

**PROGESTERONE-INDUCED $[Ca^{2+}]_i$ OSCILLATIONS AND REGULATION OF
HUMAN SPERM BEHAVIOUR**

by

ELIS TORREZAN GONÇALVES RAMALHO NITÃO

A thesis submitted to

The University of Birmingham

For the degree of

DOCTOR OF PHILOSOPHY

School of Biosciences

College of Life and Environmental Sciences

University of Birmingham

2019

UNIVERSITY OF
BIRMINGHAM

University of Birmingham Research Archive

e-theses repository

This unpublished thesis/dissertation is copyright of the author and/or third parties. The intellectual property rights of the author or third parties in respect of this work are as defined by The Copyright Designs and Patents Act 1988 or as modified by any successor legislation.

Any use made of information contained in this thesis/dissertation must be in accordance with that legislation and must be properly acknowledged. Further distribution or reproduction in any format is prohibited without the permission of the copyright holder.

ABSTRACT

Ca^{2+} signalling is crucial to modulate sperm motility and changes in the intracellular calcium concentration $[\text{Ca}^{2+}]_i$ may underlie 'switching' of sperm swimming behaviour in human spermatozoa, which is important for sperm progression in the female tract. I investigated the mechanism by which progesterone induces $[\text{Ca}^{2+}]_i$ oscillations and also investigated the role of $[\text{Ca}^{2+}]_i$ oscillations for sperm swimming behaviour and penetration ability into mucus. Sperm were loaded with Ca^{2+} -indicator fluo4/AM, treated with different agonists and analysed in single live-cell imaging and functional assays were also performed in free-swimming sperm. Approximately 25% of the human sperm population exhibit $[\text{Ca}^{2+}]_i$ oscillations, independently of sperm capacitation. $[\text{Ca}^{2+}]_i$ rise first in flagellum then spread actively to the head, apparently triggering CICR. Membrane potential (V_m), Slo3 channels and CatSper channels contribute to $[\text{Ca}^{2+}]_i$ oscillations generation. $[\text{Ca}^{2+}]_i$ oscillations occur in free-swimming spermatozoa and are associated with switching of sperm swimming behaviour in both low and high viscosity environments: drives velocity, sperm turning, hyperactivated motility and regulates attachment/detachment from substrate. Consistent with the involvement of CatSper in generation of $[\text{Ca}^{2+}]_i$ oscillations, regulation of sperm swimming velocity and cell progression are dependent on CatSper channels. Additionally, sperm ability to penetrate into mucus environment is also dependent on CatSper activity.

ACKNOWLEDGEMENTS

I would like to express my immense appreciation to my supervisor, Dr. S.J. Publicover, for the opportunity and for his unconditional guidance and support through the whole process of my PhD. I also wish to thank my co-supervisor Dr. Linda Lefievre (College of Medical and Dental Sciences – University of Birmingham) for her valuable advices and intellectual contributions. I must also thank Dr. Timo Strunker (University of Münster, Germany) for providing the novel CatSper inhibitor, RU1968-F1; Dr. Esperanza Mata-Martinez (Universidad Nacional Autónoma de México, México), Dr. Hector Guidobaldi (Universidad Nacional de Cordoba, Argentina) and Dr. Sean Brown (University of Abertay Dundee, Scotland) for their precious collaboration.

I take this opportunity to acknowledge the donors who actively provided samples, which were crucial to make my research work possible. I would also like to thank the School of Biosciences (University of Birmingham) for providing the services and facilities for continuing the project and CAPES foundation (Federal Government of Brazil) for the financial support throughout my PhD. My deepest gratitude to the members of my research group, particularly Cosmas Achikanu and Sarah Costello, to everyone in the 8th floor and to all friends I have met in Birmingham during my PhD studies.

Finally, I am incredibly grateful to all my family, especially my parents Regina and Hostilio, for their unconditional love, for being my source of strength and mostly for their understanding of my absence. I am extending a special thanks to my life partner, Tim Banasik, for all his love, care and support.

TABLE OF CONTENTS

CHAPTER ONE: INTRODUCTION

1.1	Research background.....	1
1.2	Fertilisation.....	2
1.2.1	Oogenesis.....	3
1.2.2	Spermatogenesis.....	6
1.2.3	Sperm transport in the female reproductive tract	12
1.2.4	Capacitation.....	15
1.2.5	Hyperactivation.....	19
1.2.6	Sperm chemotaxis.....	22
1.2.7	Spermatozoa-Zona pellucida interaction.....	24
1.2.8	Acrosome reaction and sperm-egg fusion.....	25
1.3	Ion channels in sperm physiology	27
1.3.1	Sperm calcium-signalling components.....	28

1.3.1.1	Canonical transient receptor potential (TRPC) channels.....	29
1.3.1.2	Voltage-gated Ca ²⁺ channels (CaV).....	30
1.3.1.3	Cyclic nucleotide-gated Ca ²⁺ channels (CNG).....	31
1.3.1.4	CatSper channels.....	32
1.3.1.5	Mobilisation of Ca ²⁺ from intracellular stores.....	35
1.3.2	Potassium (K ⁺) channels (Slo3).....	39
1.3.3	Chloride (Cl ⁻) transporters.....	41
1.3.4	Voltage-gated proton channel (Hv1).....	42
	Research Aims.....	44

CHAPTER TWO: MATERIALS & METHODS

2.1	Chemicals.....	45
2.2	Media preparation.....	45
2.3	Donor recruitment.....	46
2.4	Preparation and capacitation of spermatozoa.....	46
2.5	Single-cell imaging of [Ca ²⁺] _i	47

2.6	[Ca ²⁺] _i oscillations analysis.....	49
2.7	Fluorescent free-swimming cell tracking.....	50
2.8	Penetration of artificial viscous medium (Kremer's assay).....	51
2.9	Computer-assisted sperm analysis (CASA).....	53
2.10	Fluorimetric measurement of changes in [Ca ²⁺] _i	54
2.11	Whole-cell patch clamping.....	54
2.12	Statistical analysis.....	55

CHAPTER THREE: MEMBRANE POTENTIAL CONTRIBUTES TO GENERATION OF [Ca²⁺]_i OSCILLATIONS

3.1	ABSTRACT.....	56
3.2	INTRODUCTION.....	58
	CHAPTER AIMS.....	60
3.3	RESULTS.....	61
3.3.1	Progesterone induces [Ca ²⁺] _i oscillations in human spermatozoa.....	61
3.3.2	Level of capacitation and [Ca ²⁺] _i oscillations induced by	

	progesterone.....	63
3.3.3	[Ca ²⁺] _i oscillations require extracellular Ca ²⁺	65
3.3.4	Spatiotemporal characteristics of [Ca ²⁺] _i oscillations induced by progesterone.....	67
3.3.5	Membrane potential (V _m) regulates [Ca ²⁺] _i oscillations.....	70
3.3.5.1	Hyperpolarisation (-79 mV) effect on [Ca ²⁺] _i oscillations.....	71
3.3.5.2	Depolarisation (-4 mV) effect on [Ca ²⁺] _i oscillations.....	74
3.3.5.3	V _m close to resting potential (-38 mV) effect on [Ca ²⁺] _i oscillations....	78
3.4	DISCUSSION.....	81

CHAPTER FOUR: RU1968-F1, A NEW PHARMACOLOGICAL TOOL TO INVESTIGATE CATSPER IN HUMAN SPERMATOZOA

4.1	ABSTRACT.....	84
4.2	INTRODUCTION.....	85
	CHAPTER AIMS.....	87
4.3	RESULTS.....	88

4.3.1	RU1968 inhibits Ca^{2+} response induced by progesterone spermatozoa.....	88
4.3.2	Effect of RU1968 on the progesterone-induced $[\text{Ca}^{2+}]_i$ transient.....	89
4.3.3	RU1968 removal promotes $[\text{Ca}^{2+}]_i$ rebound peak.....	92
4.4	DISCUSSION.....	94

CHAPTER FIVE: INVESTIGATION OF THE MECHANISM OF $[\text{Ca}^{2+}]_i$ OSCILLATIONS

5.1	ABSTRACT.....	96
5.2	INTRODUCTION.....	98
	CHAPTER AIMS.....	100
5.3	RESULTS.....	101
5.3.1	CatSper channels contribution to $[\text{Ca}^{2+}]_i$ oscillations.....	101
5.3.2	Slo3 channels contribution to $[\text{Ca}^{2+}]_i$ oscillations.....	105
5.3.3	Chloride ion contribution to $[\text{Ca}^{2+}]_i$ oscillations.....	107
5.3.3.1	Cystic fibrosis transmembrane conductance regulator (CFTR) and $[\text{Ca}^{2+}]_i$ oscillations.....	109

5.3.3.2	Ca²⁺-dependent Cl⁻ channels (CaCCs) and [Ca²⁺]_i oscillations.....	109
5.4	DISCUSSION.....	112

**CHAPTER SIX: INVESTIGATION OF THE MECHANISM BY WHICH SKF-96365
MODULATES THE GENERATION OF [Ca²⁺]_i OSCILLATIONS**

6.1	ABSTRACT.....	116
6.2	INTRODUCTION.....	118
	CHAPTER AIMS.....	120
6.3	RESULTS.....	121
6.3.1	SKF-96365 induces/enhances [Ca²⁺]_i oscillations in cells pre-treated with progesterone.....	121
6.3.2	SKF-96365 <i>per se</i> induces [Ca²⁺]_i oscillations in human spermatozoa.	123
6.3.3	SKF-96365-induced [Ca²⁺]_i oscillations are sensitive to membrane hyperpolarisation.....	127
6.3.4	SKF-96365-induced [Ca²⁺]_i oscillations are sensitive to membrane depolarization.....	128
6.3.5	SKF-96365-induced [Ca²⁺]_i oscillations are dependent of CatSper	

	channels.....	131
6.3.6	SKF-96365-induced $[Ca^{2+}]_i$ oscillations are dependent of sperm capacitation.....	133
6.4	DISCUSSION.....	135

CHAPTER SEVEN: PHYSIOLOGICAL ROLE OF $[Ca^{2+}]_i$ OSCILLATIONS IN HUMAN SPERMATOZOA

7.1	ABSTRACT.....	137
7.2	INTRODUCTION.....	139
	CHAPTER AIMS.....	141
7.3	RESULTS.....	142
7.3.1	$[Ca^{2+}]_i$ oscillations occur in free-swimming cells.....	142
7.3.2	$[Ca^{2+}]_i$ oscillations drives velocity/detachment in human spermatozoa.....	143
7.3.3	$[Ca^{2+}]_i$ oscillations drives turning and hyperactivated motility.....	146
7.3.4	High viscosity induces Ca^{2+} transient and $[Ca^{2+}]_i$ oscillations.....	150
7.3.5	High viscosity effect on Ca^{2+} response is dependent of CatSper.....	153

7.3.6	[Ca²⁺]_i oscillations drives velocity in high viscosity environment.....	154
7.3.7	Swimming velocity and cell progression is inhibited by CatSper blockade.....	155
7.3.8	Sperm ability to penetrate into artificial viscous medium.....	157
7.3.9	Effect of CatSper inhibition in sperm penetration of artificial viscous medium.....	158
7.3.10	Changes in membrane potential inhibit sperm penetration into viscous medium.....	164
7.4	DISCUSSION.....	166

CHAPTER EIGHT: GENERAL DISCUSSION

8.1	Key findings.....	169
8.2	Thesis discussion.....	170
8.3	Future work.....	177
	APPENDIX I.....	178

APPENDIX II: Publication and presentations of research.....	181
REFERENCES.....	183

LIST OF FIGURES

CHAPTER 1

Figure 1.1 Human female gamete.....	4
Figure 1.2 Human female oogenesis and gamete maturation.....	6
Figure 1.3 Germ cells and Sertoli cells organisation in seminiferous tubules.....	7
Figure 1.4 Human male spermatogenesis and gamete maturation.....	9
Figure 1.5 Human male spermiogenesis phases.....	11
Figure 1.6 Sperm transport in the female reproductive tract.....	14
Figure 1.7 Signalling pathways of fast and slow events associated with sperm capacitation.....	19
Figure 1.8 Comparison of hyperactivated and non-hyperactivated flagellar beat pattern.....	20
Figure 1.9 Different types of motility patterns in human spermatozoa.....	21
Figure 1.10 Model for behaviour of human spermatozoa in a chemoattractant gradient.....	23
Figure 1.11 Diagram of acrosome reaction at the apical head of sperm cell.....	25
Figure 1.12 Diagram of acrosome reaction leading to sperm-egg fusion.....	27

Figure 1.13 Classic schematic representation of CatSper localisation and composition in human sperm cell.....	33
Figure 1.14 Model for $[Ca^{2+}]_i$ change propagation triggered by activation of CatSper.	35
Figure 1.15 Schematic diagram of Ca^{2+} signalling components involved on mobilisation of Ca^{2+} from intracellular stores.....	33
Figure 1.16 Molecular architecture of sperm Slo3 channel.....	40
 CHAPTER 2	
Figure 2.1 Schematic representation of the swim-up technique.....	47
Figure 2.2 Screenshot of iQ3 software showing the regions of interest (ROI).....	48
Figure 2.3 Calculation of $[Ca^{2+}]_i$ oscillations amplitude and frequency.....	49
Figure 2.4 Schematic representation of the Kremer's assay.....	52
Figure 2.5 Schematic representation of different designs performed in Kremer's assay.....	53
 CHAPTER 3	
Figure 3.1 Progesterone chemical structure depiction.....	59
Figure 3.2 Typical biphasic (transient + sustained phase) Ca^{2+} response induced by progesterone in human spermatozoa.....	61

Figure 3.3 Progesterone induces $[Ca^{2+}]_i$ oscillations in populations of human spermatozoa: ‘rapid’ transients with high amplitude.....	62
Figure 3.4 Ca^{2+} profiles in human spermatozoa populations are not different in non-capacitated cells or after 4 hours and 7 hours of capacitation.....	63
Figure 3.5 Degree of capacitation affects the frequency of $[Ca^{2+}]_i$ oscillations but not amplitude in human spermatozoa populations.....	64
Figure 3.6 $[Ca^{2+}]_i$ oscillations require extracellular Ca^{2+}	66
Figure 3.7 Ca^{2+} transient induced by progesterone start at the flagellum and propagate towards the sperm head.....	68
Figure 3.8 $[Ca^{2+}]_i$ oscillations induced by progesterone start at the flagellum and propagate towards the sperm head.....	69
Figure 3.9 Confirmation of manipulation of V_m using valinomycin with the technique of whole-cell patch clamp.....	70
Figure 3.10 V_m hyperpolarisation abolishes progesterone-induced $[Ca^{2+}]_i$ oscillations.....	72
Figure 3.11 Proportion of ‘oscillating’ population under different membrane potential values.....	73
Figure 3.12 V_m hyperpolarisation alters the frequency and amplitude of progesterone-induced $[Ca^{2+}]_i$ oscillations.....	73
Figure 3.13 Depolarisation (-4 mV) partially inhibits progesterone-induced $[Ca^{2+}]_i$ oscillations in sperm cells.....	75

Figure 3.14 Depolarisation slightly alters the frequency of $[Ca^{2+}]_i$ oscillations and inhibits amplitude.....	76
Figure 3.15 Progesterone-induced $[Ca^{2+}]_i$ oscillations generation is dependent on the value of V_m	77
Figure 3.16 V_m close to resting potential (-38 mV) abolishes progesterone-induced $[Ca^{2+}]_i$ oscillations in sperm cells.....	79
Figure 3.17 V_m close to resting potential (-38 mV) alters the frequency and amplitude of $[Ca^{2+}]_i$ oscillations.....	79
 CHAPTER 4	
Figure 4.1 Molecular structure of the potential CatSper inhibitor RU1968.....	86
Figure 4.2 RU1968 inhibits Ca^{2+} response induced by progesterone in a dose-dependent curve.....	88
Figure 4.3 RU1968 inhibits the transient peak induced by progesterone in a dose-dependent way.....	90
Figure 4.4 RU1968 alters the amplitude distribution of $[Ca^{2+}]_i$ transients induced by progesterone in a dose-dependent way.....	91
Figure 4.5 Low concentrations of RU1968 inhibit the frequency distribution of the highest transient amplitudes induced by progesterone.....	92
Figure 4.6 Latency to rebound is dependent on the RU1968 concentration.....	93

Figure 4.7 Rebound peak duration is dependent on the RU1968 concentration.....	93
---------------------------------------------------------------------------------------	-----------

CHAPTER 5

Figure 5.1 CatSper blocker (RU1968F1 – 10 μ M) inhibits [Ca ²⁺] _i oscillations frequency in human sperm cells, but not their amplitude.....	102
-------------------------------------------------------------------------------------------------------------------------------------------------------------------------------	------------

Figure 5.2 Different concentrations of CatSper blocker (RU1968F1) affect the proportion of ‘oscillating’ population.....	103
---------------------------------------------------------------------------------------------------------------------------------	------------

Figure 5.3 CatSper blocker (RU1968F1 – 30 μ M) inhibits [Ca ²⁺] _i oscillations frequency and amplitude in human sperm cells.....	104
--------------------------------------------------------------------------------------------------------------------------------------------------------------------	------------

Figure 5.4 Slo3 blocker (quinidine) completely inhibits [Ca ²⁺] _i oscillations generation in human sperm cells.....	106
---------------------------------------------------------------------------------------------------------------------------------------------------	------------

Figure 5.5 Absence of extracellular Cl ⁻ decreases [Ca ²⁺] _i oscillations frequency in sperm cells, but not their amplitude.....	108
---------------------------------------------------------------------------------------------------------------------------------------------------------------------------	------------

Figure 5.6 CFTR channels blocker (CFTR(inh)-172) does not affect [Ca ²⁺] _i oscillations generation in human sperm cells.....	110
------------------------------------------------------------------------------------------------------------------------------------------------------------	------------

Figure 5.7 Ca ²⁺ -dependent Cl ⁻ channels blocker (niflumic acid – NFA) does not affect [Ca ²⁺] _i oscillations generation in human sperm cells.....	111
---------------------------------------------------------------------------------------------------------------------------------------------------------------------------------------------------------	------------

Figure 5.8 Proposed model for [Ca ²⁺] _i oscillations generation in human sperm cells...	115
-----------------------------------------------------------------------------------------------------------------------	------------

CHAPTER 6

Figure 6.1 SKF-96365 induces or enhances [Ca ²⁺] _i oscillations in cells pre-treated with progesterone.....	122
-------------------------------------------------------------------------------------------------------------------------------------------	------------

Figure 6.2 SKF-96365 induces a transient Ca^{2+} response in a concentration-dependent manner in the whole sperm cell population.....	124
Figure 6.3 SKF-96365 <i>per se</i> induces $[\text{Ca}^{2+}]_i$ oscillations in human spermatozoa.....	126
Figure 6.4 Hyperpolarisation inhibits the frequency and amplitude of SKF-induced $[\text{Ca}^{2+}]_i$ oscillations.....	128
Figure 6.5 Depolarisation inhibits the frequency and amplitude of SKF-induced $[\text{Ca}^{2+}]_i$ oscillations.....	130
Figure 6.6 RU1968 completely inhibits initial $[\text{Ca}^{2+}]_i$ transient induced by SKF-96365.....	132
Figure 6.7 RU1968 completely inhibits $[\text{Ca}^{2+}]_i$ oscillations induced by SKF-96365...	132
Figure 6.8 SKF-induced ‘oscillating’ population is dependent of sperm capacitation..	133
 CHAPTER 7	
Figure 7.1 $[\text{Ca}^{2+}]_i$ oscillations drives velocity in human spermatozoa.....	144
Figure 7.2 $[\text{Ca}^{2+}]_i$ oscillations drives attachment/detachment in human spermatozoa...	145
Figure 7.3 Correlation between $[\text{Ca}^{2+}]_i$ and velocity.....	147
Figure 7.4 Correlation between $[\text{Ca}^{2+}]_i$ and straightness.....	148
Figure 7.5 Correlation between $[\text{Ca}^{2+}]_i$ and fractal dimension.....	149

Figure 7.6 High viscosity induces Ca^{2+} transient with half amplitude of P4-induced transient in human spermatozoa.....	151
Figure 7.7 High viscosity does not change the characteristics of P4-induced $[\text{Ca}^{2+}]_i$ oscillations in human spermatozoa.....	152
Figure 7.8 CatSper blocker (RU1968) completely inhibits Ca^{2+} transients and $[\text{Ca}^{2+}]_i$ oscillations generation induced by MCL and P4 in human sperm cells.....	153
Figure 7.9 $[\text{Ca}^{2+}]_i$ oscillations drives velocity in high viscosity environment.....	154
Figure 7.10 CatSper blocker inhibits $[\text{Ca}^{2+}]_i$ oscillations and progression of cell.....	156
Figure 7.11 Sperm penetration into artificial viscous medium assay expressed in number of ‘penetrating’ cells.....	157
Figure 7.12 RU1968 inhibits sperm penetration into artificial viscous medium in a dose-dependent way.....	159
Figure 7.13 RU1968 inhibits stimulation induced by progesterone (3 μM) of sperm penetration of artificial viscous medium – design (1).....	160
Figure 7.14 RU1968 inhibits progesterone effect on sperm penetration when added to the viscous medium – design (2).....	161
Figure 7.15 RU1968 inhibits the sperm progression and motility when added to the viscous medium.....	163
Figure 7.16 Valinomycin inhibits sperm penetration into artificial viscous media induced by progesterone, affecting sperm track speed (VCL).....	165

LIST OF TABLES

Table 7.1 $[Ca^{2+}]_i$ oscillations characteristics under different temperatures (25 °C and 31°C) in immobilised and free-swimming sperm cells..... **143**

LIST OF ABBREVIATIONS

ABC	ATP binding cassette
ALH	Amplitude of lateral head displacement
AR	Acrosome reaction
ARSA	Arylsulfatase A
ART	Assisted reproductive technology
ATP	Adenosine triphosphate
AM	Acetoxymethyl
BCF	Beat frequency
BSA	Bovine serum albumin
Ca²⁺	Calcium ion
[Ca²⁺]_i	Intracellular calcium concentration
[Ca²⁺]_o	Extracellular calcium concentration
CaCC	Ca ²⁺ -activated Cl ⁻ channel
CaCl₂	Calcium chloride
cADP	Cyclic adenosine diphosphate ribose
CaV	Calcium voltage channel
CaCl₂·2H₂O	Calcium chloride dihydrate
cAMP	Cyclic adenosine monophosphate
CASA	Computer assisted sperm analysis
CatSper	Sperm specific cation channel
C₆H₁₁KO₇	Potassium gluconate

CICR	Calcium induce calcium release
Cl⁻	Chloride ion
cm	Centimetre
CNG	Cyclic nucleotide-gated Ca ²⁺
cNMP	3',5'-cyclic monophosphates
CO₂	Carbon dioxide
cp	Centipoise
cpm	Cycle per minute
DAG	Diacylglycerol
DMSO	Dimethyl sulfoxide
DNA	Deoxyribonucleic acid
E_{Cl}	Chloride equilibrium potential
EGTA	Ethylene glycol-bis (β-aminoethyl ether)-N,N,N',N'-tetraacetic acid
E_K	Potassium equilibrium potential
ER	Endoplasmic reticulum
f	Frequency
fig	Figure
Fluo4-AM	Glycine,N-[4-[6-[(acetyloxy)methoxy]-2,7difluoro-3-oxo3h-xanthen-9-yl]-2-[2-[2-bis[2-[(acetyloxy)methoxy]-2-oxoethyl]amino]-5-methylphenoxy]ethoxy]phenyl]-N-[2-(acetyloxy)methoxy]-2-oxoethyl](acetyloxy)methyl ester
FSH	Follicle-stimulating hormone
H⁺	Proton ion
HC-056456	CatSper channel inhibitor
HCl	Hydrochloric acid
HCO₃⁻	Bicarbonate

HEPES	4-(2-hydroxyethyl)-1-piperazineethanesulfonic acid
H₂O₂	Hydrogen peroxide
HSPA2	Heat shock protein 2
Hv1	Proton channel 1
HVA	High voltage-activated
Hz	Hertz
IC50	Half maximal inhibitory concentration
ICSI	Intracytoplasmic sperm injection
IP₃	Inositol 1,4,5-trisphosphate
IP₃R	Inositol triphosphate
IUI	Intrauterine insemination
IVF	<i>in vitro</i> fertilization
K⁺	Potassium ion
KCl	Potassium chloride
kDa	Kilodalton
KSper	Sperm specific potassium ion channel
LH	Luteinizing hormone
LIN	Linearity
LVA	Low voltage-activated
M	Molar
MCL	Methylcellulose
MDL12330A	CatSper channel inhibitor
MDMA	Multi Dimensional Motion Analysis
MgCl₂	Magnesium chloride

MgSO₄·7H₂O	Magnesium sulphate heptahydrate
min	Minute
mL	Millilitre
mm	Millimetre
mOsm	Milliosmole
μM	Micromolar
mM	Millimolar
mV	Milivolts
Na⁺	Sodium ion
NAADP	Nicotinic acid-adenine dinucleotide phosphate
NaC₆H₁₁O₇	Sodium gluconate
NaCl	Sodium chloride
NaHCO₃	Sodium bicarbonate
NaOH	Sodium hydroxide
Na⁺/H⁺	Sodium/proton exchanger
Na⁺/HCO₃⁻	Sodium/bicarbonate ion exchanger
NBC	Na ⁺ / HCO ₃ ⁻ co-transporters
NC	Non-capacitated
NH₄Cl	Ammonium chloride
NFA	Niflumic acid
nM	Nanomolar
nm/sec	Nanometre per second
NNC55-0396	Catsper channel inhibitor
ODFs	Outer dense fibers

p	Probability
P4	Progesterone
pHi	Intracellular pH
PHN	Posterior head/neck
PKA	Protein kinase A
PLC	Phospholipase C
PIP2	Phosphatidylinositol-4,5-bisphosphate
PMCA	Plasma membrane calcium –ATPase pump
ROI	Region of interest
ROS	Reactive oxygen species
RNE	Redundant nuclear envelope
RU1968-F1	CatSper channel inhibitor
sec	Second
RyR	Ryanodine receptor
sAC	Soluble adenylyl cyclase
SACY	Soluble adenylyl cyclase
SD	Standard deviation of the mean
sEBSS	Supplemented Earle's balanced salt solution
SEM	Standard error of the mean
Ser	Serine
SERCA	Sarcoplasmic endoplasmic Ca^{2+} ATPase
Slo3	Sperm specific potassium ion channel
sNHE	Na^+/H^+ exchanger
SOC	Store-operated Ca^{2+} channel

SOD	Superoxide dismutase
SPAM1	Sperm adhesion molecule 1
SPCA	Secretory pathway Ca ²⁺ ATPase
STIM	Stromal interaction molecule
STR	Straightness
T	Period (minutes)
Thr	Threonine
TM	Transmembrane
TRPC	Transient receptor potential canonical
Tyr	Tyrosine
VAP	Average path velocity
VCL	Curvilinear velocity
VLN	K ⁺ ionophore valinomycin
V_m	Membrane potential
WHO	World health organisation
w/v	Weight per volume
ZP	Zona pellucida
ZP 1-4	Zona pellucida protein 1-4

CHAPTER ONE: INTRODUCTION

1.1 Research background

The World Health Organization (WHO) considers infertility as “a disease of the reproductive system defined by the failure to achieve a clinical pregnancy after 12 months or more of regular unprotected sexual intercourse” and this disorder has been recognised as a public health issue across the globe (Zegers-Hochschild et al, 2009). The estimated proportion of couples in reproductive age (15 - 49 years) affected by infertility is more than 20% (approximately 210 million people worldwide) (Slama et al , 2012) and 40 - 50% is attributed to the male partner (Hirsh, 2003; Brugh and Lipshultz, 2004). Male infertility affects approximately 7% of all men in the world and it is associated to sperm dysfunction in most of the cases (Irvine, 1998; Sharpe, 2012, Lotti and Maggi, 2014). According to the WHO, the reference values for human semen are: volume: 1.5 mL, sperm concentration: 15 million spermatozoa/mL, total sperm number: 39 million spermatozoa per ejaculate, morphology: 4% normal forms, vitality: 58% live and progressive motility: 32% (Cooper et al, 2010). Therefore, the main causes for male fertility issues include low sperm concentration (oligospermia), abnormal sperm morphology (teratospermia) and poor sperm motility (asthenospermia). The impaired motility of spermatozoa is responsible for a great number of male infertility occurrences. At the moment, men do not have a choice of a non-invasive pharmacological treatment for sperm dysfunction and to improve fertility. In fact, the only infertility therapy option is ART (Assisted Reproductive Technology), which depends on the severity of the infertility condition. Common methods of ART to overcome male infertility involve: intrauterine insemination (IUI) - soft cases; *in vitro* fertilisation (IVF) - moderate

cases; and intra-cytoplasmic sperm injection (ICSI) - extreme sperm dysfunction cases. However, ART procedures can be very expensive, complex and highly invasive. The lack of progress in non-invasive treatment alternatives is due to the limited understanding of cellular and molecular functions of the mature spermatozoa (Aitken and Henkel, 2011; Barratt et al, 2011). Important studies are being made concerning Ca^{2+} signalling as a major key to understand the regulation of sperm motility and male fertility (Publicover et al, 2007; Costello et al, 2009; Lishko et al, 2011; Alasmari et al, 2013). Spermatozoa need to undergo several events to be competent for a successful fertilisation, such as capacitation, hyperactivation, chemotaxis towards the egg, acrosome reaction, binding and fusion with egg membrane. Most of these events are Ca^{2+} -dependent (Marquez and Suarez, 2004; Eisenbach and Giojalas, 2006; Kaupp et al, 2006; Publicover et al, 2007). Although some progress in this area has been made, a number of questions associated with Ca^{2+} signalling and sperm function remains unclear.

1.2 Fertilisation

Fertilisation is a complex multi-event process in which a female and a male haploid gamete, named egg and sperm cell, combine their genetic information to produce a genetically different organism. It involves maturation and development of the spermatozoa and eggs, followed by sperm transport through the female reproductive tract and ending with sperm-egg interaction and then fusion of the gametes plasma membranes (Yanagimachi, 1994). To successfully fertilise an egg, sperm cells need to undergo a succession of biochemical and physiological changes in the female reproductive tract since human spermatozoa are not yet competent for fertilisation when freshly ejaculated (Yanagimachi, 1994; Aitken, 1997; Urner

and Sakkas, 2003). These events are dependent on several factors such as hormones, pH, ions, reactive oxygen species (ROS), temperature, and are regulated by different signaling pathways. However, changes in the intracellular Ca^{2+} concentration ($[\text{Ca}^{2+}]_i$) is a modulation mechanism that plays a significant role in most of fertilisation steps (Publicover et al, 2007; Costello et al, 2009).

1.2.1 Oogenesis

Oogenesis is the production of the female gamete from primordial germ cells, resulting in an egg containing all the constituents and machinery necessary to start metabolism and development, such as organelles, maternal mRNAs, cytoplasmic proteins, growth factors and metabolic substrates. In the human female, oogenesis begins during fetal development when primordial germ cells multiply to form thousand diploid oogonia (Witschi, 1948; Hashimoto and Eguchi, 1955). The first meiosis event of the oogonium occurs during the embryo development and the primary oocyte remains arrested in the sustained diplotene stage of the first meiotic prophase for approximately 12 years, when females reaches puberty (Pinkerton et al, 1961; Baker and Franchi, 1967; Byskov and Hoyer, 1994). In fact, some oocytes are arrested in meiotic prophase for almost 50 years. Each oocyte becomes surrounded by a layer of epithelial granulosa cells and a layer of mesenchymal thecal cells, which together forms the primordial follicle (Gougeon, 1996). At birth, the ovary contains around 400,000 primordial follicles however, over the lifetime of woman, only about 400 primordial follicles get matured (Peters et al, 1975). Human females have a periodic ovulation pattern, which is associated with the maturing and releasing of gamete. During this period, a

primordial follicle undergoes a stage of follicular growth (follicular phase) with the stimuli of follicle-stimulating hormone (FSH) (Wassarman, 1988; Gupta et al, 1997).

The oocyte forms an extracellular matrix called the zona pellucida (ZP) by secreting glycoproteins (ZP1 to ZP4, in humans) (Chamberlin and Dean, 1990; Harris et al, 1994, Lefièvre et al, 2004). The follicle undergoes a 500-fold increase in volume and become among the largest cells in the body. Oocyte diameter increases from 10 μm in a primordial follicle reaching 100 μm in a fully developed follicle. Simultaneously with oocyte growth an increase in the number of follicular granulosa cells occurs, which form several layers of cumulus cells around the oocyte (Buccione et al, 1990). In response to hormonal stimulation, oocyte resumes the first meiotic division and it is divided in two daughter cells; one cell has barely any cytoplasm, called first polar body, whereas the other cell has nearly the entire volume of cellular components, referred as secondary oocyte (Erickson, 1986; Gondos et al, 1986) (fig. 1.1).

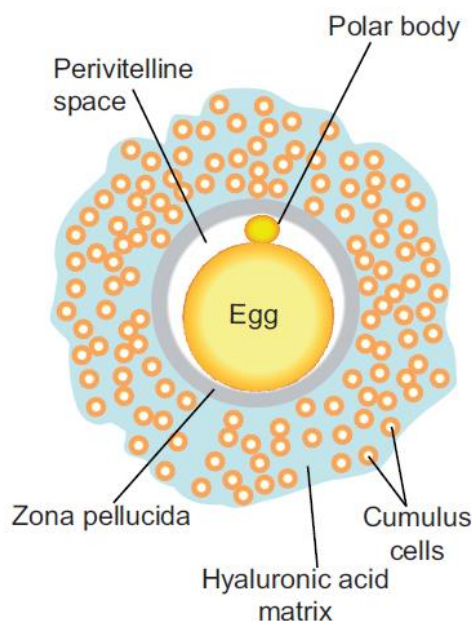


Figure 1.1 Human female gamete. Egg and polar body surrounded by zona pellucida (formed by ZP1-ZP4 glycoproteins) and by cumulus cells layer inserted in hyaluronic acid matrix (image reproduced from Okabe, 2013).

The physical release of the mature oocyte from the follicle is triggered by luteinising hormone (LH) which initiates the process of ovulation by the stimulation of steroidogenesis and plasminogen activator, causing increase on prostaglandin synthesis and latent collagenase (Lemaire et al, 1973; Beers et al, 1975; Downs and Longo, 1983). After the rupture of the follicle, the remaining cells developed into the corpus luteum, under the continued effect of LH (luteal phase). The corpus luteum secretes steroid hormones including estrogen, but mainly progesterone. Progesterone is important to stimulate the uterine wall thickening and blood vessels growth for facilitate embryo implantation after egg fertilisation (Lessey et al, 1996).

If the fertilisation does not occur, the corpus luteum becomes degenerated, progesterone secretion stops, and the uterine wall sheds. If fertilisation occurs, the egg undergoes the second division of meiosis, similar to the first one, with unequal cytokinesis. Most of the cytoplasm is reserved by the fertilised egg and a second polar body remains with negligible cytoplasm (fig. 1.2).

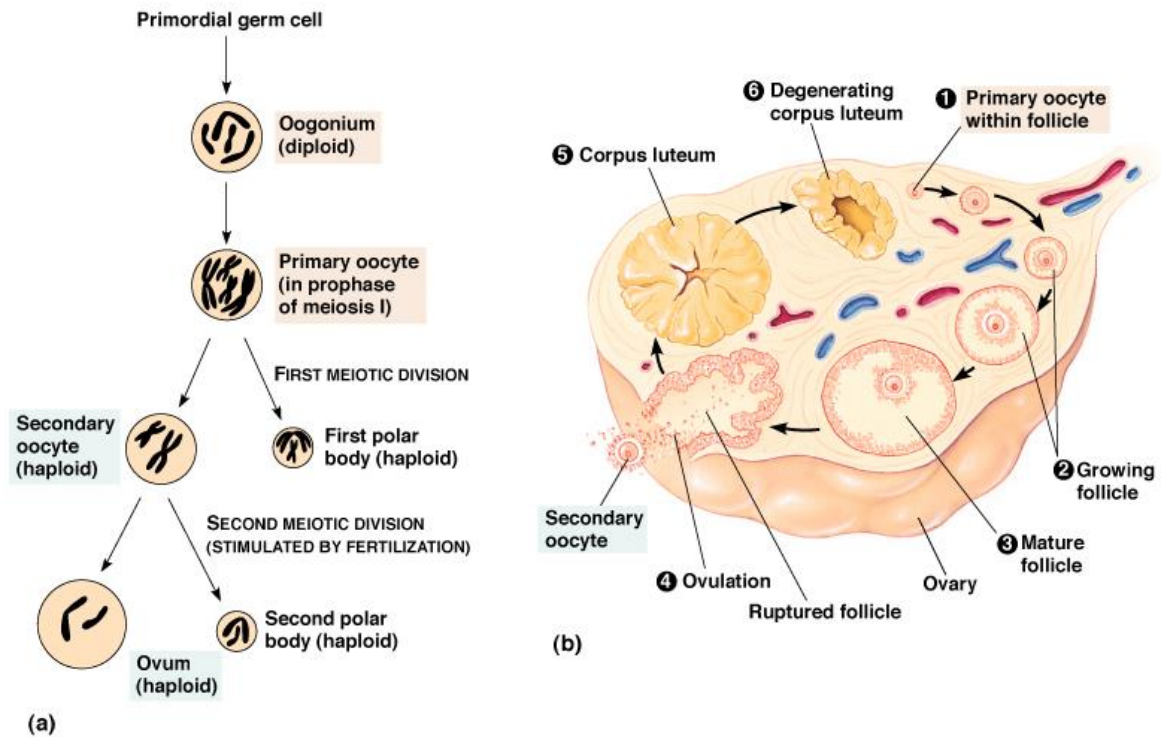


Figure 1.2 Human female oogenesis and gamete maturation. (a) Diagram of oogenesis process from the primordial germ cell to ovum development. (b) The process of female gamete maturation in human female ovary: 1 - primordial follicle development; 2 and 3 - follicular phase; 4 - ovulation and gamete releasing; 5 - luteal phase; 6 - corpus luteum degeneration (image reproduced from Campbell et al, 1999).

1.2.2 Spermatogenesis

Spermatogenesis differs from oogenesis in several ways. While oogenesis develops an egg containing all the constituents necessary to start metabolism, spermatogenesis forms a gamete differentiated for motility. During embryonic development, primordial germ cells become integrated into the sex cords of the male embryo, where they remain until maturation. The sex cords, which develop into the seminiferous tubules, have an epithelium that includes Sertoli cells (Wartenberg, 1978; Martineau et al, 1997; Tilmann and Capel, 1999). Sertoli cells are activated by follicle-stimulating hormone (FSH) to facilitate the maturation of

primordial germ cells into sperm cells, mainly nourishing the developing sperm cells through the different stages of spermatogenesis (Griswold, 1998) (fig. 1.3).

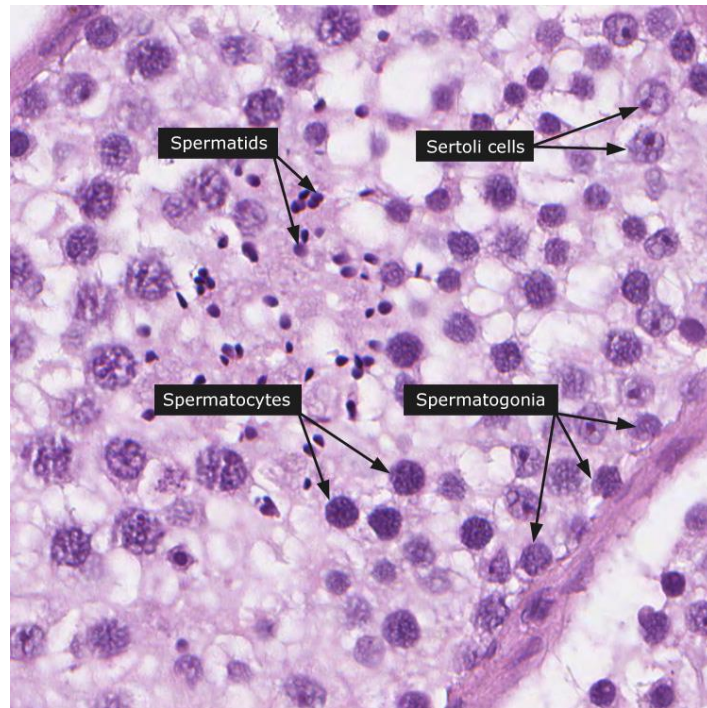


Figure 1.3 Germ cells and Sertoli cells organisation in seminiferous tubules. Cross section from seminiferous tubule showing different stages of germ cells maturation: undifferentiated spermatogonia (in the basal layer) and mature spermatocytes and spermatids (closer to the lumen); and Sertoli cells organised in concentric layers (image reproduced from The Human Protein Atlas: available on www.proteinatlas.org).

Spermatogenesis begins with the division of primordial germ cells into smaller cells called type A spermatogonia. Type A spermatogonia are stem cells, capable of self-renewal, and they are found adjacent to the outer basement membrane of seminiferous tubules. In rodents, there are four different types A spermatogonia (1 – 4), however, only type A4 can differentiate into the intermediate spermatogonium, which are committed to becoming sperm cells. However, in human type A spermtogonia can be classified in only two types: A dark

(Ad) and A pale (Ap) spermatogonia (Clermont, 1972). An intermediate spermatogonium undergoes mitotic division both to maintain the stem cell population and to form the type B spermatogonia, which are the precursors of the primary spermatocytes (Huckins, 1971; Oakberg, 1971; De Rooij, 1973; Tegelenbosch and De Rooij 1993, De Rooij and Russell, 2000).

Diploid primary spermatocytes undergo first meiotic division producing haploid secondary spermatocytes. The secondary spermatocytes complete the second meiosis division, which generates four spermatids, connected to each other through cytoplasmic bridges. The cytoplasmic bridges are important to facilitate diffusion of proteins and mRNAs between the cytoplasm of the two cells (Dym and Fawcett 1971; Braun et al, 1989). During these several divisions from type A1 spermatogonium to spermatid, the cells migrate from the basement membrane of the seminiferous tubule towards its lumen (fig. 1.4).

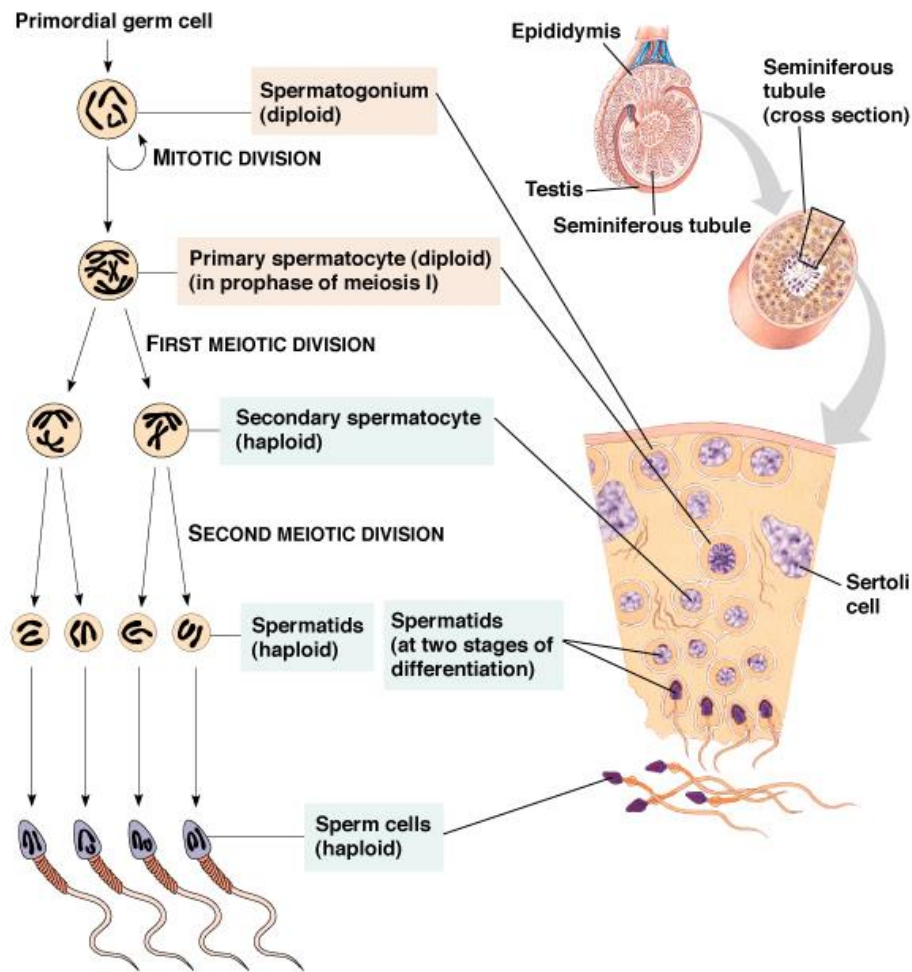


Figure 1.4 Human male spermatogenesis and gamete maturation. Diagram of spermatogenesis process from the primordial germ cell to mature sperm cell. The process of male gamete maturation in human occurs in the seminiferous tubules and the different types of cells observed during spermatogenesis can be found in a particular region of the tubule (image reproduced from Campbell et al, 1999).

The spermatid, in the first stage of differentiation, is a round and unflagellated cell and it needs to go through a process called spermiogenesis to differentiate into a functional sperm cell. The first step of spermiogenesis involves the developing of the acrosomal vesicle from the Golgi apparatus, also called Golgi phase (Clermont et al, 1993; Smith et al, 1990; Susi et al, 1971; Tang et al, 1982; Oko and Clermont, 1998). Then, the cap phase initiates and the acrosome vesicle starts to be positioned covering the sperm nucleus. Concomitant to the cap formation, the centrioles begin to form the sperm flagellum at the posterior pole of the

nucleus (Clermont et al, 1993; Oko and Clermont, 1998). By the end of this phase, the spermatid rotates so that the cap and nucleus will be directed toward the basal membrane of the seminiferous tubule and the developing flagellum will extend into the lumen.

During the acrosomal phase of spermiogenesis, the nucleus flattens and the DNA condensing histones are removed and replaced by protamines. The DNA becomes supercondensed and the transcription in the nucleus is completely inhibited (Burgos and Fawcett, 1956; Peschon et al, 1987; Russell et al, 1990; Braun, 2001). Also, the formation of the tail continues and approximately 100 mitochondria concentrate at the flagellum midpiece, being responsible for the aerobic functioning of the sperm cell. From the midpiece to the principal piece of the sperm flagellum, nine outer dense fibers (ODFs) extend and surround the internal cytoskeleton structure of the flagellum, the axoneme (Fawcett et al, 1975; Guraya, 1987). The ODFs together with tubuli doublets confer the flagellum 9+2 structure and are important to the flagellum protection and in regulating sperm motility (Linck et al, 1981; Baltz et al, 1990; Sutovsky and Manandhar, 2006; Linck et al, 2016). The most distal end piece of flagellum contains essentially the central flagellum surrounded by the plasma membrane. Just before the sperm cell is liberated from the luminal surface, the maturation phase, most of the cytoplasm and redundant organelles such as Golgi complexes, endoplasmic reticulum, lysosomes, peroxisomes, and ribosomes are removed as residual bodies and phagocytosed by surrounding Sertoli cells (Dietert, 1966; Sakai and Yamashina, 1989). The mature spermatozoon cell consists: the head, with the nucleus and acrosome; and the flagellum, which is divided in middle piece (containing mitochondria), principal piece (responsible for motility) and the end piece (containing few structural components) (fig. 1.5).

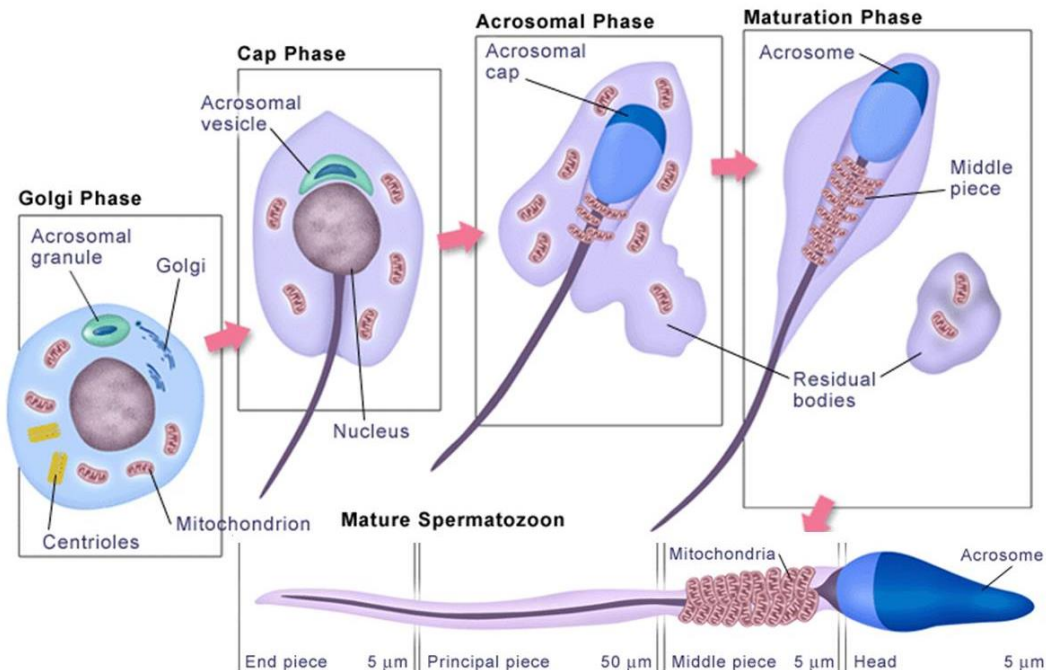


Figure 1.5 Human male spermiogenesis phases. Spermiogenesis consists in the developing of the acrosomal vesicle from Golgi apparatus (Golgi phase); formation of acrosomal cap and flagellum (cap phase); nucleus elongation and mitochondria deposition at the flagellum midpiece (acrosomal phase); and elimination of cytoplasm excess and redundant organelles as residuals bodies (maturation phase) (image reproduced from Campbell et al, 1999).

The developing of spermatogonial stem cell to mature sperm cell takes approximately 65 days, in human (Dym, 1994). Daily, around 100 million sperm cells are produced in each human testicle, in a rate of approximately 1000 spermatozoa produced per second (Amann and Howards, 1980). Approximately 200 million sperm cells are released during the ejaculation. The estimative is that human male can produce approximately 10^{12} to 10^{13} sperm cells during a lifetime (Reijo et al, 1995).

After sperm production and maturation in the testes, cells are transported to the epididymis, where they are stored and undergo a plasma membrane remodelling by the addition of epididymal proteins to its surface (Frenette et al, 2002; Busso et al, 2007). Epididymal sperm now encounter the seminal fluid secreted by several glands including seminal glands and prostate. The seminal fluid contains immune response inhibitors and also

plays an important role in coating the sperm plasma membrane. This coat involve proteins also named as “decapacitation factors” which are implicated in sperm stabilisation and survival during the transport through the female reproductive tract, prevention of premature capacitation and also proteins required for the sperm’s ability to bind to the zona pellucida and undergo oocyte fusion (Eng and Oliphant, 1978; Reddy et al, 1982; Cooper, 2002; Cuasnicu et al, 2002).

1.2.3 Sperm transport in the female reproductive tract

At ejaculation, the seminal fluid with millions sperm cells is deposited in the female reproductive tract. However, only a limited number of sperm succeeds in reaching the fallopian tubes (oviducts), and even less are capable of fertilising the egg. The first interaction of the sperm cells with the female tract is with the anterior vagina. Sperm cells then start to abandon the seminal fluid and enter the cervix in order to escape vaginal acid (typically pH between 3.8 – 4.5) and immune responses (Sobrero and Macleod, 1962). Under estrogen stimulation, the cervix secretes highly hydrated mucus, which represents a greater barrier to abnormal sperm with poor morphology and motility. The cervical mucus acts as a sperm selection system since only a fraction of the ejaculated sperm actually enter the cervix (Hanson and Overstreet, 1981; Barros et al, 1984; Katz et al, 1990, 1997).

The transport of sperm through the uterus is boosted by muscular contractions of the myometrium and take less than 10 min since sperm cells can swim at a rate around 5 mm/min in an aqueous medium and the human uterine cavity is quite small in length (Mortimer and Swan, 1995). After traversing the uterine cavity, sperm cells reach the uterotubal junction, which also plays a role as a selective barrier to the sperm. Anatomically, the uterotubal lumen

is thick walled and exhibits a twisty and very narrow lumen often filled with viscous mucus (Hafez and Black, 1969; Jansen, 1980). All these characteristics together regulate the sperm progression and just few thousands cells manage to swim through the uterotubal junction to get into the oviduct (also known as Fallopian tube) (Bedford, 1970; Shalgi et al, 1992; Holt and Van Look 2004; Nakanishi et al, 2004).

Although only identified in other mammalian species, a storage region (sperm reservoir) in the tubal isthmus is also believed to be found in humans (Suarez and Pacey, 2006). A sperm reservoir provides conditions that maintain sperm viability until ovulation, suppression of motility providing sperm interaction with oviductal epithelium (Kervancioglu et al, 1994). Also the storage of sperm in the tubal isthmus prevents polyspermy since only 100 to 1000 sperm cells reach the oocyte in the ampulla (the last portion of the oviduct) (Hunter and Leglise, 1971; Hunter, 1972, 1973).

During the hosting period in the tubal isthmus, sperm cells undertake capacitation and hyperactivation, which permits them to proceed on the way to the tubal ampulla. After release from the oviductal epithelium, sperm may be guided to the oocyte by taxis mechanisms, mainly chemotaxis. Also hyperactivated motility aids sperm in penetrating mucus in the oviduct, the cumulus cells layer and zona pellucida of the oocyte, so that male gamete may finally fuse with the oocyte plasma membrane (Ho and Suarez, 2001; Rathi et al, 2001; Suarez, 2008; Quill et al, 2003; Suarez and Ho, 2003; Darszon et al, 2011; Alasmari et al, 2013) (fig. 1.6).

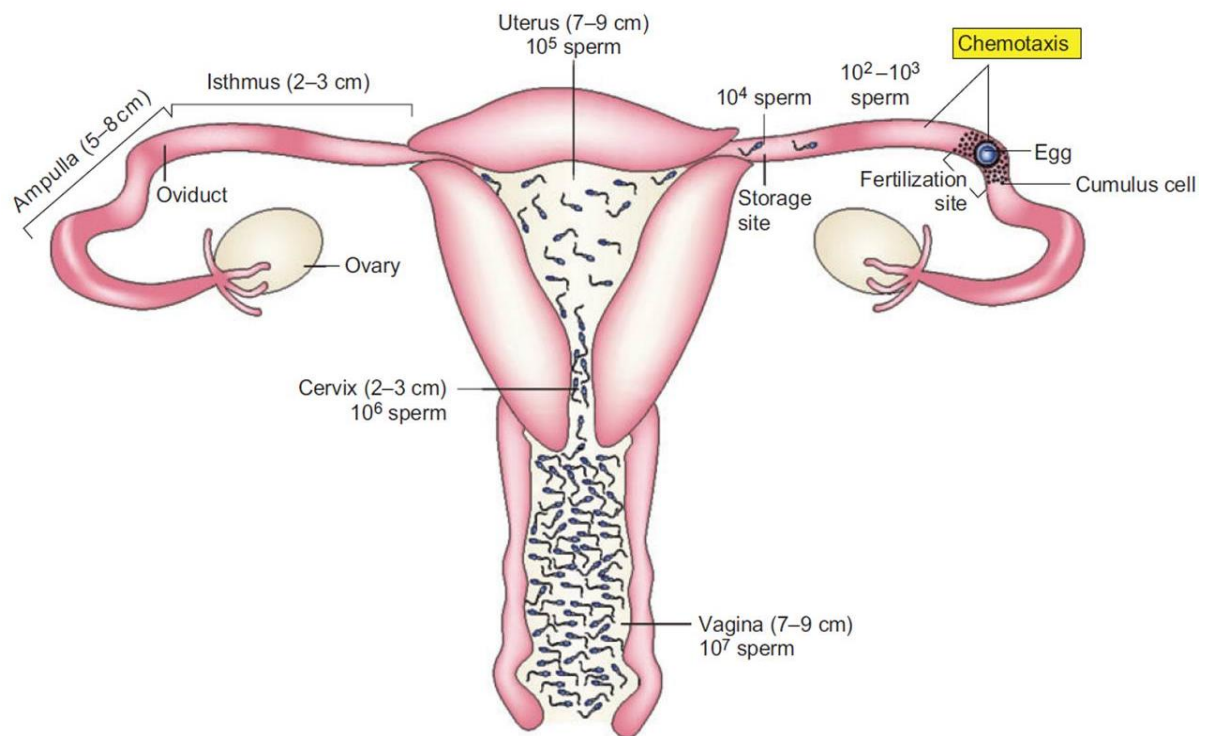


Figure 1.6 Sperm transport in the female reproductive tract. The diagram shows the dimensions of female reproductive tract organs and the amount of sperm cells that may reach each organ to fertilise an egg. Sperm cells are deposited in the anterior vagina, however just a few proceed into the cervix. After transverse the uterine cavity, they reach the uterotubal junction and enter into the isthmus, where they can be attached in the sperm reservoir. In the storage site, sperm undergoes capacitation and hyperactivation and only a small fraction is guided by chemotaxis towards to the egg-cumulus complex (image reproduced from Eisenbach and Giojalas, 2006).

After fertilisation, any remaining sperm cells in the female reproductive tract may be phagocytosed and eliminated (Chakraborty and Nelson, 1975; Mortimer and Templeton, 1982; Rasweiler, 1987).

1.2.4 Capacitation

Freshly ejaculated sperm cells are not competent to fertilise an egg and they must reside in the female mammalian reproductive tract to undergo multiple physiological and biochemical modifications to become capacitated for fertilisation (De Lamirande et al, 1997; Jonge, 2005). This process, known as capacitation, was first reported in rabbit and rat sperm by the scientists Chueh Chang (1951) and Colin Russell Austin (1951; 1952). In humans, capacitation starts at the cervical mucus, after the sperm cells migrate from the acidic environment of the vagina, and takes place predominantly in the oviduct, more specifically in the ampulla of the Fallopian tubes (Rathi et al, 2001).

The modifications associated with the capacitation process include: efflux of cholesterol from the sperm plasma membrane promoting an increase in membrane fluidity; increase in bicarbonate (HCO_3^-) concentration, tyrosine phosphorylation, cyclic adenosine monophosphate (cAMP) levels and intracellular Ca^{2+} concentrations, changes protein kinase A (PKA) activity and consequently in protein phosphorylation. All these changes confer upon the sperm the ability to gain hyperactivated motility pattern, chemotactic behaviour, interact with the ZP, undergo the acrosome reaction (AR) and initiate oocyte plasma membrane fusion (Yanagimachi, 1994).

Recently, capacitation has been divided into: (1) fast and early events that allow activated spermatozoa to swim from the seminal fluid into the cervical mucus present in the female tract (Mortimer et al, 1986) and (2) slow and late events that comprise change of movement (hyperactivation) and the ability to carry out the acrosome reaction stimulated by a physiological agonist (Salicioni et al, 2007; Visconti, 2009).

Fast and early events: occur a few seconds after the sperm are ejaculated and includes mainly an increase in bicarbonate (HCO_3^-) and intracellular Ca^{2+} . Sperm cells encounter two main sources of HCO_3^- during capacitation process: (1) from the semen and (2) from the luminal fluid in oviduct. Although the epididymal fluid contains relatively low concentrations of HCO_3^- , the semen from mammals is rich in bicarbonate and human semen presents an average of 22 mM (Huggins et al, 1942; Liu et al, 2012). On the other hand, luminal fluid of the oviduct contains very high concentration of HCO_3^- , varying between 35 mM and 90 mM depending on the ovulatory phase (Vishwakarma, 1962; Maas et al, 1977).

The HCO_3^- enters the sperm through the co-transporter $\text{Na}^+/\text{HCO}_3^-$ (Demarco et al, 2003) and studies suggests that Ca^{2+} influx also occurs through the sperm-specific Ca^{2+} channel CatSper. Once in the sperm cell, HCO_3^- promotes fast responses (order of minutes) inducing sAC/cAMP and PKA signalling pathway activation (Harrison and Miller, 2000). The bicarbonate promotes increase in the intracellular pH and stimulates the abundant sperm soluble adenylyl cyclase (SACY) (Litvin et al, 2003). The sperm specific Na^+/H^+ exchanger (sNHE) is also required to activate the soluble adenylyl cyclase (SACY), by regulating the increase of pH_i (Quill et al, 2006; Wang et al, 2007). sNHE is localised on the principal piece of the sperm flagellum and null sperm mice are immotile and are not able to fertilise an oocyte (Wang et al, 2003).

SACY increases the intracellular levels of cAMP and, consequently, the activation of protein kinase A (PKA). PKA regulates several proteins by phosphorylating at serine/threonine (Ser/Thr) residues. PKA may also be associated in regulating the activation of CatSper channels by promoting alterations to membrane potential, which, consequently, increases $[\text{Ca}^{2+}]_i$ and induces hyperactivated motility in sperm cells (Wennemuth et al, 2003). Also, the HCO_3^- can stimulate a collapse of the sperm plasma membrane asymmetry due to

activation of scramblase enzymes, which translocate membrane phospholipids between the lipid bilayer (Gadella and Harrison, 2000); this facilitates removal of cholesterol by acceptor proteins in the external leaflet of plasma membrane (Salicioni et al, 2007; Visconti, 2009).

Slow and late events: begin by an organised destabilisation of the sperm plasma membrane. In ejaculated sperm, coating substances and other components of the seminal plasma overlay the acrosomal region of the sperm head and have to be removed before capacitation can occur, mainly by the dissociation of cholesterol from the sperm plasma membrane (Cross, 1998, 2003; Flesch and Gaella, 2000; Travis and Kopf, 2002). The shedding of cholesterol is probably caused by the capacitation-dependent activation of a reverse sterol transporter that specifically lifts free sterols out of the sperm plasma membrane lipid bilayer and transfer free sterol monomers toward an acceptor. It may involve efflux pumps of the superfamily of ABC (for ATP binding cassette) transporters such as ABCA1 and ABCA17 (Selva et al, 2004; Morales et al, 2012) or scramblases, which are activated via a bicarbonate adenylate cyclase PKA signalling pathway. After being released from the sperm plasma membrane, the cholesterol can be transferred to proteins present in the oviductal fluid during its journey in the female tract, such as albumin (Neild et al, 2005).

Albumin in the surrounding medium decreases cholesterol content of the sperm plasma membrane up to 40% (Cross, 1998), and this effect is HCO_3^- -dependent (Gadella and Harrison, 2000; Gadella and Van Gerstel, 2004). Cholesterol efflux, from sperm plasma membrane, increases membrane fluidity in the acrosomal region and also facilitates the Ca^{2+} -influx into the sperm cell during acrosome reaction (Iborra et al, 2000; Neild et al, 2005; Yoshimoto et al, 2017). The phenomenon is associated with the activation of several membrane signal transduction pathways related to capacitation.

In addition to being dependent in HCO_3^- , the alterations of the sperm plasma membrane is also assisted by oxidative stress. Recently, studies have described that sterols can be oxidised during capacitation, increasing their hydrophilicity therefore facilitating their transfer to albumin (Brouwers et al, 2011). Moreover, antioxidants can inhibit this process and interrupt the capacitation of the spermatozoa (O'Flaherty et al, 1997; Boerke et al, 2013).

Downstream sAC/cAMP/PKA signalling pathway, activation of tyrosine kinases occurs on a long-term basis (more than an hour), which phosphorylates diverse proteins at tyrosine (Tyr) residues (Visconti et al, 1999; Ficarro et al, 2003). The crosstalk between both sAC/cAMP/PKA signalling pathway and tyrosine kinase signalling pathway has been reported on few studies (Naz and Rajesh, 2004; Signorelli et al, 2012; Sati et al, 2014; Jin and Yang, 2017). Phosphorylation of proteins is a posttranslational modification event and is an important mechanism to regulate various cellular processes. PKA activation leads to the phosphorylation of several proteins in serine and threonine residues, which can activate several kinases or inhibit phosphatases and consequently produce an increase in the phosphorylation of tyrosine residues. The proteins that undergo tyrosine phosphorylation during capacitation are not completely identified yet. However, it is known that Tyr-phosphorylated proteins in human sperm include ion channels; metabolic enzymes and structural proteins (Ficarro et al, 2003). Increased protein-tyrosine phosphorylation is noted in the sperm tail and it might play a role in regulation of sperm to generate hyperactivated motility (fig. 1.7).

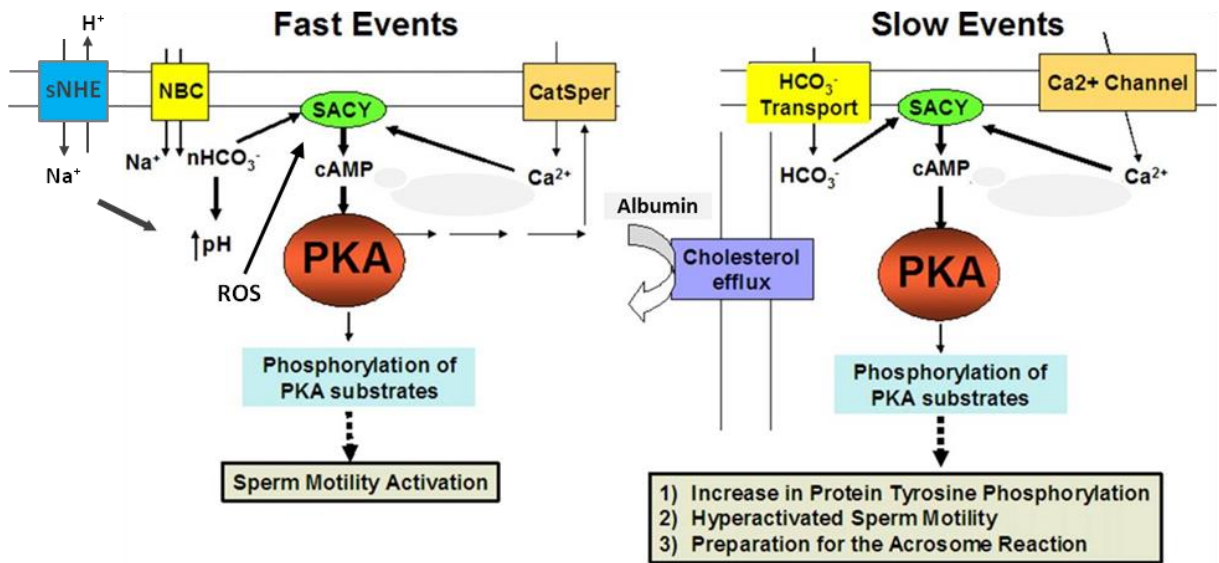


Figure 1.7 Signalling pathways of fast and slow events associated with sperm capacitation. Fast events: increase in pH_i , Ca^{2+} and ROS (mainly, H_2O_2) through activation of Na^+/HCO_3^- cotransporter (NBC) and Na^+/H^+ exchanger (sNHE), CatSper channels and oxidases, respectively. They might stimulate adenylyl cyclase SACY to increase cAMP levels. cAMP enhances PKA activity, which leads to sperm motility activation. Slow events: increase in HCO_3^- and Ca^{2+} facilitates cholesterol efflux and PKA activation, which leads to increase in protein tyr phosphorylation, hyperactivated motility and acrosome reaction (image modified from Visconti, 2009).

Interestingly, the cAMP/PKA signalling pathway activation can be completely bypassed when mice spermatozoa are treated with Ca^{2+} ionophore, A23187 (Tateno et al, 2013). Treatment with A23187 in the presence of PKA inhibitor or in the absence of HCO_3^- induces acrosome-reacted and fertilisation-competent sperm cells and normal offspring (Tateno et al, 2013).

1.2.5 Hyperactivation

Accompanied by capacitation, mammalian sperm must undergo a change in its motility. It involves a transition from activated swimming state, characterised by linear and progressive trajectories caused by low-amplitude and symmetrical flagellar beating (Suarez et

al, 1983), to hyperactivated motility with an increase in the amplitude of the flagellar curvature (Yanagimachi, 1994; Ho et al, 2002). A full hyperactivated spermatozoon displays a vigorous and more powerful swimming pattern characterised by asymmetrical flagellar bends and high amplitude whip-like movements producing a non-progressive figure-of-eight pattern (Morales et al, 1988, Aitken and Nixon, 2013) (fig. 1.8).

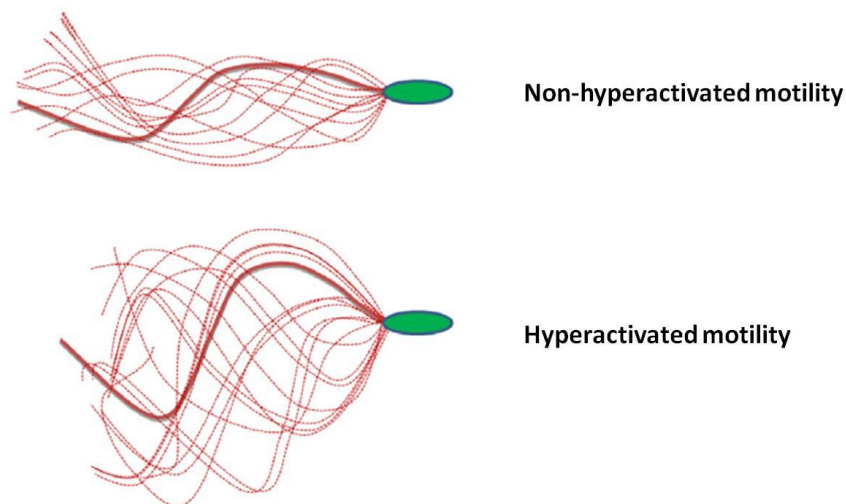


Figure 1.8 Comparison of hyperactivated and non-hyperactivated flagellar beat pattern. Non-hyperactivated sperm cell exhibits low-amplitude and symmetrical flagellar beating promoting linear and progressive trajectories while hyperactivated sperm cells shows increase in the amplitude of the flagellar curvature and asymmetrical whip-like flagellar beating inducing figure-of-eight pattern (image reproduced from Singh and Rajender, 2015).

Hyperactivated motility was first described by Ryuzo Yanagimachi (1969) while studying the effect of follicular fluid in hamster spermatozoa. He observed that sperm show vigorous movement as they penetrate the oocyte's zona pellucida. Over the years, scientists have been trying to determine how to define swimming patterns in sperm cells. The most accepted evaluation is through the use of computer-assisted sperm analysis (CASA), although this system is only able to track the head movements, indirectly assessing the flagellar bend amplitude. Mortimer and colleagues (1998) established that in human sperm the threshold values for hyperactivation movement measured by CASA should be: curvilinear velocity

(VCL) $\geq 150\mu\text{m/s}$, linearity (LIN) $<50\%$, amplitude of lateral head displacement (ALH) $\geq 7\mu\text{m}$. Also CASA allowed the identification of two types of hyperactivated motility in human spermatozoa: progressive hyperactivated (or transition phase) and non-progressive hyperactivated motility (star-pin phase) (Mortimer and Mortimer, 1990) (fig. 1.9).

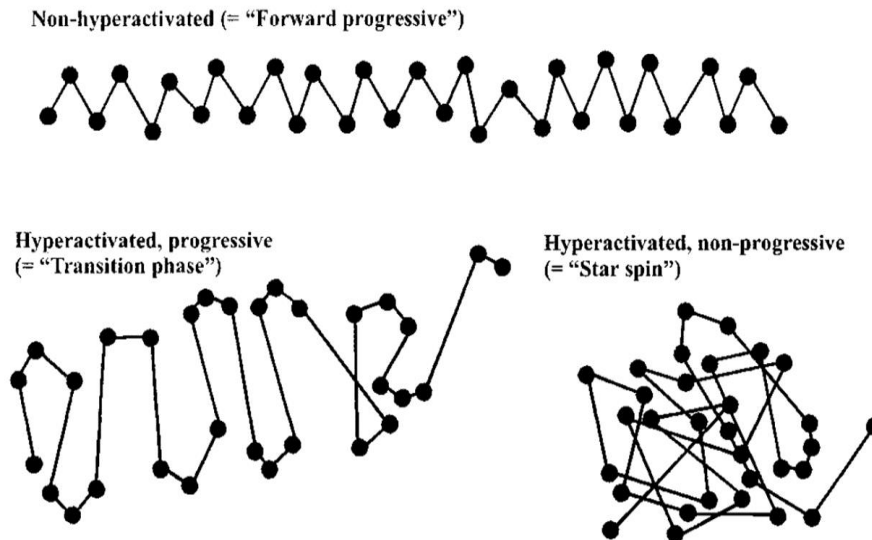


Figure 1.9 Different types of motility patterns in human spermatozoa. Non-hyperactivated spermatozoa exhibiting linear and progressive trajectory, with low ALH; Progressive hyperactivated (or transition phase); and non-progressive hyperactivated motility (star-pin phase), showing high ALH and VCL values, with low LIN (image reproduced from Mortimer, 2000).

It has been proposed that hyperactivation is required by sperm to assist progression up the oviduct (Stauss et al, 1995; Ho and Suarez, 2001; Quill et al, 2003), to facilitate sperm to detach from the oviductal epithelium (Demott and Suarez, 1992) and to provide the propulsive force necessary for penetrating the dense matrix of the zona pellucida (Rathi et al, 2001; Suarez, 2008) and finally interact and fuse with the egg plasma membrane (Darszon et al, 2011). However, the molecular basis of hyperactivation is still being elucidated. It is generally accepted that hyperactivation is a calcium-dependent phenomenon since it is

associated with an increase in cytoplasmic Ca^{2+} (Yanagimachi, 1988, 1994) and can be induced by treatment with Ca^{2+} ionophores, such as A23187 or ionomycin (Suarez et al, 1992; Marquez and Suarez, 2007). The main Ca^{2+} source for hyperactivated motility is from the extracellular environment and the sperm-specific flagellar CatSper channel has been suggested to regulate the influx of Ca^{2+} through the plasma membrane and, thereby, the swimming behaviour of spermatozoa (Kirichok et al, 2006; Chang and Suarez, 2011). In addition to extracellular Ca^{2+} , hyperactivation may also be achieved by release of calcium from internal stores, possibly the redundant nuclear envelope located at the base of the sperm flagellum (Ho and Suarez, 2003; Aitken and McLaughlin, 2007).

Hyperactivated motility has been considered as a part of capacitation however, the pathways leading to hyperactivation and acrosome reaction are not completely coupled. Hyperactivation can occur independently of acrosomal responsiveness in mouse and hamster sperm; therefore they seem to be separated processes (Neill and Olds-Clarke, 1987; Marquez and Suarez, 2004).

1.2.6 Sperm chemotaxis

Only few capacitated sperm cells are released from the isthmus sperm reservoir at one time and numbers of sperm in ampulla are low, such that guidance is crucial in order to guarantee the meeting between sperm and oocyte (Eisenbach and Giojalas, 2006). Several molecules identified in follicular fluid have been suggested as sperm attractants, such as N-formylated peptides (Iqbal et al, 1980), atrial natriuretic peptide (Zamir et al, 1993) and the female steroid hormone progesterone (Villanueva-Diaz et al, 1995).

In the female reproductive tract, the cumulus cell layer secretes progesterone at micromolar concentrations and forms a gradient from the interior to the margin in the surrounding area of the egg. Capacitated human spermatozoa are sensitive to picomolar concentrations of progesterone, inducing $[Ca^{2+}]_i$ increase and can modulate movement patterns (Teves et al, 2009; Lishko et al, 2011; Strünker et al, 2011). Human sperm cells have been reported to exhibit movement and flagellar beating oriented towards the source of the attractant. As hyperactivation may result in a change in the swimming direction and both sperm chemotaxis and hyperactivation require extracellular Ca^{2+} , it suggested that hyperactivation may be the mechanism responsible to the changing of swimming direction during chemotaxis (Armon and Eisenbach, 2011). However, with a raise in the chemoattractant concentration, turns and asymmetrical flagellar beating may be repressed, such that the cell swims in nearly straight line (Armon and Eisenbach, 2011) (fig. 1.10).

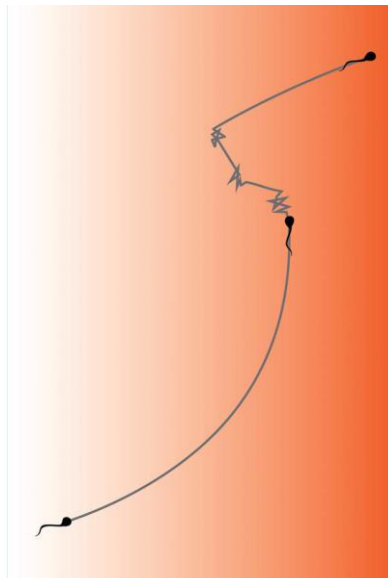


Figure 1.10 Model for behaviour of human spermatozoa in a chemoattractant gradient. Chemoattractant gradient concentration is shown as the different intensity of the background colour. In contact with the chemoattractant, sperm show bursts of highly asymmetrical flagellar beating consistent with hyperactivated motility. However, as the chemoattractant concentration increases hyperactivation is inhibited and sperm starts swim in a progressive and straight trajectory (image reproduced from Armon and Eisenbach, 2011).

1.2.7 Spermatozoa-Zona pellucida interaction

After penetrating the cumulus cells layer, sperm cells start interaction and binding to the zona pellucida (ZP). The ZP is secreted during oogenesis and consists of a porous glycoprotein matrix, which surrounds the oocyte. In human, the ZP comprises four sulfated glycoproteins: hZP1 (100 kDa), hZP2 (75 kDa), hZP3 (55 kDa) and hZP4 (65 kDa) (Bauskin et al, 1999; Lefièvre et al, 2004; Chiu et al, 2008; Gupta and Bhandari, 2011). Functions of the ZP include interaction between oocytes and follicle cells during oogenesis, species-specific fertilisation, prevention of polyspermy, induction of acrosomal exocytosis and protection of the embryo before implantation (Yanagimachi, 1994; Zhao and Dean, 2002; Hoodbhoy et al, 2005).

The classical model of spermatozoa–ZP interaction involves simple binding through a single receptor–ligand, followed by induction of acrosome reaction. However, recent studies reveal a more complicated process and a surprisingly a large number of sperm molecules may be involved in spermatozoa–ZP interaction (Gadella, 2008). The current suggestion is that the sperm ZP receptor is a structure involving multiple receptor molecules that together become a functional complex.

The binding of sperm to the ZP stimulates G-proteins, consequently increases the pH of the cytosol, and initiates a depolarisation of the plasma membrane which results in opening of CatSper channels (Florman et al, 1989; Xia and Ren, 2009). Influx of Ca^{2+} can induce additional release of Ca^{2+} from intracellular stores. This increase of Ca^{2+} in the cytosol mediates the phosphorylation of proteins and finally results in the acrosome reaction.

1.2.8 Acrosome reaction and sperm-egg fusion

The final step previous to fertilisation is the sperm acrosome reaction. The acrosome is a single Golgi-derived secretory granule located at the apical head of sperm, which contains hydrolytic enzymes. When the sperm cell encounters the cumulus cells layer or the zona pellucida, it undergoes a process called acrosome reaction (AR). AR involves fusion of the sperm plasma membrane with the outer membrane of the acrosome at multiple sites (fig 1.11), leading to the release of a variety of hydrolytic and proteolytic enzymes, which are vital for sperm penetration through the zona pellucida (Yanagimachi, 1994). AR is also important to promote the exposure of the inner acrosome membrane as a new cell surface membrane (Nolan and Hammerstedt, 1997; Jungnickel et al, 2001) and the equatorial segment in the sperm plasma membrane acquires ability to fuse with egg since proteins crucial to the fusion become exposed (fig. 1.11). These events are critical and necessary for fertilisation to occur.

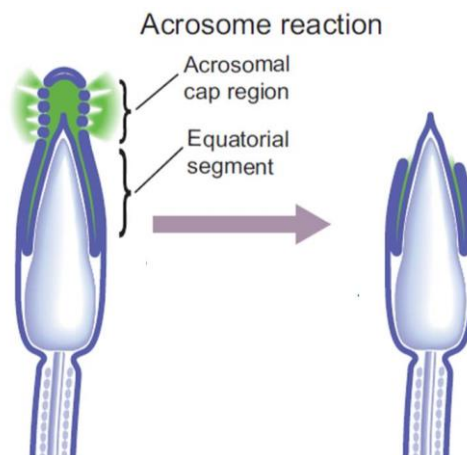


Figure 1.11 Diagram of acrosome reaction at the apical head of sperm cell. The outer and the inner acrosomal membrane fuse during acrosome reaction, leading to the release of hydrolytic and proteolytic enzymes. The acrosome exocytosis exposes a new cell surface domain in the sperm membrane, including proteins required to sperm-egg fusion at the equatorial segment (image reproduced from Okabe, 2013).

Zona pellucida glycoprotein ZP3 and progesterone secreted by the cumulus cells are recognised as physiological factors that are crucial to acrosome reaction and are associated to the oocyte (Osman et al, 1989; Suarez and Ho, 2003). Sperm interaction with the zona pellucida triggers a number of initial responses which are required in order to produce the sustained Ca^{2+} influx that leads to the acrosome reaction and progesterone is also able to stimulate a Ca^{2+} influx into spermatozoa through activation of CatSper (Darszon et al, 2011). The Ca^{2+} influx generates a large and rapid increase in intracellular Ca^{2+} concentration, appearing first at the principal piece then spreading throughout the head, and followed by a sustained increase of intracellular Ca^{2+} concentration. Extracellular calcium is required for $[\text{Ca}^{2+}]_i$ increase and for acrosome reaction achievement, but mobilisation of Ca^{2+} stored in cell organelles as acrosome or mitochondria is also important to the phenomenon (Florman et al, 1989; Blackmore et al, 1990).

More recently, Jin and co-workers (2011) have demonstrated that acrosome reaction is not necessarily triggered by the contact between sperm and the proteins in zona pellucida. Actually, most of mouse spermatozoa undergoes the acrosome reaction before contact with zona pellucida and are still capable to penetrate it and to bind and fuse with the oocyte. Further studies showed that fertilising mouse spermatozoa can start acrosome reaction even before progressing from the isthmus to the ampulla in the oviduct (Hino et al, 2016). Moreover, between acrosome-intact and acrosome-reacted sperm that penetrate the cumulus, the acrosome-reacted ones are more likely to reach the membrane of oocyte (Hino et al, 2016).

Only acrosome reacted spermatozoon can fuse with the oocyte plasma membrane. The acrosome exocytosis exposes the protein IZUMO1 at the equatorial segment in the sperm plasma membrane, which is essentially required for sperm-egg fusion (Inoue et al, 2005;

Satouh et al, 2012). The egg protein receptor that interacts directly with the sperm IZUMO1 was recently described as JUNO (Bianchi et al, 2014) (fig. 1.12).

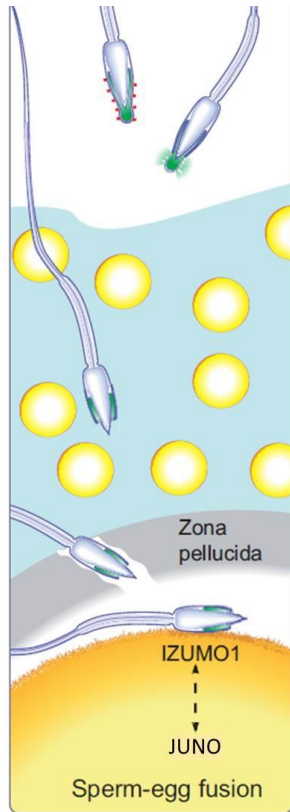


Figure 1.12 Diagram of acrosome reaction leading to sperm-egg fusion. Sperm cell penetrates the cumulus cells layer and ZP and then undergoes the acrosome reaction. Exposed IZUMO1 interacts with JUNO presented in the egg plasma membrane, promoting the sperm-egg fusion (image reproduced from Okabe, 2013).

1.3 Ion channels in sperm physiology

Ion channels are membrane proteins that operate as a pore mediating the selective transport of ions, such as K^+ , Na^+ and Ca^{2+} . The action of these proteins exploits ionic gradients generated by ion pumps across the cell, establishing membrane potential (V_m) and electrical currents, which are crucial to the modulation of several cell functions: such as

regulation of intracellular pH (pH_i), transcellular transport, cell volume, cell signalling pathways, enzymes activation/inactivation. In sperm cells, ion channels play an indispensable role in a variety of critical events in order to guarantee a successful fertilisation. Ion fluxes have been described on the regulation of sperm capacitation in the female reproductive tract, hyperactivated motility, chemotaxis and the acrosome reaction (Eisenbach, 1999; Visconti et al, 2002; Darszon et al, 2005). Sperm cell express a number of plasma membrane and intracellular ion channels, including the sperm exclusive channels CatSper for Ca^{2+} and Slo3 for K^+ (Ren et al, 2001; Carlson et al, 2003; Castellano et al, 2003; Darszon et al, 2006; Hernández-González et al, 2006; Navarro et al, 2007; Pinto et al, 2009; Xu et al, 2007; Lishko et al, 2010).

1.3.1 Sperm calcium-signalling components

The maintenance and regulation of intracellular calcium concentration ($[\text{Ca}^{2+}]_i$), is of great importance and is carried out by proteins and co-factors that import, export and sequester Ca^{2+} . Typically the concentration of Ca^{2+} in the cytoplasm is kept under 10^{-7} M while external Ca^{2+} concentration and Ca^{2+} concentration inside cellular organelles are higher and can vary between 10^{-4} and 10^{-3} M (Berridge, 2004). In spermatozoa, alteration in the intracellular Ca^{2+} concentration ($[\text{Ca}^{2+}]_i$) is a modulation mechanism of most fertilisation steps, especially in the swimming behaviour and flagellar beat pattern (Publicover et al, 2007; Costello et al, 2009).

Sperm cells exhibit a diversity of plasma membrane Ca^{2+} channels and also possess Ca^{2+} stores, such as the acrosomal vesicle and redundant nuclear envelope (RNE) in the neck of the sperm. The variety of plasma membrane Ca^{2+} channels localised in the sperm includes:

canonical transient receptor potential (TRPC) channels (Castellano et al, 2002, 2003; Trevino et al, 2001), voltage-gated Ca^{2+} channels (Carlson et al, 2005; Trevino et al, 2004; Wennemuth et al, 2000), cyclic nucleotide-gated Ca^{2+} channels (Wiesner et al, 1998) and the sperm-specific CatSper (Ren et al, 2001; Quill et al, 2003).

1.3.1.1 Canonical transient receptor potential (TRPC) channels

The TRPC is a subfamily of the transient receptor potential (TRP) channel superfamily, which is divided according to the structure of the protein motif. They are nonselective cation channels, being permeable to both monovalent and divalent cations and consist of a set of six transmembrane domains (TM1-TM6) and an additional hydrophobic pore region between TM5 and TM6 (Vannier et al, 1998). These channels are widely distributed in a diversity of cell types and are proposed to play role as store-operated and second messenger-operated channels, mainly by regulating Ca^{2+} signalling (Li et al, 2011).

In mammals, seven genes encoding TRPCs have been reported in both spermatogenic cells and mature spermatozoa (TRPC1-7) (Trevino et al, 2001; Jungnickel et al, 2001; Castellano et al, 2003; Nilius et al, 2007). Several studies are being made to understand the TRPCs contribution for sperm physiology and fertilisation process. TRPC1 has been identified exclusively in the sperm flagellum and may be involved in the sperm activation process (Nilius et al, 2007). On the other hand, TRPC2 has been suggested to play a role in the ZP3-sperm interaction and consequently on the mediation of Ca^{2+} influx during acrosome reaction (Jungnickel et al, 2001). TRPC3 has also been reported on the sperm flagellum and associated with sperm capacitation and sperm motility (Castellano et al, 2003; Ru et al, 2015). TRPC4 has also been detected in the sperm flagellum, suggesting a role in sperm motility

(Castellano et al, 2003). Just recently a specific antibody for TRPC5 was developed and Zhu and colleagues (2018) reported that TRPC5 levels are positively correlated with sperm motility and superoxide dismutase (SOD) activity. TRPC6 has been identified in both acrosomal region and sperm flagellum and may be required to sperm activation and acrosome reaction (Castellano et al, 2003).

1.3.1.2 Voltage-gated Ca^{2+} channels (CaV)

Voltage-gated Ca^{2+} (CaV) channels are transmembrane proteins sensitive to changes in membrane potential (V_m), mediating Ca^{2+} influx to the cell cytoplasm. CaVs have been classified according to their electrophysiological and pharmacological properties, mainly on the level of membrane depolarisation required for their activation: high voltage-activated (HVA), which includes L-, N-, P/Q-, and R-types currents, and low voltage-activated (LVA) channels, T-type currents (Reuter, 1983; Nilius et al, 1985). The molecular structure of CaVs consists in a pore-forming $\alpha 1$ subunit, an intracellular β subunit, a single transmembrane $\alpha 2/\delta$ subunit and several membrane-spanning γ domain (Catterall, 1995, Walker and De Waard, 1998; Canti et al, 2003). CaVs can also be grouped in three subfamilies according to the genes encoding the $\alpha 1$ domain: CaV1, CaV2 and CaV3. CaV1 conducts L-type currents and has four members (CaV1.1–CaV1.4); CaV2 conducting P/Q-type currents (CaV2.1), N-type currents (CaV2.2) and R-type currents (CaV2.3); and CaV3 conducting only T-type currents (CaV3.1–CaV3.3) (Catterall, 2000; Ertel et al, 2000; Burgess et al, 2001).

In mammals, CaV channels activity has been identified in both spermatogenic cells and mature spermatozoa (Arnoult et al, 1996, 1999; Lievano et al, 1996; Wennemuth et al, 2000; Jagannathan et al, 2002a, 2002b). Subunits of CaV1.2, CaV2.1 and CaV2.3 were

detected on the midpiece of the sperm flagellum (Westenbroek and Babcock, 1999). Subunits of the three members of CaV3 channel (T-type currents) were localised in both midpiece and principal piece of flagellum and as well as the head (Trevino et al, 2004; Darszon et al, 2006). These findings led to the believe that CaVs were the main channels regulating Ca²⁺ signals in the mature sperm cell and that they would play a crucial key role in the acrosome reaction process (Florman et al, 1998; Darszon et al, 1999, 2006; Publicover and Barratt, 1999). However, a variety of studies showed that gene knockout had no effect on spermatogenesis or male infertility in mice: CaV1.3 (Platzer et al, 2000), CaV2.2 (Ino et al, 2001), CaV2.3 (Saegusa et al, 2000; Sakata et al, 2002), CaV3.1 (Kim et al, 2001; Escoffier et al, 2007), CaV3.2 (Chen et al, 2003; Escoffier et al, 2007).

1.3.1.3 Cyclic nucleotide-gated Ca²⁺ channels (CNG)

Cyclic nucleotide-gated Ca²⁺ (CNG) channel is part of a heterogenous superfamily of ion channels which consists of six membrane-spanning segments (S1–S6), a pore domain localised between S5 and S6 and a single cyclic nucleotide-binding site for 3',5'-cyclic monophosphates (cNMPs) next to the COOH-terminal region of the protein (Kaupp, 1995; Kaupp and Seifert 2002; Brown et al, 2006). CNGs are nonselective channels that are activated by both cAMP and cGMP binding, are weakly voltage sensitive and mediate the influx of divalent cations, mainly Ca²⁺ (Brown et al, 2006; Mazzolini et al, 2010).

The first sperm ion channel cloned and described was a CNG channel from mouse testis (Weyand et al, 1994). In mammals, the CNG channels are classified in two subfamilies according to the genes encoded: CNGA and CNGB. Kaupp and Seifert (2002) demonstrated the expression of A3, B1 and B3 CNGs subunits in testis. As well as TRPCs and CaVs

channels, CNG channels expression has also been reported in both spermatogenic cells and mature sperm (Weyand et al, 1994; Wiesner et al, 1998). CNGA3 and CNGB1 has been localised within the sperm flagellum by several studies (Wiesner et al, 1998; Kaupp and Seifert, 2002; Carlson et al, 2003), which suggested a role in the modulation of sperm motility. In marine invertebrates, cGMP signalling pathway has been shown to regulate Ca^{2+} influx and CNGs play a role in sperm chemotaxis (Kaupp et al, 2003; Strünker et al, 2006; Darszon et al, 2008; Kaupp et al, 2008). However, Brenker and colleagues (2012) reported that cyclic nucleotides, in fact, does not increase $[\text{Ca}^{2+}]_i$ in mouse and human spermatozoa and the activation of ion channels by ligand is actually due to its action on CatSper channels and not on CNGs.

1.3.1.4 CatSper channels

Between all types of Ca^{2+} channels present on the sperm plasma membrane, only the sperm-specific channel CatSper has been shown to be critical for a successful fertilisation and for male fertility (Ren et al, 2001; Quill et al, 2003). Several studies have shown that sperm from mutant mice, which could not express CatSper proteins, failed to switch from progressive motility to hyperactivated motility and also failed to penetrate the zona pellucida of oocytes preventing fertilisation. However, those sperm were not immotile as they exhibited progressive motility and could undergo acrosome reaction (Ren et al, 2001; Quill et al, 2003; Jin et al, 2007; Qi et al, 2007).

CatSper channels are constituted of multiple proteins. Proteins that compose the pore complex includes CatSper 1-4 proteins, containing six transmembrane segments, with a voltage-sensor S4 domain and a Ca^{2+} selective pore region (Ren et al, 2001; Quill et al, 2003;

Lobley et al, 2003; Qi et al, 2007; Navarro et al, 2008; Kirichok and Lishko, 2011). In addition to the subunits CatSper 1-4, CatSper is also associated with the auxiliary proteins CatSper β , CatSper γ , and CatSper δ (Liu et al, 2007; Wang et al, 2009; Chung et al, 2011; Lishko et al, 2012), which can regulate channel activity. CatSper proteins are strictly localised on the plasma membrane of the sperm principal piece of the flagellum (Ren et al, 2001; Carlson et al, 2005; Jin et al, 2007) (fig. 1.13). Recently, Chung and colleagues (2017) reported two more genes, Gm7068 and Tex40, which encode new accessory proteins in the CatSper channel complex: CatSper ϵ and CatSper ζ . These newly identified accessory proteins are believed to be relevant to hyperactivation and fertilising ability (Chung et al, 2017).

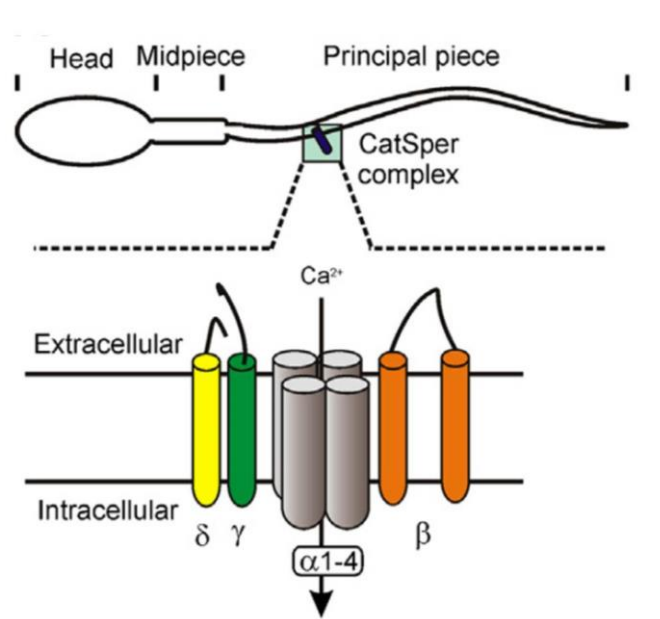


Figure 1.13 Classic schematic representation of CatSper localisation and composition in human sperm. Catsper is localised in the principal piece of flagellum and is composed of four pore-forming subunits (CatSper 1-4 proteins) and auxiliary proteins CatSper β , CatSper γ , and CatSper δ (image reproduced from Cai et al, 2015).

CatSper are sensitive to increasing of intracellular pH, are voltage-dependent and can be stimulated by progesterone, prostaglandins and other ligands (Ren et al, 2001; Quill et al, 2001; Kirichok et al, 2006; Navarro et al, 2008; Lishko et al, 2011; Strünker et al, 2011; Brenker et al, 2012). Together membrane potential, pH_i , and progesterone work collectively to regulate Ca^{2+} influx into spermatozoa, a process that is critical for proper sperm function and successful fertilisation (Ren et al, 2001; Quill et al, 2003; Carlson et al, 2003, 2005; Qi et al, 2007; Xia et al, 2007). CatSper channels are the primary source of Ca^{2+} flux into the cytosol necessary for sperm to ascend beyond the oviductal reservoir (Ho et al, 2009), for hyperactivation (Kirichok et al, 2006) and are required for sperm penetration in the zona pellucida surrounded the oocyte (Ren et al, 2001; Quill et al, 2003).

The $[\text{Ca}^{2+}]_i$ changes promoted by CaSper activation are not limited to the initial region in the principal piece of the flagellum but propagates through the sperm midpiece and head within a few seconds. The suggested model is that Ca^{2+} from the flagellum diffuses forward, raising $[\text{Ca}^{2+}]_i$ at the sperm neck and can mobilise stored Ca^{2+} by Ca^{2+} -induced Ca^{2+} release (CICR) (Correia et al, 2015) (fig. 1.14).

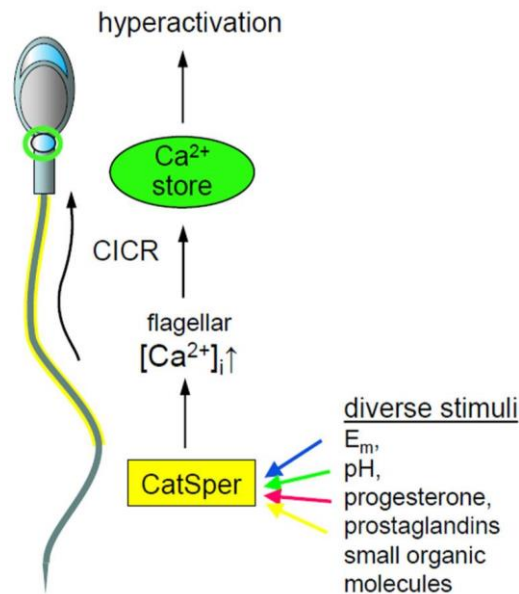


Figure 1.14 Model for $[Ca^{2+}]_i$ change propagation triggered by activation of CatSper. CatSper activation occurs by different stimuli and leads to influx of Ca^{2+} . Consequent increase in $[Ca^{2+}]_i$ diffuses from the flagellum to the sperm neck, stimulating mobilisation of stored Ca^{2+} by Ca^{2+} -induced Ca^{2+} release (CICR) (modified from Correia et al, 2015).

1.3.1.5 Mobilisation of Ca^{2+} from intracellular stores

As sperm cells do not have an endoplasmic reticulum (ER), which is the main Ca^{2+} storage organelle in somatic cells, other membranous structures may act as releasable Ca^{2+} stores, such as the acrosome (surrounding the anterior nucleus), mitochondria (in the midpiece) and some irregular membranous structures (in the neck), also called redundant nuclear envelope (RNE) (Costello et al, 2009, Correia et al, 2015). Inositol trisphosphate receptors (IP3Rs), ryanodine receptors (RyRs) and Ca^{2+} -ATPases have been localised on the acrosome and the mid-piece of human sperm cells (Ho and Suarez, 2001, 2003; Naaby-Hansen et al, 2001; Harper et al, 2004; Park et al, 2011) and are crucial for the mediation of

Ca²⁺ release from the stores and, therefore, for the regulation of several physiological processes on the spermatozoa (fig. 1.15).

Inositol trisphosphate receptors (IP3Rs): are activated by the second messenger inositol 1,4,5-trisphosphate (IP3), which is the product of the phosphatidylinositol-4,5-bisphosphate (PIP2) hydrolysis. The opening of these channels, by the binding of IP3 in the site located N-terminus, releases Ca²⁺ from the stores into the cytoplasm (Bezprozvanny et al, 1991; Seo et al, 2012). IP3Rs have been reported in sperm cells of a variety of mammals and are localised in the acrosomal vesicle and also in redundant nuclear envelope (RNE), suggesting their involvement with the acrosome reaction (Dragileva et al, 1999; Kuroda et al, 1999; Naaby-Hansen et al, 2001; Ho and Suarez, 2001; 2003; Jimenez-Gonzalez et al, 2006).

Ryanodine receptors (RyRs): are activated by the second messengers cyclic adenosine diphosphate ribose (cADPR) and nicotinic acid-adenine dinucleotide phosphate (NAADP) (Billington et al, 2006; Jimenez-Gonzalez et al, 2006; Ogunbayo et al, 2011), which are both products of the action of ADP-ribosyl cyclase enzymes, such as CD38 (Cosker et al, 2010). Activation of RyRs can also occur by the increase of Ca²⁺ concentration in the cytoplasm, triggering Ca²⁺ induced Ca²⁺ release (CICR) mechanisms (Bedu-Addo, 2008; Darszon et al, 2011). RyRs isoforms have been detected in mammalian spermatogenic cells, as well as in mature spermatozoa (Giannini et al, 1995; Treviño et al, 1998). So far, RyRs have been localised in the acrosome-intact and acrosome-reacted sperm cell, in the posterior head/neck (PHN) region and also in the neck (Treviño et al, 1998; Harper et al, 2004; Park et al, 2011).

Store-operated Ca^{2+} channels (SOCs): are activated in response of an initial release of Ca^{2+} from stores, leading to an influx of extracellular Ca^{2+} via plasma membrane (Putney, 1986). This process is important to keep a sustained Ca^{2+} signal in the cytoplasm and also to provide Ca^{2+} in order to refill the stores (Jimenez-Gonzalez et al, 2006; Correia et al, 2015). The proteins involved in the SOC mechanism are still being elucidated; so far it has been reported the participation of STIM1 (stromal interaction molecule), which acts as a Ca^{2+} store sensor to detect the luminal Ca^{2+} concentration. In a Ca^{2+} depletion situation, STIM1 changes its conformation leading to the consequently activation of Orai, which forms a Ca^{2+} -permeable membrane channel (Strange et al, 2007; Wang et al, 2008; Lefievre et al, 2012). SOC constitution may also involve TRPC channel members that could interact with STIM1 and Orai complex (Abramowitz and Birnbaumer, 2009; Cahalan, 2009; Kim et al, 2009; Feng et al, 2010). In sperm cells, these proteins (STIM1, Orai and TRPC) have all been detected and are localised predominantly on the neck and the acrosome region (Castellano et al, 2003; Darszon et al, 2012; Lefievre et al, 2012). SOC are being believed to play a role in the acrosome reaction: IP_3 generation mobilises Ca^{2+} from intracellular stores, mainly acrosome, promoting an increase in $[\text{Ca}^{2+}]_i$ and a subsequent activation of SOC mechanism. Sustained Ca^{2+} influx then results in the acrosome reaction (Florman, 1994; O'Toole et al, 2000; Breitbart, 2002; Fukami et al, 2003).

Ca^{2+} -ATPases: in order to maintain the resting Ca^{2+} intracellular level and to promote the refilling of the Ca^{2+} stores, the cell exhibits a variety of Ca^{2+} pumps driven by the hydrolysis of ATP and also Ca^{2+} exchangers (co-transporters). In sperm cells, the Ca^{2+} pumps consist of plasma membrane calcium ATPase (PMCA), sarcoplasmic-endoplasmic reticulum Ca^{2+} ATPase (SERCA) and the secretory pathway Ca^{2+} ATPase (SPCA) (Jimenez-Gonzalez et al,

2006; Bedu-Addo, 2008; Michelangeli and East, 2011). PMCAs have been detected in the head of sea urchin sperm cells (Gunaratne and Vacquier, 2005) and may regulate acrosome reaction in invertebrates. However, in mammalian sperm cells, these pumps are located exclusively in the principal piece of the flagellum and are associated with the modulation of motility, hyperactivation and male fertility. PMCA4 knockout mice are infertile and show impaired motility (Okunade et al, 2004; Schuh et al, 2004; Jimenez-Gonzalez et al, 2006). SERCA was identified in the acrosome and mid piece of several mammalian spermatozoa, including human, suggesting that they contribute with the Ca^{2+} homeostasis after mobilisation from the stores (Rossato et al, 2001; Lawson et al, 2007). SPCAs, specifically the isoform SPCA1, have been detected restricted to the posterior head and midpiece region in human spermatozoa and in the midpiece (on the single mitochondrion) in sea urchins sperm cells (Wootton et al, 2004; Harper et al, 2005; Harper and Publicover, 2005; Gunaratne and Vacquier, 2005). SPCA may also interact with Orai Ca^{2+} channel, suggesting its role on the refilling of Ca^{2+} stores (Feng et al, 2010).

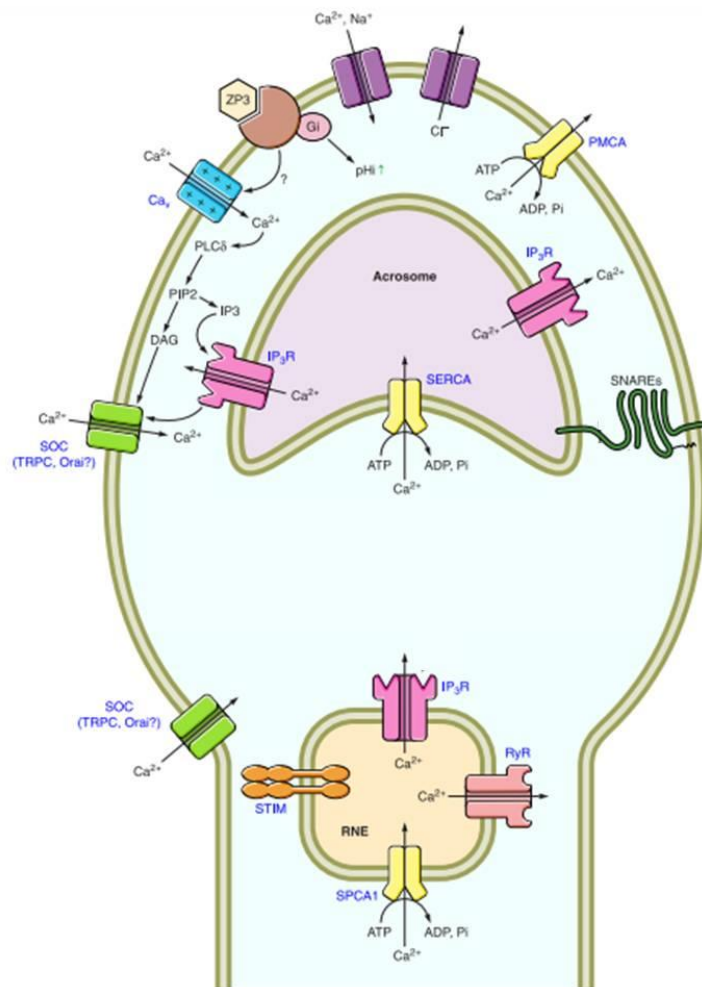


Figure 1.15 Schematic diagram of Ca^{2+} signalling components involved on mobilisation of Ca^{2+} from intracellular stores. Mobilisation from acrosome is mainly due to activation of IP3Rs by the binding of IP3, product of PIP2 hydrolysis on the plasma membrane. On the other hand, mobilisation from the RNE involves opening of both IP3Rs and RyRs. Release of Ca^{2+} from stores, promotes the activation of SOCs responsible for the sustained $[\text{Ca}^{2+}]_i$ increase. This mechanism involves STIM and possibly Orai and TRPC channels. The refilling of stores is mediated mainly by SERCA channels (in the acrosome) and SPCA1 in the RNE. PMCA, in the plasma membrane, contribute to keep Ca^{2+} homeostasis (image modified from Darszon et al, 2011).

1.3.2 Potassium (K^+) channels (Slo3)

Potassium (K^+) channels are membrane proteins that mediate the flow of K^+ ions, generating an electrical gradient and setting the resting membrane potential (V_m) in many cell

types. K^+ channels are classified in four groups according to its activation or conductive characteristics: voltage-gated K^+ channels (sensitive to changes on V_m), ion-activated K^+ channels (sensitive to Ca^{2+} and others second messengers), inwardly rectifying K^+ channels (allows current more easily in the inward direction), and tandem pore domain K^+ channels (constitutively opened or with high basal activation) (Hodgkin and Keynes 1955; Doyle et al, 1998; Coetzee et al, 1999; Hibino et al, 2010; Kim and Nimigean, 2016). Several studies have demonstrated the occurrence of several types of K^+ channels in both spermatogenic cells and spermatozoa (Wu et al, 1998; Felix et al, 2002; Navarro et al, 2007; Martinez-Lopez et al, 2009; Santi et al, 2010). However, the only K^+ current that was shown to be expressed in sperm, potentially setting resting membrane potential is a pH-sensitive K^+ current, originally named $I_{K_{Sper}}$ (Navarro et al, 2007) and now identified to be carried by an exclusive sperm-specific K^+ channel, the Slo3 (Santi et al, 2010; Zeng et al, 2011). Slo3 molecular structure consists in seven transmembrane helices (S0–S6), that function as a voltage sensor, and a large cytoplasmic C-terminal domain that forms a structure called “gating ring”, which is involved in the pH-sensitivity of Slo3 (Xia et al, 2004; Leonetti et al, 2012) (fig. 1.16).

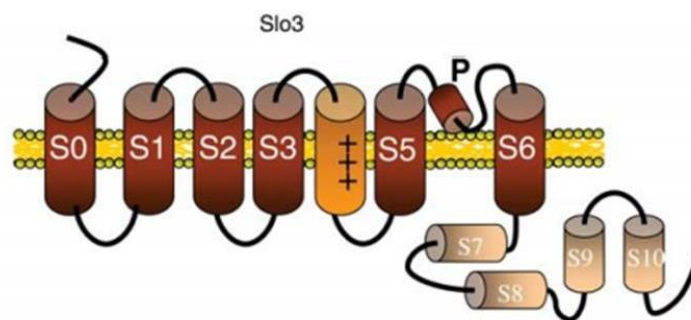


Figure 1.16 Molecular architecture of sperm Slo3 channel. Predicted membrane topology of Slo3 channel exhibiting seven transmembrane helices (S0–S6) and a large intracellular C-terminal domain, probably associated to its pH sensitiveness (image reproduced from Kirichok and Lishko, 2011).

Similarly to CatSper channels, Slo3 channels are voltage-gated, activated by intracellular alkalinisation and are localised in the principal piece of the sperm flagellum (Navarro et al, 2007). Recently, Brenker and co-workers (2014) showed that Slo3, in human sperm, can also be activated by Ca^{2+} , suggesting a potential interplay between this channel and CatSper: during progesterone response, CatSper opens leading to an increase in $[\text{Ca}^{2+}]_i$, which can activate Slo3. It has been demonstrated that Slo3 are important to sperm physiology and critical steps of the fertilisation, such as sperm osmoregulation, acrosomal exocytosis and sperm motility (Santi et al, 2010; Tang et al, 2010; Zeng et al, 2011).

1.3.3 Chloride (Cl^-) transporters

The anion chloride (Cl^-) can be transported through a variety of systems across the biological membranes, including Cl^- channels and specialised Cl^- carriers (Jentsch et al, 2005; Nilius and Droogmans, 2003). The Cl^- channels are identified in four different families according to structure: CLC channels, CFTR channels, γ -aminobutyric (GABA)-gated and related glycine-gated neurotransmitter receptors and Ca^{2+} -activated Cl^- channels (CaCC). The Cl^- carrier proteins consist of $\text{Cl}^-/\text{HCO}_3^-$ exchangers and electroneutral cation-chloride cotransporters. Cl^- transporters in sperm cells was described by Hogg et al (1994) and Espinosa et al (1998), who showed the presence of an anion channel in epididymal mouse sperm compatible with the Ca^{2+} -activated Cl^- channels (CaCC). Later, the occurrence of CaCCs was also reported in human spermatozoa (Orta et al, 2012). CLC channel, more specifically CLCN3, was observed in the sperm flagellum (Yeung et al, 2005). CFTRs have been detected in both human and mouse spermatozoa by different laboratories (Chan et al,

2006; Hernandez-Gonzalez et al, 2007; Li et al, 2010; Xu et al, 2007). The contribution of Cl^- transporters has been described in sperm physiology, capacitation process, motility and also during the acrosome reaction. In sperm cells, Cl^- is shown to be important to the cell volume modulation and osmotic stress protection (Furst et al, 2002; Yeung et al, 2005; Cooper and Yeung, 2007). Several studies reported that the intracellular concentration of Cl^- increases during capacitation (Meizel and Turner, 1996; Hernandez-Gonzalez et al, 2007), suggesting the participation of Cl^- transporters. Capacitation and most of its associated processes, such as increase in tyrosine phosphorylation, in cAMP levels, hyperactivated motility and acrosome reaction, are inhibited when mouse or human spermatozoa are incubated in media with Cl^- concentrations lowered or absent (Hernandez-Gonzalez et al, 2007; Wertheimer et al, 2008; Chen et al, 2009; Orta et al, 2012; Figueiras-Fierro et al, 2013). Additionally, CFTR mutations have been associated with male infertility in patients (Popli and Stewart, 2007).

1.3.4 Voltage-gated proton channel (Hv1)

Voltage-gated proton channels (Hv) are membrane proteins that selectively mediate the flow of protons (H^+) across cell membranes and regulate intracellular alkalinisation. Critical steps of fertilisation appear to be modulated by intracellular $[\text{H}^+]$ signalling, such as sperm capacitation, initiation of motility, hyperactivation, chemotaxis and also the acrosome reaction. Human sperm cells exhibit a large voltage-gated H^+ current and expression of Hv1 proteins in the flagellum, which suggests a major role for these channels in regulation of pH_i (Lishko et al, 2010). Hv1 is constituted by four transmembrane domains and functions as a dimer in the plasma membrane (Ramsey et al, 2006; Sasaki et al, 2006), each subunit acts as

an independent H⁺ channel (Koch et al, 2008; Lee et al, 2008; Tombola et al, 2008). Furthermore, Hv1 is activated by membrane depolarisation and shows slow kinetics of activation and deactivation, conducting outward rectified current (Ramsey et al, 2006; Sasaki et al, 2006; DeCoursey, 2010). Since Hv1 channels are located in the principal piece of the spermatozoa flagellum colocalised with CatSper channels, which are sensitive to alkalinisation, it has been suggested that participates in the regulation of sperm motility due to its possible indirect action on CatSper (Lishko et al, 2010). As Hv1 currents are not detected in mouse (Lishko et al, 2010), it has not been possible to study the fertility levels on null mutants.

Research aims

Ca^{2+} signalling is crucial for most fertilisation steps in human spermatozoa, especially for the swimming behaviour and flagellar beat pattern. The aim of this thesis was to further characterise the Ca^{2+} responses generated by progesterone, eliciting whether and how they contribute to sperm behaviour in human spermatozoa and sperm penetration ability into viscous medium. To address our research aims, we propose the following specific aims:

- (1) What are the Ca^{2+} responses promoted by progesterone in human sperm population? What are the characteristics of progesterone-induced $[\text{Ca}^{2+}]_i$ oscillations in human spermatozoa? Does membrane potential (V_m) regulate progesterone-induced $[\text{Ca}^{2+}]_i$ oscillations generation? – chapter 3.
- (2) Is RU1968, originally described as a sigma ligand, a potent pharmacological tool to investigate Ca^{2+} CatSper channel activity? Does RU1968 inhibit the CatSper-dependent $[\text{Ca}^{2+}]_i$ increase induced by progesterone? – chapter 4.
- (3) What is the molecular mechanism involved on the generation of progesterone-induced $[\text{Ca}^{2+}]_i$ oscillations? – chapter 5.
- (4) Does SKF-96365, a classic SOCE inhibitor, modulate $[\text{Ca}^{2+}]_i$ oscillations generation? – chapter 6.
- (5) Are progesterone-induced $[\text{Ca}^{2+}]_i$ oscillations associated with switching of sperm behaviour and sperm ability to penetrate viscous medium? Does CatSper channels activity contribute to these events? – chapter 7.

CHAPTER TWO: MATERIALS & METHODS

2.1 Chemicals

Progesterone [4-pregnene-3, 20-dione], valinomycin, niflumic acid, CFTR(inh-172), quinidine, salts for the preparation of supplemented Earle's balanced salt solution (sEBSS) and Cl⁻ free medium, methylcellulose, dimethylsulphoxide (DMSO), ethylene glycol-bis(β -aminoethyl ether)-N,N,N',N'-tetraacetic acid (EGTA) and HEPES were all obtained from Sigma-Aldrich, Poole, UK; Fluo4-AM and Pluronic F-127 (20% dilution DMSO) from Invitrogen - Molecular Probes, Cambridge Bioscience, UK; pH buffer tablets of pH 9.2 and 4 for calibrating the pH meter were from Fisher scientific, UK. Poly-D-lysine from BD – Biosciences, Bedford, UK; bovine serum albumin (BSA) from United States Biological, Swampscott, USA; SKF 96365 from Calbiochem, San Diego, USA; CristaSeal wax from Hawksley, Oxford, UK; and RU1968-F1 courtesy from Timo Strunker's lab team.

2.2 Media preparation

The standard medium used in the experiments was supplemented Earle's balanced salt solution (sEBSS). sEBSS consists in NaCl (116.4 mM), KCl (5.4 mM), CaCl₂ (1.8 mM), MgCl₂ (1 mM), glucose (5.5 mM), NaHCO₃ (25 mM), Na pyruvate (2.5 mM), Na lactate (19 mM), MgSO₄ (0.81 mM), HEPES (15 mM) and 0.3% bovine serum albumin (BSA). The pH was adjusted to 7.4 and osmolarity to 285 – 295 mOsm.

A high 100 mM K⁺ medium was prepared as a modified sEBSS, where concentration of KCl was increased from 5.4 mM to 100 mM and NaCl was decreased in the same

proportion: from 116.4 mM to 21.8 mM in order to keep the osmolarity at 285 – 295 mOsm. The same principle was used to prepare 25 mM K⁺ medium (25 mM KCl and 96.8 NaCl). To prepare a nominally Cl⁻ free medium, NaCl and KCl were replaced by sodium gluconate (NaC₆H₁₁O₇) and potassium gluconate (C₆H₁₁KO₇), respectively. To prepare a nominally Ca²⁺ free medium, CaCl₂ (1.8 mM) was omitted from the sEBSS recipe and replaced by NaCl.

2.3 Donor recruitment

Semen samples were provided by healthy research donors in accordance with the Human Fertilisation and Embryology Authority Code of Practice (University of Birmingham Life and Health Sciences ERC-07-009 and ERN-12-0570). Donors gave informed consent and samples were analysed according to criteria set by the World Health Organisation guidelines (Cooper et al, 2010). Different donors were used in the triplicates of each experiment.

2.4 Preparation and capacitation of spermatozoa

Semen was provided by masturbation after 2–3 days of sexual abstinence. The sample was kept in incubator (36 °C, 5.5% CO₂) for 30 minutes to liquefy and then prepared by swim-up. 200 μL aliquots of semen were gently layered beneath 1 ml of sEBSS (supplemented Earle's balanced salt solution) + 0.3% BSA. Tubes were incubated for 1 hour (36 °C, 5.5% CO₂) at an angle of 45° - to create maximum surface area for cells to swim up (fig. 2.1). The upper 0.7 ml containing the motile spermatozoa portion was collected and the cell concentration was assessed in Neubauer counting chamber (0.1 mm depth) under a Nikon

eclipse TS 100 microscope. The cell concentration was adjusted to 3×10^6 in aliquots of 100 μL and cells were left to capacitate for 4-5 hours in incubator (36°C , 5.5% CO_2).

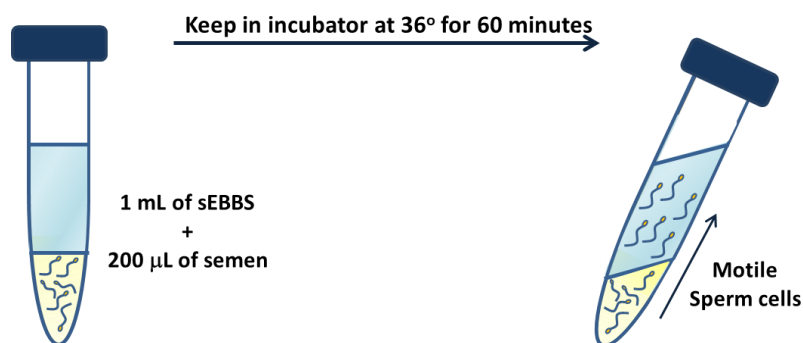


Figure 2.1 Schematic representation of the swim-up technique. 200 μL aliquots of semen is added in 1 mL of sEBSS (supplemented Earle's balanced salt solution) + 0.3% BSA (bovine serum albumin) and then incubated (36°C , 5.5% CO_2) at an angle of 45° for 60 minutes in order to separate the motile sperm portion from the fluid components and debris.

2.5 Single-cell imaging of $[\text{Ca}^{2+}]_i$ in immobilised sperm

Cell concentration was adjusted to 1.5×10^6 in aliquots of 200 μL and incubated with 5 μM of fluo4-AM for 30 minutes (36°C , 5.5% CO_2). Cells were then transferred to an imaging chamber, the base of which was a coverslip coated with 0.001% poly-D-lysine and incubated for an additional 5 minutes to allow cells to settle. The chamber was installed on the stage of an inverted fluorescence microscope (Nikon TE300) connected to the perfusion apparatus and perfused with fresh medium to remove unattached cells and excess dye. All experiments were performed at 25°C in a continuous flow of sEBSS, with a perfusion rate of 0.6 ml/minute. Time-lapse fluorescence imaging was performed with an Andor Ixon 897E cooled EMCCD camera controlled by Andor iQ3 software (Andor Technology, Belfast, UK).

Fluorescence excitation was at 485 nm and emission at 520 nm. Images were obtained at 0.2, or 2.5 Hz using a 40x or a 60x oil objective. An initial control period was recorded (at least 3 minutes) with sEBSS only before application of any stimuli.

Analysis of images and background correction was processed using iQ3 software. Regions of interest (ROI) were drawn typically around the head and neck of each sperm cell (or in three different regions of the sperm cell, head, neck and flagellum, when stated) and the average intensity was obtained for each and plotted against time (fig. 2.2).

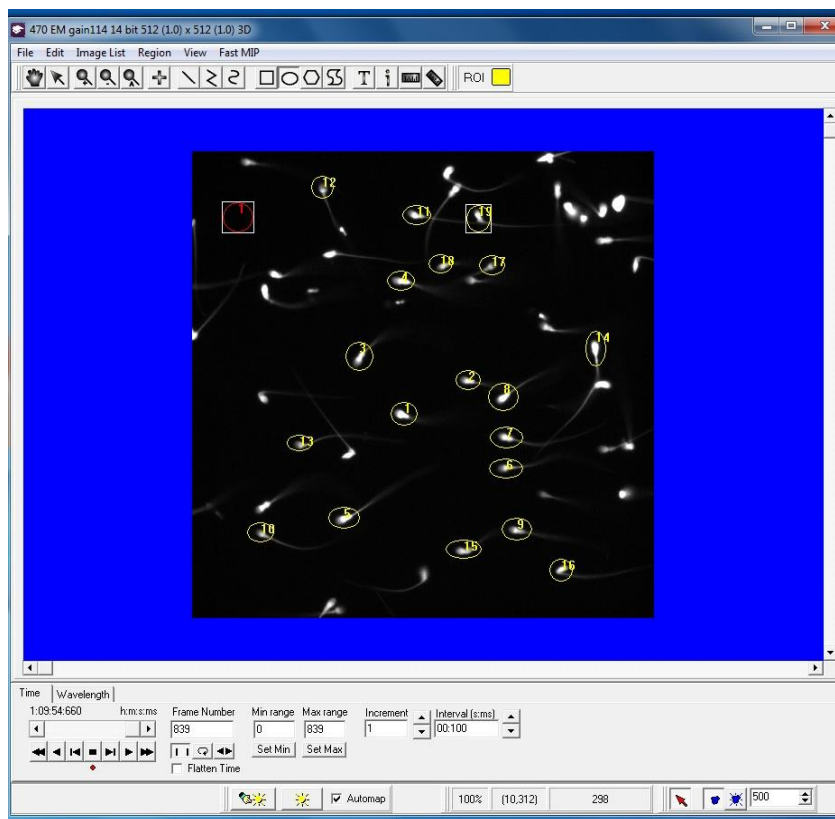


Figure 2.2 Screenshot of iQ3 software showing the regions of interest (ROI). The entire head and neck of each sperm cell (yellow circles) was considered for fluorescence analysis.

After background correction, raw intensity values were imported into Microsoft Excel and normalised using the equation from (Nash et al, 2010):

$$R = [(F - F_{\text{basal}}) / F_{\text{basal}}] \times 100\%$$

R = normalised fluorescence intensity

F = fluorescence intensity at time t

F_{basal} = mean of values of F during the control period (perfusion with sEBSS only)

2.6 $[\text{Ca}^{2+}]_i$ oscillation analysis

$[\text{Ca}^{2+}]_i$ oscillations induced by progesterone stimulation were analysed for their amplitude and frequency. In each cell the amplitude of oscillations was normalised to the amplitude of the initial progesterone-induced transient (considered as 100%). Oscillation amplitude was calculated as the difference between the highest point at the peak ('a' in fig 2.3) and the mean of the points preceding the signal rise ('b' in fig 2.3). $[\text{Ca}^{2+}]_i$ 'ripples' with amplitude > 20% of the initial transient peak amplitude were not considered oscillations. The frequency of $[\text{Ca}^{2+}]_i$ oscillations was assessed by dividing the number of $[\text{Ca}^{2+}]_i$ oscillation cycles by the period of measurement (fig. 2.3).

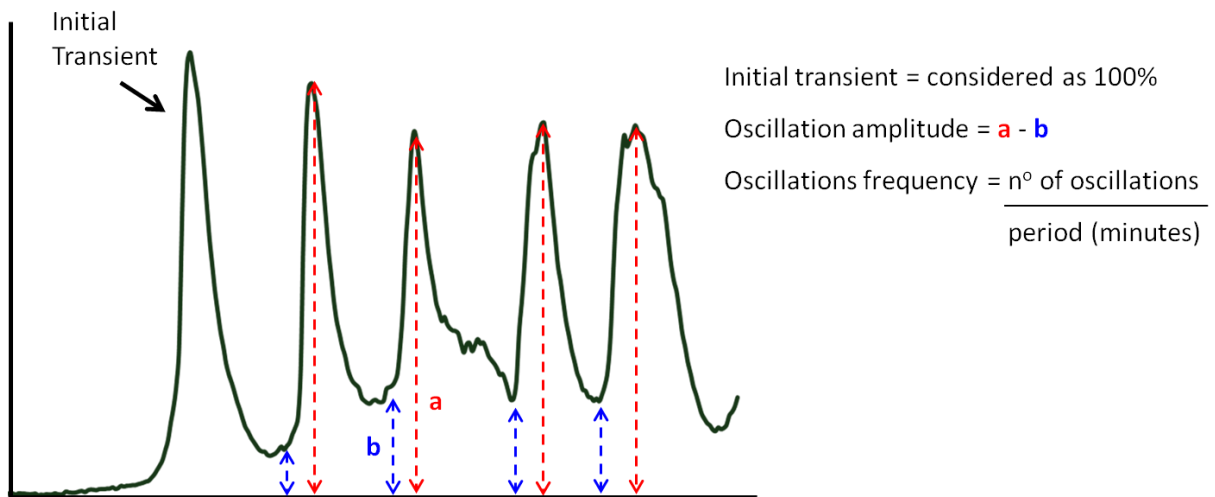


Figure 2.3 Calculation of $[\text{Ca}^{2+}]_i$ oscillations amplitude and frequency. Initial transient peak was considered as 100% and $[\text{Ca}^{2+}]_i$ oscillations amplitude was calculated subtracting the peak from points preceding the signal rise. The frequency of $[\text{Ca}^{2+}]_i$ oscillations is the ratio of number of $[\text{Ca}^{2+}]_i$ oscillations over period.

2.7 Fluorescent free-swimming cell tracking

After capacitation cell concentration was adjusted to 1.0×10^6 in aliquots of 100 μL , labelled with Ca^{2+} probe fluo4-AM (5 μM) for 30 minutes (36 °C, 5.5% CO_2). Cells were then centrifuged (700 rcf 10 minutes; Eppendorf 5417R) and resuspended twice in order to remove excess dye. Free swimming cells were then transferred into Hamilton-Thorn 2X-Cel chambers (20 μm depth) (Dual Sided Sperm Analysis Chamber, Hamilton Thorn Biosciences, Beverly, MA, USA) that were pre-warmed at 36°C. The chamber was then attached to the platform of a thermostatic controller (Warner TC-324B), adjusted to 25°C or 36.5°C, mounted on the stage of a Nikon eclipse TE300 inverted fluorescence microscope. Time-lapse fluorescence imaging (excitation 485 nm; emission 520 nm) was performed at 2.5 or 10 Hz using a 10x objective and a cooled Andor Ixon 897E EMCCD camera controlled by Andor iQ3 software (Andor Technology, Belfast, UK). For each recording a sperm cell was randomly selected and manually followed for at least 5 minutes by re-centring the cell when it approached the edge of the field of view. Images were analysed and processed uin MetaMorph® NX Microscopy Automation & Image Analysis Software (version 2.0 Molecular Devices 2011), using the Multi Dimensional Motion Analysis (MDMA) application module to track the position of the sperm head. Additional analysis on sperm tracks (calculation of fractal dimension and kinematic variables) was performed by Dr. Hector A. Guidobaldi (Universidad Nacional de Cordoba, Argentina) using a recently developed plugin for ImageJ.

2.8 Penetration of Artificial Viscous Medium (Kremer's assay)

An *in vitro* physiological assay was developed to assess the sperm penetration ability and therefore its fertilising capacity (Kremer, 1965). An artificial viscous medium of methylcellulose (1%, w/v, 4000 cp) was prepared in sEBSS + 0.3% BSA and left overnight at 4 °C with mild shaking to guarantee solubilisation. When drugs were to be included in the methylcellulose column they were added at this stage. The viscous medium was then introduced into 5 cm long flattened glass capillary tubes (dimensions: 1.2 x 4.8-mm and 0.4-mm inner depth; CM scientific - UK), being careful to avoid inclusion of air bubbles, and one end of the tube was sealed with CristaSeal wax (Hawksley – UK). 100 μ L aliquots of capacitated sperm cells at a concentration of 3×10^6 / ml were placed in a sperm reservoir where they could be treated with agonists and inhibitors. After ten minutes of treatment, the open end of the capillary tube was then inserted into the sample and incubated (36 °C, 5.5% CO₂) for one hour. Using phase contrast microscopy (final magnification x200), the number of spermatozoa was counted at 0 (just inside the methylcellulose), 1, 2, 3 and 4 cm from the base of the tube. Under the microscope, three fields of view were selected and in each field, three focal planes were counted, yielding 9 fields altogether (fig. 2.4).

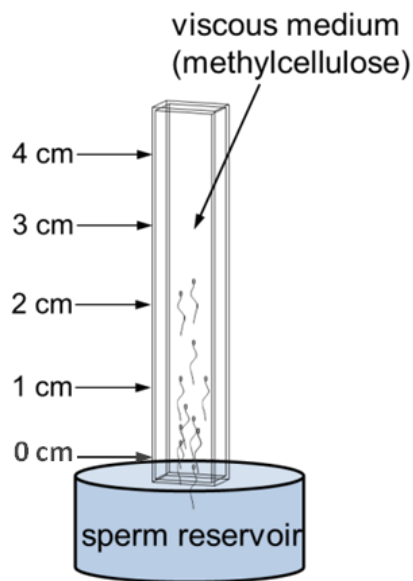


Figure 2.4 Schematic representation of the Kremer's assay. An aliquot of sperm cells ($3 \times 10^6 / \text{mL}$) was kept in a reservoir in contact with the open extremity of the capillary tubes filled with artificial viscous medium of methylcellulose (1%, w/v) prepared in sEBSS + 0.3% of BSA. Samples were incubated (36°C , 5.5% CO_2) for one hour and the number of spermatozoa penetrated at 0, 1, 2, 3 and 4 cm was evaluated under phase contrast microscopy.

Two different types of penetration experiment were performed: the 'classical' design where cells were exposed to drugs in the sperm reservoir (1) or a specific design when one drug was added to the saline with cells and other was included in the viscous medium inside the capillary tubes (2) (fig. 2.5).

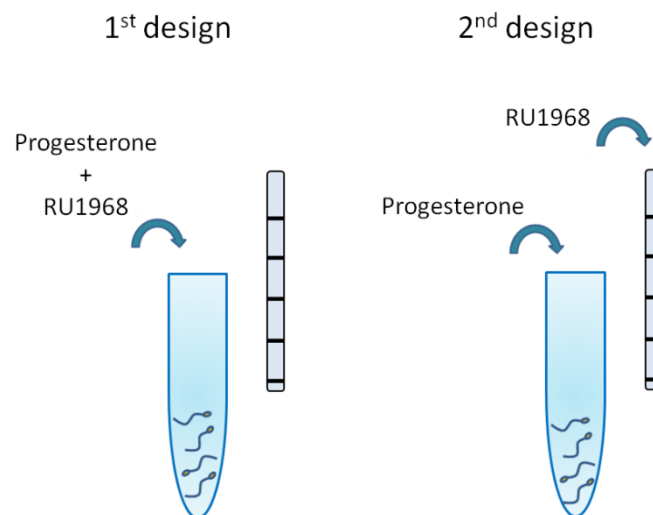


Figure 2.5 Schematic representation of different designs performed in Kremer's assay. First design: both drugs (RU1968F1 and progesterone) were added to sperm reservoir. Second design: progesterone was added to sperm reservoir and RU1968F1 was added to the viscous medium inside the capillary tubes.

2.9 Computer-assisted sperm analysis (CASA)

To assess motility of sperm in methylcellulose, the rectangular section capillary tubes from the Kremer's assay were placed on a heated stage (37°C) of an Olympus CX41 microscope connected to a Hamilton Thorn CEROS CASA system (HTM-CEROS; Hamilton Thorne, Inc. Beverly, MA, USA). Motility of cells at various penetration distances, on 3 different planes of focus, were analysed under a 10x negative phase contrast objective (final magnification of $\times 100$). 30 images were recorded at a frame rate of 60 Hz. Kinematics parameters evaluated were: Track Speed/curvilinear velocity (VCL - $\mu\text{m/s}$), Amplitude of Lateral Head Displacement (ALH - μm), Beat Cross Frequency (BCF - Hz), Linearity (LIN - %) and Hyperactivation. Hyperactivation was identified using the standard criteria of: $\text{VCL} \geq 150 \mu\text{m/s}$, $\text{Linearity} \leq 50 \%$ and $\text{ALH} \geq 7 \mu\text{m}$ (Mortimer et al, 1995).

2.10 Fluorimetric measurement of changes in $[Ca^{2+}]_i$

Following capacitation (section 2.4), cell concentration was adjusted to 5×10^6 / ml and labelled with Ca^{2+} probe fluo4-AM (5 μ M) for 30 minutes (36 °C, 5.5 % CO_2). The cells were then centrifuged (Eppendorf 5417R) twice for 10 minutes in 700 rcf in order to remove excess of the dye and re-suspended in fresh medium. Supernatant of the last washing process was used for background subtraction from experimental values. Sperm cells were transferred to 96-wells plate and fluo4 fluorescence was measured over time using a fluorometer (FluoStar Omega BMG Labtech, Offenburg, Germany) at 492 nm excitation and 520 nm emission and temperature of 30 °C. Changes in $[Ca^{2+}]_i$ was acquired using top optics, measured in parallel in multiple wells, 20% photomultiplier gain and 5s cycle time.

2.11 Whole-cell patch clamping

Whole-cell patch clamping experiments were performed in collaboration with Dr. Sean Brown, University of Abertay Dundee – Scotland. The current clamp protocol used can be found in Mansell et al (2014) as described: “The electrophysiological properties of individual spermatozoa were investigated using the whole cell recording technique (Hamill et al, 1981; Kirichok et al, 2006; Lishko et al, 2011). The recording pipettes (10–18 $M\Omega$) were fabricated from borosilicate glass and filled with standard pipette solution. Gigaohm seals were obtained by bringing the pipette tip into gentle contact with the cytoplasmic droplet, which lies just behind the sperm head, and the patch of membrane spanning the pipette tip then ruptured by applying suction in conjunction with 1 ms voltage pulses (see Lishko et al, 2010). Our standard recording conditions were designed to preserve physiologically relevant

Na⁺, K⁺ and Cl⁻ gradients and V_m. Resting V_m was measured directly by monitoring (5 KHz acquisition, data low pass filtered at 3 KHz) the zero current potential (see Hamill et al, 1981).”

2.12 Statistical analysis

The data were analysed using Microsoft Excel or GraphPad Prism5 performing paired or unpaired t tests, one way ANOVA followed by Tukey's test or two-way ANOVA followed by Bonferroni's post-hoc, as appropriate. Results were expressed as mean ± standard error of the mean (SEM) or mean ± standard deviation (SD), when indicated. Results were considered significant when ***p ≤ 0.001, **p ≤ 0.01 and *p ≤ 0.05. All experiments were performed at least three times independently.

CHAPTER THREE: MEMBRANE POTENTIAL CONTRIBUTES TO GENERATION OF $[Ca^{2+}]_i$ OSCILLATIONS

3.1 Abstract

Progesterone regulates Ca^{2+} influx into spermatozoa, which is crucial for regulation of sperm motility. $[Ca^{2+}]_i$ oscillations may underlie ‘switching’ of sperm behaviour in human spermatozoa, which is believed to be important for sperm progression in the female tract. I have investigated the contribution of membrane potential (V_m) to $[Ca^{2+}]_i$ oscillations induced by progesterone. Manipulation of V_m was performed using the K^+ ionophore valinomycin (VLN-1 μ M), alone or with high K^+ media (25 mM and 100 mM) and confirmed by whole-cell patch clamping. $[Ca^{2+}]_i$ signalling was assessed by loading sperm cells with the Ca^{2+} -indicator fluo-4-AM and stimulating them with 3 μ M progesterone. Approximately 25% of cells exhibited $[Ca^{2+}]_i$ oscillations after progesterone stimulation, independently of the level of sperm capacitation. $[Ca^{2+}]_i$ oscillations were dependent on extracellular Ca^{2+} and $[Ca^{2+}]_i$ rose first in the flagellum, consistent with activation of CatSper, then spread actively to the head, apparently triggering Ca^{2+} store release. ‘Clamping’ of V_m at -79 mV (with VLN only) abolished progesterone-induced $[Ca^{2+}]_i$ oscillations, but basal $[Ca^{2+}]_i$ activity was still observed. $[Ca^{2+}]_i$ oscillations were completely recovered upon VLN washout. ‘Clamping’ of V_m at -38 mV (with VLN/25 mM K^+) was less effective in reducing progesterone-induced $[Ca^{2+}]_i$ oscillations frequency and amplitude. When V_m was clamped to -4 mV (with VLN/100 mM K^+) progesterone-induced $[Ca^{2+}]_i$ oscillations was more resistant and recovery of inhibited oscillations upon VLN washout was slower. Our results show that V_m contributes

to generation of progesterone-induced $[Ca^{2+}]_i$ oscillations, probably by regulating CatSper (and consequently triggering of CICR).

3.2 Introduction

The steroid female hormone progesterone (P4; fig 3.1) is released by cumulus cells surrounding the ovulated egg and may be involved in the stimulation of several sperm functions, such as hyperactivated motility, sperm chemotaxis towards the egg, acrosome reaction, binding to oocyte zona pellucida and, finally, penetration (Roldan et al, 1994; Harper et al, 2004; Eisenbach and Giojalas, 2006; Publicover et al, 2007; Qi et al, 2007; Xia et al, 2007). Progesterone regulates Ca^{2+} influx into spermatozoa, mostly by activation of CatSper channels (the primary route for Ca^{2+} entry into sperm cells) which are also sensitive to increasing of intracellular pH, changes in membrane potential (V_m) and other ligands (Ren et al, 2001; Quill et al, 2001; Kirichok et al, 2006; Navarro et al, 2008; Brenker et al, 2012).

Sperm cells stimulated with progesterone in different concentrations respond with complex alterations in $[\text{Ca}^{2+}]_i$ and flagellar movement. Typically, progesterone induces a rapid, biphasic and dose-dependent Ca^{2+} entry into human spermatozoa. The biphasic response consists in a first transient peak followed by a long-lasting plateau and sustained phase (Blackmore et al, 1990; Kirkman-Brown et al, 2000). Interestingly, later studies have reported that, in a sub-population of sperm, progesterone can also induce $[\text{Ca}^{2+}]_i$ oscillations after the first transient peak instead of a stable plateau phase (Kirkman-Brown et al, 2004; Aitken and McLaughlin, 2007). The functional significance of changes in $[\text{Ca}^{2+}]_i$ is not yet clear but it appears that they may play a role in the regulation of sperm motility and underlie ‘switching’ of sperm behaviour in human spermatozoa, which is believed to be important for sperm progression in the female tract (Jaiswal et al, 1999; Harper and Publicover, 2005).

The characteristics of $[Ca^{2+}]_i$ oscillations in most somatic cells are compatible with a cyclical emptying/refilling of intracellular Ca^{2+} stores, mediated by generation of second messengers such as IP_3 (Berridge, 1993). Initial studies on $[Ca^{2+}]_i$ oscillations in human sperm indicate that Ca^{2+} store mobilisation is involved but also suggest a strong dependence on extracellular Ca^{2+} (Harper et al, 2004). One possibility is that Ca^{2+} influx triggers secondary release of stored Ca^{2+} (Correia et al, 2015). In particular, since CatSper is voltage-sensitive, periodic depolarisation of V_m could lead to cyclical activation of Ca^{2+} -influx via CatSper and, consequently, generate $[Ca^{2+}]_i$ oscillations, as has been observed in other cell types (Lieste et al, 1998; Mizutani et al, 2014).

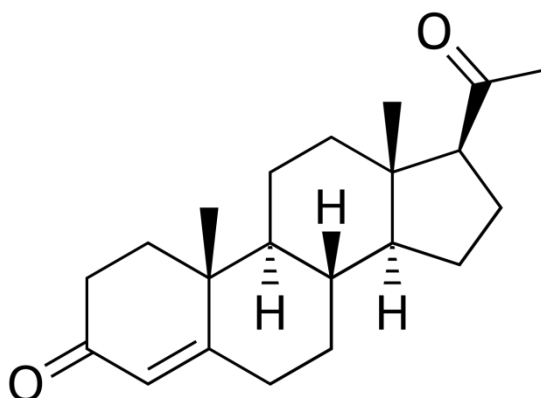


Figure 3.1 Progesterone chemical structure depiction. Progesterone is composed of $C_{21}H_{30}O_2$ arranged as a four fused rings, with molecular weight of 314.469 g/mol (image reproduced from PubChem: available on <https://pubchem.ncbi.nlm.nih.gov>).

Chapter Aims

The aims of this chapter were to characterise the Ca^{2+} responses induced by progesterone in human spermatozoa and to investigate the contribution of membrane potential (V_m) to progesterone-induced $[\text{Ca}^{2+}]_i$ oscillations.

3.3 Results

3.3.1 Progesterone induces $[Ca^{2+}]_i$ oscillations in human spermatozoa

Previous studies have been reported that progesterone can induce $[Ca^{2+}]_i$ oscillations after the transient phase in a subpopulation of human spermatozoa (Kirkman-Brown et al, 2004; Aitken and McLaughlin, 2007). I investigated the Ca^{2+} response profiles induced by progesterone, using single cell imaging technique. As previously reported in several studies sperm cells stimulated with progesterone exhibit a biphasic Ca^{2+} response (fig. 3.2). Immediately after progesterone addition, a high transient peak occurs with approximately 200% fluorescence intensity increase when compared to control period. The transient phase lasts about 2-3 minutes and is followed by a long-lasting plateau and sustained phase until progesterone removal.

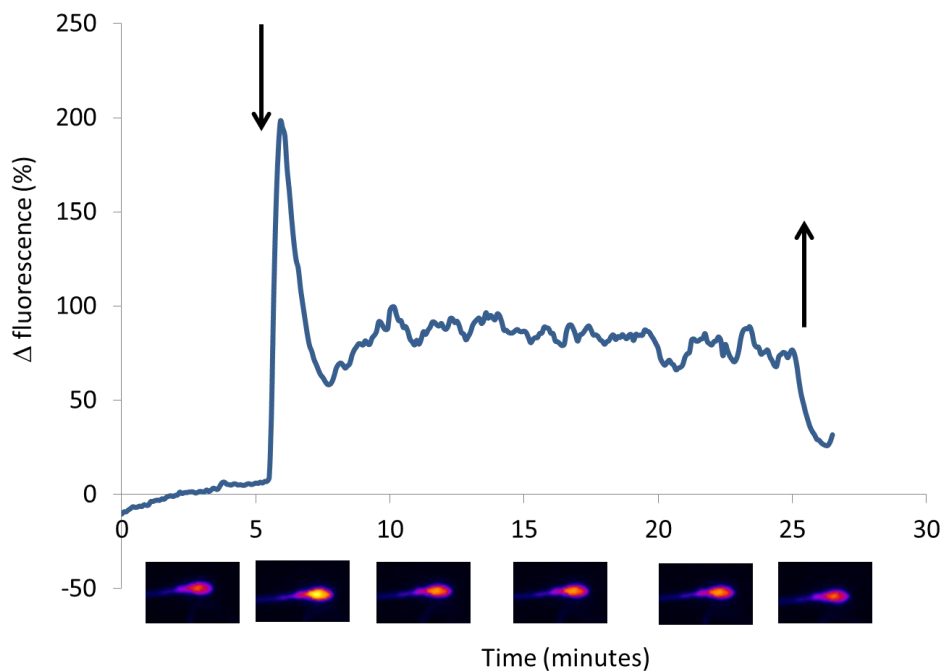


Figure 3.2 Typical biphasic (transient + sustained phase) Ca^{2+} response induced by progesterone in human spermatozoa. First arrow represents the moment of progesterone addition while the second arrow shows the progesterone removal. Pictures show the Ca^{2+} intensity in a single human spermatozoon over the course of time. The histogram is an average of the Ca^{2+} response intensity of 100 sperm cells.

However, when individual cells were analysed a stable sustained phase following the initial transient peak was not observed in all cells. Instead, in some cells $[Ca^{2+}]_i$ oscillations was observed and exhibited ‘rapid’ $[Ca^{2+}]_i$ spikes with kinetics similar to the initial progesterone $[Ca^{2+}]_i$ transient response (fig. 3.3). Although amplitude, frequency and duration of the $[Ca^{2+}]_i$ oscillations was very variable between the ‘oscillating’ cells. Therefore, I established that a $[Ca^{2+}]_i$ oscillation shows at least 20% of the initial transient peak amplitude and lasts less than 2 minutes per cycle. Moreover, basal $[Ca^{2+}]_i$ activity with slower kinetics and lower amplitude was also observed, which has been already previously reported in human spermatozoa (Sanchez-Cardenas et al, 2014; Kelly et al, 2018; Mata-Martinez et al, 2018).

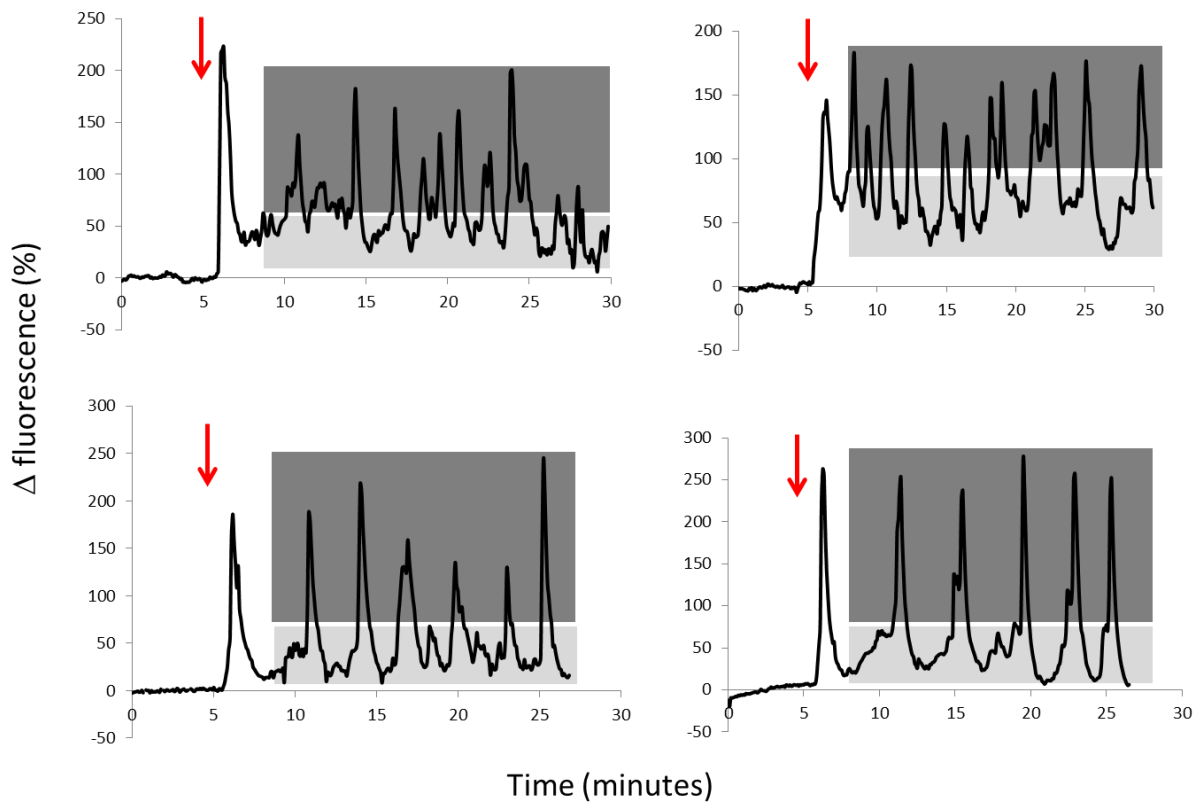


Figure 3.3 Progesterone induces $[Ca^{2+}]_i$ oscillations in populations of human spermatozoa: ‘rapid’ transients with high amplitude. Dark grey shading shows progesterone-induced $[Ca^{2+}]_i$ oscillations while light grey shading shows basal Ca^{2+} activity, red arrows show addition and removal of 3 μ M progesterone. Graphs are representative histograms generated from single cell images.

3.3.2 Level of capacitation and $[Ca^{2+}]_i$ oscillations induced by progesterone

Human sperm cells reach maximum level of tyrosine phosphorylation, which is a well-established marker of capacitation, over 3-4 hours incubation in sEBSS (O'Flaherty et al, 2004; Bedu-Addo et al, 2005; Moseley et al, 2005). And different levels of capacitation may affect the proportion of 'oscillating' cells (Kirkman-Brown et al, 2004). I investigated the percentage of cells that exhibit different Ca^{2+} responses according to the duration of sperm capacitation by incubating in non-capacitating medium for 4 hours or under capacitating conditions for 4 hours or 7 hours. The proportion of cells exhibiting $[Ca^{2+}]_i$ oscillations after progesterone stimulation was approximately 25% in non-capacitated cells and the ones capacitated for 4 and 7 hours ($n=70$ cells per condition; $p<0.001$; fig. 3.4).

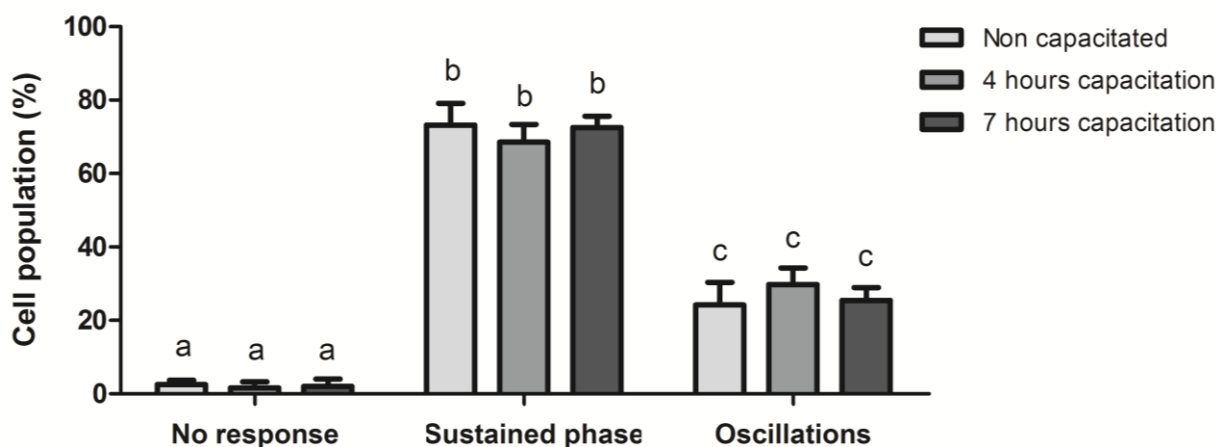


Figure 3.4 Ca^{2+} profiles in human spermatozoa populations are not different in non-capacitated cells or after 4 hours and 7 hours of capacitation. Graph represents the percentage of cells that exhibits different Ca^{2+} responses after progesterone stimulation according to the duration of sperm capacitation. Treatment groups with the same letters were not significantly different according to two-way ANOVA followed by Bonferroni's post-hoc ($p<0.001$). Bars show mean \pm SEM of 3 experiments.

I also analysed the characteristics of the progesterone-induced $[Ca^{2+}]_i$ oscillations generated when cells were capacitated or not (fig 3.5A). The amplitude of $[Ca^{2+}]_i$ oscillations did not change between the populations incubated under the three capacitating conditions, approximately 45% Δ fluorescence when compared to the initial transient peak (fig 3.4C). However, whereas in cells capacitated for 4 or 7 hours the frequency of $[Ca^{2+}]_i$ oscillations was similar (0.26 ± 0.2 cpm; $p < 0.05$; (fig 3.4B), in non-capacitated cells oscillations occurred at a slower rate (0.21 ± 0.01 cpm; $n = 400$ $[Ca^{2+}]_i$ oscillations from 70 cells; $p < 0.05$; (fig 3.5B). Therefore, subsequent experiments were performed with sperm cells incubated in capacitating media for at least 4 hours.

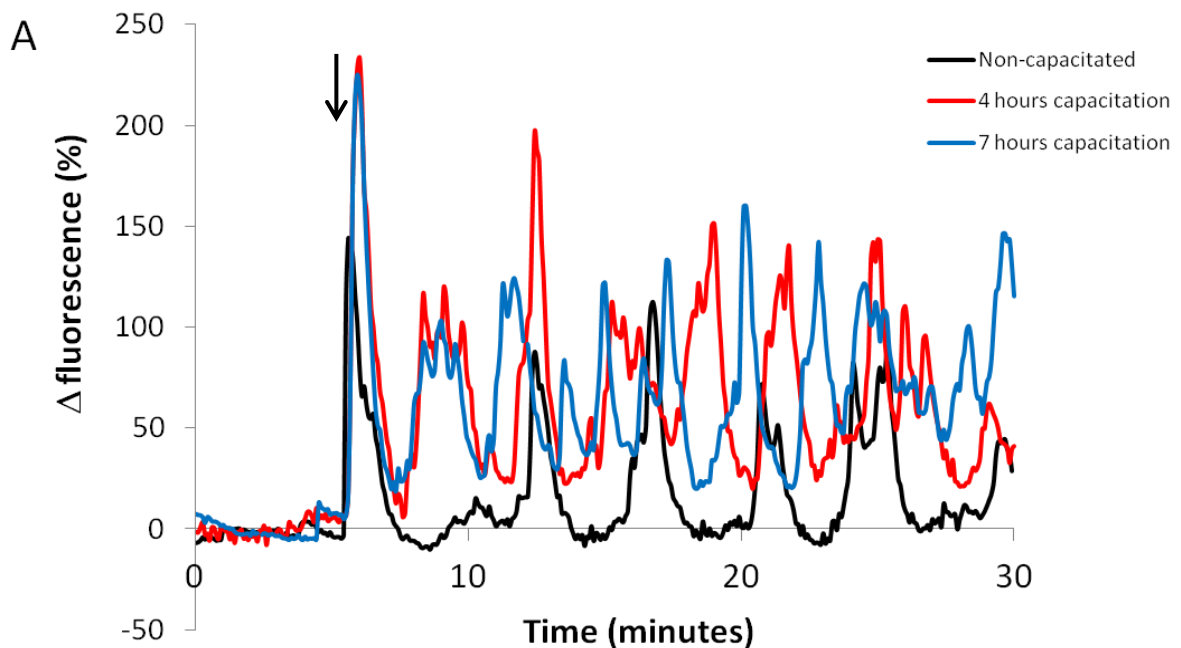


Figure 3.5 Degree of capacitation affects the frequency of $[Ca^{2+}]_i$ oscillations but not amplitude in human spermatozoa populations. (A) Graph is representative ‘oscillating’ cell traces generated from single cell images on non-capacitated (black), after 4 hours of capacitation (red) and 7 hours of capacitation (blue) populations of spermatozoa. Arrow shows addition of 3 μ M progesterone.

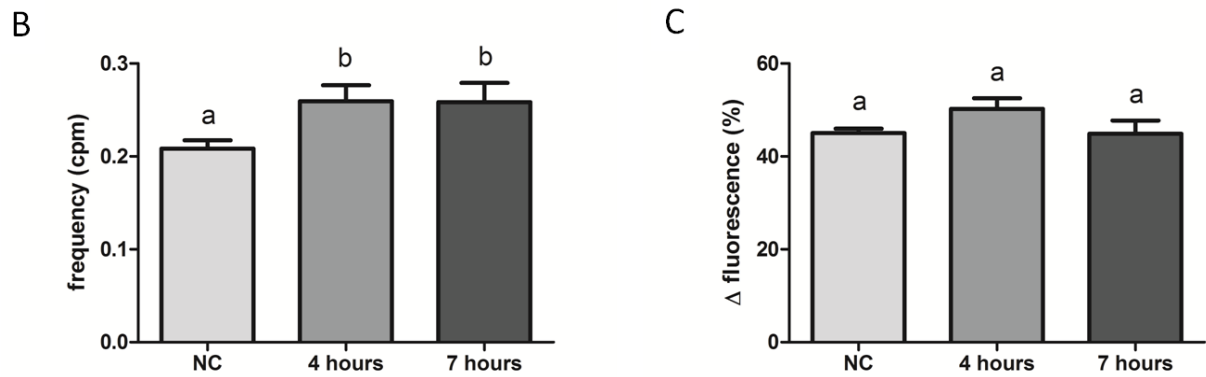


Figure 3.5 Capacitation affects the frequency of $[Ca^{2+}]_i$ oscillations but not amplitude in human spermatozoa populations. (B) Graph shows the frequency of $[Ca^{2+}]_i$ oscillations occurrence per minute in the ‘oscillating’ population and bars show mean \pm SEM of 3 experiments. (C) Graph shows the amplitude of $[Ca^{2+}]_i$ oscillations in sperm population under the 3 capacitating conditions. Amplitude was calculated using the mean response of each $[Ca^{2+}]_i$ oscillation considering the initial transient peak as 100% and bars show mean \pm SEM of experiments. A $[Ca^{2+}]_i$ oscillation was considered when reached at least 20% of the initial transient peak amplitude. NC = non-capacitated. Treatment groups with the same letters were not significantly different according to one-way ANOVA followed by Tukey’s post-test ($p < 0.05$).

3.3.3 $[Ca^{2+}]_i$ oscillations require extracellular Ca^{2+}

Previously, Harper and colleagues (2004) showed that generation of $[Ca^{2+}]_i$ oscillations in human spermatozoa was blocked in Ca^{2+} -free medium (buffered with EGTA). But when cells were exposed to low- Ca^{2+} medium (sEBSS with no added Ca^{2+} ; $\approx 10^{-6}M$ Ca^{2+}) oscillations persisted and became slightly larger. In order to investigate this further, I performed a similar experiment but with a longer exposure to low- Ca^{2+} medium (sEBSS with no added Ca^{2+}). Progesterone was used to stimulate $[Ca^{2+}]_i$ oscillations and later low- Ca^{2+} medium was introduced for 30 minutes. Perfusion of this medium initially increased oscillation amplitude as described by Harper et al (2004) but then gradually abolished the oscillations during the course of time, inhibiting completely after 12.3 ± 0.5 minutes of treatment ($n=51$ cells from 3 experiments; data not shown). The longest time a $[Ca^{2+}]_i$

oscillation pattern persisted during low- Ca^{2+} medium perfusion was 22.7 minutes of treatment. Addition of EGTA to remove any remaining trace of Ca^{2+} in the extracellular environment further decreased $[\text{Ca}^{2+}]_i$ (fluo4 fluorescence) to levels below the control phase. The subsequent addition of standard sEBSS (1.8 mM of Ca^{2+}) promoted a large $[\text{Ca}^{2+}]_i$ increase (fig. 3.6).

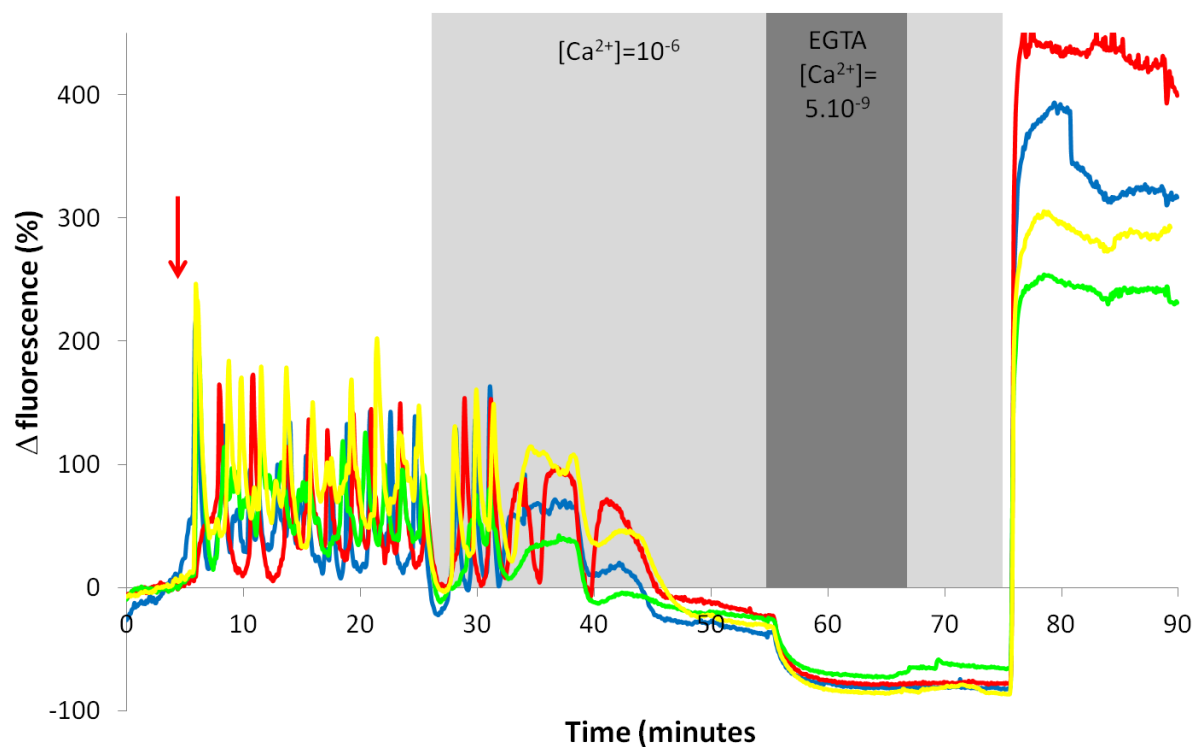


Figure 3.6 $[\text{Ca}^{2+}]_i$ oscillations require extracellular Ca^{2+} . Absence of extracellular Ca^{2+} abolishes $[\text{Ca}^{2+}]_i$ oscillations induced by progesterone in human spermatozoa. Panel shows single cells traces (4 cells from different set of experiments) generated from single cell images obtained in a time-lapse experiment. Light grey shading shows perfusion of Ca^{2+} free (lower trace) medium, dark grey shading shows addition of the Ca^{2+} chelator EGTA (2 mM) and red arrow shows addition of progesterone (3 μM). Experiments were performed, in collaboration with Dr. Esperanza Mata-Martínez, Universidad Nacional Autónoma de México.

3.3.4 Spatiotemporal characteristics of $[Ca^{2+}]_i$ oscillations induced by progesterone

To investigate the spatiotemporal characteristics of $[Ca^{2+}]_i$ oscillations induced by progesterone, I performed single-cell images in high speed – 2.5 Hz and 5 Hz and 60x oil objective. The occurrence of $[Ca^{2+}]_i$ elevation was investigated separately in three regions of the sperm cell (flagellum, neck, head). After progesterone addition, a transient followed by oscillations was observed in all three regions. It was clear that the progesterone-induced $[Ca^{2+}]_i$ transient initiate in the flagellum then spread actively towards the sperm head, through the neck (fig. 3.7A). This sequence is consistent with activation of CatSper by progesterone since the channels are restrictedly found in the principal piece of the sperm flagellum. The time delay Ca^{2+} signal propagates from the flagellum to the neck or head during the initial transient peak was 3.1 ± 0.4 and 3.6 ± 0.5 seconds (n=22 cells from 10 experiments, $p < 0.001$), respectively (fig. 3.7B).

Analysis of $[Ca^{2+}]_i$ oscillations which followed the initial transient showed a similar pattern, indicating that oscillations were also triggered in the flagellum. However, once reaching neck and head, Ca^{2+} oscillations exhibited higher amplitude than observed in the flagellum, which suggests that the Ca^{2+} signal then triggers Ca^{2+} store release (fig. 3.8A). The time delay Ca^{2+} signal propagates in the sperm cell during oscillations generation was 3.1 ± 0.5 seconds (to the neck) and 4.2 ± 0.5 seconds (to the head) (n=22 cells from 10 experiments, $p < 0.001$) (fig. 3.8B).

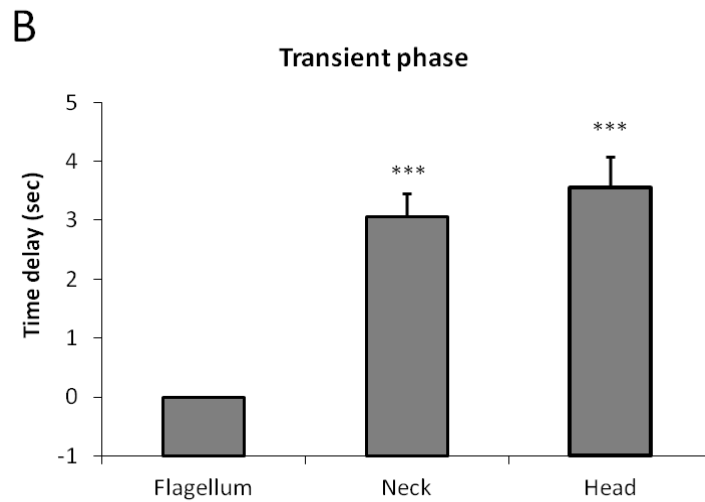
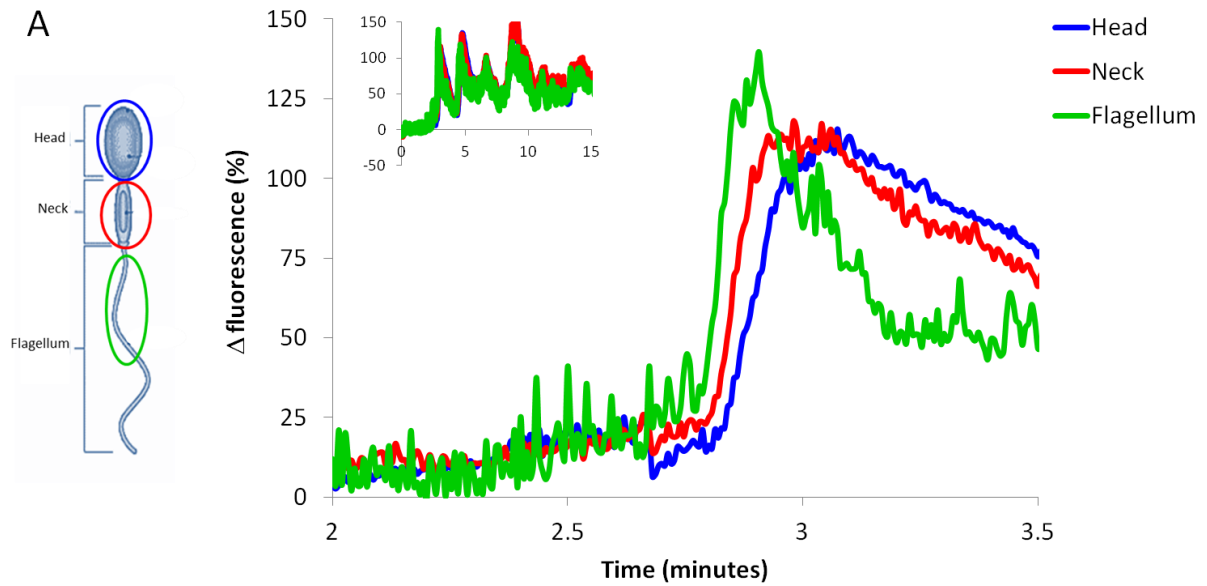


Figure 3.7 Ca^{2+} transient induced by progesterone start at the flagellum and propagate towards the sperm head. **(A)** Traces show Ca^{2+} rising during the first $[Ca^{2+}]_i$ oscillation in three different regions of the sperm cell, flagellum (green), neck (blue) and head (red). Representative histogram was generated by single-cell images obtained in a time-lapse experiment recorded in high speed of 2.5 Hz. **(B)** Delays to the neck and head were calculated considering flagellum as the start point – 0 seconds. A total of 60 $[Ca^{2+}]_i$ oscillations was analysed from 22 sperm cells recorded in 10 experiments performed independently. Comparisons were conducted with one-way ANOVA followed by Tukey’s post-hoc. *** $p < 0.001$, when compared to “flagellum”.

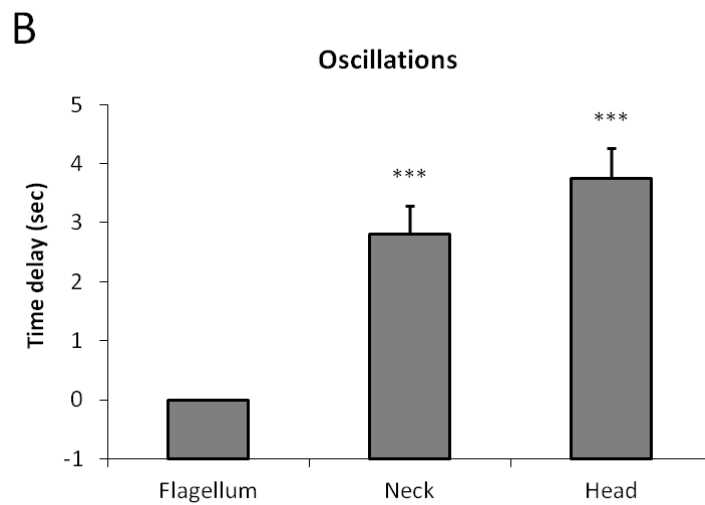
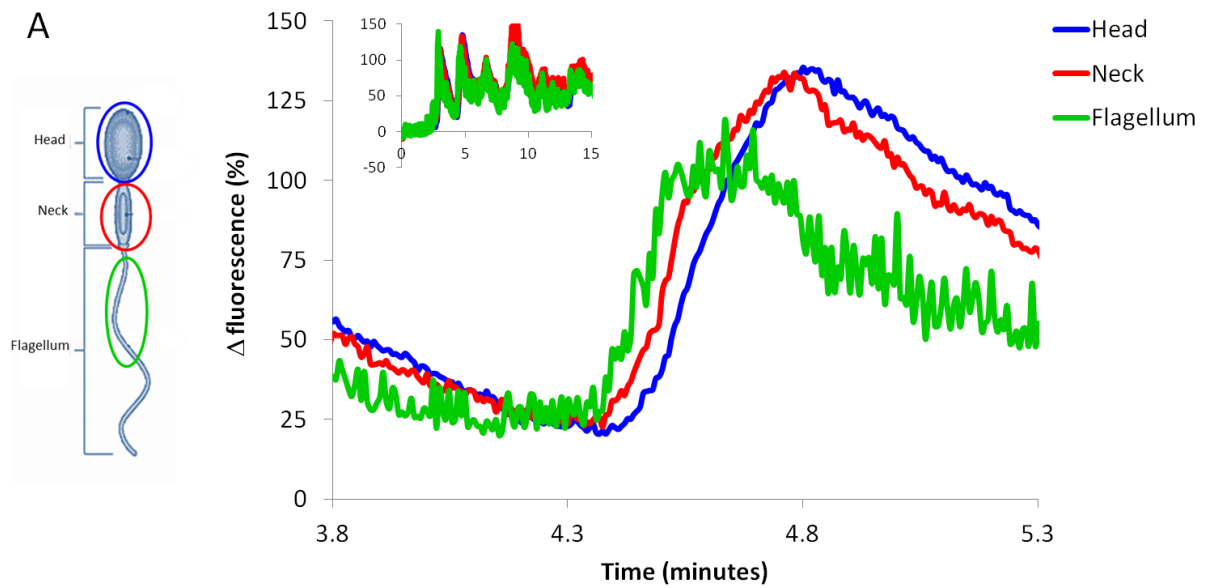


Figure 3.8 $[Ca^{2+}]_i$ oscillations induced by progesterone start at the flagellum and propagate towards the sperm head. **(A)** Traces show Ca^{2+} rising during the first $[Ca^{2+}]_i$ oscillation in three different regions of the sperm cell, flagellum (green), neck (blue) and head (red). Representative histogram was generated by single-cell images obtained in a time-lapse experiment recorded in high speed of 2.5 Hz. **(B)** Delays to the neck and head were calculated considering flagellum as the start point – 0 seconds. A total of 60 $[Ca^{2+}]_i$ oscillations was analysed from 22 sperm cells recorded in 10 experiments performed independently. Comparisons were conducted with one-way ANOVA followed by Tukey’s post-hoc. *** $p < 0.001$, when compared to “flagellum”.

3.3.5 Membrane potential (V_m) regulates $[Ca^{2+}]_i$ oscillations

Periodic changes in membrane potential may lead to cyclical activation of voltage dependent Ca^{2+} -influx pathways and, consequently, generate $[Ca^{2+}]_i$ oscillations (Lieste et al, 1998). To investigate the contribution of changes in membrane potential on $[Ca^{2+}]_i$ oscillations, manipulation of V_m was performed using K^+ ionophore valinomycin (VLN - $1\mu M$) to clamp V_m to E_K . Calculated values of E_K for standard sEBBS and high K^+ sEBSS ($100\text{ mM } K^+$) were -79 mV and -4 mV . This was assessed using whole-cell current clamp, which showed that $1\text{ }\mu M$ valinomycin was sufficient to control V_m and that recorded values approximated to those estimated by calculation (fig. 3.9).

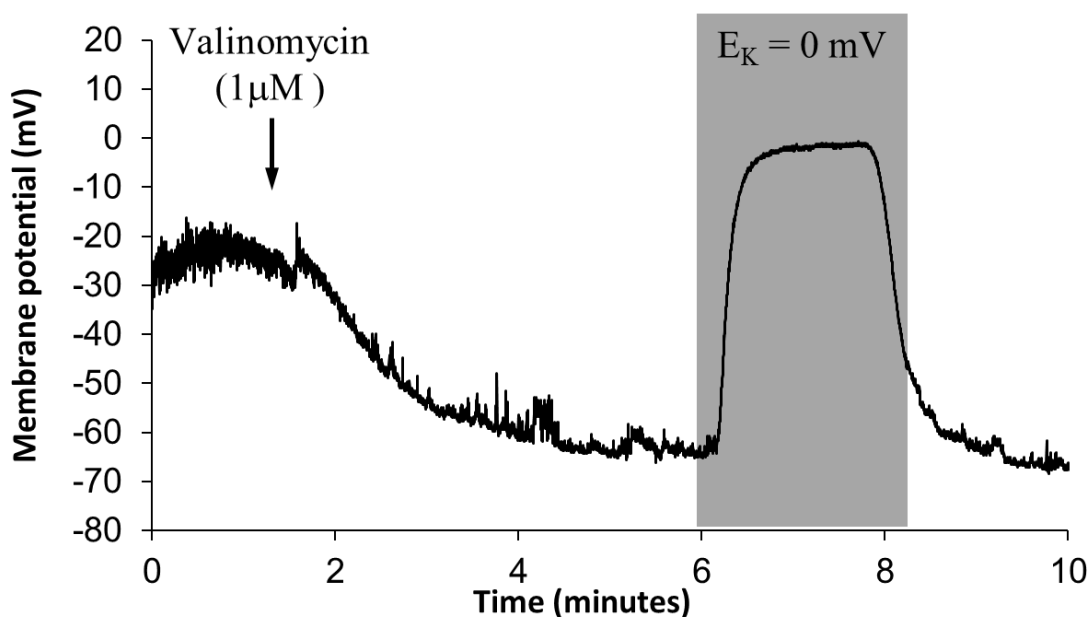


Figure 3.9 Confirmation of manipulation of V_m using valinomycin with the technique of whole-cell patch clamp. Arrow shows the time of addition of $1\text{ }\mu M$ VLN, grey shading show treatment period with $100\text{ mM } K^+$ media. Experiments were performed by Dr. Sean Brown, University of Abertay Dundee.

3.3.5.1 Hyperpolarisation (-79 mV) effect on $[Ca^{2+}]_i$ oscillations

Pre-treatment with VLN (to clamp V_m at -79 mV) had no effect on the initial progesterone-induced $[Ca^{2+}]_i$ transient but abolished progesterone-induced $[Ca^{2+}]_i$ oscillations. However, basal $[Ca^{2+}]_i$ activity was still observed. $[Ca^{2+}]_i$ oscillations pattern were completely recovered when VLN was removed (fig. 3.10A). Similar results were obtained when valinomycin was added after progesterone stimulation. The $[Ca^{2+}]_i$ oscillating sub-population was completely inhibited upon hyperpolarisation by VLN application (fig 3.10B). Furthermore, as observed in the pre-treatment experiments, $[Ca^{2+}]_i$ oscillations pattern was completely recovered upon VLN washout (fig. 3.10B).

In experiments where VLN was added after progesterone $[Ca^{2+}]_i$ oscillations persisted in approximately $11.6 \pm 3.4\%$ of the oscillating sub-population (fig 3.11). In these cells frequency of $[Ca^{2+}]_i$ oscillations was greatly reduced from 0.52 ± 0.02 cpm to 0.08 ± 0.02 cpm (420 $[Ca^{2+}]_i$ oscillations from 50 cells; $p < 0.001$; fig. 3.11A). When V_m was subsequently restored by VLN washout the frequency of $[Ca^{2+}]_i$ oscillations recovered. Additionally, the amplitude of $[Ca^{2+}]_i$ oscillations after hyperpolarisation was also affected: reduction of $86.4 \pm 2.2\%$ (420 $[Ca^{2+}]_i$ oscillations from 50 cells; $p < 0.001$; fig. 3.12A). Restoring V_m completely recovered the amplitudes, as they exhibited the same levels of the $[Ca^{2+}]_i$ oscillations before hyperpolarisation (fig. 3.12B).

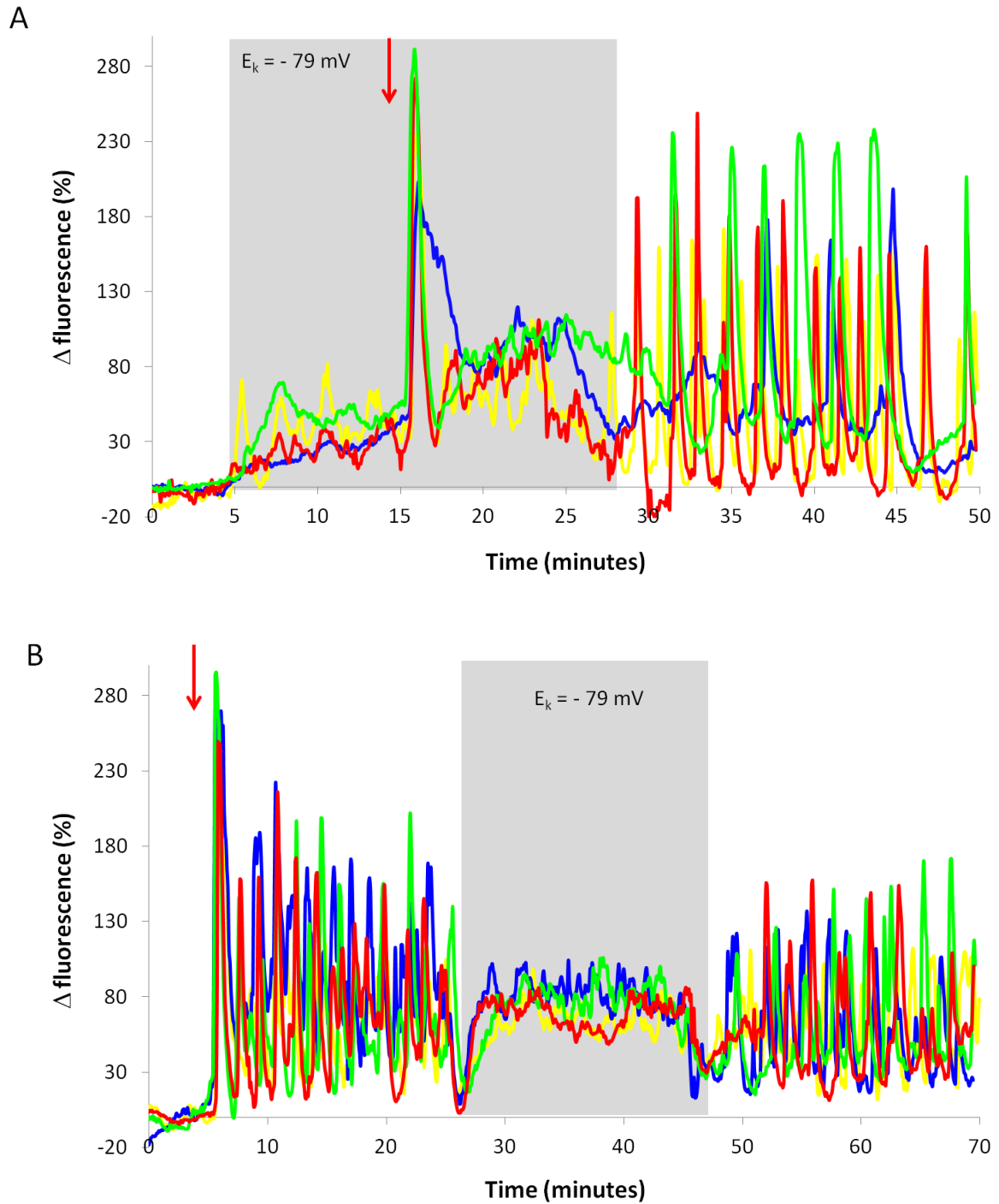


Figure 3.10 Vm hyperpolarisation abolishes progesterone-induced $[Ca^{2+}]_i$ oscillations. $[Ca^{2+}]_i$ oscillations profile was completely recovered when valinomycin was removed and Vm was restored. Panels show single cell traces (4 cells from different set of experiments) generated from single cell images obtained in a time-lapse experiment. Grey shading shows pre-treatment (A) or post-treatment (B) with VLN (1 μ M), red arrow shows addition of progesterone (3 μ M).

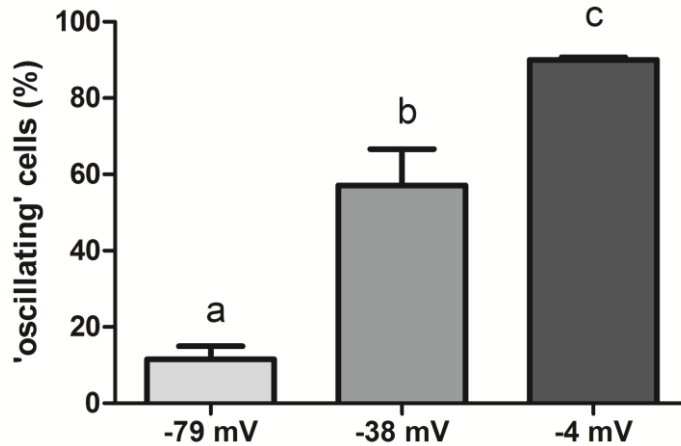


Figure 3.11 Proportion of 'oscillating' population under different membrane potential values. Membrane potential was manipulated to hyperpolarisation: -79 mV; close to resting potential: -38 mV; and depolarisation: -4 mV. Bars show mean \pm SEM of a total of 50 cells per condition from 3 different experiments. Treatment groups with the same letters were not significantly different according to one-way ANOVA followed by Tukey's post-hoc ($p < 0.001$).

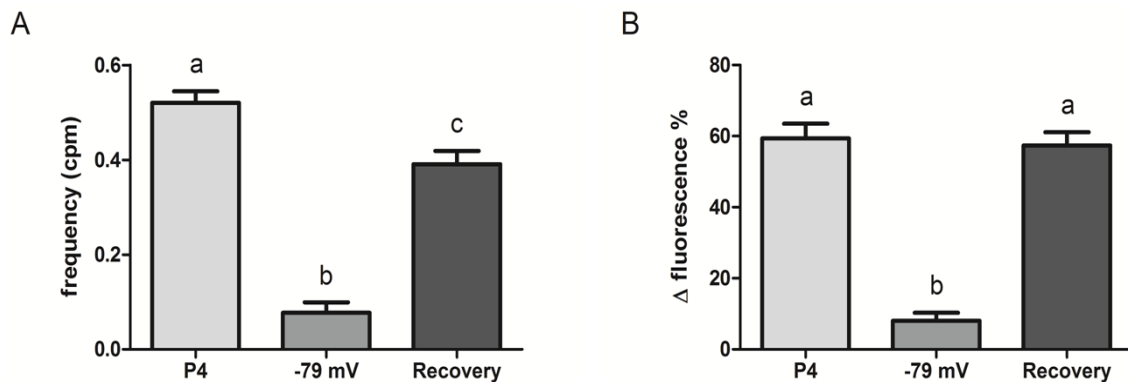


Figure 3.12 Vm hyperpolarisation alters the frequency and amplitude of progesterone-induced [Ca²⁺]_i oscillations. Graphs show the frequency of [Ca²⁺]_i oscillations occurrence per minute in the 'oscillating' population (A) and the amplitude of [Ca²⁺]_i oscillations in sperm population (B) under the three conditions: progesterone alone and regular Vm (first bar), hyperpolarisation Vm E_K = -79 mV (second bar) and restored Vm (third bar). Amplitude was calculated using the mean response of each [Ca²⁺]_i oscillation considering the initial transient peak as 100% and bars show mean \pm SEM of 3 experiments. A [Ca²⁺]_i oscillation was considered when reached at least 20% of the initial transient peak amplitude. Treatment groups with the same letters were not significantly different according to one-way ANOVA followed by Tukey's post-hoc ($p < 0.001$).

3.3.5.2 Depolarisation (-4 mV) effect on $[Ca^{2+}]_i$ oscillations

In order to investigate whether the $[Ca^{2+}]_i$ oscillations would be affected by membrane potential depolarisation, sperm cells were exposed to 1 μ M VLN combined with 100 mM K^+ (estimated $E_K = -4$ mV). Pre-treatment with VLN/100 mM K^+ increased resting $[Ca^{2+}]_i$ (fig 3.13A) and resulted in a slight increased peak, but did not inhibit nor alter the amplitude of the initial transient response induced by progesterone. Depolarisation prevented generation of progesterone-induced $[Ca^{2+}]_i$ oscillations following the initial progesterone transient, but basal $[Ca^{2+}]_i$ activity was still observed (fig. 3.13A). When cells were treated with VLN/100 K^+ after exposure to progesterone $[Ca^{2+}]_i$ oscillations persisted in most cells (fig 3.13B).

The proportion of oscillating sub-population upon depolarisation was approximately $90.1 \pm 0.6\%$ of the cells (fig. 3.11). Furthermore, membrane depolarisation had little effect on rate of generation of progesterone-induced $[Ca^{2+}]_i$ oscillations, frequency being reduced by only $17.7 \pm 0.01\%$ ($n=260$ $[Ca^{2+}]_i$ oscillations from 25 cells; $p<0.05$; fig. 4.14A) during perfusion with VLN/100 K^+ but after washout, the $[Ca^{2+}]_i$ oscillation frequency was further decreased (by $57.7 \pm 0.02\%$) and recover did not occur within the period of recording. However, amplitude in oscillating cells decreased by $49.9 \pm 2.1\%$ ($n=260$ $[Ca^{2+}]_i$ oscillations from 25 cells; $p<0.001$; fig. 3.14B).

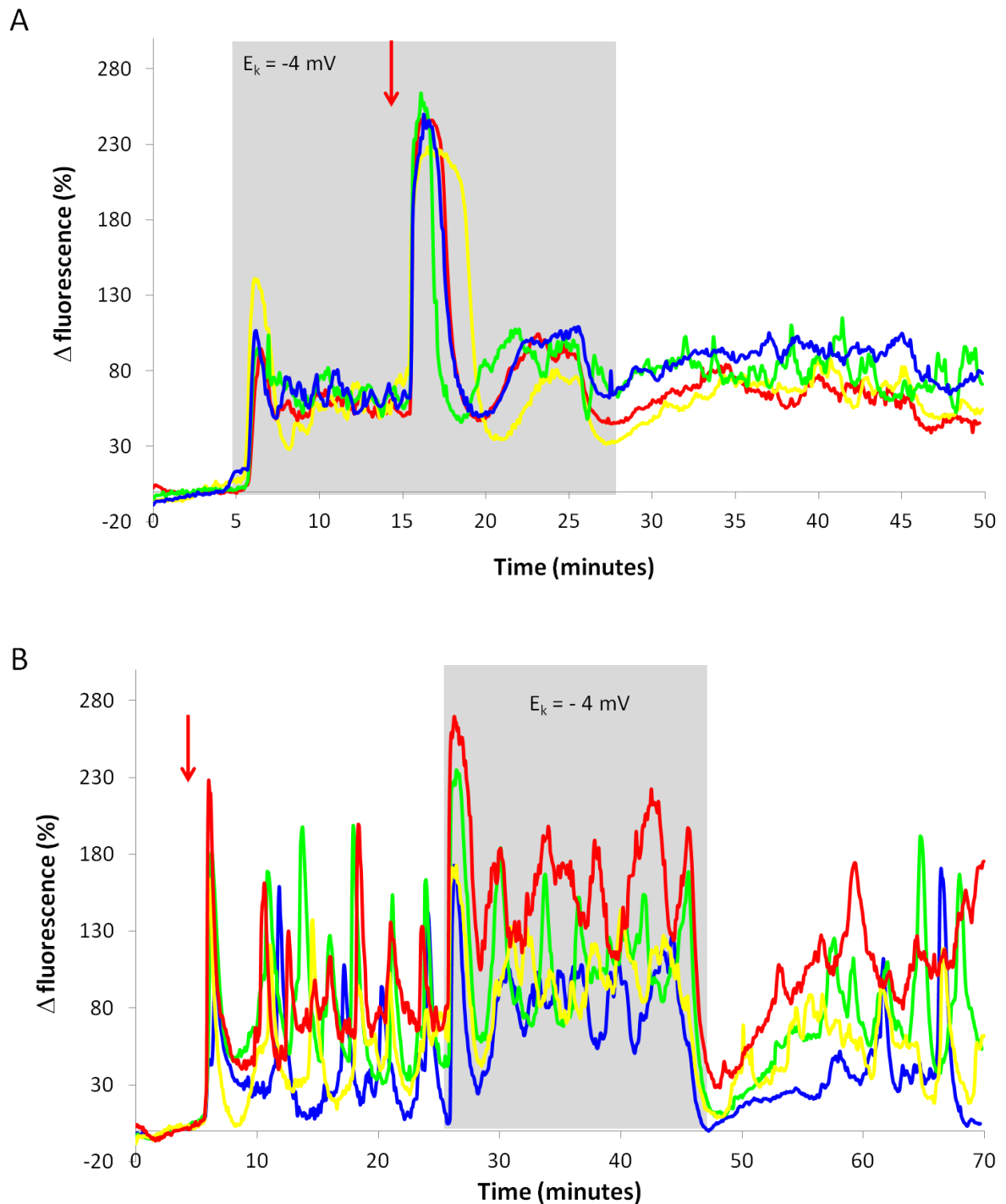


Figure 3.13 Depolarisation (-4 mV) partially inhibits progesterone-induced $[Ca^{2+}]_i$ oscillations in sperm cells. $[Ca^{2+}]_i$ oscillations profile was not completely recovered when VLN/100 mM K^+ was removed. Panels show representative single cells traces (4 cells from different set of experiments) generated from single cell images obtained in a time-lapse experiment. Grey shading shows pre-treatment (A) or post-treatment (B) with VLN/100 mM K^+ , red arrow shows addition of progesterone (3 μ M).

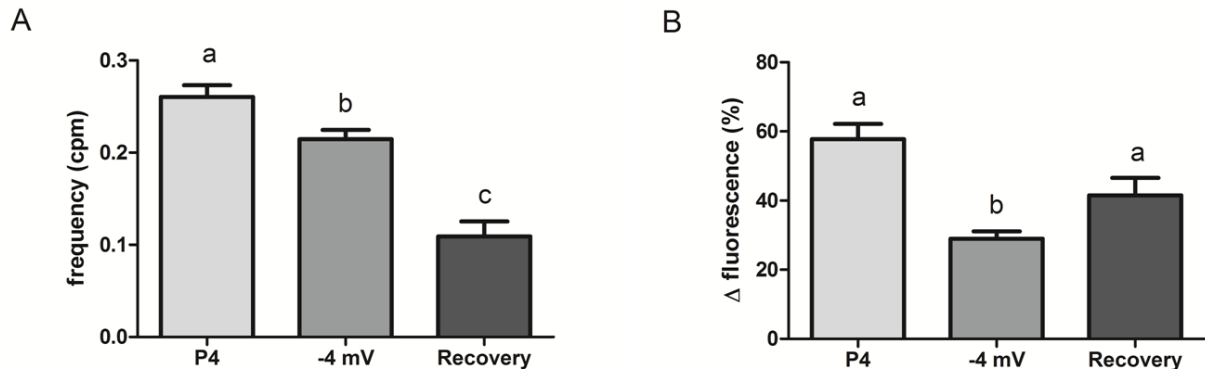


Figure 3.14 Depolarisation slightly alters the frequency of $[Ca^{2+}]_i$ oscillations and inhibits amplitude. Graphs show the frequency of $[Ca^{2+}]_i$ oscillations occurrence per minute in the ‘oscillating’ population (A) and the amplitude of $[Ca^{2+}]_i$ oscillations in sperm population (B) under the three conditions: progesterone alone treatment and regular Vm (first bar), depolarisation Vm $E_K = -4$ mV (second bar) and restored Vm (third bar). Amplitude was calculated using the mean response of each $[Ca^{2+}]_i$ oscillation considering the initial transient peak as 100% and bars show mean \pm SEM of 260 $[Ca^{2+}]_i$ oscillations from 25 cells acquired in 3 experiments. A $[Ca^{2+}]_i$ oscillation was considered when reached at least 20% of the initial transient peak amplitude. Treatment groups with the same letters were not significantly different according to one-way ANOVA followed by Tukey’s post-hoc ($p < 0.05$).

In order to confirm that the effect of clamping Vm with VLN was dependent on the value of Vm, I performed experiments where, after establishing the progesterone-induced $[Ca^{2+}]_i$ oscillations, the membrane potential was first depolarised with VLN/100 mM K^+ and subsequently hyperpolarised with VLN in standard sEBSS ($E_K = -79$ mV) (fig. 3.15A). As previously described in figure 3.14, membrane depolarisation reduced $[Ca^{2+}]_i$ oscillations amplitude, but slightly altered the frequency. However, hyperpolarisation after depolarisation largely affected both amplitude and frequency of oscillations. Frequency was decreased by $95 \pm 0.01\%$ ($p < 0.001$; fig. 3.15B) and amplitude by $91.3 \pm 2.7\%$ ($p < 0.001$; fig. 3.15C), when compared to $[Ca^{2+}]_i$ oscillations before any membrane potential alteration. The $[Ca^{2+}]_i$ oscillations recovery was also affected, once frequency returns only to $42.3 \pm 0.01\%$ and amplitude $68.5 \pm 4.1\%$ ($n = 140$ $[Ca^{2+}]_i$ oscillations from 15 cells; $p < 0.001$) in comparison to the $[Ca^{2+}]_i$ oscillations generated in resting membrane potential (fig. 3.15B and C).

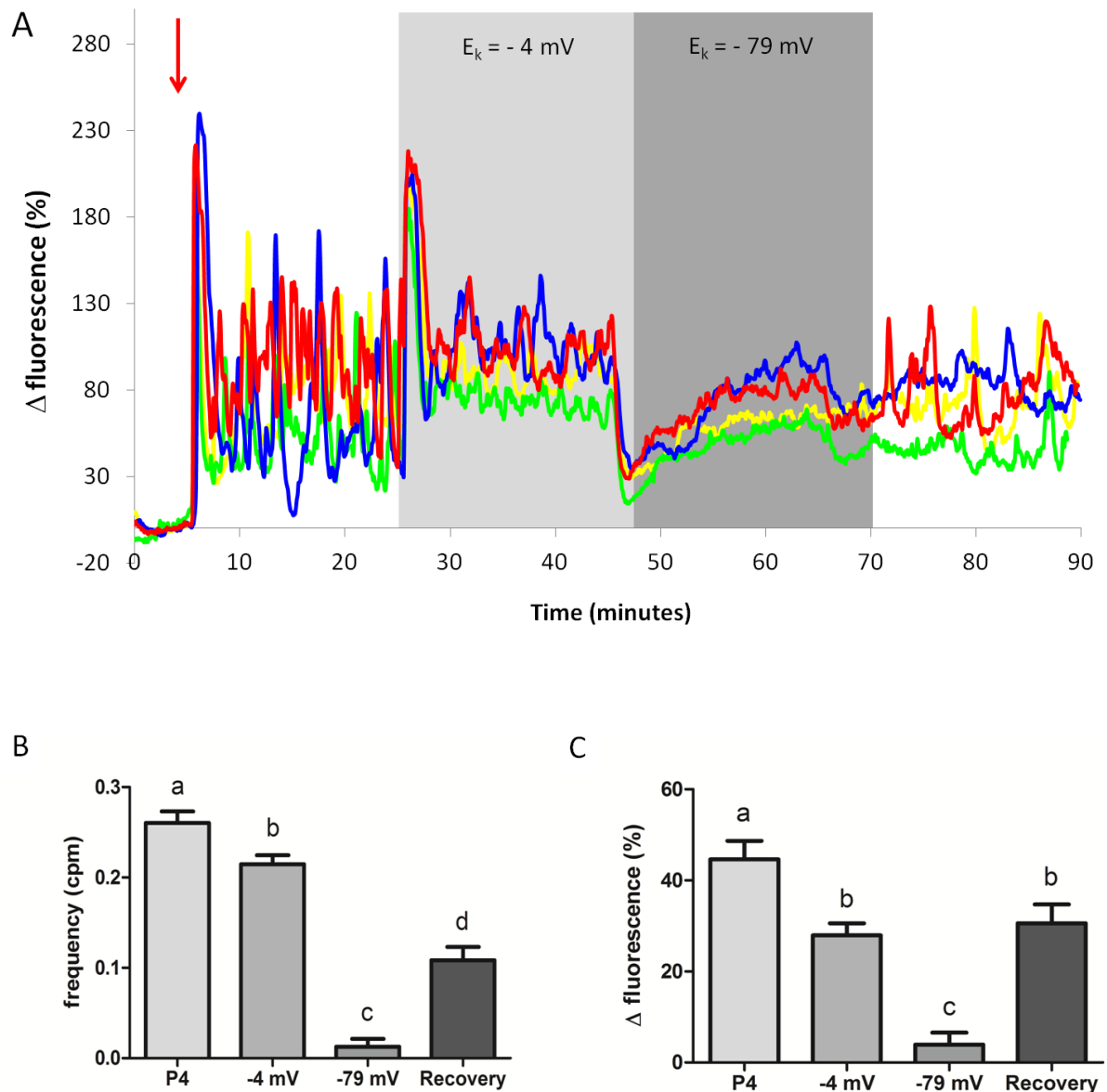


Figure 3.15 Progesterone-induced $[Ca^{2+}]_i$ oscillations generation is dependent on the value of V_m . (A) Panel shows single cell traces (4 cells from different set of experiments) generated from single cell images obtained in a time-lapse experiment. Dark grey shading indicates depolarised V_m (-4 mV), light grey shading indicates hyperpolarised V_m (-79 mV), red arrow shows addition progesterone (3 μ M). Graphs show the frequency of $[Ca^{2+}]_i$ oscillations occurrence per minute in the ‘oscillating’ population (B) and the amplitude of $[Ca^{2+}]_i$ oscillations in sperm population (C) under the four conditions: progesterone alone and regular V_m (first bar), depolarisation V_m $E_K = -4$ mV (second bar), hyperpolarisation V_m $E_K = -79$ mV (third bar) and restored V_m (forth bar). Amplitude was calculated using the mean response of each $[Ca^{2+}]_i$ oscillation considering the initial transient peak as 100% and bars show mean \pm SEM of 140 $[Ca^{2+}]_i$ oscillations from 15 cells acquired in 3 experiments. Treatment groups with the same letters were not significantly different according to one-way ANOVA followed by Tukey’s post-hoc ($p < 0.001$).

3.3.5.3 V_m close to resting potential (-38 mV) effect on $[Ca^{2+}]_i$ oscillations

Estimates of resting potential of capacitated mammalian sperm vary but values of -30 to -40 mV are typical (Espinosa and Darszon, 1995; Munoz-Garay et al, 2001; Demarco et al, 2003; Hernandez-Gonzalez et al, 2006; De La Vega-Beltran et al, 2012 and fig 3.9). To investigate whether the $[Ca^{2+}]_i$ oscillations might persist if V_m was clamped at a value close to resting potential I applied valinomycin in saline containing 25 mM K^+ (estimated $E_K = -38$ mV). Spermatozoa were stimulated with progesterone (3 μ M) then saline with 25 mM K^+ and valinomycin was applied after $[Ca^{2+}]_i$ oscillations had become established. Similar to the effects of hyperpolarised conditions, progesterone-induced $[Ca^{2+}]_i$ oscillations were inhibited and basal $[Ca^{2+}]_i$ activity was still observed. Progesterone-induced $[Ca^{2+}]_i$ oscillations were completely recovered when V_m was restored (fig. 3.16). The proportion of oscillating cells at $V_m = -38$ mV was approximately $57.1 \pm 9.5\%$ (fig. 3.11). Moreover, in those cells where $[Ca^{2+}]_i$ oscillations persisted, the effect on frequency was less marked than at -79 mV (compare fig 3.12A and 3.17A). When V_m was subsequently restored the frequency was recovered (fig. 3.17A). Amplitude of $[Ca^{2+}]_i$ oscillations was also less sensitive to clamping at -38 mV than at -79 mV (compare fig 3.12B and 3.17B). After restoring V_m by VLN washout $[Ca^{2+}]_i$ oscillations amplitude recovered to the levels recorded before V_m manipulation (fig. 3.17B).

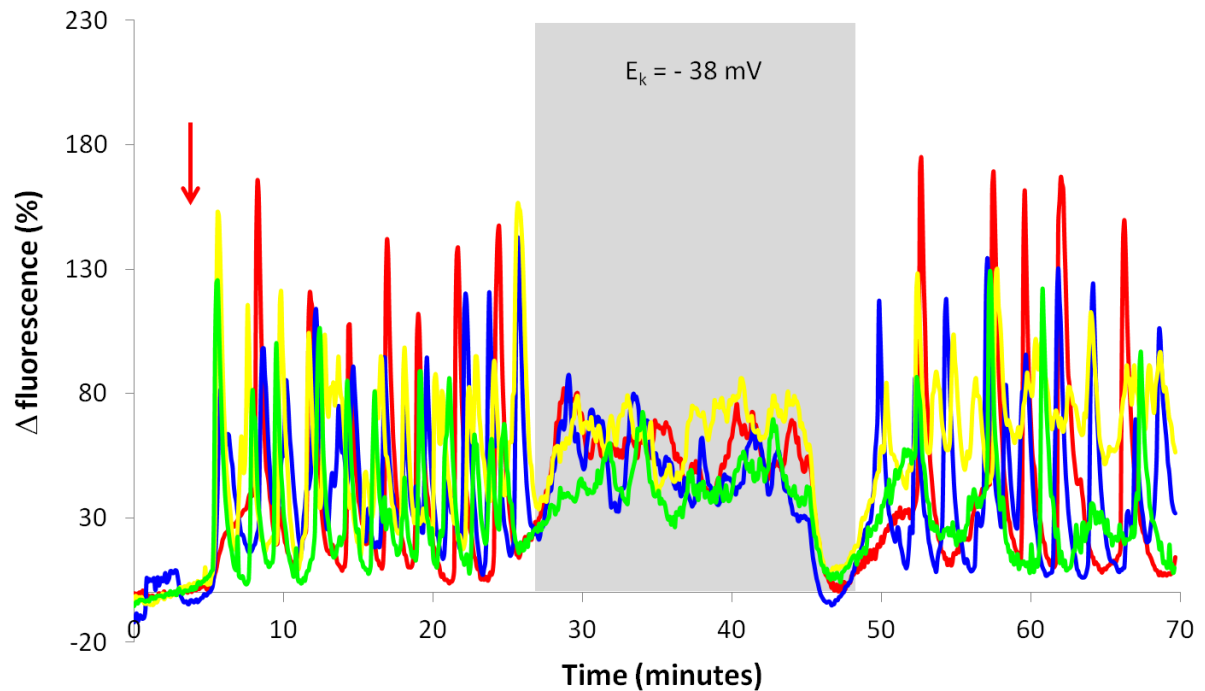


Figure 3.16 V_m close to resting potential (-38 mV) abolishes progesterone-induced $[Ca^{2+}]_i$ oscillations in sperm cells. $[Ca^{2+}]_i$ oscillations profile was completely recovered when VLN/25 mM K^+ was removed and V_m was restored. Representative histogram was generated from single cell images obtained in a time-lapse experiment. Grey shading shows treatment with VLN 25 mM K^+ , red arrow shows addition of progesterone (3 μ M).

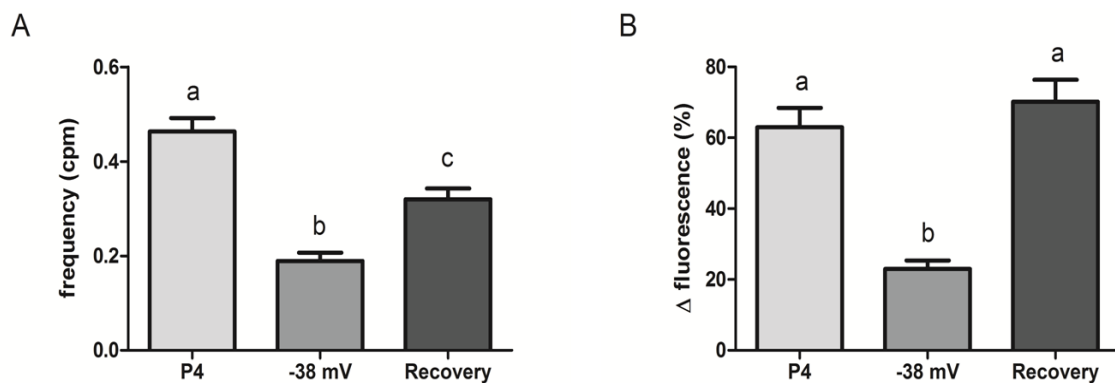


Figure 3.17 V_m close to resting potential (-38 mV) alters the frequency and amplitude of $[Ca^{2+}]_i$ oscillations. Graphs show the frequency of $[Ca^{2+}]_i$ oscillations occurrence per minute in the 'oscillating' population (A) and the amplitude of $[Ca^{2+}]_i$ oscillations in sperm population (B) under the three conditions: progesterone alone treatment and regular V_m (first bar), V_m $E_K = -38$ mV (second bar) and restored V_m (third bar). Amplitude was calculated using the mean response of each $[Ca^{2+}]_i$ oscillation considering the initial transient peak as 100% and bars show mean \pm SEM of 3 experiments. A $[Ca^{2+}]_i$ oscillation was considered when reached at least 20% of the initial transient peak amplitude. Treatment groups with the same letters were not significantly different according to one-way ANOVA followed by Tukey's post-hoc ($p < 0.001$).

Collectively, our results showed that progesterone induces $[Ca^{2+}]_i$ oscillations in human spermatozoa: 'rapid' transients resembling the initial progesterone transient. I also characterised that these oscillations require extracellular Ca^{2+} and that $[Ca^{2+}]_i$ rose first in the flagellum, consistent with activation of CatSper channels, then spread actively to the head, apparently triggering Ca^{2+} store release. Also, membrane potential contributes to progesterone-induced $[Ca^{2+}]_i$ oscillations generation.

3.4 Discussion

Ca^{2+} signalling is critical for regulation of sperm motility and in human spermatozoa is mainly mediated by influx of extracellular Ca^{2+} through CatSper channels. Progesterone, released by the cumulus cells layer surrounding the oocyte, can activate CatSper channels and typically induces a rapid and biphasic Ca^{2+} entry into spermatozoa. Several studies have described progesterone biphasic response as an initial transient peak, which lasts approximately 1 to 2 minutes, followed by a long-lasting plateau, named sustained phase (Blackmore et al, 1990; Meizel and Turner, 1991, Kirkman-Brown et al, 2000; fig 3.2). Similar response was also described in sea urchin sperm cells. Gonzalez-Martinez and colleagues (2001) and Hirohashi and Vacquier (2003) showed that peptides released by sea urchin egg promotes Ca^{2+} fluctuations.

Interestingly, single-cell imaging analysis showed that approximately a quarter of the sperm cell population exhibits cyclical $[\text{Ca}^{2+}]_i$ oscillations after progesterone exposure instead of the typical long-lasting plateau phase (figs. 3.3 and 3.4). In hamster spermatozoa, Suarez and colleagues (1993) showed that high frequency spontaneous $[\text{Ca}^{2+}]_i$ oscillations occurs in hyperactivated sperm and are related to flagellar bending. In sea urchin sperm, $[\text{Ca}^{2+}]_i$ oscillations were identified both spontaneously and also after stimulation with speract, an oligopeptide released by the egg of *Strongylocentrotus purpuratus*, and they may also be related to motility activity (Wood et al, 2003). $[\text{Ca}^{2+}]_i$ oscillations have also been recognised in human sperm cells. In 2004, Kirkman-Brown and colleagues and also Harper and colleagues showed that human sperm exhibit $[\text{Ca}^{2+}]_i$ oscillations in response to progesterone and their kinetics are slow, each cycle lasting approximately 2 to 3 minutes. A similar pattern of $[\text{Ca}^{2+}]_i$ oscillations was later observed in studies published by Aitken and McLaughlin

(2007) and Bedu-Addo and colleagues (2007) in the same type of cell. Although $[Ca^{2+}]_i$ oscillations have been previously described, the Ca^{2+} signalling pathways involved in this behaviour are not completely clear yet.

Our data shows that Ca^{2+} oscillations induced by progesterone occur in the whole sperm cell, initiating the flagellum and then propagating forward towards the sperm head, through the neck (figs. 3.7 and 3.8). This characterisation is important as it suggests that $[Ca^{2+}]_i$ oscillations may start due to activation of CatSper channels, which are found only in the principal piece of the sperm flagellum. Moreover the $[Ca^{2+}]_i$ oscillation amplitudes observed in the neck and head of the sperm were greater than initially started at the flagellum. This enhanced signal must be achieved by further Ca^{2+} mobilisation, probably releasing Ca^{2+} from intracellular stores by CICR, in response to CatSper-mediated Ca^{2+} entry (fig. 3.7). As $[Ca^{2+}]_i$ oscillations may start through activation of CatSper channels and these channels are regulated by membrane potential (V_m), we decided to investigate the contribution of changes in V_m to the generation of $[Ca^{2+}]_i$ oscillations. Our results demonstrates that progesterone-induced $[Ca^{2+}]_i$ oscillations were completely inhibited by membrane hyperpolarisation (fig. 3.10, 3.11 and 3.12). However, $[Ca^{2+}]_i$ oscillations were highly resistant when membrane potential was depolarised (fig 3.13 and 3.14). Furthermore, membrane potential close to resting V_m had intermediate effects on the $[Ca^{2+}]_i$ oscillations, not completely inhibiting frequency or amplitude (fig. 3.16 and 3.17). These observations differ from those described by Kirkman-Brown and colleagues (2004). In their work valinomycin did not change the proportion of oscillating cells or alter the characteristics of the $[Ca^{2+}]_i$ oscillations, suggesting that V_m was not involved in $[Ca^{2+}]_i$ oscillations generation in human sperm cells. The reason for this difference is not clear but we suspect that the valinomycin used in that study did not effectively clamp V_m . Therefore, our work is the first report that changes in membrane

potential may contribute to the generation of progesterone-induced $[Ca^{2+}]_i$ oscillations in human sperm, suggesting that CatSper may be involved in this oscillation profile, potentially triggering CICR.

CHAPTER FOUR: RU1968-F1, A NEW PHARMACOLOGICAL TOOL TO INVESTIGATE CATSPER IN HUMAN SPERMATOZOA

4.1 Abstract

The sperm-specific CatSper channel has been shown to modulate the intracellular Ca^{2+} concentration ($[\text{Ca}^{2+}]_i$), to regulate sperm behaviour and to be crucial for fertilisation and male fertility (Ren et al, 2001; Quill et al, 2003; Publicover et al, 2008; Lishko et al, 2010; Alvarez et al, 2014). Currently, NNC-0396, mibefradil, MDL12330A and HC-056456 are the drugs being used as pharmacological tools to study CatSper; however, they are not selective and promote toxic effects to the sperm cells. I aimed to characterise the action of RU1968, a potential CatSper inhibitor resynthesised by Dr. Timo Strunker's lab group (University of Münster – Germany). $[\text{Ca}^{2+}]_i$ signalling was assessed by loading sperm cells with the Ca^{2+} -indicator fluo-4-AM, pre-treating them with different concentrations of RU1968 and then stimulating with progesterone (P4 - 3 μM). RU1968 shows a dose dependent effect on the transient phase induced by P4. RU1968 - 30 μM inhibited the peak by $74.9 \pm 7.5\%$; while the highest concentration 50 μM promoted an $81.6 \pm 0.9\%$ peak inhibition. Moreover, when the inhibitor was removed a rebound peak was observed. The time for peak recovery and duration of peak was dependent on the drug concentration. The peak recovery took up to 247.5 ± 47.5 seconds to occur (RU1968 - 50 μM) and longest peak duration occurred after RU1968 30 μM and 50 μM removal, 303.8 ± 44.6 and 445.7 ± 17.4 seconds, respectively. These data together with those obtained by the collaborators of Dr. Timo Strunker (Rennhack et al, 2018) suggest that RU1968 is effective in inhibiting CatSper and could be used as a new pharmacological tool in the study of these Ca^{2+} channels.

4.2 Introduction

CatSper is a sperm-specific Ca^{2+} channel which has been shown to be critical for a successful fertilisation and for male fertility (Ren et al, 2001; Quill et al, 2003). CatSper is sensitive to increasing of intracellular pH, is dependent of voltage and can be stimulated by progesterone, prostaglandins and other ligands, which modulates Ca^{2+} influx into sperm cells (Ren et al, 2001; Quill et al, 2001; Kirichok et al, 2006; Navarro et al, 2008; Lishko et al, 2011; Brenker et al, 2012). The localisation of these Ca^{2+} channels is strictly on the plasma membrane of the principal piece of the sperm flagellum (Ren et al, 2001; Carlson et al, 2005; Jin et al, 2007) constituting the primary source of Ca^{2+} flux into the cytosol. $[\text{Ca}^{2+}]_i$ signals are necessary for regulation of hyperactivated motility, which enables sperm to ascend beyond the oviductal reservoir (Kirichok et al, 2006; Ho et al, 2009) and penetrate the zona pellucida surrounding the oocyte (Ren et al, 2001; Quill et al, 2003, 2007). The role of CatSper channels in sperm hyperactivated motility and in the fertilisation process has been well studied in mice, particularly through generation of CatSper-null mice which produces 'normal' sperm lacking the channel (Ren et al, 2001). The importance of these channels in human sperm is still debatable. Some studies show that mutations in human CatSper genes and CatSper dysfunction could be associated with infertility (reviewed in Hildebrand et al, 2010; Williams et al, 2015), but the number of cases analysed was very low and sperm motility parameters varied largely between different samples. A better method to investigate this relationship would be to express or mutate CatSper channels in cultured cells however such technique has not been achieved yet. The identification of specific CatSper channel blockers can provide a powerful tool to investigate Ca^{2+} signalling in sperm and help to address the physiological role and temporal aspects of CatSper in human sperm.

Currently, NNC-0396, mibefradil, MDL12330A and HC-056456 are the drugs being

used as CatSper inhibitors (Carlson et al, 2009; Lishko et al, 2011; Strünker et al, 2011; Brenker et al, 2012) however, they show evidence of side effects: in addition to inhibition of CatSper they also inhibit Slo3 channels, might promote acrosomal exocytosis and sustained increase of cytosolic Ca^{2+} and also show toxicity to the sperm cells (Navarro et al, 2007; Carlson et al, 2009; Brenker et al, 2012, 2014; Mansell et al, 2014; Tamburrino et al, 2014; Chavez et al, 2017).

Shaefer and colleagues (2000) reported that the bis-TFA salt named RU1968 (fig. 4.1), which was classically described as a steroidal sigma ligand, could act as a potent inhibitor of human sperm activation, more specifically by blocking Ca^{2+} influx induced by progesterone and prostaglandin E1. However, the mechanism of RU1968 in spermatozoa remained unclear and was not shown to be dependent of activation of sigma receptors (Shaefer et al, 2000). The laboratory team of Dr. Timo Strunker (University of Münster – Germany) has been resynthesizing RU1968 and, in collaboration with other groups, revisited its mechanism of action in sperm from humans, mice, and sea urchins, in order to elucidate whether the drug would actually modulate CatSper in a more effective fashion than the usual drugs used as pharmacological tools to investigate CatSper channels.

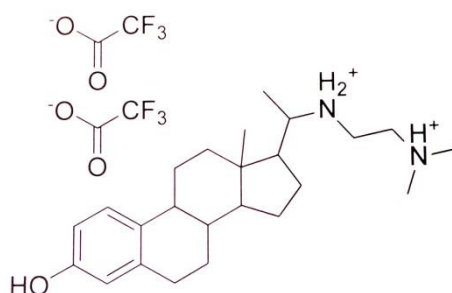


Figure 4.1 Molecular structure of the potential CatSper inhibitor RU1968. RU1968 is a bis-trifluoroacetate salt molecule, resynthesised by Dr. Timo Strunker's lab team, which presents a molecular weight of 598.63 and chemical formula $\text{C}_{28}\text{H}_{40}\text{F}_6\text{N}_2\text{O}_5$.

Chapter Aims

The aim of this chapter was to characterise the action of RU1968, re-synthesised by Dr. Timo Strunker's group, and its effects on the Ca^{2+} CatSper channel. I wanted to investigate whether the drug could inhibit the CatSper-dependent $[\text{Ca}^{2+}]_i$ increase induced by progesterone.

4.3 Results

4.3.1 RU1968 inhibits Ca^{2+} response induced by progesterone

In order to characterise the action of RU1968 on Ca^{2+} CatSper channels, I performed Ca^{2+} imaging experiments to confirm if the pharmacological tool could inhibit the effect induced by progesterone. Progesterone alone induces a biphasic Ca^{2+} response in human sperm cells – a transient peak followed by a sustained phase. RU1968 inhibited the transient phase induced by progesterone in a dose dependent way. Moreover, when the inhibitor was removed a rebound peak was observed (fig. 4.2 and 4.3).

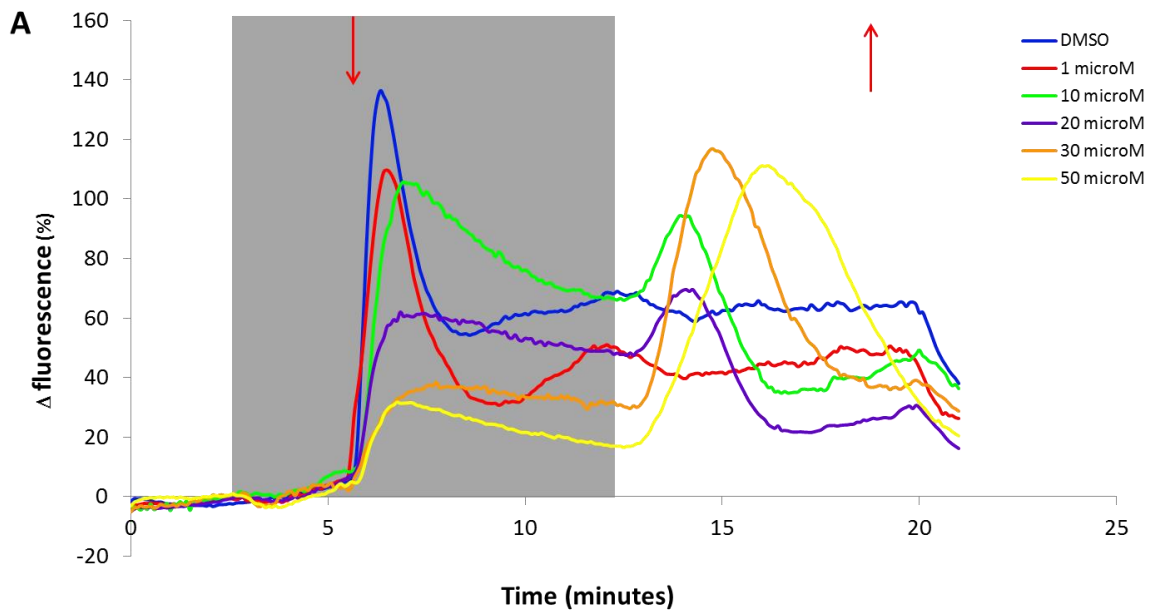


Figure 4.2 RU1968 inhibits Ca^{2+} response induced by progesterone in a dose-dependent curve. (A) Graph shows mean effects of treatment with DMSO (blue; n = 10 experiments, 440 cells), 1 μM RU1968 (red; n = 4 experiments 218 cells), 10 μM RU1968 (green; n=3 experiments, 127 cells), 20 μM RU1968 (purple; n=3 experiments, 157 cells), 30 μM RU1968 (orange, n=3 experiments, 129 cells), 50 μM RU1968 (yellow, n= 3 experiments, 123 cells). Grey shading shows period of treatment with RU1968 or DMSO, red arrows show addition and removal of 3 μM progesterone.

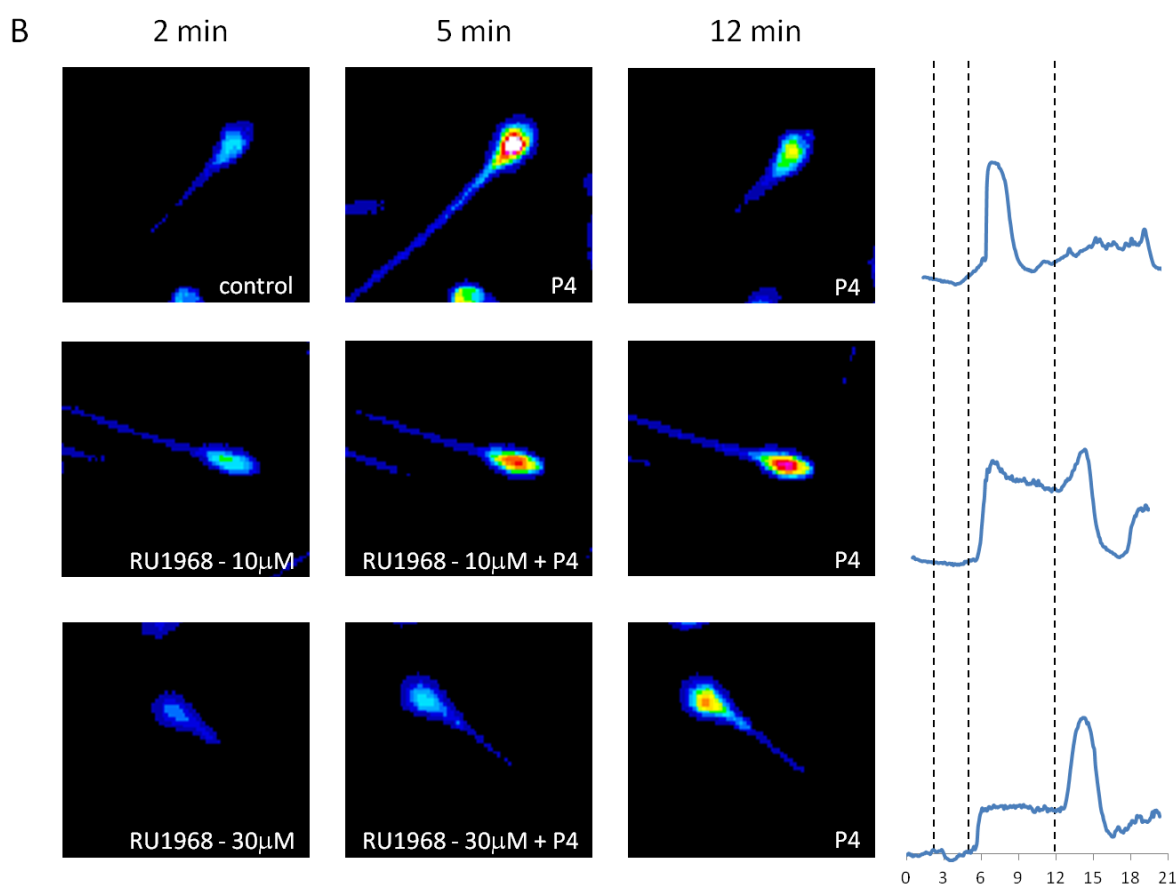


Figure 4.2 RU1968 inhibits Ca^{2+} response induced by progesterone in a dose-dependent curve. Panel (B) shows representative images of three individual cells and their respective Ca^{2+} traces (right) in response to addition of RU1968 (at minute 2), stimulation with progesterone (at minute 5) and RU1968 removal (at minute 12). Upper row = control cell treated with P4 only; middle row = cell pre-treated with $10 \mu\text{M}$ RU1968 and treated with P4; lower row = cell pre-treated with $30 \mu\text{M}$ RU1968 and treated with P4. Ca^{2+} signals are shown under a 32 bit look-up table, in which white represents maximum fluorescence intensity and dark blue means minimum fluorescence intensity.

4.3.2 Effect of RU1968 on the progesterone-induced $[\text{Ca}^{2+}]_i$ transient

The concentrations $1 \mu\text{M}$ and $10 \mu\text{M}$ of RU1968 inhibited the transient peak by $17.0 \pm 9.6\%$ and $25.4 \pm 3.0\%$, respectively. At higher concentrations ($20\text{-}50 \mu\text{M}$) the effect was saturated as peak inhibition of $20 \mu\text{M}$, $30 \mu\text{M}$ and $50 \mu\text{M}$ were not statically significant different. RU1968 $20 \mu\text{M}$ showed a $56.6 \pm 8.7\%$ of peak inhibition; $30 \mu\text{M}$ inhibited the peak

in $74.8 \pm 7.5\%$; while the highest concentration $50 \mu\text{M}$ caused an $81.6 \pm 0.9\%$ inhibition of peak amplitude (fig. 4.3).

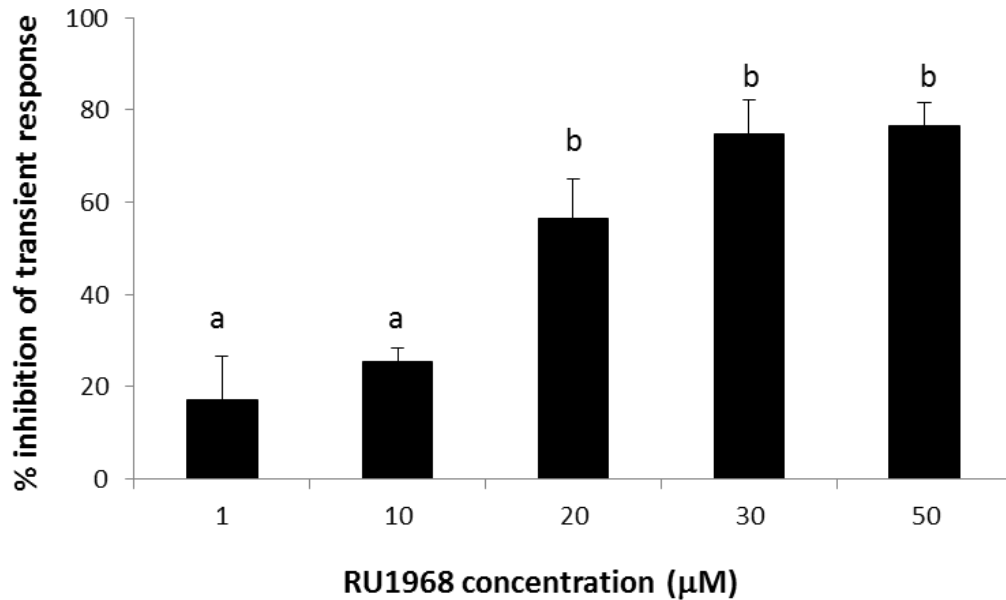


Figure 4.3 RU1968 inhibits the transient peak induced by progesterone in a dose-dependent way. Graph represents effect of different RU1968 concentrations on the amplitude of the progesterone-induced $[\text{Ca}^{2+}]_i$ peak (expressed as percentage inhibition). Treatment groups with the same letters were not significantly different according to one-way ANOVA followed by Tukey's post-test ($p < 0.05$). Inhibition was calculated using the mean response in each experiment and bars show mean \pm SEM of 3 experiments.

To further characterise the inhibition of the $[\text{Ca}^{2+}]_i$ transient in individual cells, I analysed the amplitude distribution of the transient in the presence of different RU1968 concentrations (fig. 4.4). In the presence of lower concentrations of RU1968 ($1 \mu\text{M}$ and $10 \mu\text{M}$) the most noticeable effect was a reduction in the frequency of very large $[\text{Ca}^{2+}]_i$ transients (amplitudes over $200\% \Delta$ fluorescence), the majority of cells showed transients between $50 - 150\% \Delta$ fluorescence. Higher concentrations of the drug ($20 \mu\text{M}$, $30 \mu\text{M}$ and 50

μM) completely abolished the occurrence of transient amplitudes over 200%. The proportion of the cell population which generated transient amplitudes between 0 - 50% Δ fluorescence was 43.31% (20 μM), 60.47% (30 μM) and 82.86% (50 μM).

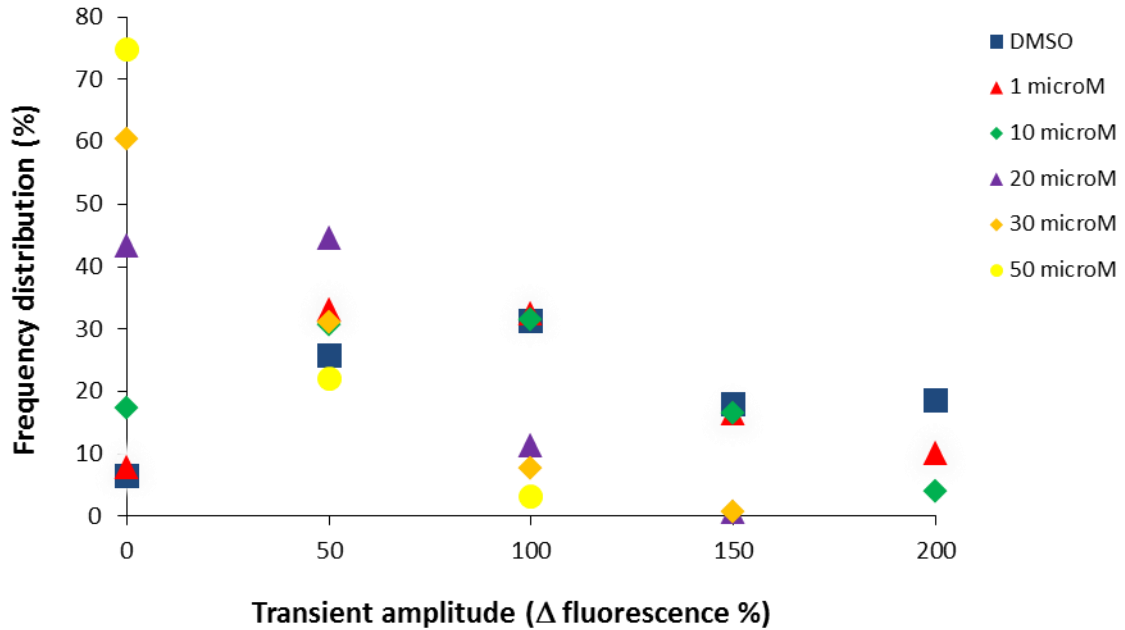


Figure 4.4 RU1968 alters the amplitude distribution of $[Ca^{2+}]_i$ transients induced by progesterone in a dose-dependent way. Graph represents the percentage of cells exhibiting different transient amplitudes in the presence of RU1968 concentrations.

As the lower doses of RU1968 (1 μM and 10 μM) primarily inhibited the occurrence very large transient responses (>200% Δ fluorescence), I decide to analyse this population in more detail. Data shows that cells treated with 1 μM and 10 μM of RU1968 exhibited maximum transient amplitudes of 285% and 385% Δ fluorescence, respectively, while in untreated cells, transient amplitudes over 500% Δ fluorescence occurred (fig. 4.5).

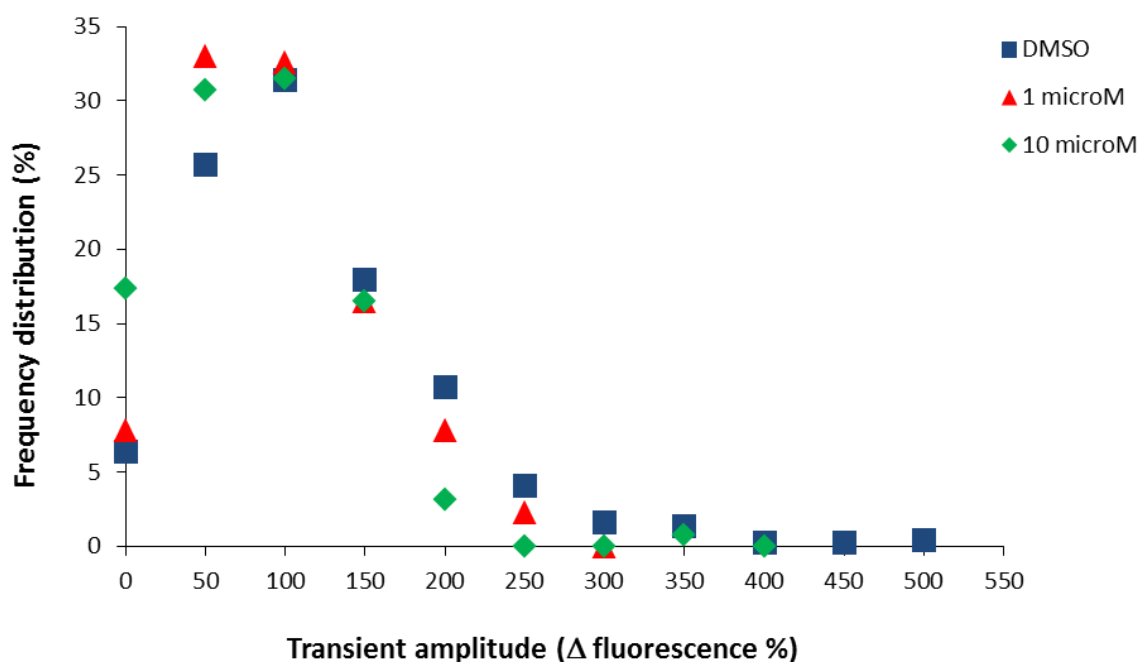


Figure 4.5 Low concentrations of RU1968 inhibit the frequency distribution of the highest transient amplitudes induced by progesterone. Graph represents the percentage of cells exhibiting different transient amplitudes in the presence of RU1968 concentrations.

4.3.3 RU1968 removal promotes $[Ca^{2+}]_i$ rebound peak

After removal of the inhibitor from the recording chamber (in the continued presence of progesterone), a rebound peak was observed (fig. 4.2). The time to maximum (latency) was dependent on the drug concentration. No rebound peak was seen with 1 μ M (inhibition in this concentration was low as showed in fig. 4.2 and fig. 4.3) but at higher doses the latency of the rebound peak was clearly dose dependent (66.7 ± 14.2 , 65.0 ± 18.0 , 116.7 ± 14.2 and 247.5 ± 47.5 s at 10 μ M, 20 μ M, 30 μ M and 50 μ M respectively; fig. 4.6).

Rebound peak also differed in its duration dependent on the drug concentration. The rebound peak after RU1968 10 μ M removal lasted 240.7 ± 29.1 s. A similar duration was also observed after 20 μ M, (242.4 ± 16.6 s) but longer durations were observed after RU1968 30 μ M and 50 μ M removal, 303.8 ± 44.6 and 445.7 ± 17.4 s, respectively (fig. 4.7).

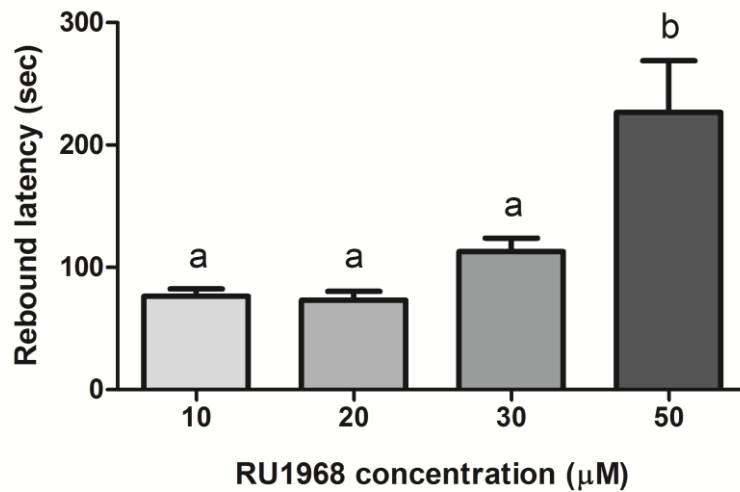


Figure 4.6 Latency to rebound is dependent on the RU1968 concentration. Bars show time to the rebound peak to occur after removal of RU1968. Latency was calculate using the mean response in each experiment and bars show mean + SEM of 3-4 experiments. Treatment groups with the same letters were not significantly different according to one-way ANOVA followed by Tukey’s post-test ($p < 0.05$).

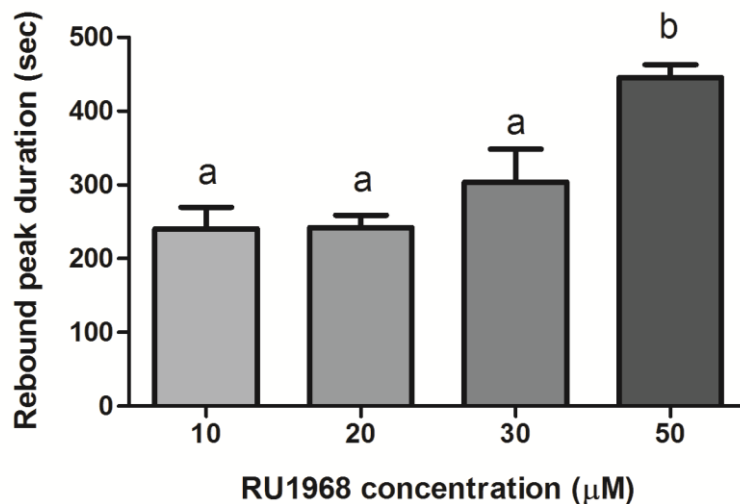


Figure 4.7 Rebound peak duration is dependent on the RU1968 concentration. Graph represents the duration of the rebound after removal of different RU1968 concentrations. Rebound peak duration was calculate using the mean response in each experiment and bars show mean + SEM of 3-4 experiments. Treatment groups with the same letters were not significantly different according to one-way ANOVA followed by Tukey’s post-test ($p < 0.05$).

4.4 Discussion

The aim of these experiments was to confirm the effectiveness of RU1968 as a pharmacological tool to investigate CatSper channels. Besides the results shown in this chapter, Dr. Timo Strunker's lab group and other collaborators worked in different techniques and biological models to confirm the RU1968 specificity in blocking CatSper. These data have been recently published (Rennhack et al, 2018).

Results in Ca^{2+} fluorimetry show that RU1968 blocks Ca^{2+} influx induced by progesterone and prostaglandin E1 in a dose dependent manner, IC_{50} values of $4 \pm 2 \mu\text{M}$ and $3.8 \pm 0.5 \mu\text{M}$, respectively (Rennhack et al, 2018). A previous study with classical drugs used as CatSper inhibitors, mibefradil and NNC55-0396, shows that both drugs inhibit Ca^{2+} responses promoted by progesterone and prostaglandin E1 but the potency was lower than RU1968 and at (effective) high doses the inhibitors promoted Ca^{2+} responses *per se*, due to a lack of specificity of the molecules for CatSper channels (Strunker et al, 2011). This lack of specificity limits the use of mibefradil and NNC55-0396 as a selective inhibition of CatSper can not be achieved. Moreover, Tamburrino and colleagues (2014) showed that mibefradil can be toxic to human sperm, thereby, affecting the data collected in live sperm experiments. In contrast, even at high micromolar concentrations of RU1968 (30 μM), the inhibitor did not affect human sperm motility or viability (Rennhack et al, 2018), suggesting that RU1968 lacks the toxic and adverse off-target actions of NNC, Mibefradil, and MDL in human sperm. Whole-cell patch clamp showed that RU1968 completely abolished CatSper channel currents with an IC_{50} of $0.4 \pm 0.3 \mu\text{M}$ in human sperm cells and only inhibits the K^{+} channel Slo3 current with an IC_{50} of $7 \pm 6 \mu\text{M}$, a 15-fold higher concentration to the one required for CatSper blockade (Rennhack et al, 2018). The classical CatSper blockers: NNC, Mibefradil, and MDL suppress CatSper currents (Lishko et al, 2011; Strunker et al, 2011; Brenker et al,

2012), but they also inhibit Slo3 (Navarro et al, 2007; Carlson et al, 2009; Brenker et al, 2014; Mansell et al, 2014) with similar potency.

The IC₅₀ values for block of progesterone-induced [Ca²⁺]_i signals by RU1968 from single-cell imaging experiments, shown in this chapter, is 17.5 + 1.2 μM, which is higher than the one calculated from Ca²⁺ fluorimetry experiments (4 ± 2 μM; Rennhack et al, 2018). This is probably due to the hydrophobicity of the molecule. Accumulation of the drug on the inside the plastic perfusion tubing may occur during perfusion, such that the sperm in the imaging chamber do not ‘see’ the applied dose. When the drug was directly added to the imaging chamber in experiments, without perfusion, the kinetics of the responses to progesterone were very slow (because mixing within the chamber is poor) but the IC₅₀ for block by RU1968 was similar to the Ca²⁺ fluorimetry experiments (Rennhack et al, 2018). However, I considered it to be important to also perform experiments under perfusion once to understand the kinetics of the drug effect, particularly drug washout. In figure 4.2, I showed that the effect of RU1968 is reversible and, after its removal in the continued presence of progesterone, a rebound peak was observed which had dose-dependent characteristics.

Collectively, the data presented in this chapter, in combination with those obtained by the other collaborators of Dr. Timo Strunker (Rennhack et al, 2018) suggest that RU1968 is an effective and acceptably selective inhibitor of CatSper channels that lacks toxic side effects in human sperm. It could be used as a new pharmacological tool in the study of these Ca²⁺ channels. An improved molecule, such as RU1968, can reveal CatSper channel properties and provide conditions to understand its roles to sperm physiology. Furthermore, RU1968 could be used as a lead structure to develop non-hormonal contraceptives, once it mimics the lack of CatSper associated with male infertility and fertilisation prevention.

CHAPTER FIVE: INVESTIGATION OF THE MECHANISM OF $[Ca^{2+}]_i$ OSCILLATIONS

5.1 Abstract

Membrane potential controls progesterone-induced $[Ca^{2+}]_i$ oscillations in human sperm cells, which may be involved in regulation of sperm motility and 'switch' of sperm behaviour. I aimed to identify the main ion channels that could contribute to generation of $[Ca^{2+}]_i$ oscillations. Progesterone-induced $[Ca^{2+}]_i$ oscillations were established for 20 minutes before treatment with different ion channels blockers. Slo3 channel block (quinidine – 0.3 mM) completely abolished progesterone-induced and basal $[Ca^{2+}]_i$ oscillations. Treatment with CatSper blocker (RU1968F1 - 30 μ M) decreased the proportion of 'oscillating' cells by $53.5 \pm 2.9\%$. Moreover, the frequency of $[Ca^{2+}]_i$ oscillations in these cells was reduced by $91.2 \pm 0.01\%$. Treatment with Cl^- free medium reduced $[Ca^{2+}]_i$ oscillation frequency in $56.7 \pm 0.02\%$ of cells but did not completely abolish $[Ca^{2+}]_i$ oscillations in any cell evaluated. Investigation of Cl^- channels (CFTR and CaCC) was conducted with the blockers CFTR(inh)-172 - 10 μ M and niflumic acid - 30 μ M, respectively. None of the drugs affected the proportion of 'oscillating' cells or altered any $[Ca^{2+}]_i$ oscillations characteristics, such as frequency and amplitude. Collectively, our data suggests that progesterone-induced $[Ca^{2+}]_i$ oscillations are generated by CatSper activation and depends on activity of Slo3. I suggest that CatSper-mediated $[Ca^{2+}]_i$ elevation may open Slo3 channels at the plasma membrane, which cause hyperpolarisation of membrane potential and closes CatSper. Re-establishment of resting $[Ca^{2+}]_i$ allows Slo3 to close, membrane potential is restored and CatSper, in the

presence of progesterone, opens again promoting increase of $[Ca^{2+}]_i$. However, the participation of Cl^- ion components is still not clear.

5.2 Introduction

The ion fluxes across the plasma membrane regulate a wide range of physiological processes including intracellular pH (pH_i), transcellular transport, cell volume, cell signalling pathways, enzymes activation/inactivation. In spermatozoa a role for membrane potential (V_m) has been described in the regulation of sperm capacitation in the female reproductive tract, chemotaxis and acrosome reaction (Eisenbach, 1999; Visconti et al, 2002; Darszon et al, 2005). In chapter 3, I showed that membrane potential also controls progesterone-induced $[\text{Ca}^{2+}]_i$ oscillations in human sperm cells, which may underlie ‘switching’ of sperm behaviour, believed to be important for sperm progression in the female tract.

The activity of K^+ channels, which modulates the flow of K^+ ions, is the primarily source underlying the establishment of membrane potential. In spermatozoa, the only K^+ current that was shown to be crucial to set the resting membrane potential is a pH-sensitive K^+ current, originally named $I_{\text{K}^{\text{Sper}}}$ (Navarro et al, 2007) and now identified to be carried by an exclusive sperm-specific K^+ channel, Slo3 (Santi et al, 2010; Zeng et al, 2011, Brenker et al, 2014). Slo3 channels are voltage-gated, activated by intracellular alkalinisation and are localised in the principal piece of the sperm flagellum (Navarro et al, 2007). They play important role on sperm physiology and critical steps of the fertilisation, such as sperm osmoregulation, acrosomal exocytosis and sperm motility (Santi et al, 2010; Tang et al, 2010; Zeng et al, 2011). Therefore, Slo3 channels would be a strong candidate on setting membrane potential, which regulates the progesterone-induced $[\text{Ca}^{2+}]_i$ oscillations generation.

In addition to K^+ fluxes, Cl^- flow might be involved in the modulation of plasma membrane potential in sperm cells. Typically, Cl^- transport across the membrane is known to be important to cell volume regulation and osmotic stress protection, which has already been

characterised in spermatozoa (Furst et al, 2002; Yeung et al, 2005; Cooper and Yeung, 2007). However, a few studies have also demonstrated that capacitation of human spermatozoa incubated in media containing low concentration of Cl^- is significantly reduced (Hernandez-Gonzalez et al, 2007; Wertheimer et al, 2008; Chen et al, 2009; Orta et al, 2012; Figueiras-Fierro et al, 2013). The capacitation-associated processes affected by absence of external Cl^- include: increase in tyrosine phosphorylation and cAMP levels, hyperactivated motility, ZP-induced acrosome reaction and hyperpolarisation of the sperm Em. The mechanisms by which Cl^- ions contributes to the modulation of the sperm membrane potential is still unclear, but estimated E_{Cl} of human sperm with 140 mM extracellular $\text{Cl}^- \approx -24$ mV (Garcia and Meizel, 1999) which would shift to +55 mV upon reduction of $[\text{Cl}^-]_o$ to 1 mM.

Changes in membrane potential can also control activation of others membrane ion channels and transporters, including the sperm-specific Ca^{2+} -permeable channel CatSper (Darszon et al, 1999, 2011; Lishko et al, 2012). CatSper is believed to be the main channel involved on the influx of extracellular Ca^{2+} in human spermatozoa, which is critical for proper sperm function and successful fertilisation (Ren et al, 2001; Quill et al, 2003; Carlson et al, 2003, 2005; Qi et al, 2007; Xia et al, 2007). CatSper channels are sensitive to increased intracellular pH, are dependent on voltage, can be stimulated by progesterone and are strictly localised on the plasma membrane of the principal piece of the sperm flagellum (Ren et al, 2001; Quill et al, 2001; Kirichok et al, 2006; Jin et al, 2007; Navarro et al, 2008; Brenker et al, 2012). The properties of the newly-described CatSper inhibitor RU1968F1, described in chapter 4, provided the possibility to investigate and understand the role of CatSper channels in the generation of progesterone-induced $[\text{Ca}^{2+}]_i$ oscillations.

Chapter Aims

The aims of this chapter were to identify the sperm cell components involved on the generation of progesterone-induced $[Ca^{2+}]_i$ oscillations and also to propose a model for its mechanism.

5.3 Results

5.3.1 CatSper channels contribution to $[Ca^{2+}]_i$ oscillations

As I previously showed in chapter 3, progesterone-induced $[Ca^{2+}]_i$ oscillations are sensitive to membrane potential and they initiate in the flagellum then spread actively towards the sperm head. Therefore, we suggested CatSper channels would be an excellent candidate to $[Ca^{2+}]_i$ oscillations mechanism since they are restricted to the sperm flagellum and their activation is dependent on membrane potential and also progesterone (Ren et al, 2001; Quill et al, 2001; Kirichok et al, 2006; Navarro et al, 2008; Brenker et al, 2012). To investigate whether CatSper is involved in $[Ca^{2+}]_i$ oscillations generation, fluo4-labelled spermatozoa were stimulated with progesterone to induce $[Ca^{2+}]_i$ oscillations and CatSper inhibition was then performed using RU1968 (10 μ M or 30 μ M). RU1968 has been proven to be an effective inhibitor of CatSper channels in human sperm (chapter 4 of this thesis; Rennhack et al, 2018). $69.6 \pm 5.9\%$ of 'oscillating' cells continued to oscillate in the presence of 10 μ M RU1968 treatment (fig 5.1A). In these cells, oscillation frequency was reduced by $38.3 \pm 0.01\%$, but amplitude was slightly increased (by $26.4 \pm 3.1\%$; $n= 455 [Ca^{2+}]_i$ oscillations from 65 cells; $p<0.001$; fig. 5.1B and C).

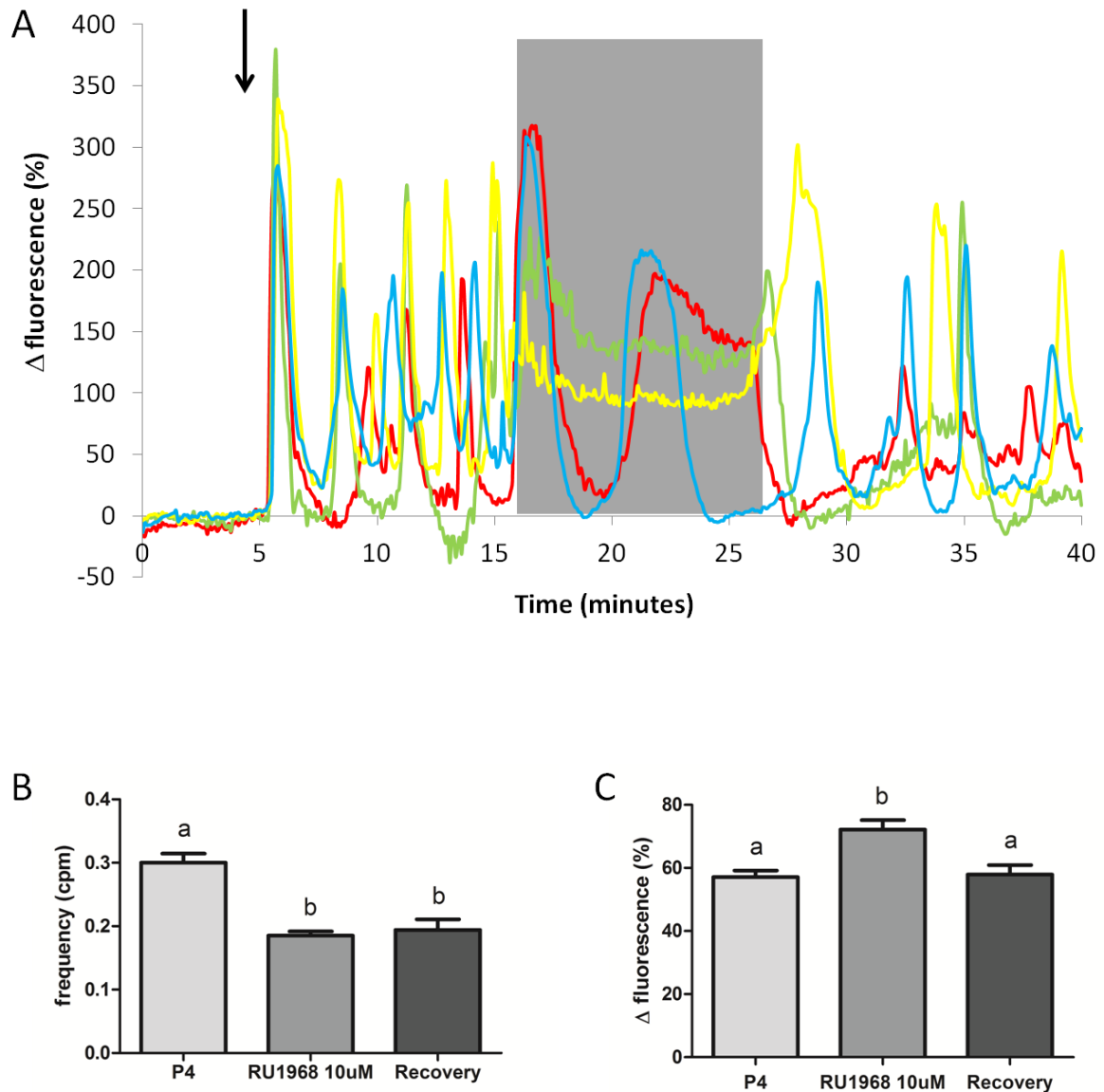


Figure 5.1 CatSper blocker (RU1968F1 – 10 μ M) inhibits [Ca²⁺]_i oscillations frequency in human sperm cells, but not their amplitude. Panel (A) shows single cells traces (4 cells from different set of experiments). Black arrow indicates addition of 3 μ M progesterone; grey shading shows period of treatment with 10 μ M RU1968. Graphs show the frequency of [Ca²⁺]_i oscillations occurrence per minute in the ‘oscillating’ population (B) and the amplitude of [Ca²⁺]_i oscillations in sperm population (C) under the three conditions: progesterone alone (first bar), progesterone plus 10 μ M RU1968 treatment (second bar) and progesterone alone (third bar). Amplitude was calculated using the mean response of each [Ca²⁺]_i oscillation considering the transient peak as 100% and bars show mean \pm SEM of 3 experiments. A [Ca²⁺]_i oscillation was considered when reached at least 20% of the transient peak amplitude. Treatment groups that do not share a letter are significantly different according to one-way ANOVA followed by Tukey’s post-hoc ($p < 0.001$). A total of 455 [Ca²⁺]_i oscillations from 65 cells were analysed.

Treatment with higher concentration 30 μM RU1968 was more effective than that observed with 10 μM RU1968. Only $7.8 \pm 2.2\%$ of ‘oscillating’ cells continued to oscillate in the presence of 30 μM RU1968 (n=80 cells per treatment; $p < 0.01$; fig. 5.2).

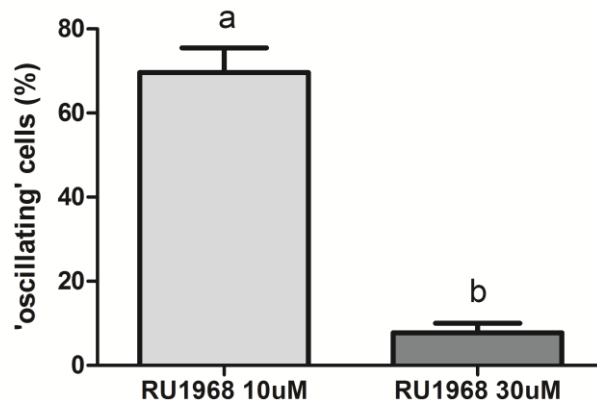


Figure 5.2 Different concentrations of CatSper blocker (RU1968F1) affect the proportion of ‘oscillating’ population. Graph shows the proportion of ‘oscillating’ cells under 10 μM RU1968 or 30 μM RU1968 treatments. An ‘oscillating’ cells was considered when exhibited at least one $[\text{Ca}^{2+}]_i$ oscillation with minimum of 20% of the transient peak amplitude. Bars show mean \pm SEM of 3 experiments. Treatment groups that do not share a letter are significantly different according to t-test ($p < 0.01$).

Interestingly, RU1968 inhibited both $[\text{Ca}^{2+}]_i$ oscillations and basal Ca^{2+} activity. The frequency of $[\text{Ca}^{2+}]_i$ oscillations was largely reduced by $91.2 \pm 0.01\%$ and their amplitude by $94.2 \pm 1.6\%$ (n=213 $[\text{Ca}^{2+}]_i$ oscillations from 35 cells; $p < 0.001$; fig. 5.3). Furthermore, after the CatSper inhibitor removal, $[\text{Ca}^{2+}]_i$ oscillations recovered completely.

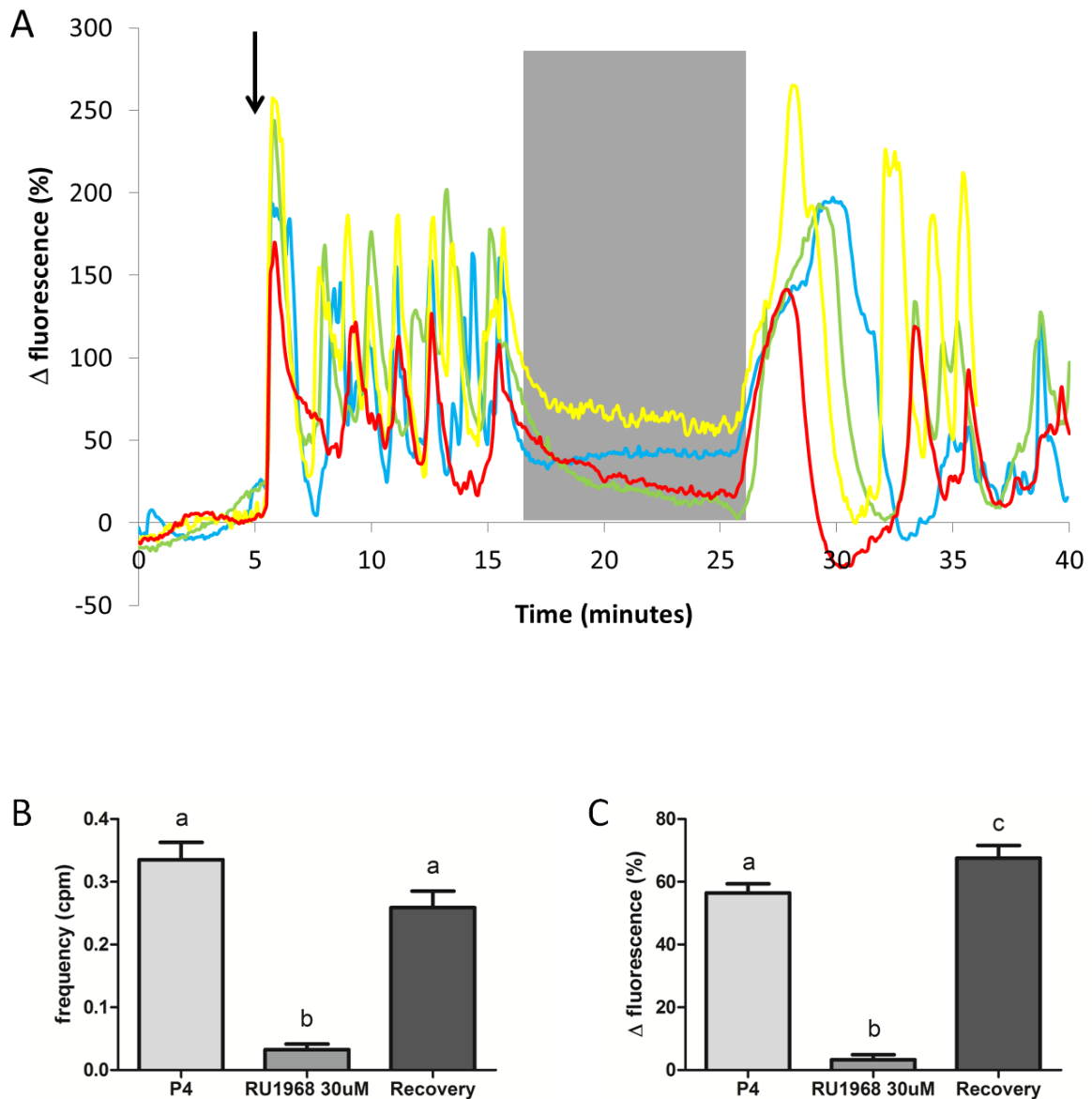


Figure 5.3 CatSper blocker (RU1968F1 – 30µM) inhibits $[Ca^{2+}]_i$ oscillations frequency and amplitude in human sperm cells. Panel (A) shows single cells traces (4 cells from different set of experiments). Black arrow indicates addition of 3 µM progesterone; grey shading shows period of treatment with 30 µM RU1968. Graphs show the frequency of $[Ca^{2+}]_i$ oscillations occurrence per minute in the ‘oscillating’ population (B) and the amplitude of $[Ca^{2+}]_i$ oscillations in sperm population (C) under the three conditions: progesterone alone (first bar), progesterone plus 30 µM RU1968 treatment (second bar) and progesterone alone treatment (third bar). Amplitude was calculated using the mean response of each $[Ca^{2+}]_i$ oscillation considering the transient peak as 100% and bars show mean \pm SEM of 3 experiments. A $[Ca^{2+}]_i$ oscillation was considered when reached at least 20% of the transient peak amplitude. Treatment groups that do not share a letter are significantly different according to one-way ANOVA followed by Tukey’s post-hoc ($p < 0.001$).

5.3.2 Slo3 channels contribution to $[Ca^{2+}]_i$ oscillations

CatSper channels are sensitive to changes in membrane potential (Darszon et al, 1999, 2011; Lishko et al, 2012) and, as reported in chapter 3, membrane potential can control $[Ca^{2+}]_i$ oscillations in sperm cells. Slo3 channels are believed to be responsible for the Ca^{2+} - activated K^+ current of human sperm (hKSper) (Santi et al, 2010; Brenker et al, 2014), which regulates plasma V_m . I investigated whether Slo3 are the principal channels involved in $[Ca^{2+}]_i$ oscillations generation. After establishing the progesterone-induced $[Ca^{2+}]_i$ oscillations for 20 minutes, the Slo3 blocker (quinidine – 0.3 mM) was added to the sperm cells. Among the classic K^+ channels blockers, quinidine has been shown to almost completely inhibit Slo3 currents (Tang et al, 2010). Quinidine treatment completely abolished $[Ca^{2+}]_i$ oscillations, including basal Ca^{2+} activity, in 100% of ‘oscillating’ cells (fig. 5.4A). Furthermore, unlike the effect of RU1968, when quinidine was removed, $[Ca^{2+}]_i$ oscillations were not restored (n=135 $[Ca^{2+}]_i$ oscillations from 25 cells; $p < 0.001$; fig. 5.4B and C).

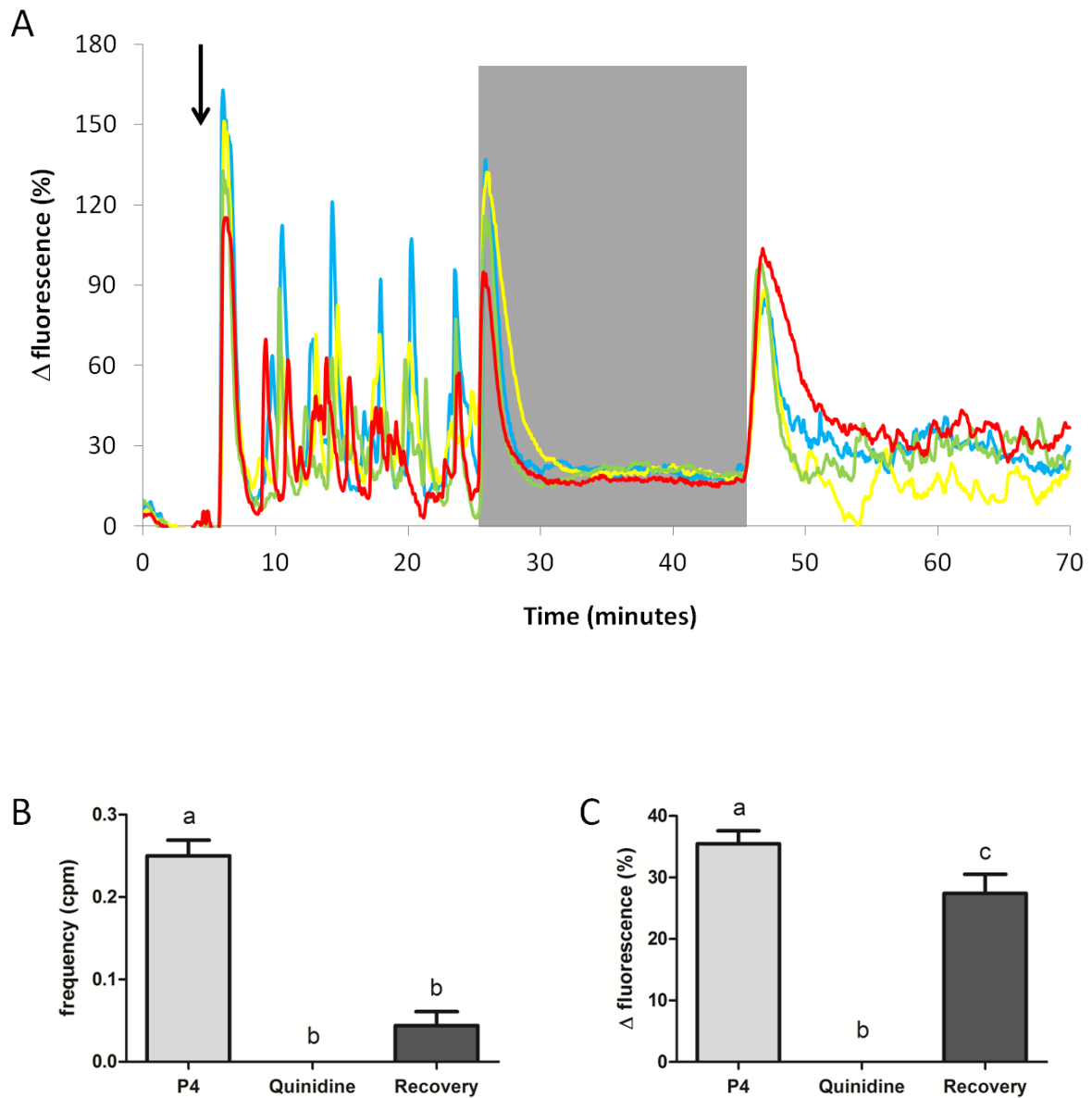


Figure 5.4 Slo3 blocker (quinidine) completely inhibits $[Ca^{2+}]_i$ oscillations generation in human sperm cells. Panel (A) shows single cells traces (4 cells from different set of experiments). Black arrow indicates addition of 3 μ M progesterone; grey shading shows period of treatment with 0.3 mM quinidine. Graphs show the frequency of $[Ca^{2+}]_i$ oscillations occurrence per minute in the ‘oscillating’ population (B) and the amplitude of $[Ca^{2+}]_i$ oscillations in sperm population (C) under the three conditions: progesterone alone treatment (first bar), progesterone plus quinidine treatment (second bar) and progesterone alone treatment (third bar). Amplitude was calculated using the mean response of each $[Ca^{2+}]_i$ oscillation considering the transient peak as 100% and bars show mean \pm SEM of 3 experiments. A $[Ca^{2+}]_i$ oscillation was considered when reached at least 20% of the transient peak amplitude. Treatment groups that do not share a letter are significantly different according to one-way ANOVA followed by Tukey’s post-hoc ($p < 0.001$).

Although quinidine treatment was greatly effective on blocking $[Ca^{2+}]_i$ oscillations, I was not able to confirm the exclusive Slo3 channels participation on $[Ca^{2+}]_i$ oscillations generation once previous patch clamp studies of human sperm revealed that quinidine and others K^+ channel blockers, such as bupivacaine and clofilium, are not selective to Slo3 channels but can also block CatSper currents (Mansell et al, 2014).

5.3.3 Chloride ion contribution to $[Ca^{2+}]_i$ oscillations

Sperm incubated in Cl^- -free medium fail to undergo several of the processes associated with capacitation, including membrane hyperpolarisation (Hernandez-Gonzalez et al, 2007; Wertheimer et al, 2008). Although Cl^- ions are not a primary determinant of sperm membrane potential, Cl^- flux may contribute directly or indirectly to regulation of V_m . Therefore, we aimed to investigate whether Cl^- ions contribute to generation of $[Ca^{2+}]_i$ oscillations. Firstly, progesterone-induced $[Ca^{2+}]_i$ oscillations were established for 20 minutes then standard saline (sEBSS) was replaced with nominally Cl^- -free medium and $[Ca^{2+}]_i$ oscillations characteristics were analysed. Absence of extracellular Cl^- failed to abolish $[Ca^{2+}]_i$ oscillations in any cell evaluated. Mean amplitude was not significantly altered by Cl^- -free conditions (n=298 $[Ca^{2+}]_i$ oscillations from 22 cells; $p < 0.001$; fig. 5.5) but mean $[Ca^{2+}]_i$ oscillation frequency was reduced by $56.7 \pm 0.02\%$.

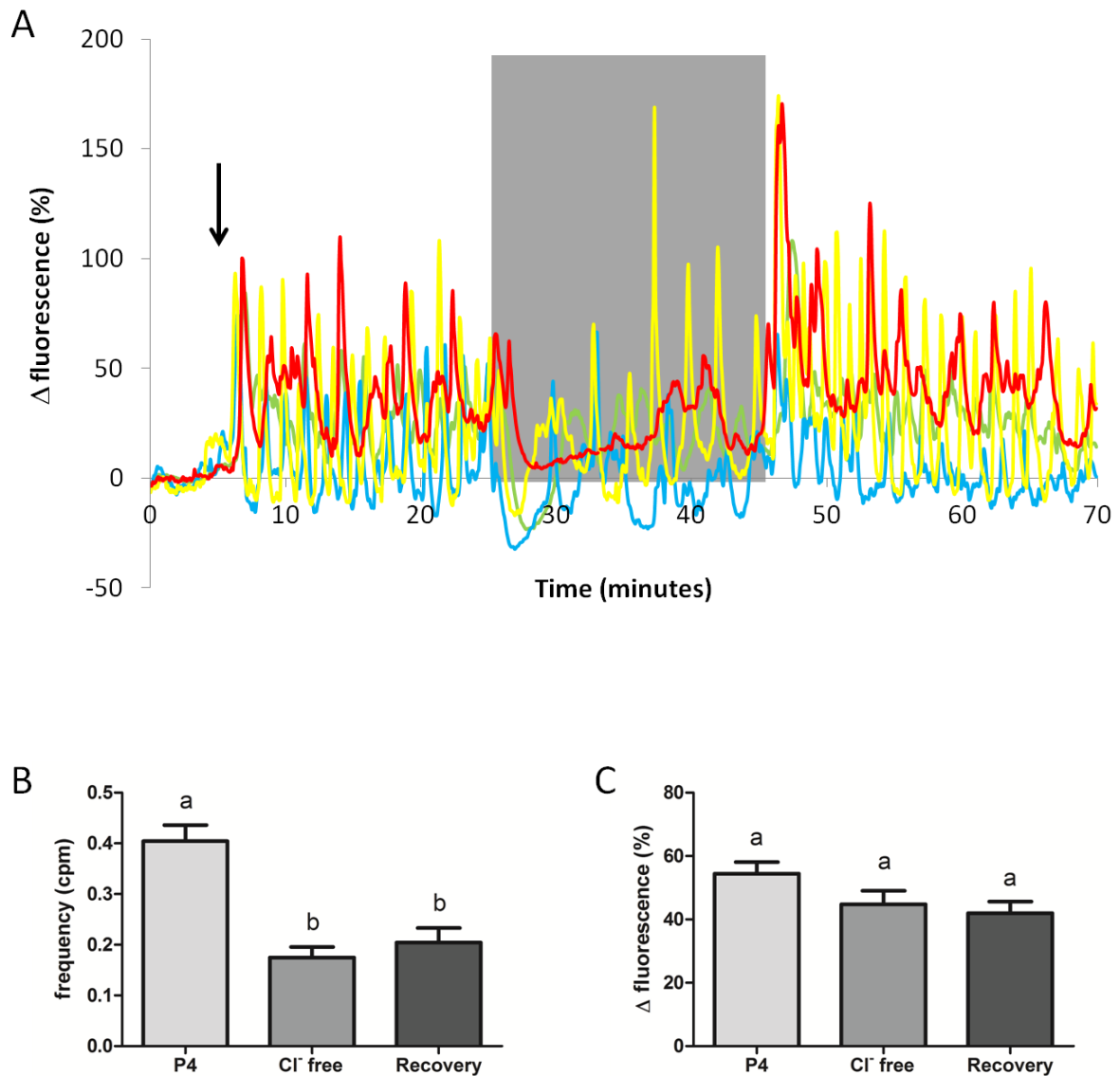


Figure 5.5 Absence of extracellular Cl^- decreases $[\text{Ca}^{2+}]_i$ oscillations frequency in sperm cells, but not their amplitude. Panel (A) shows single cells traces (4 cells from different set of experiments). Black arrow indicates addition of $3 \mu\text{M}$ progesterone; grey shading shows period of treatment with Cl^- -free medium. Graphs show the frequency of $[\text{Ca}^{2+}]_i$ oscillations occurrence per minute in the ‘oscillating’ population (B) and the amplitude of $[\text{Ca}^{2+}]_i$ oscillations in sperm population (C) under the three conditions: progesterone alone treatment and standard sEBSS (first bar), Cl^- -free sEBSS (second bar) and readdition of standard sEBSS (third bar). Amplitude was calculated using the mean response of each $[\text{Ca}^{2+}]_i$ oscillation considering the transient peak as 100% and bars show mean \pm SEM of 3 experiments. A $[\text{Ca}^{2+}]_i$ oscillation was considered when reached at least 20% of the transient peak amplitude. Treatment groups that do not share a letter are significantly different according to one-way ANOVA followed by Tukey’s post-hoc ($p < 0.001$).

5.3.3.1 Cystic fibrosis transmembrane conductance regulator (CFTR) and $[Ca^{2+}]_i$ oscillations

Cystic fibrosis transmembrane conductance regulators have been shown to be vital to sperm fertilising capacity and male fertility (Xu et al, 2007). To investigate contribution of CFTR to the generation of $[Ca^{2+}]_i$ oscillations, progesterone-induced $[Ca^{2+}]_i$ oscillations were established and subsequently the CFTR blocker (CFTR(inh)-172 - 10 μ M) was added to the sperm cells. CFTR(inh)-172 is a well-known selective CFTR antagonist (Muanprasat et al, 2004). CFTR(inh)-172 did not affect the proportion of ‘oscillating’ cells or significantly alter any $[Ca^{2+}]_i$ oscillations characteristics, such as frequency and amplitude (fig. 5.6).

5.3.3.2 Ca^{2+} -dependent Cl^- channels (CaCCs) and $[Ca^{2+}]_i$ oscillations

Ca^{2+} -dependent Cl^- channels were previously identified and characterised in human sperm cells by Orta and colleagues (2012). These channels are activated by increased $[Ca^{2+}]_i$ which can occur due to influx through plasma membrane or release from intracellular stores. In order to investigate whether $[Ca^{2+}]_i$ oscillations can regulate CaCCs and/or vice versa, I established progesterone-induced $[Ca^{2+}]_i$ oscillations for 20 minutes and then added the CaCCs blocker (niflumic acid, NFA - 30 μ M) to the sperm cells. Niflumic acid has been demonstrated to successfully block Cl^- channel in mammalian sperm (Espinosa et al, 1998; Balderas et al, 2012). Similarly to treatment with CFTR(inh)-172, niflumic acid did not affect the proportion of ‘oscillating’ cells or the characteristics of $[Ca^{2+}]_i$ oscillations (frequency and amplitude; fig. 5.7). However, $[Ca^{2+}]_i$ oscillations amplitude was slightly reduced by $27.3 \pm 2.4\%$ upon washout.

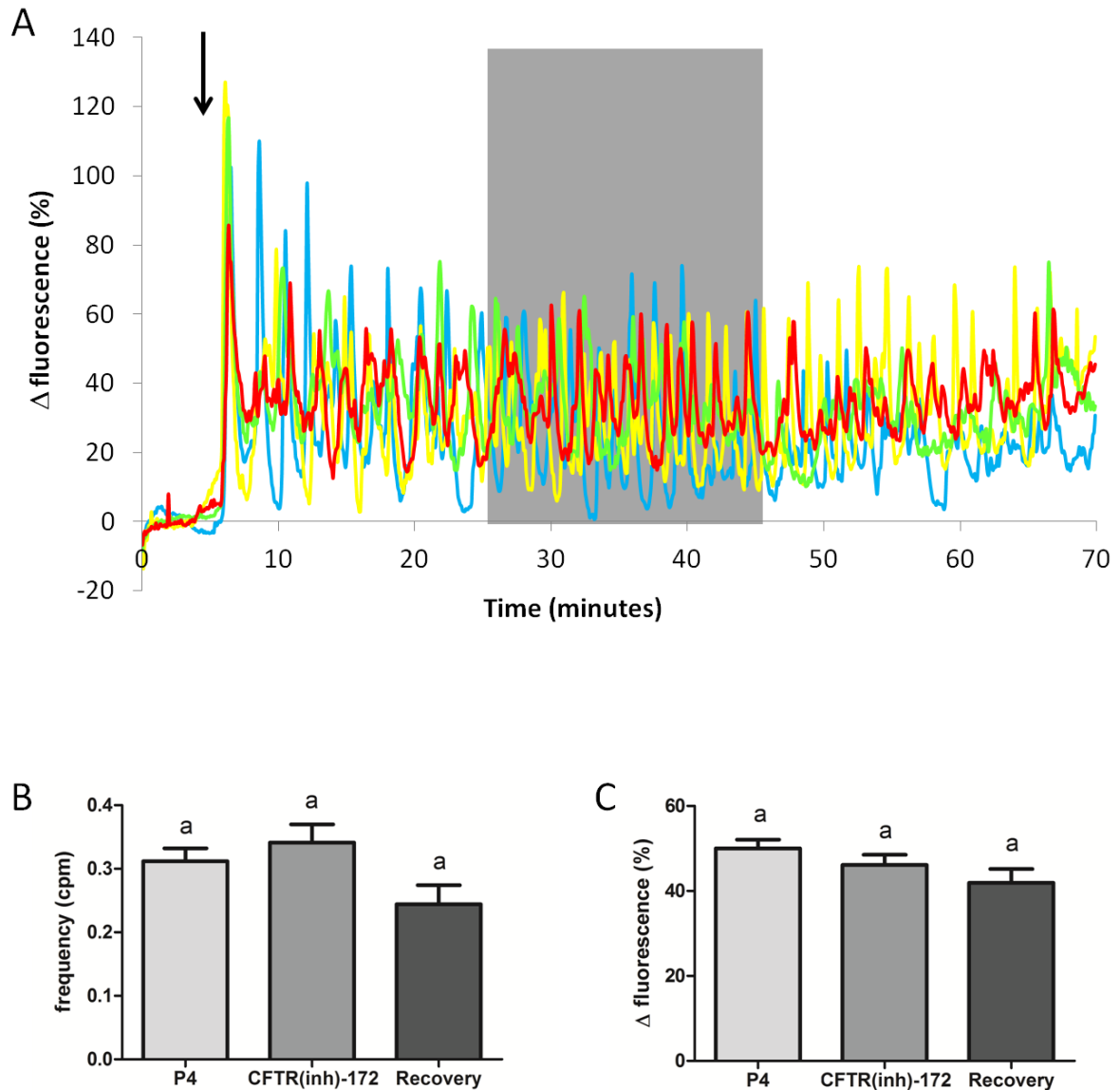


Figure 5.6 CFTR channels blocker (CFTR(inh)-172) does not affect $[Ca^{2+}]_i$ oscillations generation in human sperm cells. Panel (A) shows single cells traces (4 cells from different set of experiments). Black arrow indicates addition of 3 μ M progesterone; grey shading shows period of treatment with 10 μ M CFTR(inh)-172. Graphs show the frequency of $[Ca^{2+}]_i$ oscillations occurrence per minute in the ‘oscillating’ population (B) and the amplitude of $[Ca^{2+}]_i$ oscillations in sperm population (C) under the three conditions: progesterone alone treatment (first bar), progesterone plus 10 μ M CFTR(inh)-172 treatment (second bar) and progesterone alone treatment (third bar). Amplitude was calculated using the mean response of each $[Ca^{2+}]_i$ oscillation considering the transient peak as 100% and bars show mean \pm SEM of 3 experiments. A $[Ca^{2+}]_i$ oscillation was considered when reached at least 20% of the transient peak amplitude. Treatment groups with the same letters are not significantly different according to one-way ANOVA followed by Tukey’s post-hoc.

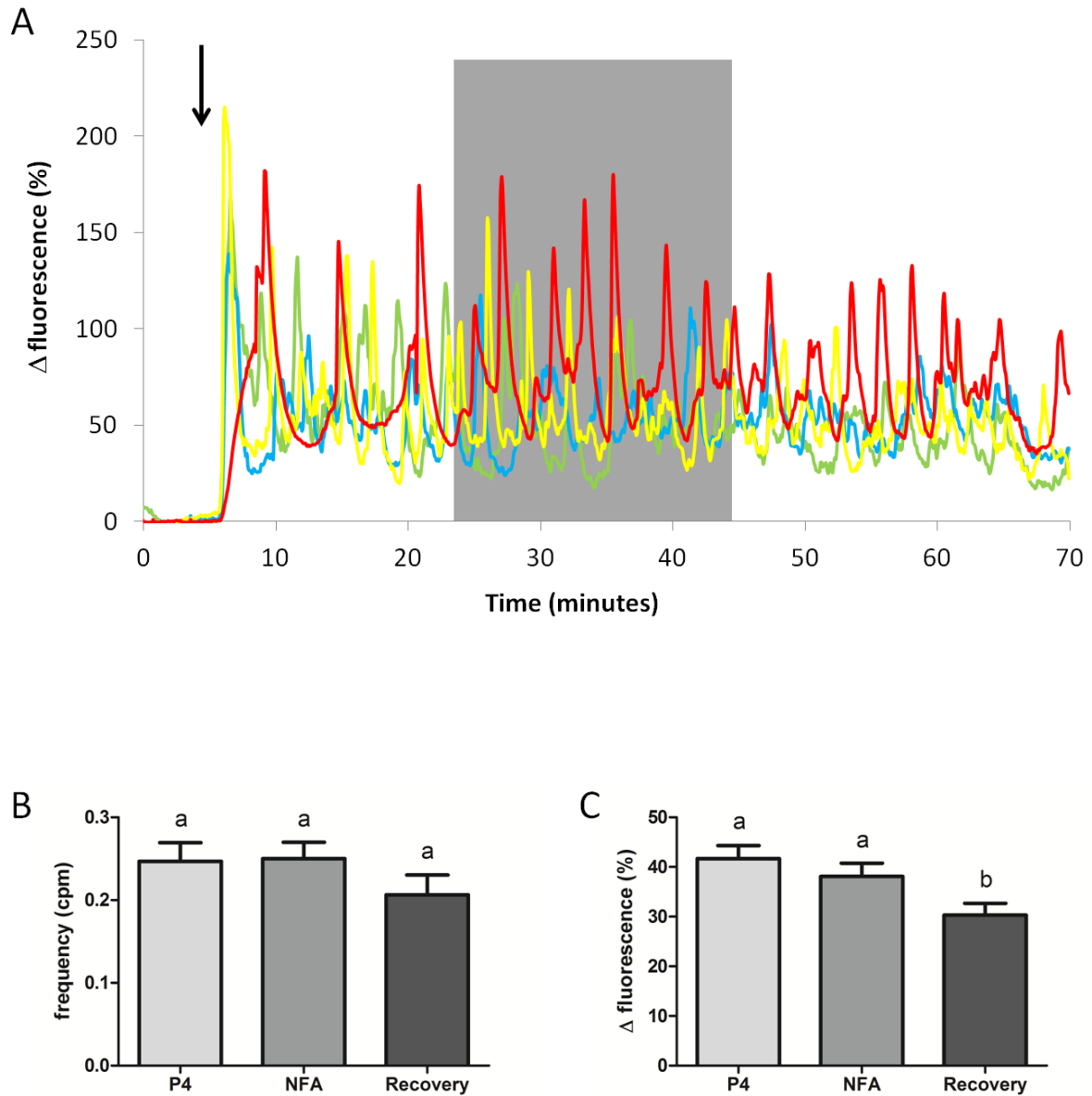


Figure 5.7 Ca^{2+} -dependent Cl^- channels blocker (niflumic acid –NFA) does not affect $[Ca^{2+}]_i$ oscillations generation in human sperm cells. Panel (A) shows single cells traces (4 cells from different set of experiments). Black arrow indicates addition of 3 μM progesterone; grey shading shows period of treatment with 30 μM NFA. Graphs show the frequency of $[Ca^{2+}]_i$ oscillations occurrence per minute in the ‘oscillating’ population (B) and the amplitude of $[Ca^{2+}]_i$ oscillations in sperm population (C) under the three conditions: progesterone alone treatment (first bar), progesterone plus 30 μM NFA treatment (second bar) and progesterone alone treatment (third bar). Amplitude was calculated using the mean response of each $[Ca^{2+}]_i$ oscillation considering the transient peak as 100% and bars show mean \pm SEM of 3 experiments. A $[Ca^{2+}]_i$ oscillation was considered when reached at least 20% of the transient peak amplitude. Treatment groups with the same letters are not significantly different according to one-way ANOVA followed by Tukey’s post-hoc ($p < 0.001$).

5.4 Discussion

Ca^{2+} signalling is critical for regulation of sperm motility and in human spermatozoa is mainly mediated by influx of extracellular Ca^{2+} through CatSper activation. Progesterone, released by the cumulus cells layer surrounding the oocyte, can activate CatSper channels and typically induces a rapid and biphasic Ca^{2+} entry into spermatozoa (Blackmore et al, 1990; Meizel and Turner, 1991, Kirkman-Brown et al, 2000). In chapter 3, I showed that approximately a quarter of the sperm cell population exhibits cyclical progesterone-induced $[\text{Ca}^{2+}]_i$ oscillations instead of the typical long-lasting plateau phase, that these oscillations are generated in the flagellar principal piece and that membrane potential contributes to their generation. Both the dependence on membrane potential and the initiation of oscillations in the flagellum suggest that CatSper plays a role in these signals. In our experiments, treatment with CatSper blocker (RU1968) inhibited oscillations in $92.2 \pm 2.2\%$ of ‘oscillating’ cells and strongly reduced the frequency of oscillations in those cells where oscillations persisted (fig. 5.2), confirming the contribution of CatSper to progesterone-induced $[\text{Ca}^{2+}]_i$ oscillations generation.

If generation of oscillations involves changes in membrane potential, it must involve the mechanisms that control V_m . Navarro and colleagues (2007) showed that K^+ current, $I_{\text{K}_{\text{Sper}}}$, is crucial to set V_m in mouse spermatozoa and, consequently, could regulate other V_m -dependent channels such as CatSper. Later, it was demonstrated that $I_{\text{K}_{\text{Sper}}}$ in both mouse and human sperm is carried by the sperm-specific Slo3 channel and mutations on Slo3 gene cause infertility in male mice, mainly to defects in sperm motility (Santi et al, 2010; Zeng et al, 2011, Brenker et al, 2014). Chávez and colleagues (2014) showed that Slo3 modulates Ca^{2+} influx into sperm through the sperm-specific Ca^{2+} channel, CatSper, suggesting they may be functionally connected. Here I have shown that treatment of human sperm with quinidine

(which potently blocks Slo3 but has little effect on Slo1 at the dose used; Tang et al, 2010), abolished $[Ca^{2+}]_i$ oscillations in all ‘oscillating’ cells (fig. 5.4), consistent with the idea that Slo3 plays a key role in this process. However, patch clamp studies of human sperm revealed that quinidine Slo3 channels can also block CatSper currents (Mansell et al, 2014). Therefore the potent effect of quinidine on $[Ca^{2+}]_i$ oscillations may be due to its action on both ion channels.

The contribution of Cl^- fluxes to the modulation of plasma membrane potential in sperm cells is not yet clear. Sperm incubated in medium where Cl^- was replaced by non-permeable anions showed no changes in its resting membrane potential (Hernandez-Gonzalez et al, 2007). However, in spermatozoa incubated in the absence of extracellular Cl^- most of capacitation-associated processes are inhibited, including membrane hyperpolarisation (Hernandez-Gonzalez et al, 2007; Wertheimer et al, 2008). I showed that replacing standard saline with Cl^- free medium did not completely abolish $[Ca^{2+}]_i$ oscillations in any cell evaluated, although the frequency of oscillations was reduced by $56.7 \pm 0.02\%$ (fig. 5.5), suggesting the Cl^- anions may contribute to $[Ca^{2+}]_i$ generation but are not essential. Several studies have reported the presence of cystic fibrosis transmembrane conductance regulator (CFTR) in both human and mouse sperm (Chan et al, 2006; Hernandez-Gonzalez et al, 2007; Xu et al, 2007; Li et al, 2010). CFTRs play role in sperm physiology by regulating pH_i and V_m , directly through Cl^- carriage across plasma membrane or indirectly through its interplay with other ion channels (Hernandez-Gonzalez et al, 2006; 2007) and have been shown be vital to sperm fertilising capacity and male fertility (Xu et al, 2007). However, our data showed that the CFTR blocker (CFTR(inh)-172) did not affect the proportion of ‘oscillating’ cells or alter the characteristics of $[Ca^{2+}]_i$ oscillations, such as frequency and amplitude (fig. 5.6). Orta and colleagues (2012) have characterised Ca^{2+} -dependent Cl^- channels (CaCCs) in human

spermatozoa and these channels are known to be activated by increased $[Ca^{2+}]_i$ which can occur due to release from intracellular stores or influx through plasma membrane. Studies with CaCCs blocker (niflumic acid - NFA) showed that NFA inhibits mouse and human sperm ZP-induced acrosome reaction and also blocks Ca^{2+} -induced hyperpolarisation determined by Cl^- in mouse spermatozoa (Espinosa et al, 1998; Orta et al, 2012; Figueiras-Fierro et al, 2013). However, our data showed that NFA has no effect on the proportion of ‘oscillating’ cells or on $[Ca^{2+}]_i$ oscillation frequency or amplitude (fig. 5.7). Therefore, further investigations need to be performed to understand the contribution of Cl^- fluxes to generation of $[Ca^{2+}]_i$ oscillations.

A tentative model generation for $[Ca^{2+}]_i$ oscillations is shown in fig 5.8. Progesterone induces opening of CatSper in the flagellum and consequent Ca^{2+} influx. The increase of $[Ca^{2+}]_i$ opens Slo3 channels, inducing efflux of K^+ , which cause hyperpolarisation of membrane potential, overcoming the effect of progesterone (Lishko et al, 2011) to cause closure of CatSper and termination of Ca^{2+} influx. Ca^{2+} sequestration mechanisms at the plasma and store membranes now re-establish Ca^{2+} concentration in the cytosol. Low intracellular Ca^{2+} allows Slo3 to close and, membrane potential is restored to its resting value. In the continuing presence of progesterone CatSper re-opens again allowing Ca^{2+} influx and the cycle restarts (fig. 5.8). Our suggestion is supported by previous studies that shows that periodic changes in membrane potential may lead to cyclical activation of voltage dependent Ca^{2+} -influx pathways and, consequently, generates $[Ca^{2+}]_i$ oscillations (Lieste et al, 1998). Also, the potential interplay between Slo3 channels and CatSper channels has been already previously suggested by other researchers (Brenker et al, 2014; Chávez et al, 2014).

It is important to note that the flagellar (CatSper-mediated) $[Ca^{2+}]_i$ signal propagates forwards and actively invades the sperm head. $[Ca^{2+}]_i$ oscillation amplitudes observed in the

neck and head of the sperm were greater than in the flagellum (despite the fact that cytoplasmic volume at the neck/head greatly exceeds that in the flagellum and therefore Ca^{2+} passively diffusing forward will be greatly diluted) and this enhanced signal must be achieved by further Ca^{2+} mobilisation, probably by Ca^{2+} -induced- Ca^{2+} release (CICR) from intracellular stores. Interventions that target Ca^{2+} store mobilisation completely inhibit $[\text{Ca}^{2+}]_i$ oscillations in somatic cells (where oscillations dependent on cyclical emptying/refilling of intracellular Ca^{2+} stores are independent of V_m ; Berridge, 1993) but in human sperm oscillations, though affected, are less sensitive (Harper et al, 2004; Mata-Martinez et al, 2018).

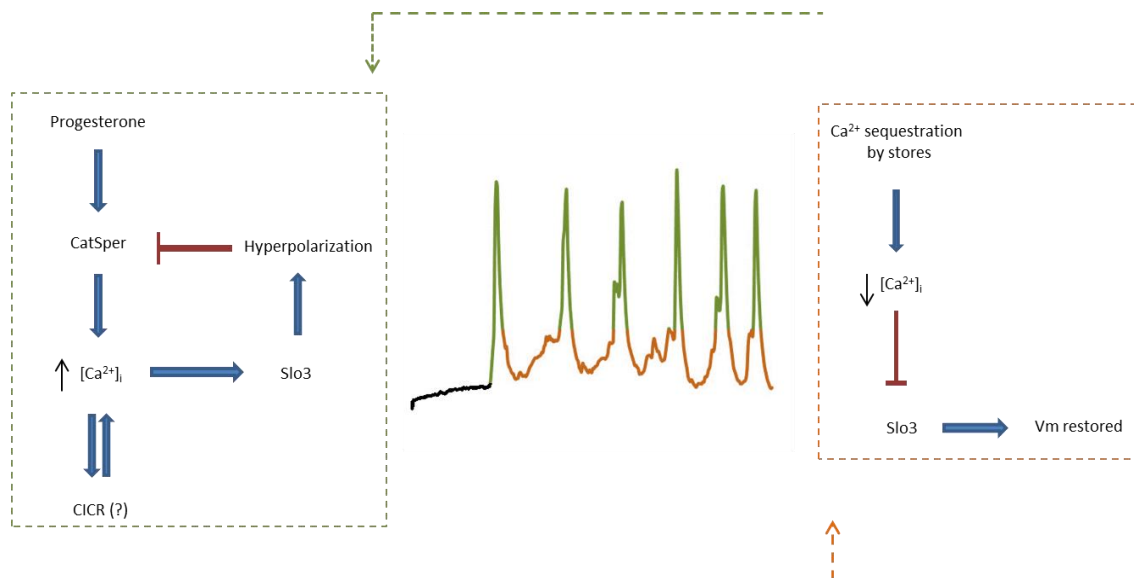


Figure 5.8 Proposed model for $[\text{Ca}^{2+}]_i$ oscillations generation in human sperm cells. Green colour represents the mechanism of the transient peaks generation: in the presence of progesterone, CatSper is activated and $[\text{Ca}^{2+}]_i$ increases, which potentially triggers mobilisation of Ca^{2+} from the stores through Ca^{2+} -induced Ca^{2+} release (CICR) system. The increase of $[\text{Ca}^{2+}]_i$ opens Slo3 channels, inducing efflux of K^+ , causing hyperpolarisation of membrane potential and consequently closes CatSper. Orange colour represents the mechanism of the peak decay: Ca^{2+} stores depletion activates Ca^{2+} sequestration mechanisms and re-establishes Ca^{2+} concentration in cytosol. Low concentration of intracellular Ca^{2+} closes Slo3, membrane potential is restored and CatSper, in the presence of progesterone, opens again promoting increase of $[\text{Ca}^{2+}]_i$. These events happen cyclically until removal of progesterone.

CHAPTER SIX: INVESTIGATION OF THE MECHANISM BY WHICH SKF-96365 MODULATES THE GENERATION OF $[Ca^{2+}]_i$ OSCILLATIONS

6.1 Abstract

$[Ca^{2+}]_i$ changes promoted by CatSper activation lead to mobilisation of stored Ca^{2+} by Ca^{2+} -induced Ca^{2+} release (Costello et al, 2009; Correia et al, 2015). The depletion of intracellular Ca^{2+} stores triggers the opening of store operated channels (SOCs) at the plasma membrane in a process termed store operated Ca^{2+} entry (SOCE). The contribution of SOCE in the response of human sperm to progesterone remains unclear. I aimed to investigate the participation of Ca^{2+} stores in generating Ca^{2+} oscillations in human sperm through the modulation of SOCE system using SKF-96365 as a pharmacological tool. Application of SKF-96365 after addition of progesterone increased the amplitude of $[Ca^{2+}]_i$ oscillations previously generated by P4 and also induced $[Ca^{2+}]_i$ oscillations in cells in which P4 was not effective. Furthermore, SKF-96365 *per se* increases $[Ca^{2+}]_i$ in a concentration-dependent manner and also induces $[Ca^{2+}]_i$ oscillations in $56 \pm 9.4\%$ of sperm cell population with faster frequency than progesterone-induced ones. SKF-induced $[Ca^{2+}]_i$ oscillations are sensitive to changes in membrane potential, both hyperpolarisation and depolarisation. Moreover, experiments with CatSper inhibitor RU1968 (30 μ M) showed that both transient peak and $[Ca^{2+}]_i$ oscillations promoted by SKF-96365 was completely inhibited, suggesting an association with the drug and the Ca^{2+} channel. In addition, unlike the effect of progesterone, induction of $[Ca^{2+}]_i$ oscillations by SKF-96365 action was dependent on sperm capacitation. More experiments need to be conducted in order to clarify the SKF-96365 mechanism of action in human spermatozoa,

especially to investigate its action on CatSper channels and other molecular targets affected by sperm capacitation.

6.2 Introduction

In sperm cells, alterations in $[Ca^{2+}]_i$ is a modulatory mechanism for many of the key steps that lead to fertilisation, including switching of flagellar beat pattern and swimming behaviour (Publicover et al, 2007; Costello et al, 2009). $[Ca^{2+}]_i$ signalling in human spermatozoa is mediated primarily by influx of extracellular Ca^{2+} , mainly through CatSper activation. However, the $[Ca^{2+}]_i$ changes promoted by CatSper activation are not limited to the initial region and propagates through the sperm midpiece and head within a few seconds. The proposed model is that Ca^{2+} from the flagellum diffuses forward, raising $[Ca^{2+}]_i$ at the sperm neck and can mobilise stored Ca^{2+} by Ca^{2+} -induced Ca^{2+} release (CICR) (Correia et al, 2015). Inositol trisphosphate receptors (IP_3Rs), ryanodine receptors (RyRs) and sarcoplasmic-endoplasmic reticulum Ca^{2+} -ATPases and secretory pathway Ca^{2+} -ATPases have been localised to the acrosome and the mid-piece of human sperm cells (Ho and Suarez, 2001; Naaby-Hansen et al, 2001; Ho and Suarez, 2003; Harper et al, 2004; Park et al, 2011). Though sperm cells do not exhibit an endoplasmic reticulum (ER), which is the main Ca^{2+} storage organelle in somatic cells, other membranous structures may act as releasable Ca^{2+} stores, such as the acrosome (surrounding the anterior nucleus), mitochondria (in the midpiece) and some irregular membranous structures in the sperm neck (Costello et al, 2009). The depletion of intracellular Ca^{2+} stores triggers the opening of store operated channels (SOCs) at the plasma membrane in a process termed store operated Ca^{2+} entry (SOCE). The linking pathway between Ca^{2+} stores and Ca^{2+} channels at plasma membrane, involves two transmembrane proteins families: stromal interacting molecules (STIM), localised at the membrane of Ca^{2+} stores, and Orai, localised at the plasma membrane (Liou et al, 2005; Prakriya et al, 2006). In human sperm both proteins STIM1 and Orai1 are present in the

sperm neck region, but the role of SOCE system to the Ca^{2+} response induced by progesterone in human spermatozoa is still speculative.

SKF-96365 was originally identified as a calcium channel blocker of receptor-mediated calcium entry, mainly of transient receptor potential canonical type (TRPC) channels, and more recently it has been used as a STIM1 protein blocker. In chapter 5, I suggested that $[\text{Ca}^{2+}]_i$ oscillations starts in sperm flagellum and potentially triggers calcium-induced calcium release, which consequently causes Ca^{2+} depletion in stores. SOCE system may be then activated in order to restore cytosolic $[\text{Ca}^{2+}]_i$ levels through mediation of Ca^{2+} influx in the plasma membrane, contributing for $[\text{Ca}^{2+}]_i$ oscillations maintenance. In the present chapter, I used SKF-96365 as a pharmacological tool to investigate the participation of Ca^{2+} stores in generating Ca^{2+} oscillations in human sperm through the modulation of SOCE system.

Chapter Aims

The aim of this chapter was to investigate the contribution of SOCE system components for the generation of progesterone-induced $[Ca^{2+}]_i$ oscillations in human sperm. For that I used SKF-96365 as an inhibitor of STIM proteins. I assessed SKF-96365 effects on intracellular Ca^{2+} response through different techniques and also its action on Ca^{2+} responses induced by progesterone and its correlation with membrane potential, CatSper channels and sperm capacitation.

6.3 Results

6.3.1 SKF-96365 induces/enhances $[Ca^{2+}]_i$ oscillations in cells pre-treated with progesterone

In order to investigate the contribution of SOCE system to $[Ca^{2+}]_i$ oscillations generation in human spermatozoa, progesterone-induced $[Ca^{2+}]_i$ oscillations were established for 20 minutes, then the STIM protein blocker (SKF-96365 – 30 μ M) was added to the sperm cells. Surprisingly, treatment with SKF-96365 after addition of progesterone showed that the drug actually enhances $[Ca^{2+}]_i$ oscillations previously generated by progesterone treatment (fig. 6.1A). The frequency and amplitude of $[Ca^{2+}]_i$ oscillations was two times larger after subsequent treatment with SKF-96365 (n= 359 $[Ca^{2+}]_i$ oscillations from 35 cells; $p < 0.001$; figs. 6.1C and 6.1D). Furthermore, SKF-96365 also generates $[Ca^{2+}]_i$ oscillations in cells in which progesterone was not effective (fig. 6.1B).

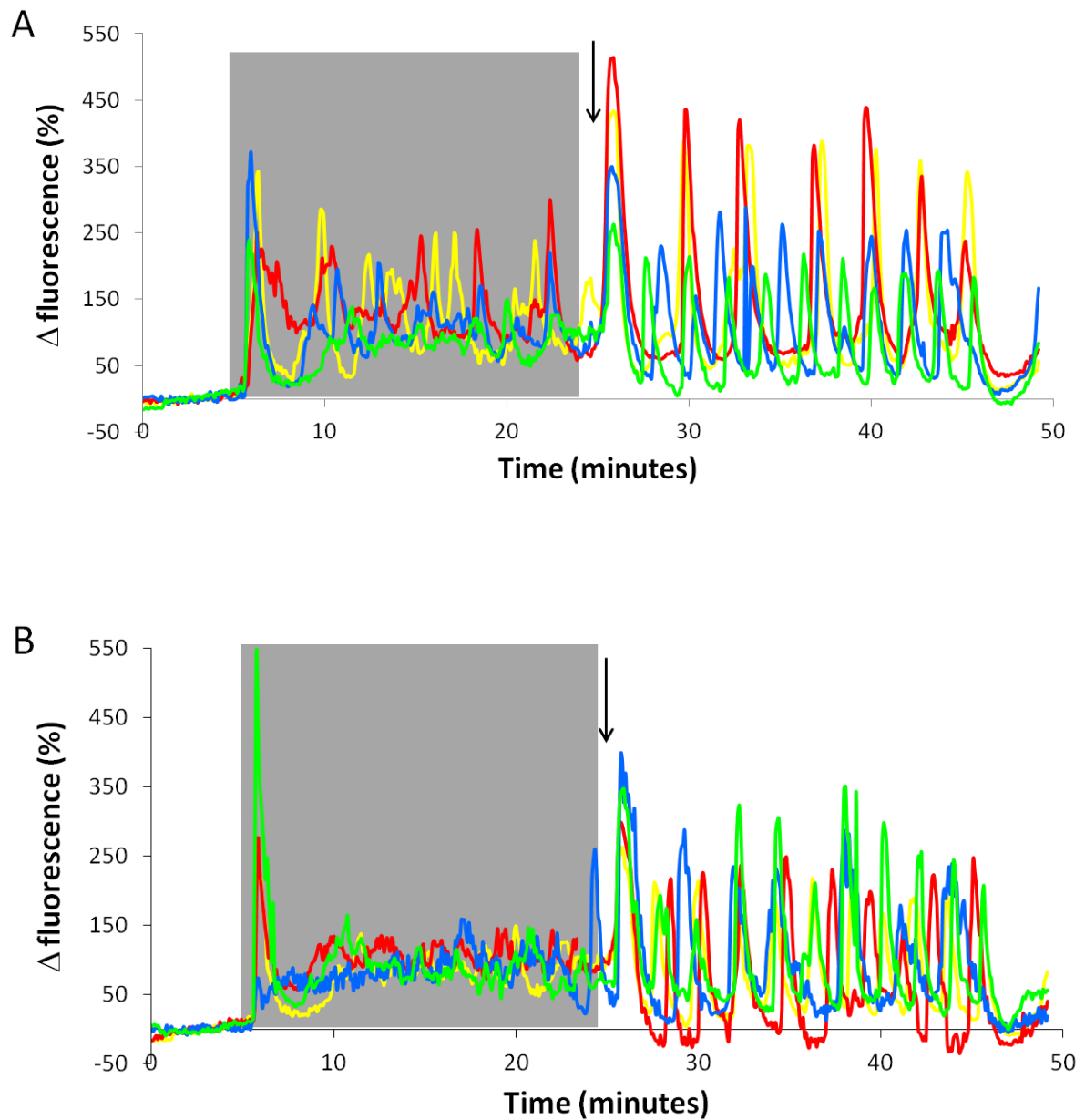


Figure 6.1 SKF-96365 induces or enhances $[Ca^{2+}]_i$ oscillations in cells pre-treated with progesterone. Panels show single cells traces (4 cells from different set of experiments): SKF 96365 enhancing progesterone pre-induced $[Ca^{2+}]_i$ oscillations (A) and generating $[Ca^{2+}]_i$ oscillations (B). Black arrow indicates addition of 30 μ M SKF-96365; grey shading shows period of treatment with 3 μ M progesterone. A total of 359 $[Ca^{2+}]_i$ oscillations from 35 cells were analysed.

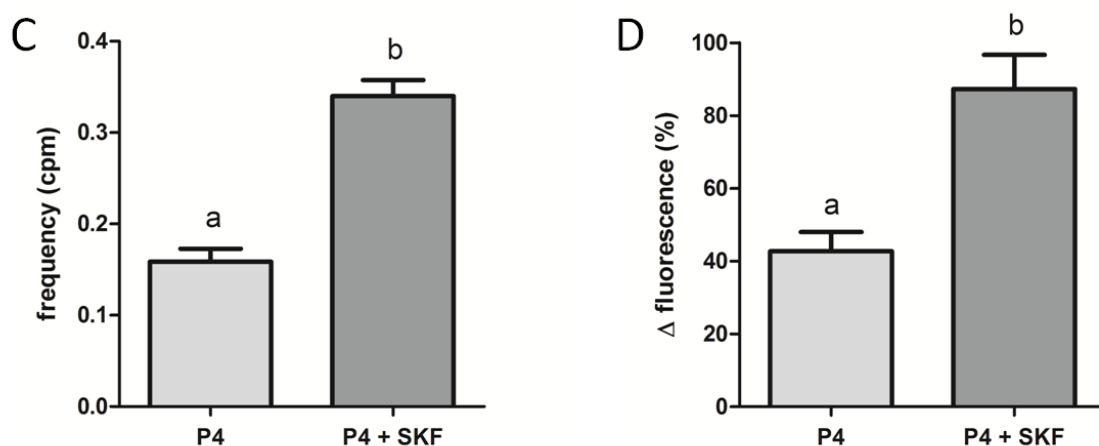


Figure 6.1 SKF-96365 induces or enhances $[Ca^{2+}]_i$ oscillations in cells pre-treated with progesterone. Graphs show the frequency of $[Ca^{2+}]_i$ oscillations occurrence per minute in the ‘oscillating’ population (C) and the amplitude of $[Ca^{2+}]_i$ oscillations in sperm population (D) under progesterone (P4) alone (first bar) and progesterone plus SKF-96365 (SKF) treatment (second bar). Amplitude was calculated using the mean response of each $[Ca^{2+}]_i$ oscillation considering the transient peak as 100% and bars show mean \pm SEM of 3 experiments. A $[Ca^{2+}]_i$ oscillation was considered when reached at least 20% of the transient peak amplitude. Treatment groups that do not share a letter are significantly different according to *t test* ($p < 0.001$). A total of 359 $[Ca^{2+}]_i$ oscillations from 35 cells were analysed.

6.3.2 SKF-96365 *per se* induces $[Ca^{2+}]_i$ oscillations in human spermatozoa

As SKF-96365 stimulates pre-induced $[Ca^{2+}]_i$ oscillations generated by progesterone, I decided to investigate whether SKF-96365 would induce $[Ca^{2+}]_i$ oscillations *per se*. Firstly, to assess the optimal concentration of SKF-96365 to be used in subsequent assays, I performed a SKF-96365 concentration curve of Ca^{2+} response. Sperm cells were labelled with Ca^{2+} indicator fluo4-AM and then exposed to different concentrations of the drug: 1.87 μ M, 3.75 μ M, 7.5 μ M, 15 μ M, 30 μ M, 60 μ M and 120 μ M. Ca^{2+} response amplitude was analysed in suspended cell populations using a fluorimeter. SKF-96365 induced an increase of $[Ca^{2+}]_i$ in a concentration-dependent manner (fig. 6.2). The effect of SKF-96365 appeared to saturate at

30 μM (increase in fluorescence at 30 and 60 μM was $54.8 \pm 14.2\%$, $58.4 \pm 10.5\%$ respectively but at 120 μM a further increase occurred. I decided to use 30 μM in imaging assays since it showed a similar effect as 60 μM . The further increase at 120 μM suggested that at this concentration the drug could be affecting other molecular targets.

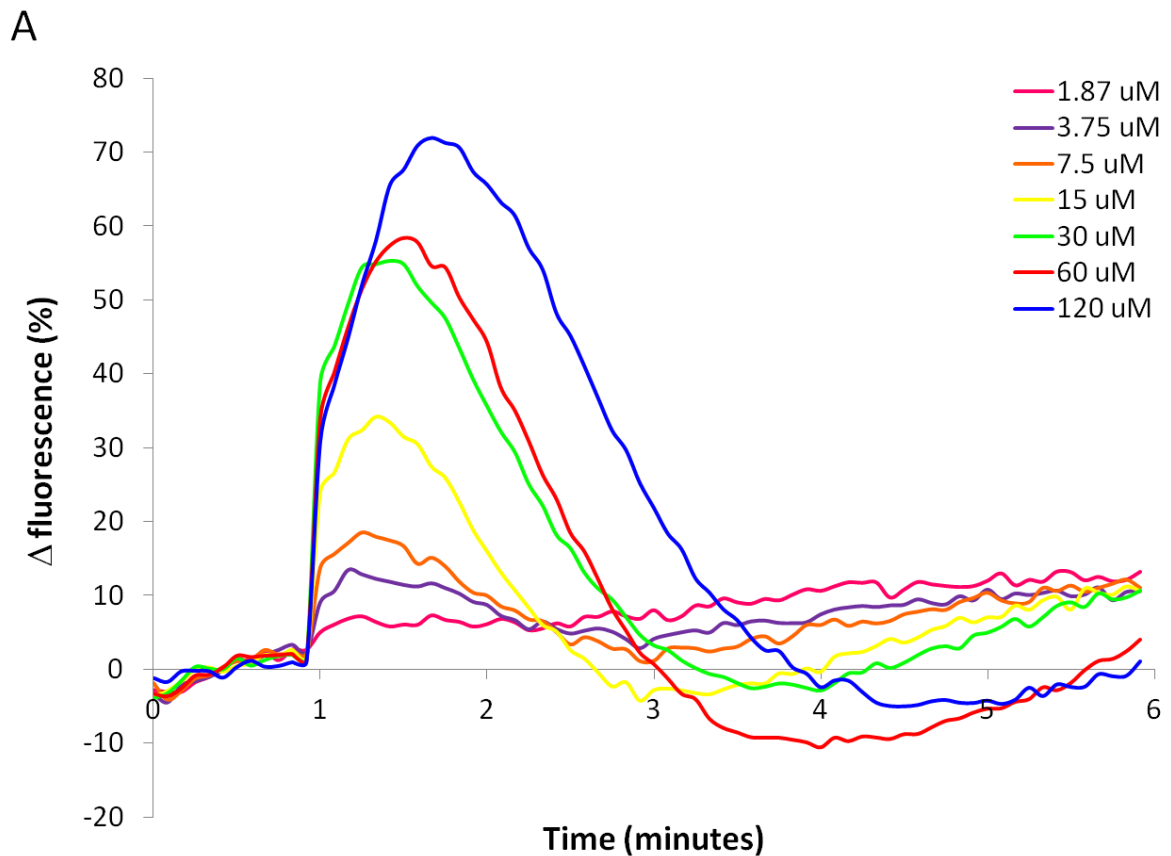


Figure 6.2 SKF-96365 induces a transient Ca^{2+} response in a concentration-dependent manner in the whole sperm cell population. Panel (A) shows the dose dependent transient induced by SKF-96365. Graph was generated from the average of experiments performed in duplicate and repeated three times independently, under fluorimeter.

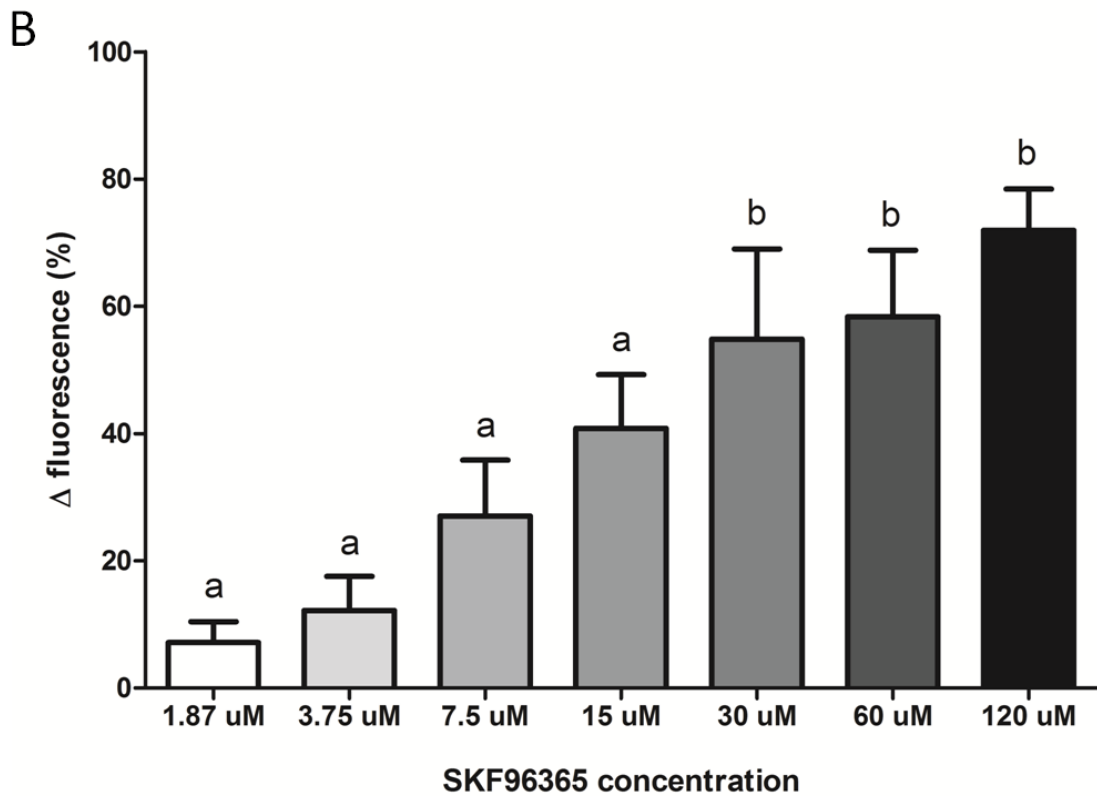


Figure 6.2 SKF-96365 induces a transient Ca^{2+} response in a concentration-dependent manner in the whole sperm cell population. (B) Histogram was generated from the average of experiments performed in duplicate and repeated three times independently, under fluorimeter. Treatment groups with the same letters were not significantly different according to one-way ANOVA followed by Tukey's post-hoc ($p < 0.001$).

Single-cell imaging experiments showed that SKF-96365 promotes an immediate transient Ca^{2+} peak with approximately half amplitude of the subsequent transient induced by progesterone ($n = 54$ cells; $p > 0.001$; figs. 6.3A and 6.3B). Interestingly, SKF-96365 also induces cyclical $[\text{Ca}^{2+}]_i$ oscillations in a large cell population $56 \pm 9.4\%$. $[\text{Ca}^{2+}]_i$ oscillations induced by SKF-96365 are faster than the ones induced by progesterone ($n = 654$ $[\text{Ca}^{2+}]_i$ oscillations from 54 cells; $p > 0.05$; figs. 6.3A and 6.3C), but their amplitude have similar size (fig. 6.3D).

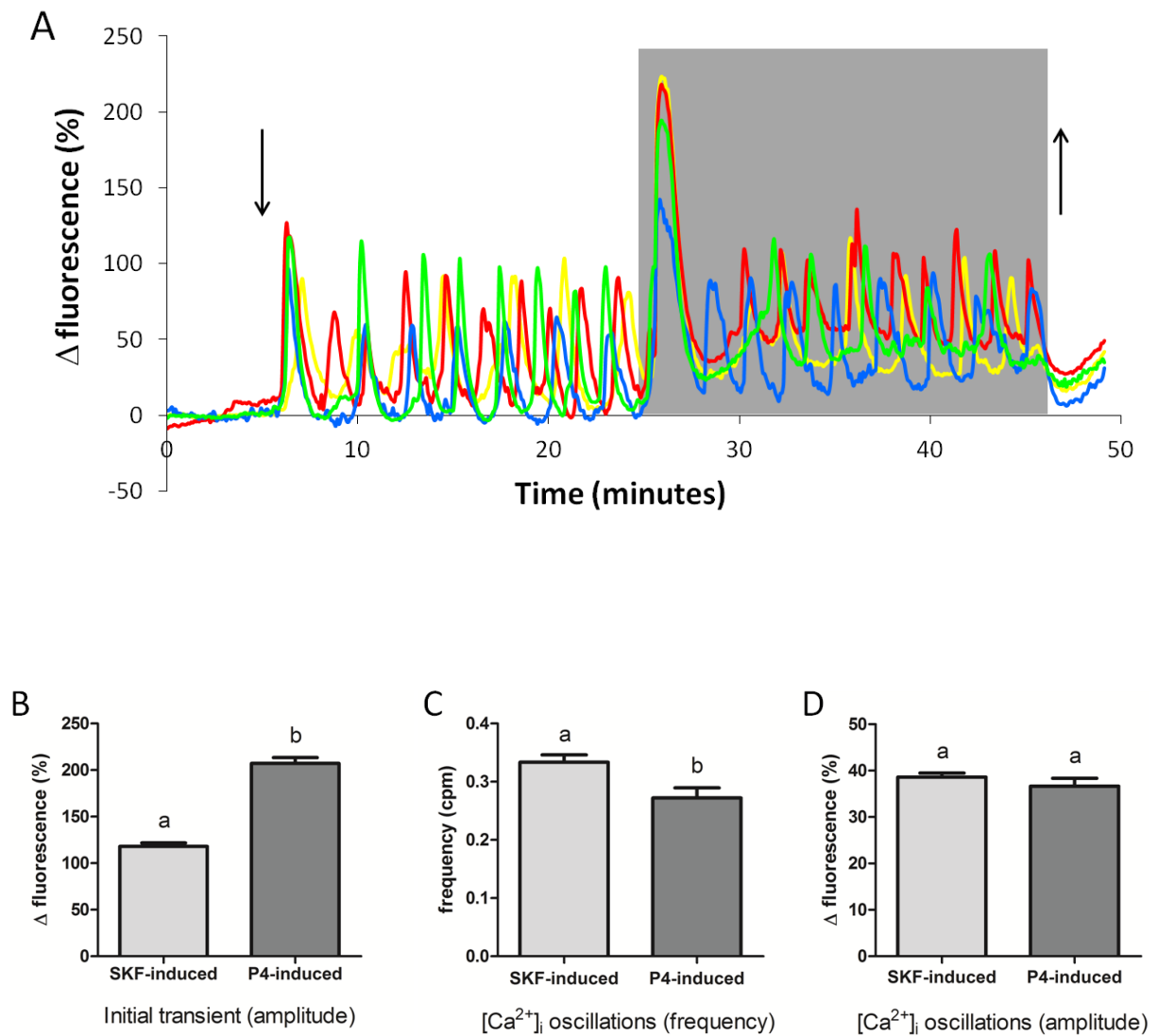


Figure 6.3 SKF-96365 *per se* induces $[Ca^{2+}]_i$ oscillations in human spermatozoa. Panel (A) shows single cells traces (4 cells from different set of experiments). Grey shading shows period of superfusion with 3 μ M progesterone; black arrows indicates addition/removal of 30 μ M SKF-96365. Graphs show the amplitude of transient peak (B) and frequency (C) and amplitude (D) of $[Ca^{2+}]_i$ oscillations induced by SKF-96365 (SKF) and progesterone (P4). Amplitude was calculated using the mean response of each $[Ca^{2+}]_i$ oscillation considering the progesterone-induced transient peak as 100% and bars show mean \pm SEM of 3 different experiments. A $[Ca^{2+}]_i$ oscillation was considered when reached at least 20% of the transient peak amplitude. Bars that do not share a letter are significantly different according to *t-test* ($p < 0.05$). A total of 654 $[Ca^{2+}]_i$ oscillations from 54 cells were analysed.

6.3.3 SKF-96365-induced $[Ca^{2+}]_i$ oscillations are sensitive to membrane hyperpolarisation

Since responses promoted by SKF-96365 and progesterone appeared very similar, I decided to analyse whether SKF-induced $[Ca^{2+}]_i$ oscillations were also sensitive to changes in membrane potential as progesterone-induced ones (see in chapter 3). After establishing SKF-induced $[Ca^{2+}]_i$ oscillations for 20 minutes, 1 μ M valinomycin, to bring V_m E_k to -79 mV, was added to the sperm cells. Membrane hyperpolarisation completely inhibited $[Ca^{2+}]_i$ oscillations in 69.8% of cell population. Similarly to the progesterone experiments, in the sub-population of cells in which oscillations persisted the frequency of $[Ca^{2+}]_i$ oscillations was much lower (0.03 ± 0.01 cpm compared to 0.32 ± 0.01 cpm; $n= 583$ $[Ca^{2+}]_i$ oscillations from 53 cells; $p>0.001$; fig. 6.4B). Amplitude of $[Ca^{2+}]_i$ oscillations after hyperpolarisation was also affected: reduction of $86.5 \pm 2.3\%$ ($n= 583$ $[Ca^{2+}]_i$ oscillations from 53 cells; $p>0.001$; fig. 6.4C). Restoring V_m allowed recovery of the frequency and the amplitude of $[Ca^{2+}]_i$ oscillations by $62.5 \pm 0.02\%$ and $69.1 \pm 4.1\%$, respectively (fig. 6.4).

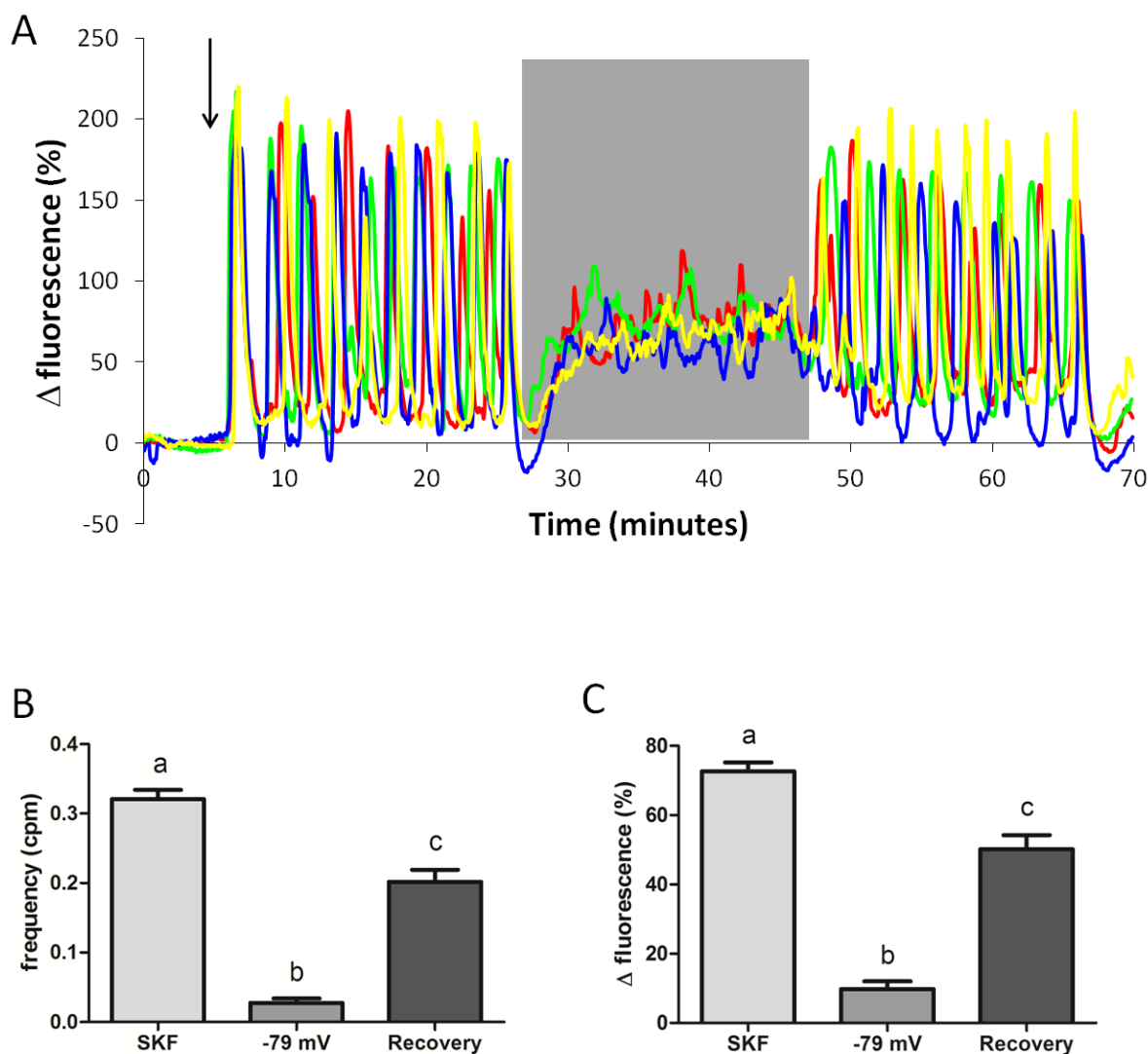


Figure 6.4 Hyperpolarisation inhibits the frequency and amplitude of SKF-induced $[Ca^{2+}]_i$ oscillations. Panel (A) shows single cell traces (4 cells from different set of experiments). Grey shading shows period of superfusion with valinomycin ($V_m E_K = -79$ mV); black arrow indicate addition of 30 μ M SKF-96365. Graphs show the frequency of $[Ca^{2+}]_i$ oscillations occurrence per minute in the ‘oscillating’ population (B) and the amplitude of $[Ca^{2+}]_i$ oscillations in sperm population (C) under the three conditions: SKF alone treatment and regular V_m (first bar), hyperpolarisation $V_m E_K = -79$ mV (second bar) and restored V_m (third bar). Amplitude was calculated using the mean response of each $[Ca^{2+}]_i$ oscillation considering the initial transient peak as 100% and bars show mean \pm SEM of 3 experiments. A $[Ca^{2+}]_i$ oscillation was considered when reached at least 20% of the initial transient peak amplitude. Treatment groups with the same letters were not significantly different according to one-way ANOVA followed by Tukey’s post-hoc ($p < 0.001$). A total of 583 $[Ca^{2+}]_i$ oscillations from 53 cells were analysed.

6.3.4 SKF-96365-induced $[Ca^{2+}]_i$ oscillations are sensitive to membrane depolarisation

To evaluate whether membrane depolarisation also affects SKF-induced $[Ca^{2+}]_i$ oscillations, combination of 1 μ M valinomycin + 100 mM K^+ EBSS (estimated $V_m E_K = -4$ mV) was superfused to the sperm cells, after pre-establishment of $[Ca^{2+}]_i$ oscillations. The proportion of cells that continued oscillating upon depolarisation was greatly reduced by 95.8%. Unlike to the observed with progesterone-induced $[Ca^{2+}]_i$ oscillations (chapter 3), membrane depolarisation had great effect on rate of generation of SKF-induced $[Ca^{2+}]_i$ oscillations. Frequency was reduced by $99.2 \pm 0.01\%$ and amplitude in oscillating cells decreased by $97.7 \pm 1.7\%$ ($n=132$ $[Ca^{2+}]_i$ oscillations from 24 cells; $p<0.001$; figs. 6.5B and 6.5B). After washout of VLN/100 K^+ , $[Ca^{2+}]_i$ oscillations did not recover within the period of recording.

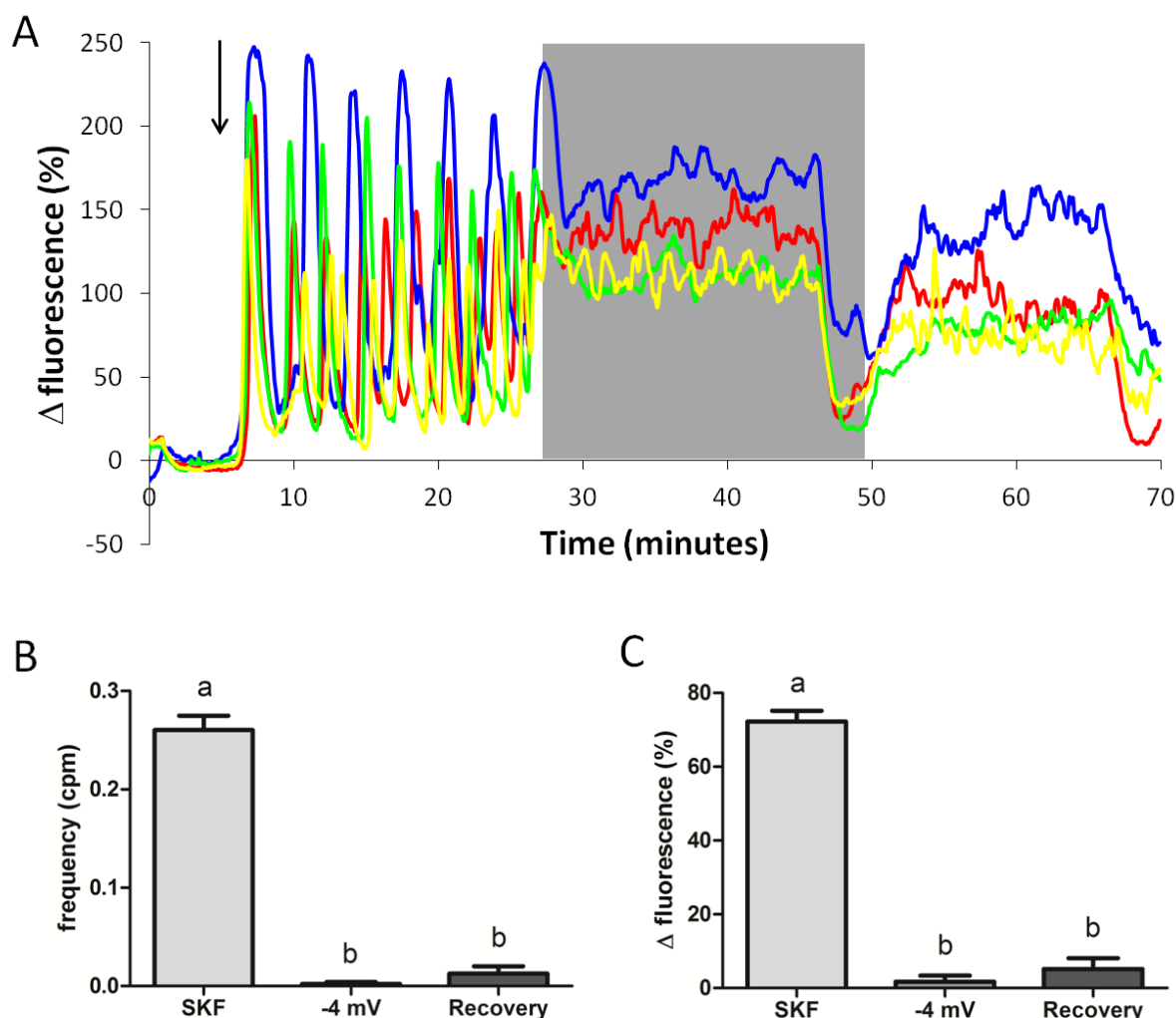


Figure 6.5 Depolarisation inhibits the frequency and amplitude of SKF-induced $[Ca^{2+}]_i$ oscillations. Panel (A) shows single cell traces (4 cells from different set of experiments). Grey shading shows period of superfusion with valinomycin/100 mM K⁺ (V_m E_K = -4 mV); black arrow indicate addition of 30 μ M SKF-96365. Graphs show the frequency of $[Ca^{2+}]_i$ oscillations occurrence per minute in the ‘oscillating’ population (B) and the amplitude of $[Ca^{2+}]_i$ oscillations in sperm population (C) under the three conditions: SKF alone treatment and regular V_m (first bar), depolarisation V_m E_K = -4 mV (second bar) and restored V_m (third bar). Amplitude was calculated using the mean response of each $[Ca^{2+}]_i$ oscillation considering the initial transient peak as 100% and bars show mean \pm SEM of 3 experiments. A $[Ca^{2+}]_i$ oscillation was considered when reached at least 20% of the initial transient peak amplitude. Treatment groups with the same letters were not significantly different according to one-way ANOVA followed by Tukey’s post-hoc ($p < 0.001$). A total of 132 $[Ca^{2+}]_i$ oscillations from 24 cells were analysed.

6.3.5 SKF-96365-induced $[Ca^{2+}]_i$ oscillations are dependent of CatSper channels

The evidence that SKF-96365 *per se* promotes cyclic changes of $[Ca^{2+}]_i$ in human sperm and also causes higher amplitudes in $[Ca^{2+}]_i$ oscillations previously induced by progesterone, suggests that the drug may have other molecular targets than STIM in human spermatozoa. I decided to evaluate whether SKF-96365 may be associated to a binding site of CatSper channels, such as progesterone. I performed experiments pre-treating spermatozoa with CatSper inhibitor RU1968 (30 μ M) and then adding SKF-96365 (30 μ M) to evaluate whether the usual Ca^{2+} transient peak promoted by SKF-96365 could also be inhibited by CatSper blocker. Figure 6.6 shows that the SKF-induced $[Ca^{2+}]_i$ transient peak was completely inhibited in the presence of CatSper inhibitor in $88 \pm 0.6\%$ of the cells, suggesting that the drug acts on the CatSper channel. Moreover, when RU1968 was added after SKF-96365 stimulation, SKF-induced $[Ca^{2+}]_i$ oscillations were also completely inhibited in $95 \pm 0.5\%$ of the cell population (fig. 6.7). Differently to what observed in progesterone treatment (chapter 5, figure 5.3) after removal of the CatSper inhibitor 27.6% of cells did not show recovery of $[Ca^{2+}]_i$ oscillations profiles.

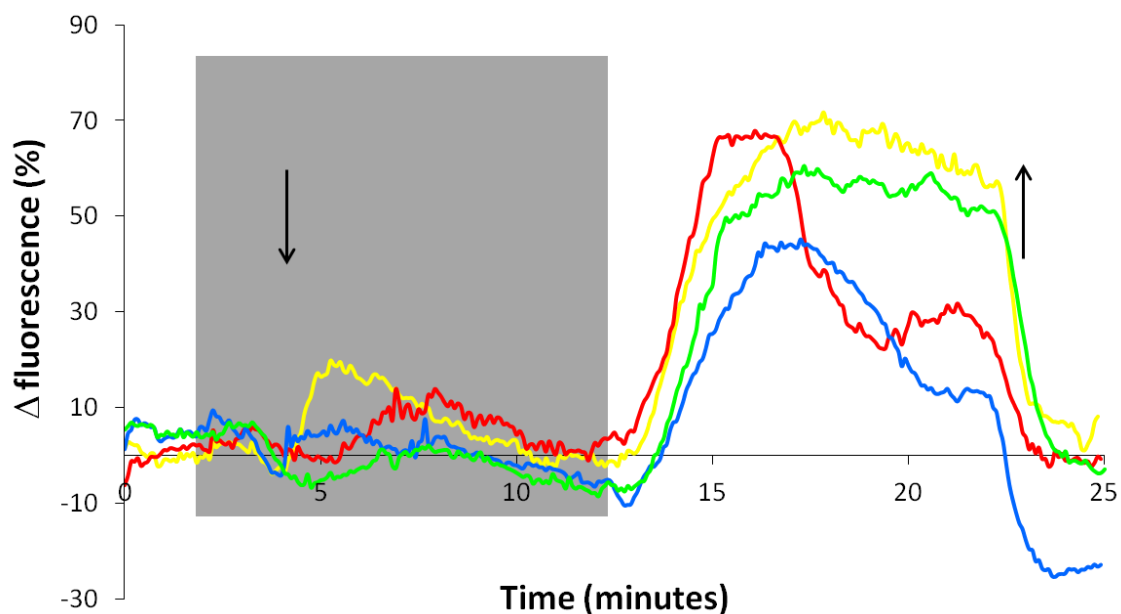


Figure 6.6 RU1968 completely inhibits initial $[Ca^{2+}]_i$ transient induced by SKF-96365. Panel shows single cells traces of different set of experiments. Grey shading shows addition of RU1968 (30 μ M), black arrows show addition/removal of SKF96396 (30 μ M). $[Ca^{2+}]_i$ transient peak was recovered when RU1968 was removed. Histogram is an average of the Ca^{2+} response intensity of 63 sperm cells obtained in three independent experiments.

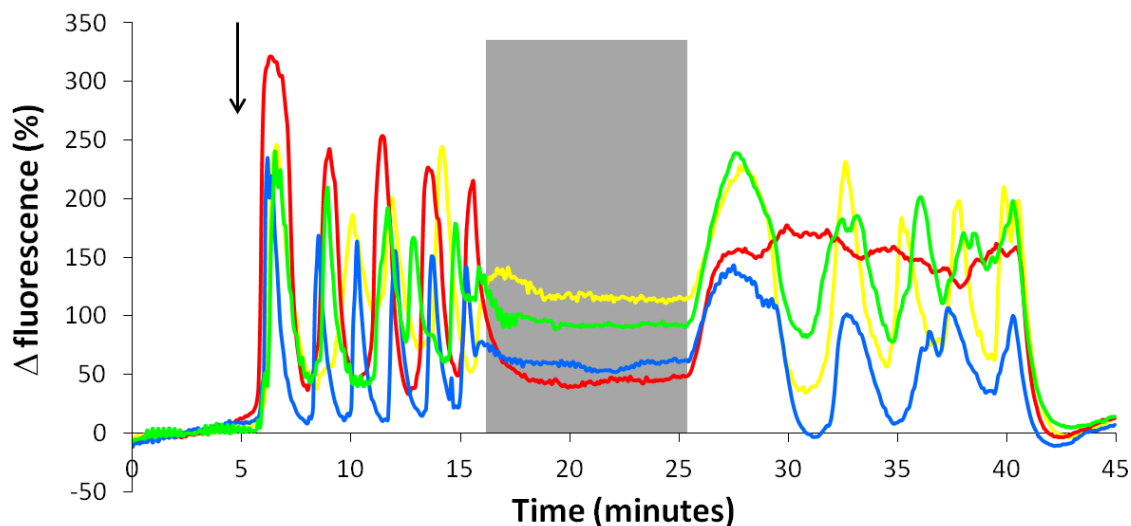


Figure 6.7 RU1968 completely inhibits $[Ca^{2+}]_i$ oscillations induced by SKF-96365. Panel shows single cells traces of different set of experiments. Grey shading shows addition of RU1968 (30 μ M), black arrow shows addition of SKF96396 (30 μ M). $[Ca^{2+}]_i$ oscillations were mostly recovered when RU1968 was removed. Histogram is an average of the Ca^{2+} response intensity of 158 sperm cells obtained in three independent experiments.

6.3.6 SKF-96365-induced $[Ca^{2+}]_i$ oscillations are dependent of sperm capacitation

In the attempt to further understand whether SKF-96365 induces $[Ca^{2+}]_i$ oscillations through the same mechanism as progesterone, I also investigated if sperm capacitation was important to SKF action. As showed in chapter 3, the proportion of ‘oscillating’ cells induced by progesterone was not affected when cells were not previously capacitated (fig. 6.8A). On the other hand, although the SKF-induced Ca^{2+} transient was not altered, the proportion of cells exhibiting $[Ca^{2+}]_i$ oscillations after SKF-96365 stimulation was greatly inhibited by the lack of capacitation: decreased by $96.2 \pm 1.5\%$ ($n= 7$ experiments; $p<0.001$; figs. 6.8A and 6.8B).

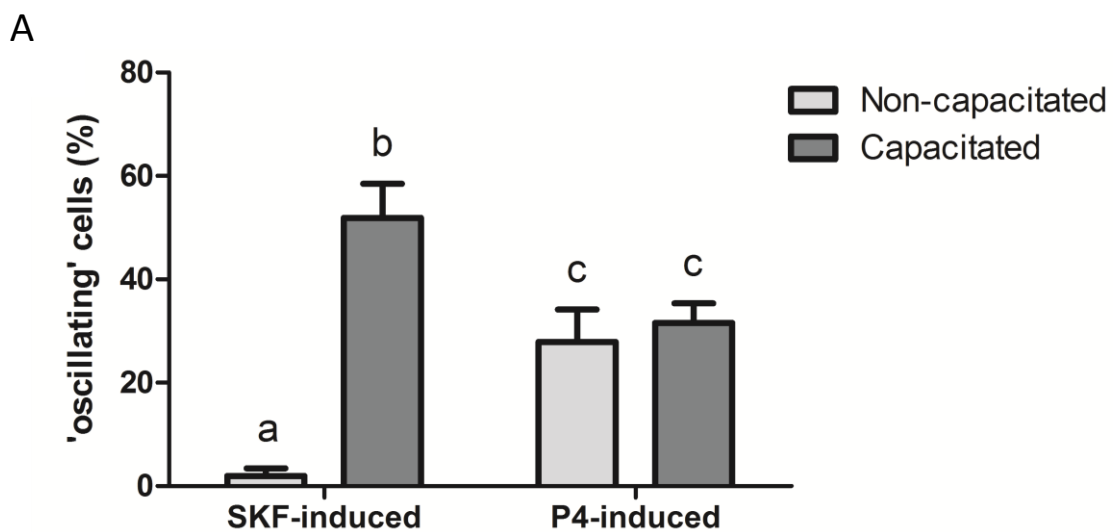


Figure 6.8 SKF-induced ‘oscillating’ population is dependent of sperm capacitation. (A) Graph represents the percentage of cells that exhibits $[Ca^{2+}]_i$ oscillations after SKF-96365 or progesterone stimulation in non-capacitated and capacitated sperm cells. Bars with the same letters were not significantly different according to two-way ANOVA followed by Bonferroni’s post-hoc ($p<0.001$). Bars show mean \pm SEM of 7 experiments.

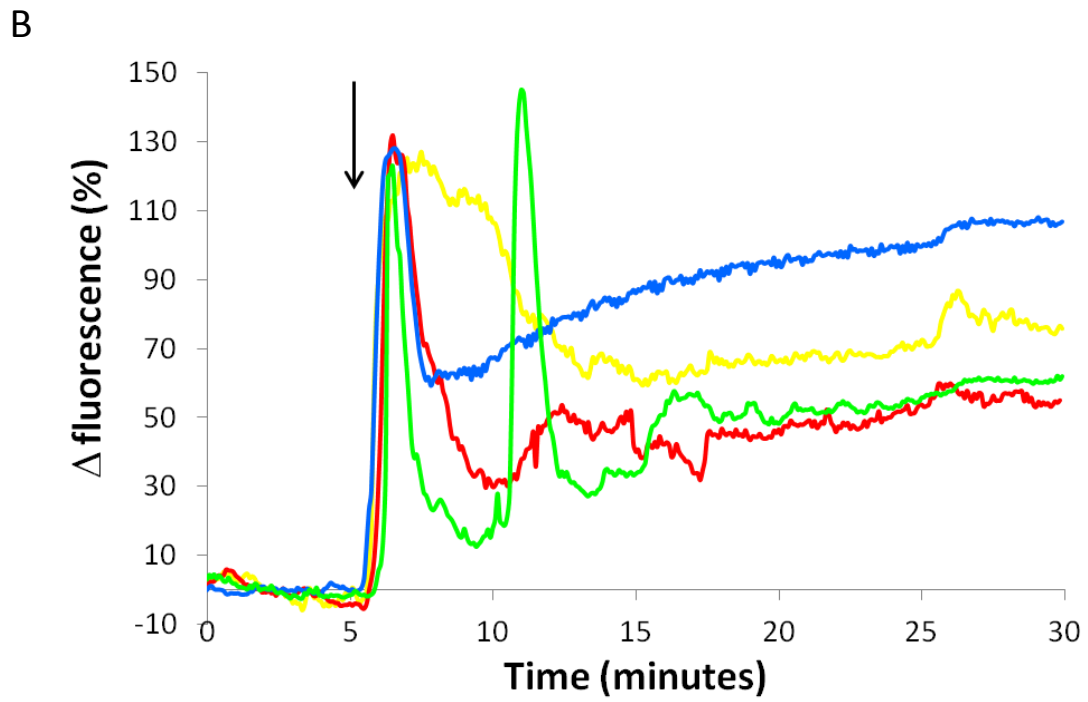


Figure 6.8 SKF-induced ‘oscillating’ population is dependent of sperm capacitation. Panel (B) shows single cells traces of different set of experiments. Black arrow shows addition of SKF96396 (30 μ M).

6.4 Discussion

SKF-96365 is a classic drug used to inhibit store operated Ca^{2+} entry (SOCE), which is a system activated by Ca^{2+} depletion in stores. I aimed to investigate whether the blockade of STIM1 protein would inhibit the maintaining of $[\text{Ca}^{2+}]_i$ oscillations induced by progesterone and confirming the contribution of Ca^{2+} stores for their generation. Surprisingly, treatment with SKF-96365 after pre-establishment of progesterone-induced $[\text{Ca}^{2+}]_i$ oscillations showed that the drug actually enhances $[\text{Ca}^{2+}]_i$ oscillations and also generates $[\text{Ca}^{2+}]_i$ oscillations in cells in which progesterone was not effective (fig. 6.1). Reducing the Ca^{2+} entry through the blockade of SOCE system may share similar behaviour reported by Harper and colleagues (2004) as they showed that in the presence of low- Ca^{2+} medium, progesterone-induced $[\text{Ca}^{2+}]_i$ oscillations were clearly enlarged and faster. However, further experiments showed that SKF-96365 *per se* induces a concentration-dependent increase of $[\text{Ca}^{2+}]_i$ in the sperm cell population (fig. 6.2) and single-cell imaging experiments showed that SKF-96365 also promotes cyclical $[\text{Ca}^{2+}]_i$ oscillations in sperm cells (fig. 6.3), suggesting that SKF-96365 probably has another molecular target in human spermatozoa as $[\text{Ca}^{2+}]_i$ oscillations induced by the drug could not be explained by the classical model: blockade of SOCE causes inhibition of Ca^{2+} influx in the plasma membrane and refilling of Ca^{2+} stores.

Several studies indicate that SKF-96365 mechanism of action has not been entirely elucidated: Schwarz and colleagues (1994) demonstrated that SKF-96365 induces increase of $[\text{Ca}^{2+}]_i$ but can also block K^+ currents; Merritt and colleagues (1990) suggested that the drug affects high voltage activated (HVA) Ca^{2+} channels and Mason and colleagues (1993) showed that SFK96365 also inhibits sarcoplasmic reticulum Ca^{2+} -ATPase; in the literature there is only one publication in sea urchin sperm showing that SKF-96365 inhibits store-operated

channels in sperm (Hirohashi and Vacquier, 2003) however, only few studies were performed to assess SKF-96365 effects in mammalian sperm: Krasznai and colleagues (2006) showed that SKF-96365 decreases human sperm motility and Trevino and colleagues (1996) demonstrated that the drug inhibits $[Ca^{2+}]_i$ increase induced by maitotoxin. My data indicate that Ca^{2+} responses promoted by SKF-96365 and progesterone are very similar. Progesterone-induced and SKF-induced $[Ca^{2+}]_i$ oscillations have both shown to be dependent of membrane potential and CatSper activity (see chapter 3 and 5; figs. 6.3 – 6.7). However, SKF-induced $[Ca^{2+}]_i$ oscillations are dependent of sperm capacitation but not progesterone-induced ones (fig. 6.8), which could be explained as progesterone might act at additional molecular targets as it has been shown that it can accelerate and induce sperm capacitation in previous studies (Foresta et al, 1992; Sumigama et al, 2015; 2017). Further investigations are necessary in order to clarify the SKF-96365 mechanism of action in human spermatozoa, mainly to understand the similarities between progesterone-induced and SKF-induced $[Ca^{2+}]_i$ oscillations generation.

CHAPTER SEVEN: PHYSIOLOGICAL ROLE OF $[Ca^{2+}]_i$ OSCILLATIONS IN HUMAN SPERMATOZOA

7.1 Abstract

Progesterone-induced $[Ca^{2+}]_i$ oscillations are dependent of CatSper activity and may be involved in the 'switching' of sperm swimming behaviour, which is crucial for a successful fertilisation. The aim was to investigate the physiological role of $[Ca^{2+}]_i$ oscillations in regulating sperm behaviour and ability to penetrate viscous medium. Fluo-4-labelled free-swimming cells stimulated with progesterone were tracked in low (sEBBS) and high (sEBBS + 1% methylcellulose, 4000 cp) viscosity environments. My data showed that correlation between $[Ca^{2+}]_i$ oscillations, sperm velocity and 'switching' of swimming behaviour behavior occurred in both environments. Moreover, changes in motility associated with $[Ca^{2+}]_i$ oscillations determined attachment/detachment to the substrate. Inhibition of CatSper activity blocked $[Ca^{2+}]_i$ oscillations (see chapter 5) and associated behaviour in both standard saline and high viscosity medium. Sperm velocity was reduced and cells turned continuously or arrested, becoming non-progressive. Superfusion with high viscosity medium (4000 cp) induces a transient $[Ca^{2+}]_i$ increase followed by oscillations with similar characteristics to the progesterone-induced ones and also dependent of CatSper channel activity. To assess the impact of CatSper in regulating sperm ability to penetrate viscous medium, spermatozoa were treated with different concentrations of RU1968 alone or in the presence of progesterone. RU1968 alone (10, 20, 30 and 50 μ M) inhibited sperm penetration into methylcellulose. Furthermore, all RU1968 concentrations tested inhibited the progesterone stimulatory effect on sperm penetration. Additionally, valinomycin treatment

also inhibited sperm penetration into artificial mucus induced by progesterone, mainly by modifying sperm velocity. Collectively, our data suggests that $[Ca^{2+}]_i$ oscillations induces 'switching' on sperm swimming behaviour and that CatSper channels might be crucial in regulating the behaviour responsible for ability of sperm to penetrate into viscous medium.

7.2 Introduction

To guarantee fertilisation, sperm must be able to modify its behaviour, which involves the transition from a linear, progressive, low-amplitude and symmetrical flagellar beating swimming state (Suarez et al, 1983) to hyperactivated motility with increased amplitude of the flagellar curvature and asymmetrical flagellar beating (Morales et al, 1988; Yanagimachi, 1994; Ho et al, 2002). Sperm hyperactivated motility is required for progression up the oviduct (Stauss et al, 1995; Ho and Suarez, 2001; Quill et al, 2003) and may provide the driving force necessary for the sperm cell to detach from the oviductal epithelium (Demott and Suarez, 1992; Ho and Suarez, 2001; Suarez and Ho, 2003). Also hyperactivated motility enhances the ability of sperm to penetrate through cervical mucus, the oviduct fluids, the cumulus cells layer and zona pellucida of the oocyte (Rathi et al, 2001; Suarez, 2008; Darszon et al, 2011; Alasmari et al, 2013).

The molecular mechanism by which sperm behavior is regulated is still being elucidated but it is generally accepted that it is a calcium-dependent phenomenon. Studies have shown that bursts of hyperactivated motility are associated with an elevation in $[Ca^{2+}]_i$ (Yanagimachi, 1988, 1994). In mouse sperm hyperactivation occurs in parallel with an increase of flagellar Ca^{2+} during capacitation (Suarez and Dai, 1995; Ho and Suarez, 2001) and it can be induced by treatment with Ca^{2+} ionophores, such as A23187 or ionomycin (Suarez et al, 1992; Marquez and Suarez, 2006). The main Ca^{2+} source for induction of hyperactivated motility is from the extracellular environment and the sperm-specific flagellar CatSper channel has been suggested to regulate the influx of Ca^{2+} through the plasma membrane and, thereby, could be involved in the regulation of swimming behaviour (Kirichok et al, 2006; Chang and Suarez, 2011). Sperm cells lacking CatSper are unable to

hyperactivate, showing defects on flagellar beat frequency and low bend amplitude, suggesting the importance of this channel to swimming behaviour (Carlson et al, 2003, 2005). Furthermore, in chapter five, I demonstrated that CatSper channels activity also leads to generation of $[Ca^{2+}]_i$ oscillations, which may underlie repeated switching of sperm behaviour.

Until the present moment, there are no studies showing the co-relation between progesterone-induced $[Ca^{2+}]_i$, the behaviour exhibited by the sperm or the ability of the sperm to penetrate viscous medium. Here I have examined $[Ca^{2+}]_i$ and motility in free-swimming sperm and have assessed the effect on mucus penetration of inhibition of CatSper.

Chapter Aims

The aims of this chapter were to investigate whether progesterone-induced $[Ca^{2+}]_i$ oscillations occur in free-swimming cells and are associated with (and responsible for) switching of sperm behaviour, which may drive its ability to penetrate viscous medium. Additionally, I also aimed to assess the contribution of CatSper channels activity to these events.

7.3 Results

7.3.1 $[Ca^{2+}]_i$ oscillations occur in free-swimming sperm cells

Single-cell imaging data presented in the previous chapters were all obtained in immobilised human spermatozoa at 25°C, which are the usual experimental conditions for sperm studies. I have shown that progesterone-induced $[Ca^{2+}]_i$ transient peak often induces the occurrence of large $[Ca^{2+}]_i$ oscillations in part of cell population, which are believed to play a role in regulating motility (Harper et al, 2004; Bedu-Addo et al, 2008) and acrosome reaction (Mata-Martinez et al, 2018). However, whether such oscillations occur in free-swimming cells is unknown. I have used time-lapse, fluorescence imaging of free-swimming human sperm to determine (a) whether $[Ca^{2+}]_i$ oscillations occur under 25 °C and 31°C and (b) whether they modify motility of the cell. Results showed that $[Ca^{2+}]_i$ oscillations occur in free-swimming spermatozoa and the proportion of ‘oscillating’ population in immobilised or free-swimming sperm cells is similar, approximately 25% (table 7.1). However, the amplitude of $[Ca^{2+}]_i$ oscillations was about three times higher when cells were allowed to swim freely than when they were attached to coverslip ($p < 0.001$; table 7.1). Similarly to immobilised cells, higher temperatures increased the frequency of $[Ca^{2+}]_i$ oscillations and consequently decreased their duration ($p < 0.01$; table 7.1).

Parameters	Immobilised cells		Free-swimming cells	
	25 °C	31 °C	25 °C	31 °C
Proportion of ‘oscillating’ cells	29.8% ^a	25% ^a	24.6% ^a	28.6% ^a
[Ca ²⁺] _i oscillations amplitude (Δ fluorescence %)	55.4 ± 1.8 ^a	57.9 ± 2.3 ^a	149.5 ± 16.2 ^b	169.9 ± 16.5 ^b
[Ca ²⁺] _i oscillations frequency (cpm)	0.3 ± 0.01 ^a	0.8 ± 0.04 ^b	0.8 ± 0.1 ^b	1.0 ± 0.1 ^c
[Ca ²⁺] _i oscillations duration (sec)	151.9 ± 4.7 ^a	56.9 ± 1.2 ^b	52.1 ± 6.2 ^b	26.8 ± 2.2 ^c

Table 7.1 [Ca²⁺]_i oscillations characteristics under different temperatures (25 °C and 31°C) in immobilised and free-swimming sperm cells. Table shows a comparison of [Ca²⁺]_i oscillations parameters detected in sperm cells under different techniques and temperatures. Data for immobilised cell at 31°C were analysed from experiments performed by Dr. Claire V. Harper. Statistics were conducted between immobilised cells and free-swimming and also between the two temperatures 25 °C and 31°C for each parameter analysed. Groups that do not share a letter are significantly different according to two-way ANOVA followed by Bonferroni’s post-test (p <0.01).

7.3.2 [Ca²⁺]_i oscillations drives velocity/detachment in human spermatozoa

Initially I incubated cells at 25°C and captured fluorescence images at 3 Hz, enabling us to identify cells in which [Ca²⁺]_i oscillations occurred and to relate the sperm’s behaviour to the changes in [Ca²⁺]_i. I observed switching of sperm behaviour which was clearly related to the changing [Ca²⁺]_i. Fig. 7.1 shows the correlated changes in [Ca²⁺]_i (blue) and velocity (red) in a cell that was tracked for almost 10 min. Large [Ca²⁺]_i oscillations are clearly visible and as [Ca²⁺]_i decays after each oscillation peak the cell slows down, such that velocity approaches zero and the sperm settles onto and ‘crawls’ on the coverslip (figs. 7.1 and 7.2).

Development of another $[Ca^{2+}]_i$ oscillation, and consequent increase in speed, allows the sperm to detach from the coverslip and swim. Plotting of velocity against $[Ca^{2+}]_i$ (fig. 7.1 inset) shows a $[Ca^{2+}]_i$ threshold, above which velocity increases when the cell is detached. Thus under these conditions $[Ca^{2+}]_i$ oscillations controls attachment/detachment from the substrate in human sperm cells. This switching of sperm behaviour occurs repeatedly following the cyclic generation of $[Ca^{2+}]_i$ oscillations (fig. 7.1). Similar behaviour between $[Ca^{2+}]_i$ signals and velocity was observed in 71.4% of sperm cells analysed.

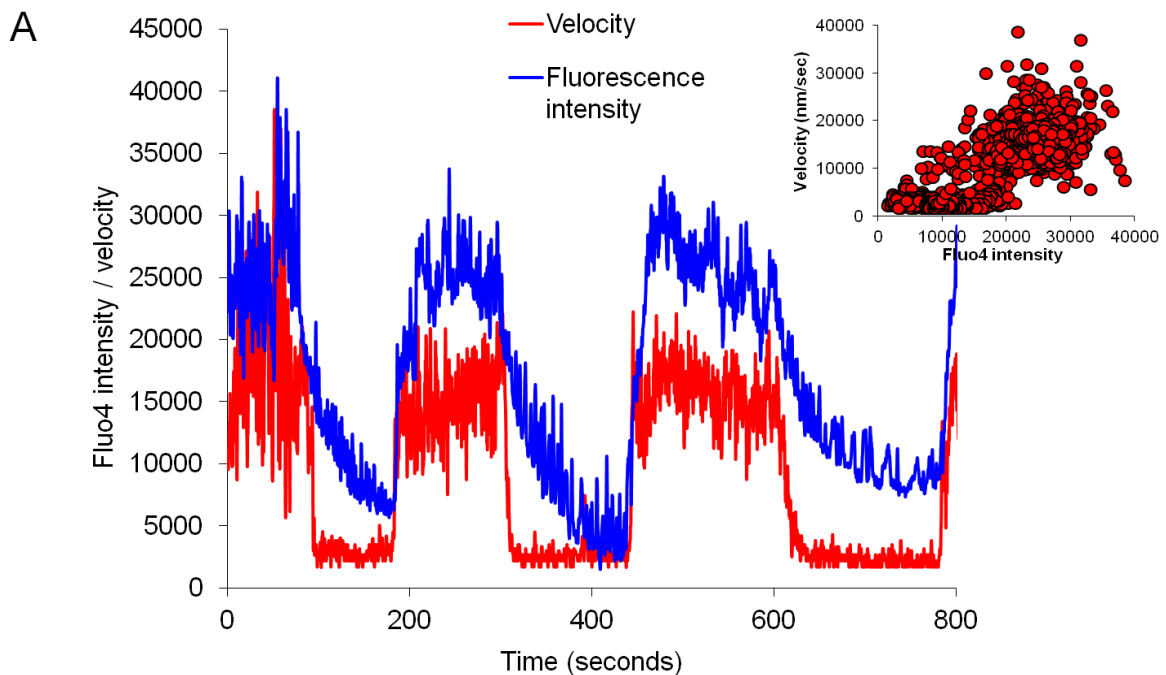


Figure 7.1 $[Ca^{2+}]_i$ oscillations drives velocity in human spermatozoa. Panel (A) shows overlay of the fluorescent intensity (blue) and velocity (red) of individual cells (velocity values were multiplied by 1000 to facilitate overlay plotting). Progesterone-induced $[Ca^{2+}]_i$ oscillations increase velocity and when $[Ca^{2+}]_i$ falls velocity drops reaching close to 0 nm/sec. Inset is a scattergram from data from panel 'A' showing correlation of fluorescent intensity and velocity.

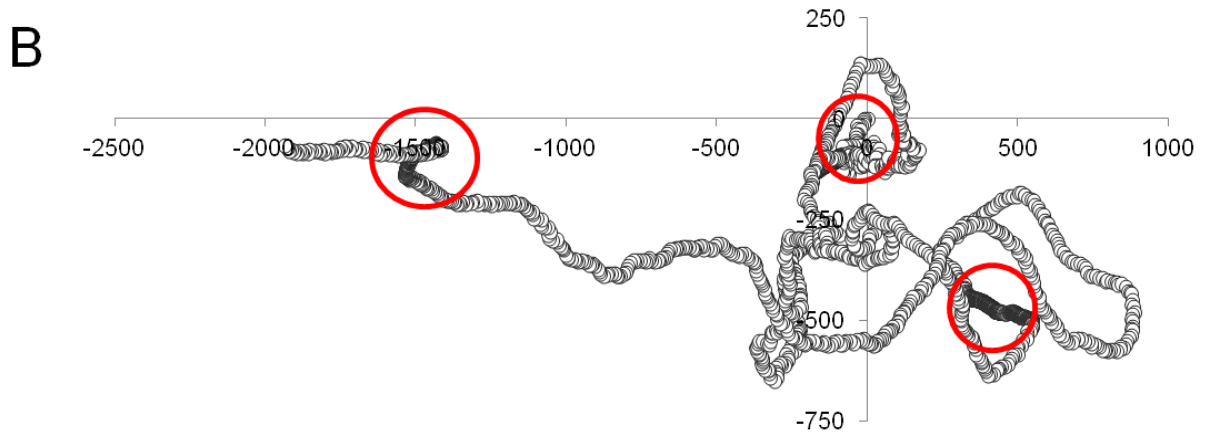


Figure 7.1 $[Ca^{2+}]_i$ oscillations drives velocity in human spermatozoa. **(B)** is the reconstructed trajectory from X-Y co-ordinates of this cell. Red circles mark periods where fluorescent intensity decreases followed by velocity.

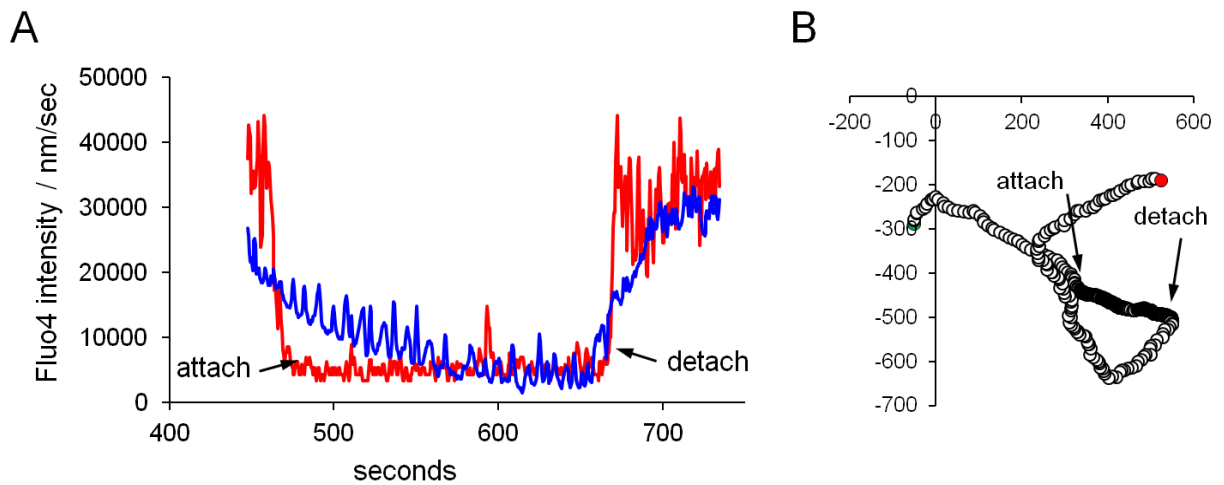


Figure 7.2 $[Ca^{2+}]_i$ oscillations drives attachment/detachment in human spermatozoa. Panel **(A)** shows a *zoom in* of a single $[Ca^{2+}]_i$ oscillation – traces represent fluorescent intensity (blue) and velocity (red). $[Ca^{2+}]_i$ oscillation decay promotes attachment of the cell to coverslip and detachment when $[Ca^{2+}]_i$ rises. **(B)** is the reconstructed trajectory from X-Y co-ordinates of a cell during this $[Ca^{2+}]_i$ oscillation. Black arrows mark periods where the cell is attaching and detaching from the substrate.

7.3.3 $[Ca^{2+}]_i$ oscillations drives turning and hyperactivated motility

We also investigated swimming behaviour of cells incubated at 31°C, using a higher frame rate (10 Hz). Videos captured in this speed provided more detail of the sperm path. Though still insufficient for CASA-type analysis (usually 60 Hz), this allowed calculation of average path velocity (VAP), straightness (STR) and fractal dimension of the sperm path derived from head position (x and y coordinates) in each video frame. At this temperature I again observed changes in behaviour associated with $[Ca^{2+}]_i$ in oscillating cells, but velocity did not fall sufficiently for cells to ‘settle’ on the coverslip as occurred at 25°C. Again, in most cells I observed correlation between $[Ca^{2+}]_i$ and velocity, cells showing bursts of acceleration during increased $[Ca^{2+}]_i$ (fig. 7.3). As a measure of hyperactivated-type motility, ‘straightness’ was calculated from the ratio of linear distance compared to smoothed distance over 10 track points (explained in fig. 7.4A). The data showed that, in many cells, the rise $[Ca^{2+}]_i$ oscillation is inversely correlated with the straightness of the cell path, which suggests that the sperm head turns more when $[Ca^{2+}]_i$ is higher (fig. 7.4B-D). I also analysed the fractal dimension of sperm trajectories, which is a parameter typically high in hyperactivated cells. Regardless the frame rate limitation, I was able to observe two cells showing a clear correlation between $[Ca^{2+}]_i$ and fractal dimension (fig. 7.5) (see Appendix I for more examples of correlation).

Decline in cell straightness and increase of fractal dimension are indicative of switching of swimming behaviour to hyperactivated motility (Cancel et al, 2000), therefore $[Ca^{2+}]_i$ oscillations may also drive hyperactivated motility in human sperm cells. Collectively, our results show that $[Ca^{2+}]_i$ oscillations occur in free-swimming human sperm and are important for modulation of sperm behaviour, regulating both velocity/detachment of the sperm (figs. 7.1 - 7.3) and its turning behaviour (figs. 7.4 and 7.5).

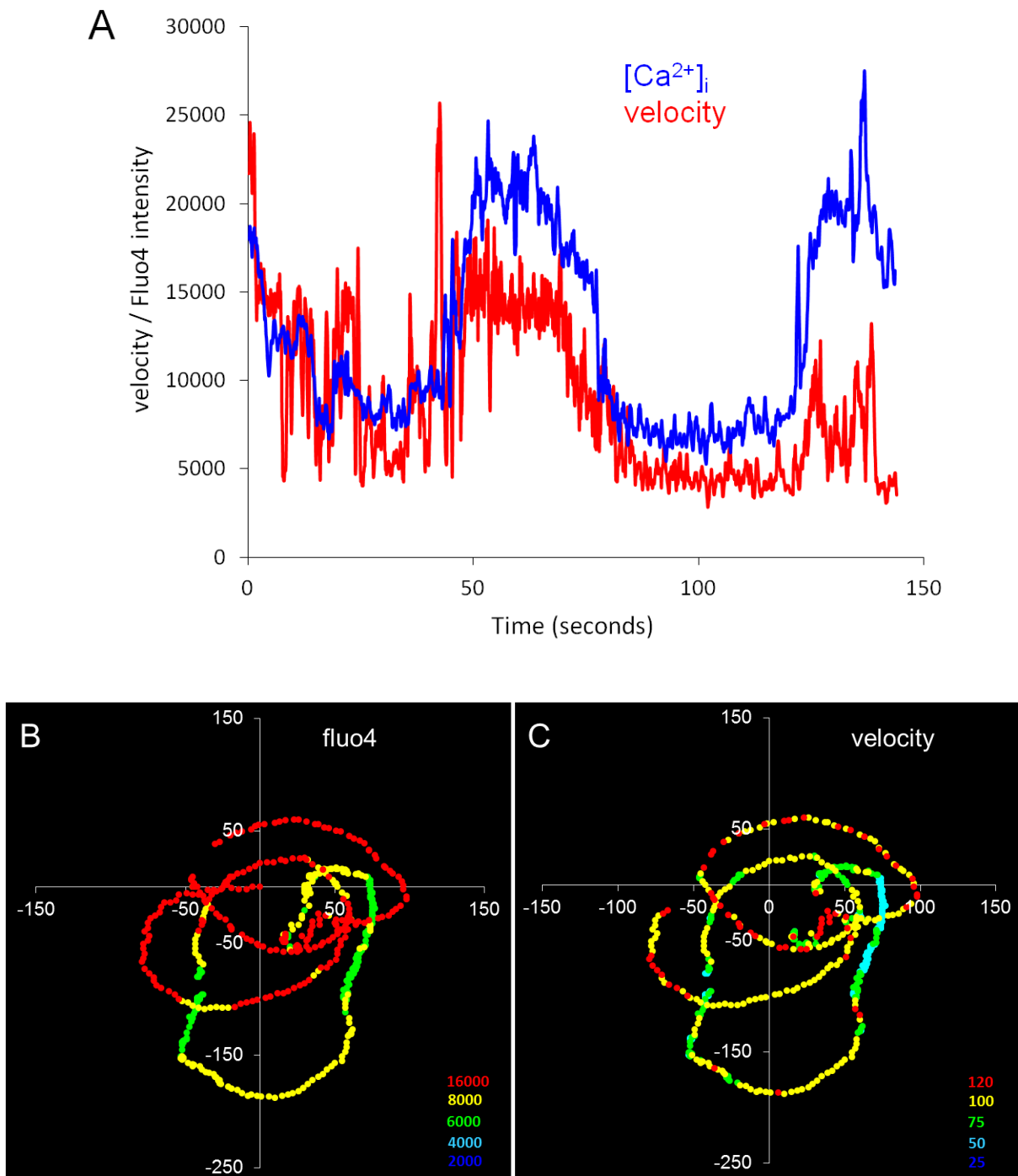


Figure 7.3 Correlation between $[Ca^{2+}]_i$ and velocity. (A) shows relationship between $[Ca^{2+}]_i$ (fluo4 fluorescence – blue) and average path velocity (VAP), in a progesterone-stimulated, free-swimming human sperm (velocity has been normalised to maximum value). Lower panel shows sperm track coordinates plotted with colour coding to indicate fluo4 fluorescence (B) and VAP (C). Analysis was performed in collaboration with Dr. Hector A. Guidobaldi, Universidad Nacional de Cordoba.

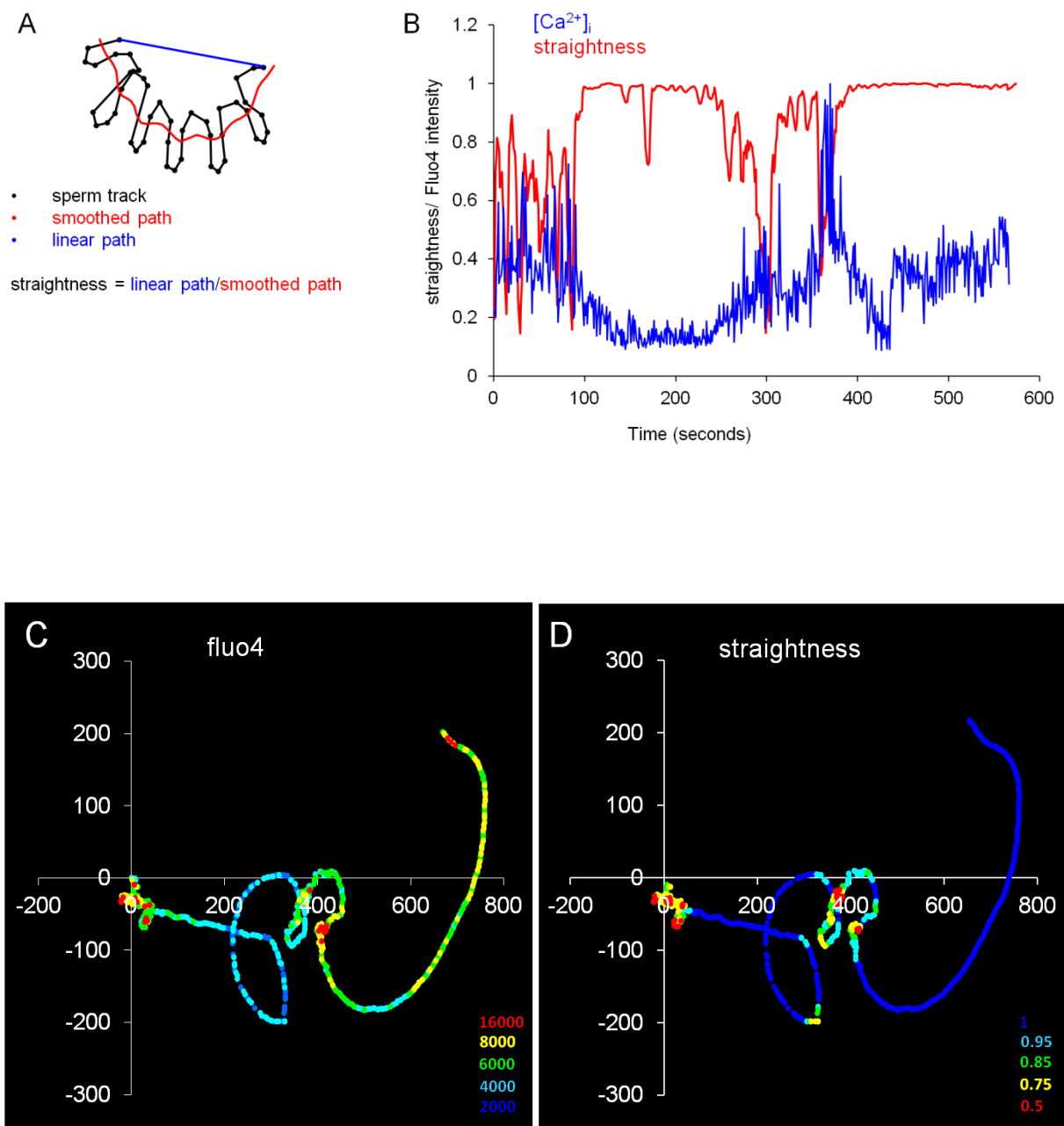


Figure 7.4 Correlation between [Ca²⁺]_i and straightness. (A) illustrates calculation of sperm path ‘straightness’. Sperm path is derived from head position (x and y coordinates) in each video frame. Smoothed path (red) is a 10 point moving average of x and y coordinates. Straightness was calculated from the ratio of linear distance (blue) compared to smoothed distance (red) over 10 track points. (B) shows relationship between [Ca²⁺]_i (fluo4 fluorescence – blue) and straightness in a progesterone-stimulated, free-swimming human sperm. Lower panel shows sperm track coordinates plotted with colour coding to indicate fluo4 fluorescence (C) and straightness (D). Analysis was performed, in collaboration with Dr. Hector A. Guidobaldi, Universidad Nacional de Cordoba.

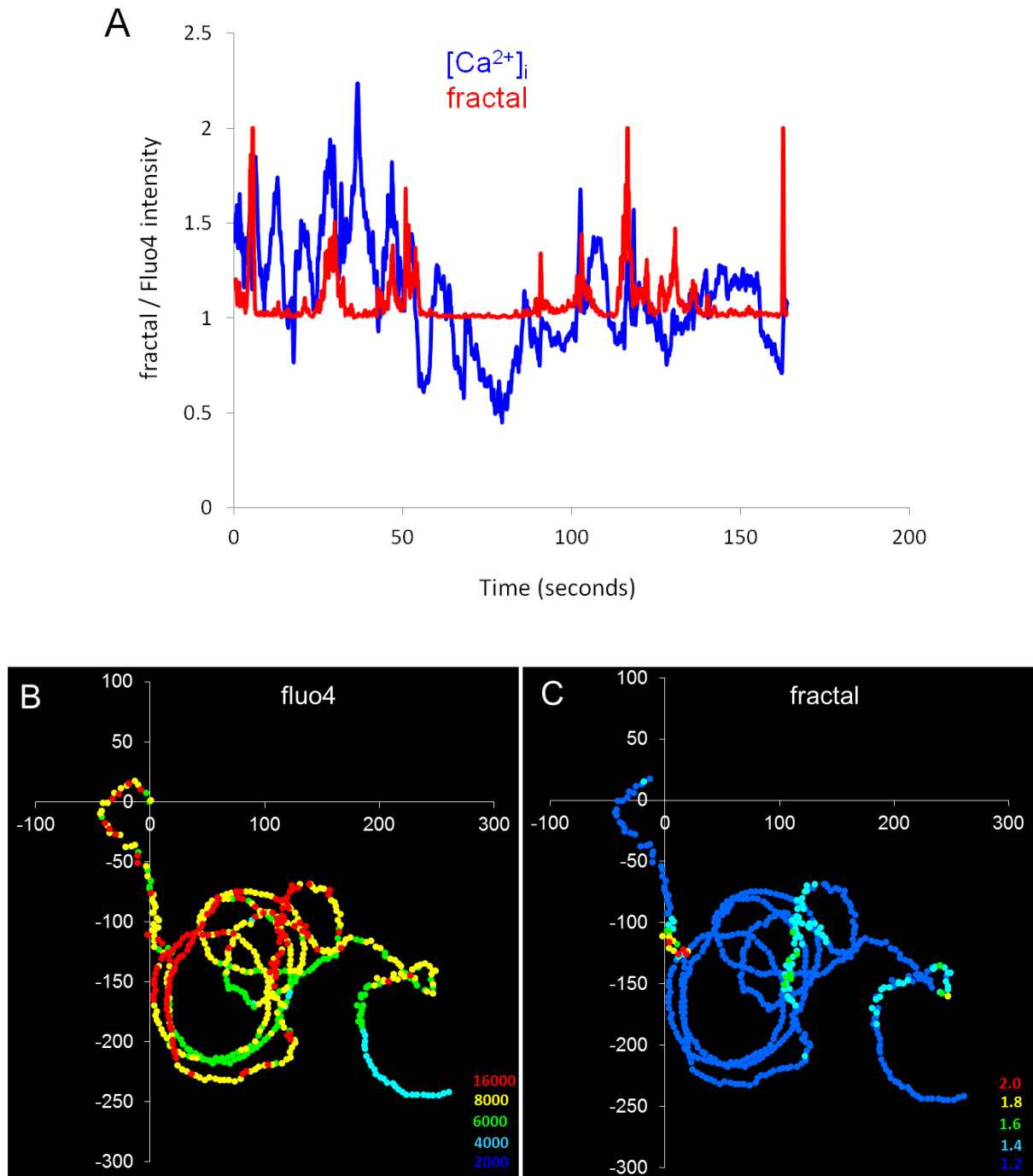


Figure 7.5 Correlation between $[Ca^{2+}]_i$ and fractal dimension. (A) shows relationship between $[Ca^{2+}]_i$ (fluo4 fluorescence – blue) and fractal dimension in a progesterone-stimulated, free-swimming human sperm. Lower panel shows sperm track coordinates plotted with colour coding to indicate fluo4 fluorescence (B) and fractal dimension (C). Analysis was performed, in collaboration with Dr. Hector A. Guidobaldi, Universidad Nacional de Cordoba.

7.3.4 High viscosity induces Ca^{2+} transient and $[\text{Ca}^{2+}]_i$ oscillations

During its journey through the female tract, a sperm cell encounters fluids with different viscosities, which range from 2800–10000 cp (Karni et al, 1971; Jansen, 1978; Suarez et al, 1997; Tung et al, 2015). To investigate how high viscosity affects $[\text{Ca}^{2+}]_i$ responses, I prepared medium using 1% (w/v) methylcellulose (MCL) to raise the viscosity to, nominally, 4000 cp. Interestingly, switch from standard sEBBS to methylcellulose perfusion induced Ca^{2+} transient which was followed by $[\text{Ca}^{2+}]_i$ oscillations in $30.9 \pm 5.9\%$ of cell population (fig. 7.6A). Subsequent application of progesterone, in the presence of methylcellulose, induced a $[\text{Ca}^{2+}]_i$ transient that resembled that seen under normal conditions and was approximately twice the amplitude of the one induced by methylcellulose ($n= 72$ cells, $p<0.001$, fig. 7.6B). Furthermore, the characteristics of the $[\text{Ca}^{2+}]_i$ oscillations induced by methylcellulose were similar to the progesterone-induced ones (fig. 7.6C and D).

When cells were first stimulated with progesterone, then exposed to methylcellulose in the continued presence of progesterone $[\text{Ca}^{2+}]_i$ oscillations persisted (fig. 7.7A) and their characteristics (amplitude and frequency) were not altered, though there was a significant reduction in these parameters when viscosity was returned to normal levels (fig. 7.7B and C).

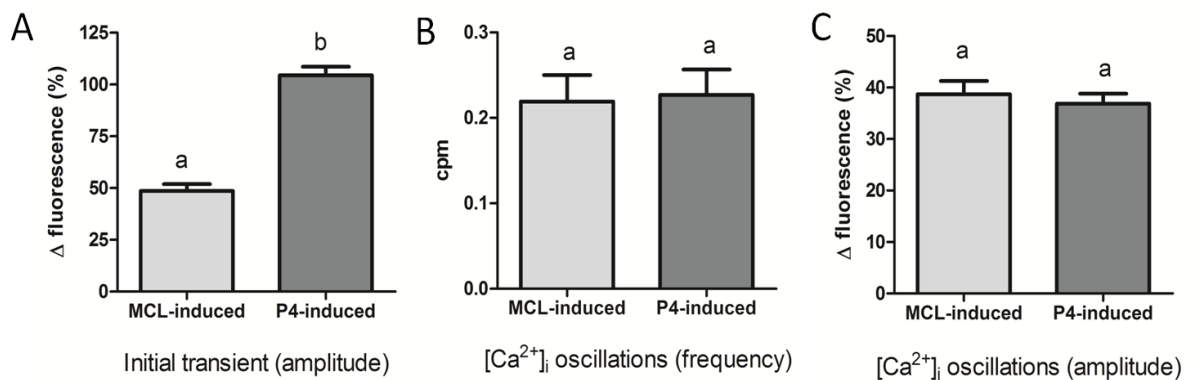
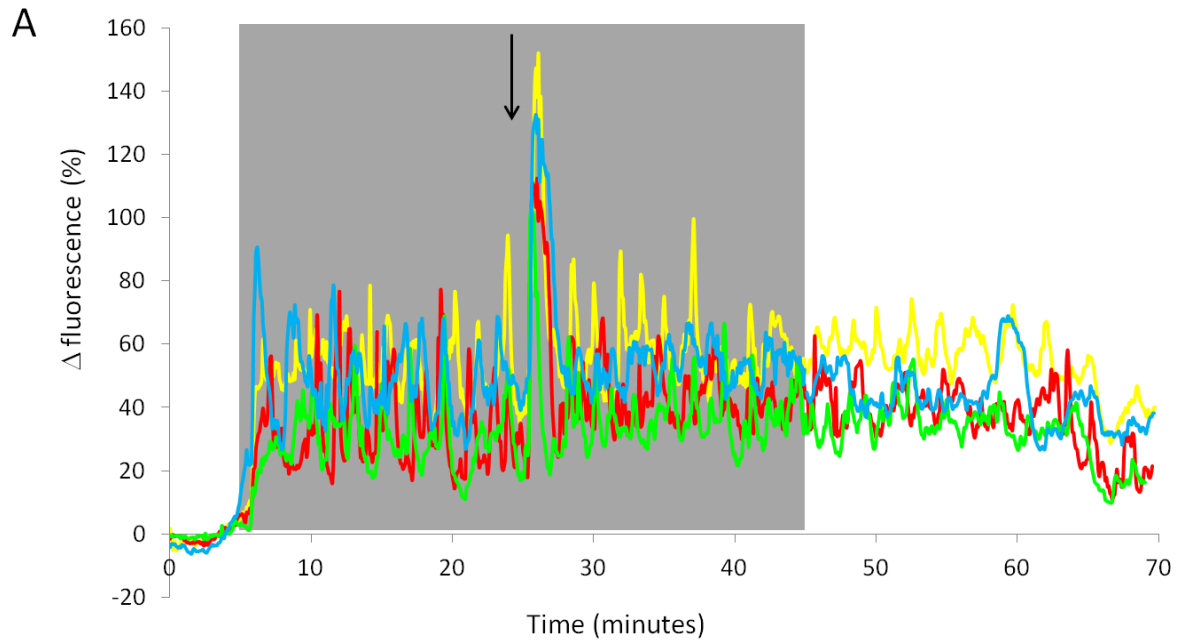


Figure 7.6 High viscosity induces Ca^{2+} transient and $[\text{Ca}^{2+}]_i$ oscillations in human spermatozoa. Panel (A) shows single cells traces (4 cells from different set of experiments). Grey shading shows period of perfusion with methylcellulose 4000 cp, black arrow indicates addition of 3 μM progesterone. Graphs show the amplitude of transient peak (B) and frequency (C) and amplitude (D) of $[\text{Ca}^{2+}]_i$ oscillations induced by methylcellulose (MCL) and progesterone (P4). Amplitude was calculated using the mean response of each $[\text{Ca}^{2+}]_i$ oscillation considering the progesterone- induced transient peak as 100% and bars show mean \pm SEM of 72 cells from 3 different experiments. A $[\text{Ca}^{2+}]_i$ oscillation was considered when reached at least 20% of the transient peak amplitude. Bars that do not share a letter are significantly different according to t-test ($p < 0.001$).

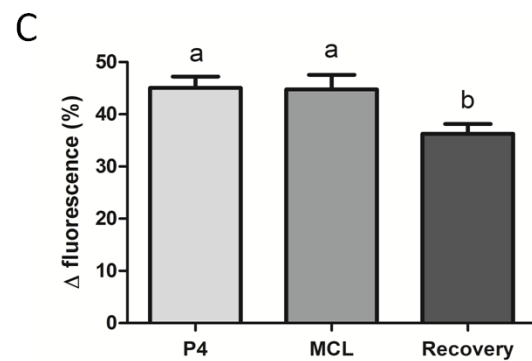
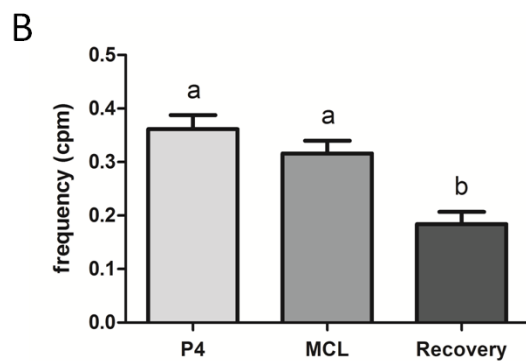
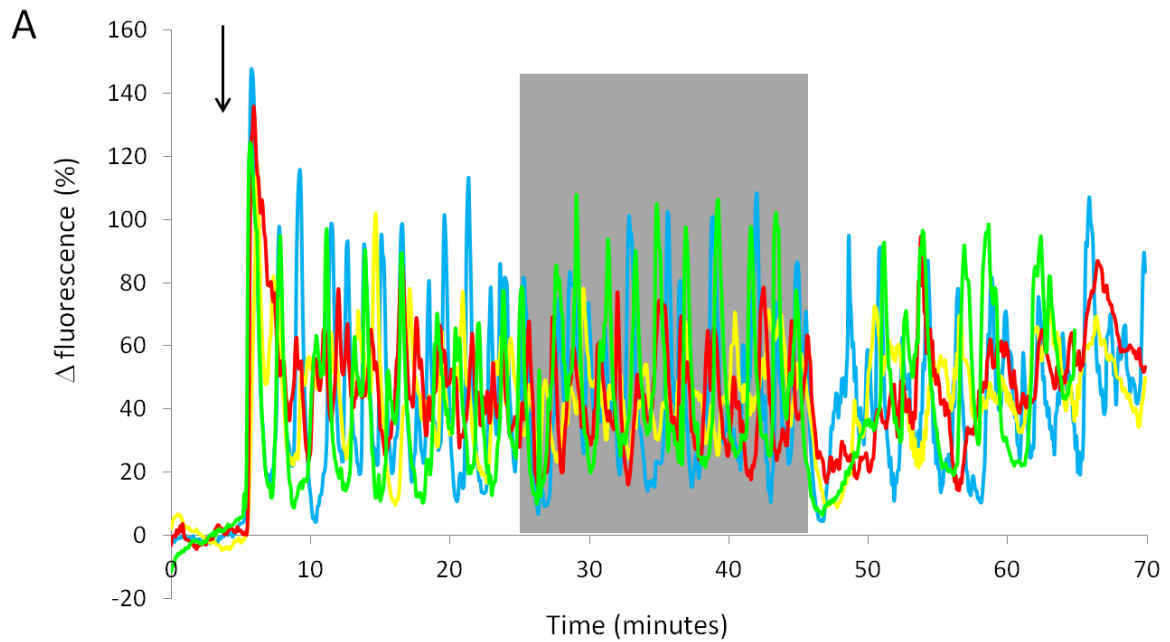


Figure 7.7 High viscosity does not change the characteristics of P4-induced $[Ca^{2+}]_i$ oscillations in human spermatozoa. Panel (A) shows single cells traces (4 cells from different set of experiments). Black arrow indicates addition of 3 μ M progesterone (P4); grey shading shows period of perfusion with methylcellulose (MCL) 4000 cp. Graphs show the frequency of $[Ca^{2+}]_i$ oscillations per minute (B) and the amplitude of $[Ca^{2+}]_i$ oscillations (C) in the ‘oscillating’ population under the three conditions: progesterone alone treatment in standard EBSS (first bar), progesterone plus methylcellulose 4000 cp (second bar) and progesterone alone treatment in standard EBSS (third bar). Amplitude was calculated using the mean response of each $[Ca^{2+}]_i$ oscillation considering the transient peak as 100% and bars show mean \pm SEM of 3 experiments. A $[Ca^{2+}]_i$ oscillation was considered when reached at least 20% of the transient peak amplitude. Treatment groups that do not share a letter are significantly different according to one-way ANOVA followed by Tukey’s post-hoc ($p < 0.001$).

7.3.5 High viscosity effect on Ca^{2+} response is dependent of CatSper

Having demonstrated that high viscosity medium induces Ca^{2+} transient followed by $[\text{Ca}^{2+}]_i$ oscillations with similar characteristics to the progesterone-induced ones, we decided to investigate whether these Ca^{2+} responses were also dependent of CatSper channels activity. Pre-treatment with RU1968 (30 μM) completely inhibited Ca^{2+} transient and $[\text{Ca}^{2+}]_i$ oscillations when both methylcellulose and subsequently progesterone were added to the sperm cells (fig. 7.8). As a control, RU1968 and methylcellulose were removed and a large Ca^{2+} peak was observed followed by $[\text{Ca}^{2+}]_i$ oscillations generation when in the presence of progesterone (n= 30 cells from 3 experiments; fig. 7.8).

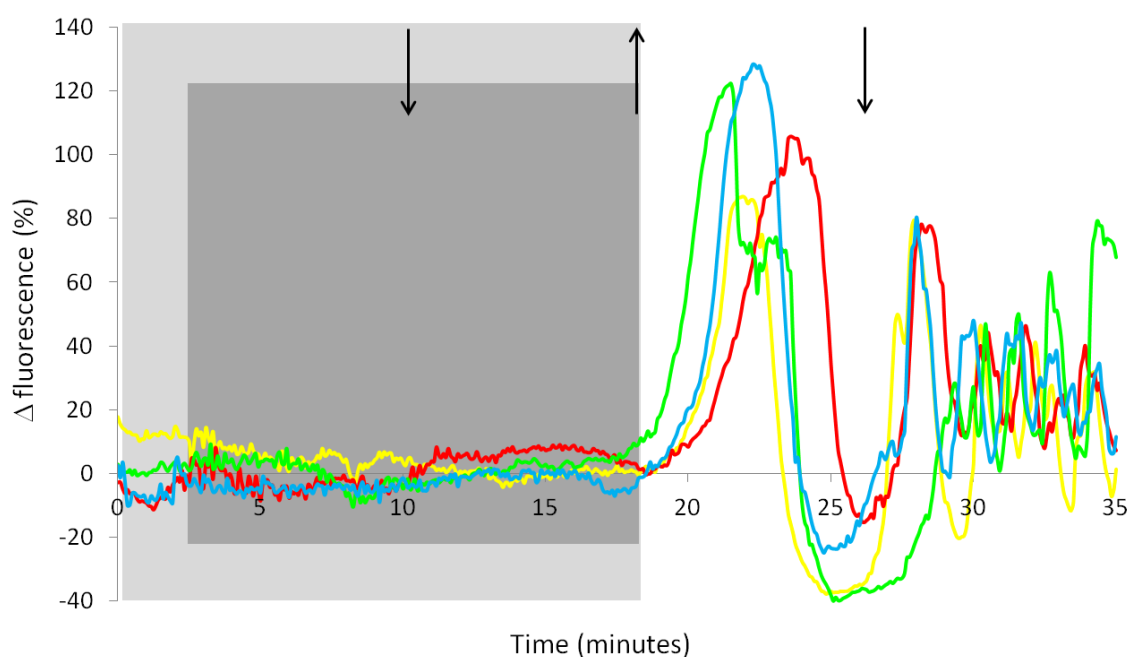


Figure 7.8 CatSper blocker (RU1968) completely inhibits Ca^{2+} transients and $[\text{Ca}^{2+}]_i$ oscillations n induced by MCL and P4 in human sperm cells. Panel shows single cells traces of different set of experiments). Light grey shading shows addition of RU1968 (30 μM), dark grey shading shows perfusion of methylcellulose (MCL) 4000 cp and black arrows show addition, removal and readdition of progesterone (3 μM). Experiments were performed in collaboration with Dr. Esperanza Mata-Martínez, Universidad Nacional Autónoma de México.

7.3.6 $[Ca^{2+}]_i$ oscillations drives velocity in high viscosity environment

To confirm that $[Ca^{2+}]_i$ oscillations also occurs in free-swimming cells in a high viscosity environment, I tracked fluo-4-labelled free-swimming sperm cells under these conditions. As observed in free-swimming cell in standard saline (fig. 7.1), spermatozoa in methylcellulose exhibited $[Ca^{2+}]_i$ oscillations (fig. 7.9). Furthermore, $[Ca^{2+}]_i$ oscillations also showed correlation with velocity in high viscosity, although the attachment/detachment from the substrate was not as clear (fig. 7.9). $[Ca^{2+}]_i$ increase induces velocity to increase and when $[Ca^{2+}]_i$ falls velocity subsequently decays, suggesting that the switching of sperm behaviour is dependent of the cyclic generation of $[Ca^{2+}]_i$ oscillations (fig. 7.9).

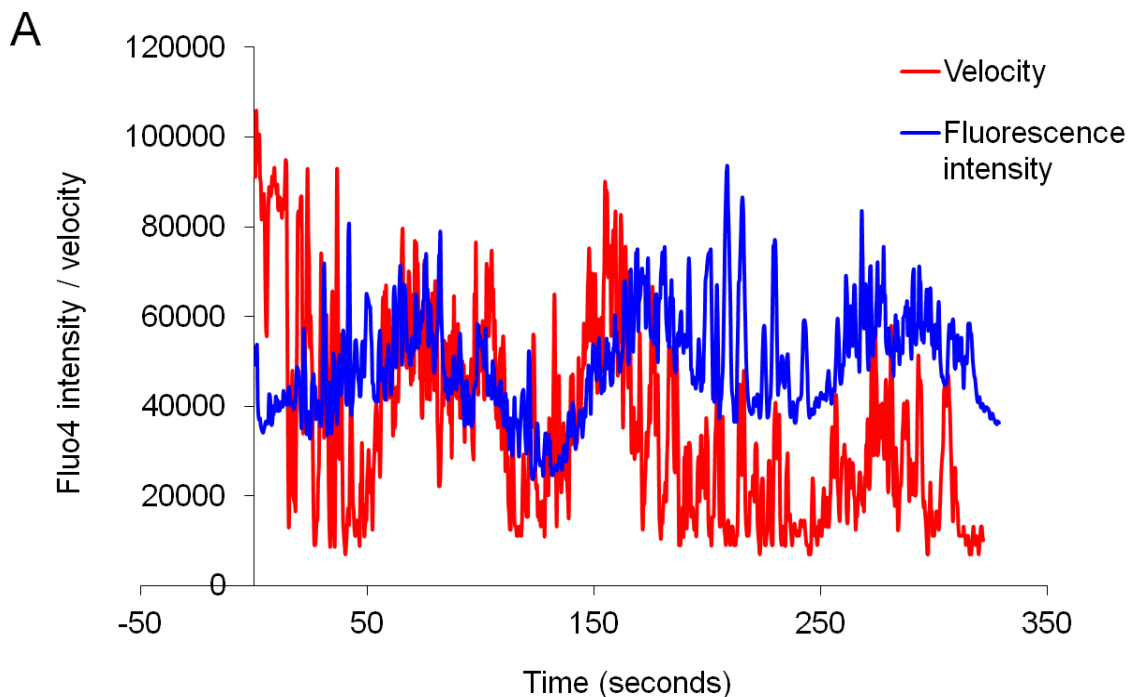


Figure 7.9 $[Ca^{2+}]_i$ oscillations drives velocity in high viscosity environment. Panel (A) shows overlay of the fluorescent intensity (blue) and velocity (red) of individual cells (velocity values were multiplied by 3000 to facilitate overlay plotting). $[Ca^{2+}]_i$ signals and velocity are correlated in methylcellulose 4000 cp - $[Ca^{2+}]_i$ increase promotes increase in velocity and when $[Ca^{2+}]_i$ falls velocity follows.

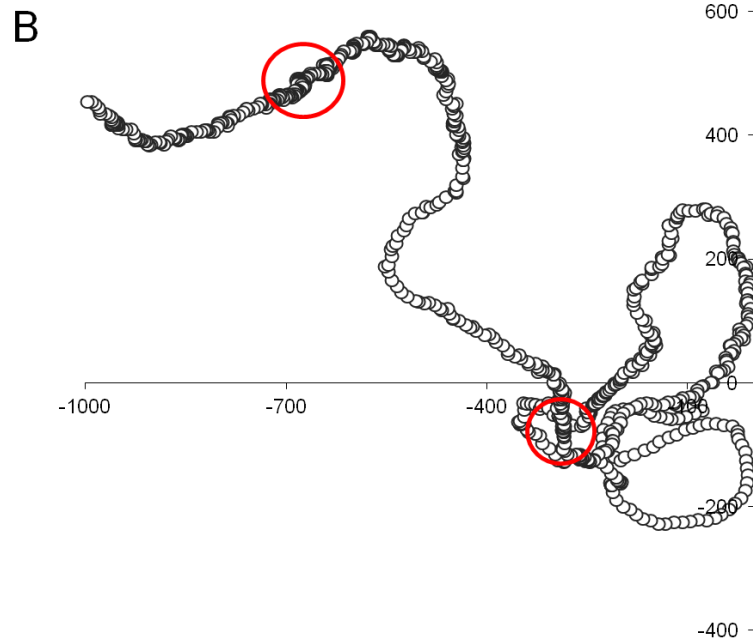


Figure 7.9 $[Ca^{2+}]_i$ oscillations drives velocity in high viscosity environment. **(B)** is the reconstructed trajectory from X-Y co-ordinates of this cell. Red circles mark periods where velocity is decreased.

7.3.7 Swimming velocity and cell progression is inhibited by CatSper blockade

In chapter 5, I demonstrated that $[Ca^{2+}]_i$ oscillations are regulated by CatSper activation. To assess whether CatSper channels are also crucial to the changes on swimming behaviour, I tracked fluo-4-labelled free-swimming sperm cells pre-treated with RU1968 (30 μ M) in the presence of progesterone (3 μ M). Similarly to its effect on immobilised cells, RU1968 inhibited $[Ca^{2+}]_i$ oscillations both in cells swimming in standard saline and in high viscosity medium (insets fig. 7.10A and B). Moreover, inhibition of CatSper both abolished variation in velocity and resulted in continuous turning of the cells such that they became effectively non-progressive. In control (untreated) cells the mean travel (distance from origin) after 3 min was approximately 1500 μ m whereas this distance was 6 times shorter when cells were treated with RU1968 (20 cells per condition; $p < 0.001$; fig. 7.10C).

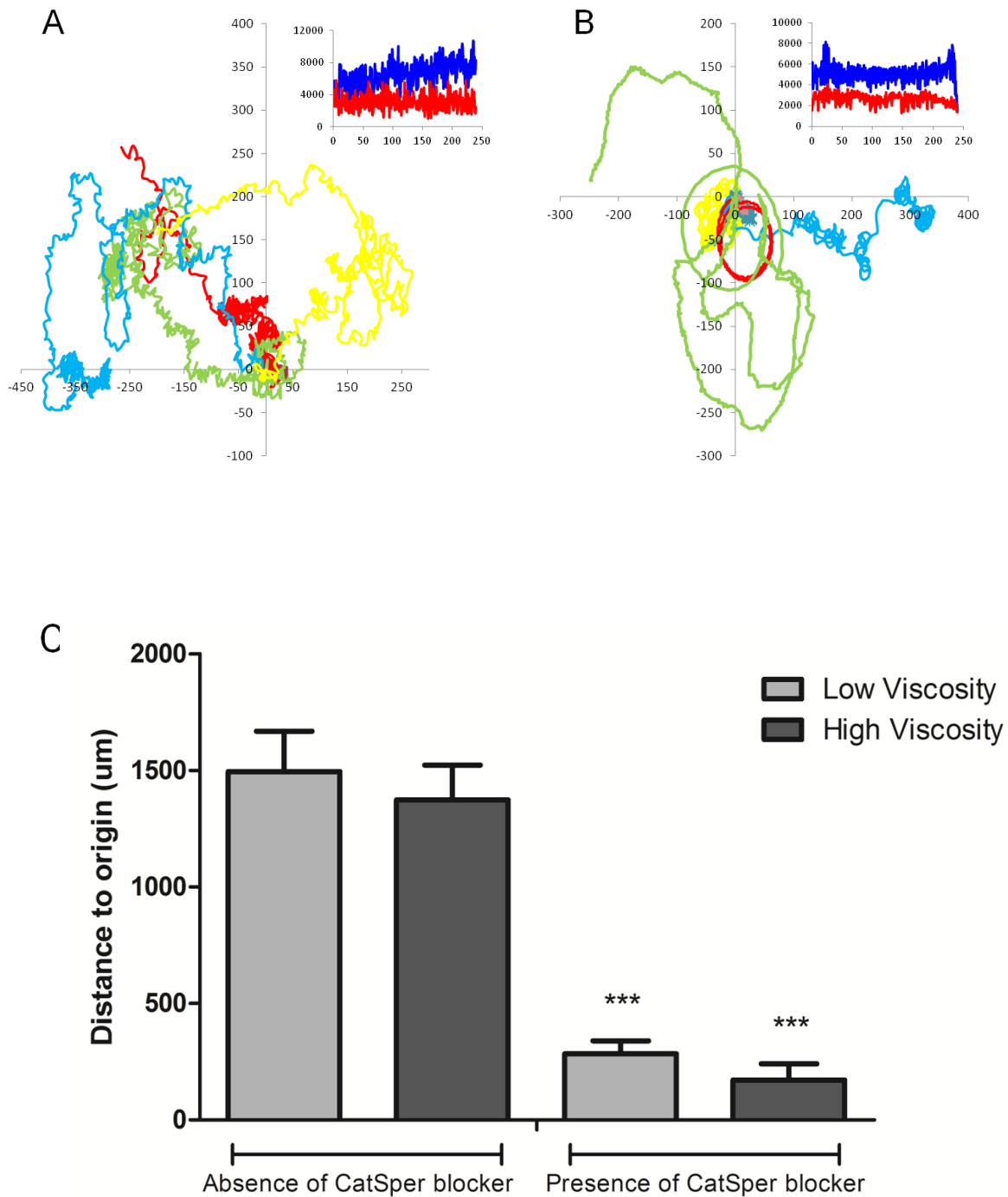


Figure 7.10 CatSper blocker inhibits $[Ca^{2+}]_i$ oscillations and progression of cell. X-Y position graphs show tracking of a group of sperm cells treated with $30 \mu\text{M}$ RU1968 + $3 \mu\text{M}$ P4 in low (panel 'a') and high (panel 'b') viscosity environment. Insets show $[Ca^{2+}]_i$ and velocity under these conditions (velocity values were multiplied by 1000 to facilitate overlay plotting). Bar graph shows the mean \pm SEM of distance (μm) of tracked cells from origin after 3 minutes of tracking. *** $p < 0.001$ when compared to group untreated with CatSper blocker under the same viscosity condition. A total of 20 cells were analysed per group.

7.3.8 Sperm ability to penetrate into artificial viscous medium

A sperm cell needs to penetrate through viscous barriers, including mucus and oviduct fluid, in order to achieve a successful fertilisation (Jansen 1978; Suarez et al, 1997; Tung et al, 2015). In these experiments the number of ‘penetrating’ cells at the start point (0 cm) varied widely (range of 40 – 157 cells) according to sperm sample (n= 20 experiments) and this wide variation affected the number of cells penetrating the viscous medium (fig. 7.11). Therefore, assays were always run in parallel with an untreated control and data were expressed as ‘% control sperm number’ (where control was considered to be 100%).

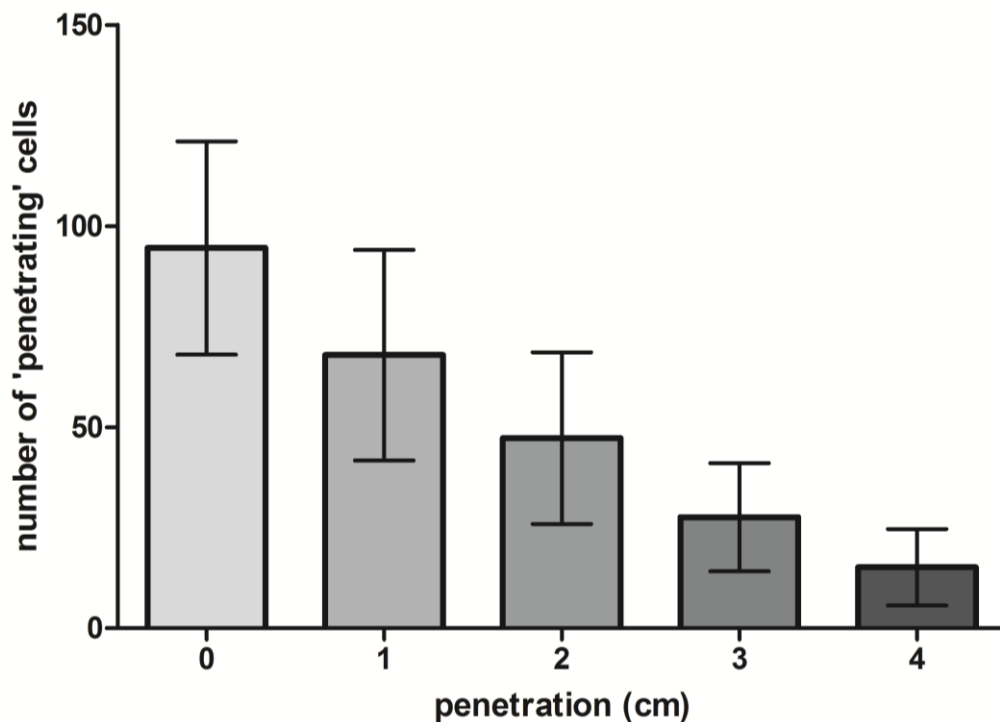


Figure 7.11 Sperm penetration into artificial viscous medium assay expressed in number of ‘penetrating’ cells. Bar graph shows the mean \pm SD of ‘penetrating’ cells at 1, 2, 3 and 4 cm into viscous medium. n=20 experiments performed in triplicates.

7.3.9 Effect of CatSper inhibition in sperm penetration of artificial viscous medium

CatSper has been implicated in regulating sperm ability to penetrate viscous medium (Alasmari et al, 2013). In order to assess whether RU1968 would inhibit this ability, spermatozoa were treated with different concentrations of the drug (added to the sperm reservoir) and the proportion of cells that penetrated artificial methylcellulose medium was analysed. 1 μ M RU1968 had negligible effect on sperm performance in the assay but significant inhibition occurred at greater concentrations (10-50 μ M). Sperm penetration at each of 1, 2, 3 and 4 cm showed a significant, dose dependent inhibitory effect of RU1968 that saturated at 30-50 μ M (n=6 experiments, p<0.01, fig. 7.12). The extent of inhibition was increased at greater penetration depth, maximum inhibition occurring at 4 cm, where cell count in the presence of 50 μ M RU1968 was only $8.1 \pm 2.2\%$ of that in the parallel control (n=6, p<0.001, fig. 7.10). Entry into the methylcellulose column (assessed by cell count at 0 cm) was reduced only slightly, even at the highest concentration used (fig. 7.12).

To further investigate the role of CatSper in regulating the behaviour that enables the sperm to penetrate viscous medium, I investigated the effect of progesterone. Two different designs were used: (1) sperm cells in the reservoir were co-treated with different concentrations of RU1968 + 3 μ M of progesterone and then allowed to penetrate into viscous medium or (2) sperm cells were treated with 3 μ M of progesterone alone in the sperm reservoir and then allowed to penetrate into viscous medium containing different concentrations of RU1968. In design (1), exposure to progesterone alone increased sperm entry into the methylcellulose (0 cm) by $72.5 \pm 10.6\%$. Moreover, this stimulatory effect was similar at all penetration distances ($60.7 \pm 6.6\%$ at 1 cm and $61.3 \pm 27.4\%$ at 4 cm) (n=5, p<0.001, fig. 7.13). All RU1968 concentrations used completely inhibited the effect of progesterone including 1 μ M RU1968 (fig. 7.13; red bars), which did not affect penetration

itself (as shown in fig. 7.10). The effect of RU1968 was again dose- and distance-dependent with maximum inhibition occurring when cells were treated with 50 μ M RU1968 and penetration assessed at 4 cm ($95.71 \pm 6.36\%$; $n=5$, $p<0.001$, fig. 7.13).

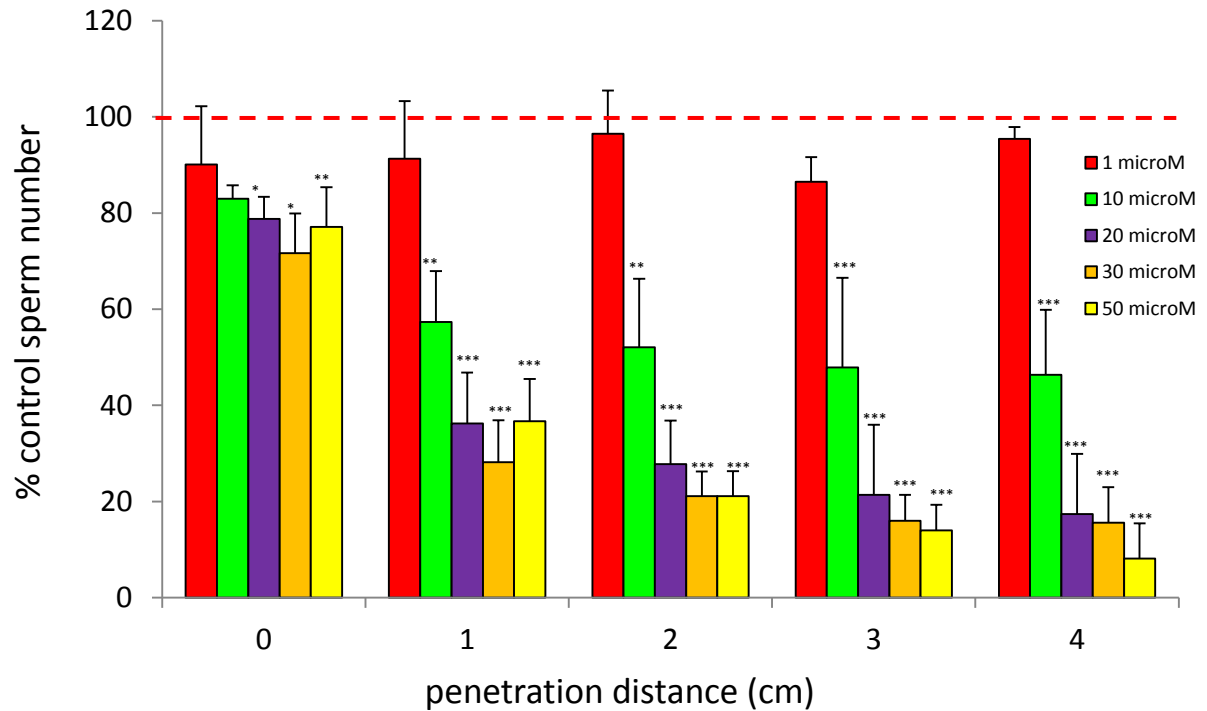


Figure 7.12 RU1968 inhibits sperm penetration into artificial viscous medium in a dose-dependent way. Bars show number of cells at 1, 2, 3 and 4 cm into viscous medium, normalised to parallel controls treated with DMSO (=100% - red dashed line); 1 μ M RU1968 (red), 10 μ M RU1968 (green), 20 μ M RU1968 (purple), 30 μ M RU1968 (orange), 50 μ M RU1968 (yellow). Comparisons were conducted with two-way ANOVA followed by Bonferroni's post-hoc. ** $p < 0.01$; *** $p < 0.001$, when compared to untreated cells at the same penetration distance. Bars show mean + SEM of five experiments.

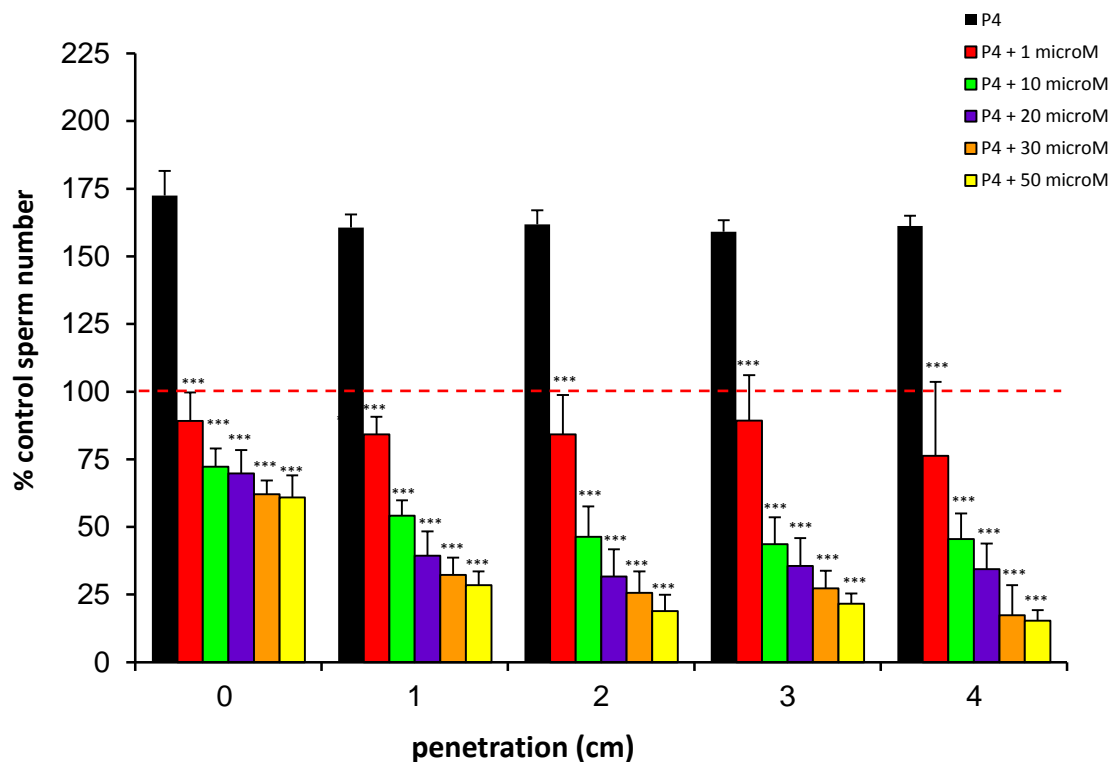


Figure 7.13 RU1968 inhibits stimulation induced by progesterone (3 μ M) of sperm penetration of artificial viscous medium – design (1). Bars show number of cells at 1, 2, 3 and 4 cm into viscous medium, normalised to parallel controls treated with DMSO (=100% - red dashed line); progesterone alone (black), progesterone and 1 μ M RU1968 (red), progesterone and 10 μ M RU1968 (green), progesterone and 20 μ M RU1968 (purple), progesterone and 30 μ M RU1968 (orange), progesterone and 50 μ M RU1968 (yellow). Comparisons were conducted with two-way ANOVA followed by Bonferroni's post-test. P4 alone was compared to untreated cells at the same penetration distance (**p < 0.001). RU1968 concentrations were compared to P4 effect alone at the same penetration distance (**p < 0.001). Bars show mean + SEM of five experiments.

The effect of RU1968 in design (2) was even more pronounced. All RU1968 concentrations inhibited the stimulatory effect of progesterone and higher doses were particularly potent: RU1968 20 μ M and 30 μ M inhibited sperm penetration to 4 cm by $94.1 \pm 0.70\%$ and $96.6 \pm 0.3\%$, respectively. 50 μ M RU1968 completely inhibited sperm penetration to distances ≥ 2 cm (n=5, p<0.001, fig. 7.14).

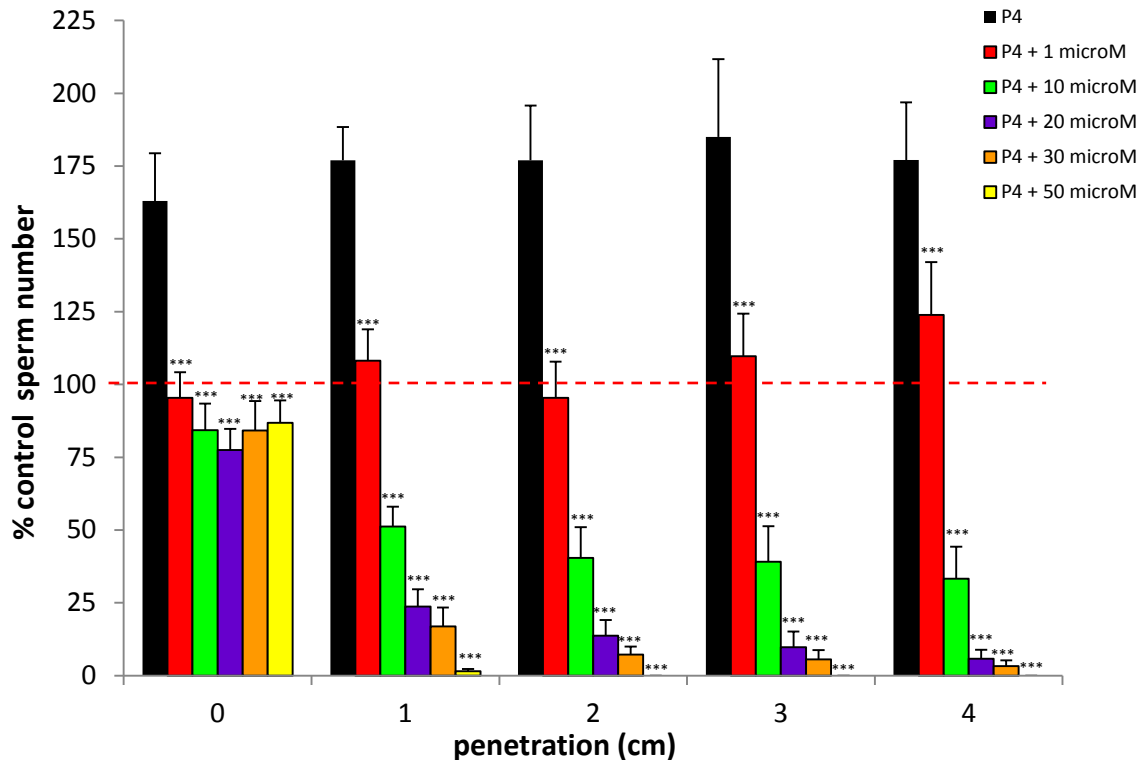


Figure 7.14 RU1968 inhibits progesterone effect on sperm penetration when added to the viscous medium – design (2). Bars show number of cells at 1, 2, 3 and 4 cm into viscous medium, normalised to parallel controls treated with DMSO (=100% - red dashed line); progesterone alone (black), progesterone and 1 μ M RU1968 (red), progesterone and 10 μ M RU1968 (green), progesterone and 20 μ M RU1968 (purple), progesterone and 30 μ M RU1968 (orange), progesterone and 50 μ M RU1968 (yellow). Comparisons were conducted with two-way ANOVA followed by Bonferroni's post-test. P4 alone was compared to untreated cells at the same penetration distance (***) $p < 0.001$. RU1968 concentrations were compared to P4 effect alone at the same penetration distance (***) $p < 0.001$. Bars show mean + SEM of five experiments.

Analysis of the motility of sperm swimming within the methylcellulose was performed with CASA software in order to assess whether the effect of RU1968 on sperm penetration (and reversal of progesterone stimulation) was reflected in kinematic parameters. Sperm cells in design (1) did not show any change in all parameters analysed: track speed (VCL), lateral amplitude of head (ALH), beat frequency (BCF), straightness, linearity and percentage of motile or progressive cells (fig. 7.15), suggesting that the pre-treatment with RU1968

abolishes the progesterone action by inhibiting the sperm entry into the mucus and, consequently, lowering the number of penetrating sperm cells. On the other hand, addition of with RU1968 to the mucus, as described in design (2), resulted in differences in the proportion of the population classified as motile and progressively motile cells (fig. 7.15). Although sperm cells could penetrate into the mucus at the start point, the lowered number of penetrating sperm is probably due to decrease of the fraction of progressively motile sperm when CatSper was inhibited by RU1968.

Collectively, these data support previous reports from Alasmari and colleagues (2013) who suggested that progesterone promotes sperm swimming in high-viscosity environment, via activation of CatSper channels. Furthermore, the drug RU1968 inhibits the effect of progesterone, mimicking the lack of functional CatSper channels, observed by Williams and colleagues (2015).

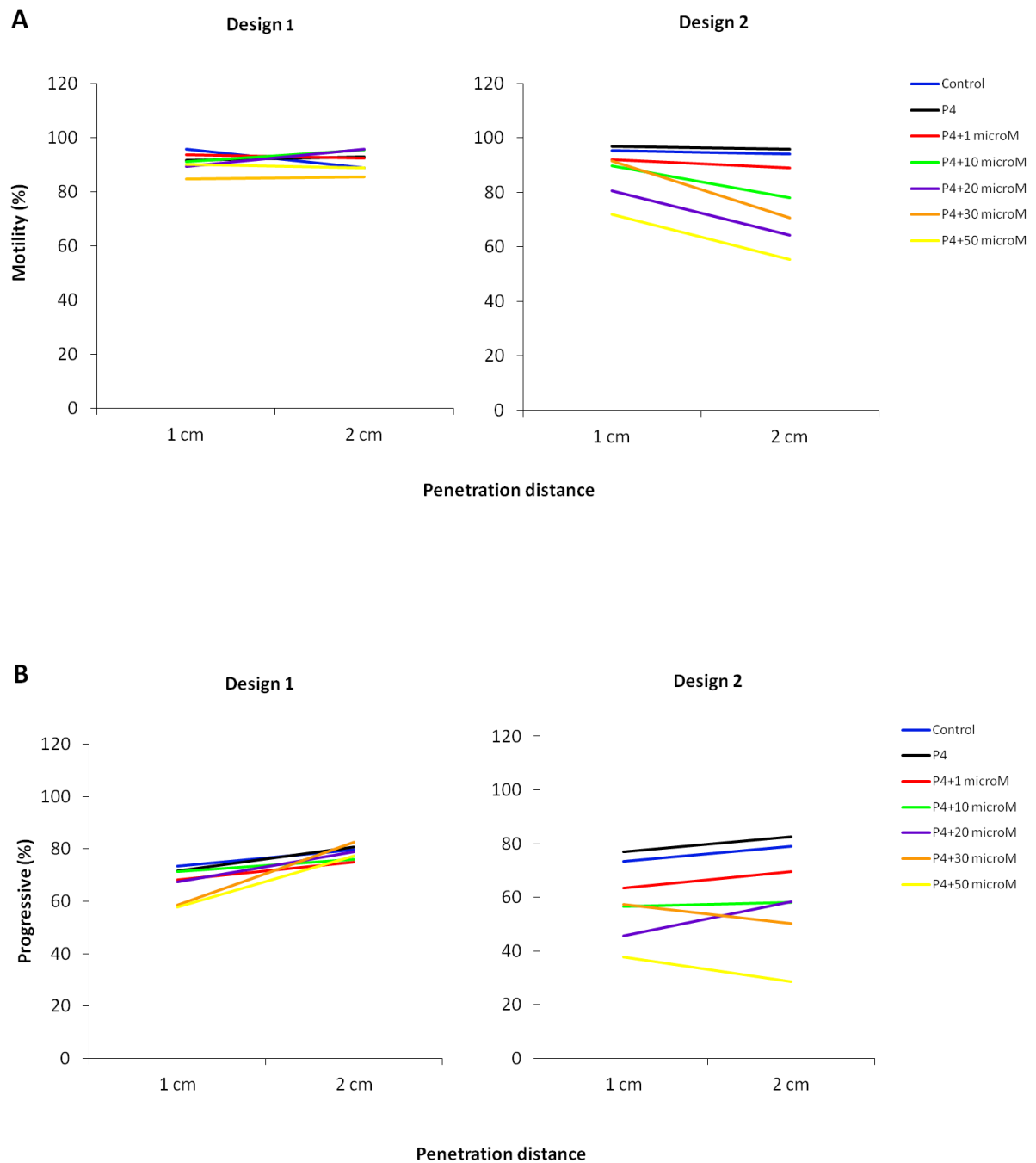


Figure 7.15 RU1968 inhibits the sperm progression and motility when added to the viscous medium. Graph represents the percentage of progressive (A) and motile (B) sperm cells in the different penetration distances in artificial viscous medium when cells were stimulated with progesterone and RU1968 was added to saline (design 1) or to the viscous medium (design 2). Parallel controls treated with DMSO (blue); progesterone alone (black), progesterone and 1 μM RU1968 (red), progesterone and 10 μM RU1968 (green), progesterone and 20 μM RU1968 (purple), progesterone and 30 μM RU1968 (orange), progesterone and 50 μM RU1968 (yellow). $n = 3$ experiments performed in triplicate.

7.3.10 Changes in membrane potential inhibit sperm penetration into viscous medium

I have demonstrated that CatSper channels are involved in swimming in high-viscosity environment and that CatSper-dependent Ca^{2+} signals in human sperm are inhibited by hyperpolarisation of V_m . To evaluate the impact of hyperpolarisation of sperm V_m on their ability to penetrate viscous medium, spermatozoa were treated with 1 μM valinomycin (VLN), alone and before or after stimulation with progesterone (3 μM). VLN was added to the sperm reservoir for 5 minutes before subsequent addition of progesterone for the same amount of time. Methylcellulose-filled tube was introduced to the reservoir and the ability of the cells to enter and penetrate artificial mucus was analysed. 3 μM progesterone significantly enhanced penetration of sperm into artificial mucus at all distances (compared to parallel controls), reaching an $80.6 \pm 11.3\%$ increase just within the methylcellulose (0 cm; $p < 0.001$; fig. 7.16A). Valinomycin alone did not have any effect on sperm penetration when compared to untreated cells (control group), however, valinomycin completely inhibited the stimulation promoted by progesterone. Assessment of sperm cell kinematic parameters within the glass capillary showed difference in curvilinear velocity of sperm (VCL) (fig. 7.16B). Progesterone enhanced significantly VCL when compared to parallel control in the same penetration distance (increase of $30.2 \pm 11.0\%$ at start point - 0 cm; $p < 0.05$) and, once again, valinomycin abolished the effect of progesterone to control levels.

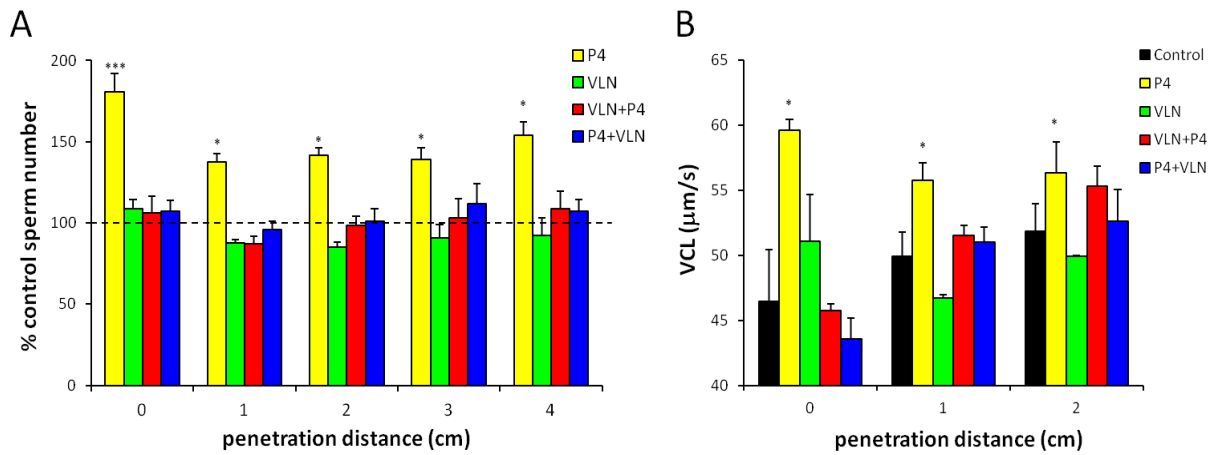


Figure 7.16 Valinomycin inhibits sperm penetration into artificial viscous media induced by progesterone, affecting sperm track speed (VCL). (A) Number of cells at each penetration distance as % of parallel control (normalised as 100% and represented as black dashed line). Mean \pm SEM of 5 different experiments performed independently. (B) Sperm VCL ($\mu\text{m/s}$) at the different penetration distances in artificial viscous media. Comparisons were conducted with paired one way ANOVA followed by Tukey's post-hoc. *** $p < 0.001$, * $p < 0.05$, when compared to untreated cells at the same penetration distance.

7.4 Discussion

Stimulation of human spermatozoa with progesterone at concentrations as low as picomolar activates CatSper (Teves et al, 2009; Lishko et al, 2011; Strünker et al, 2011). Single cell imaging of progesterone-stimulated human sperm shows that the cells generate $[Ca^{2+}]_i$ spikes and oscillations accompanied by increased sperm neck bending and flagellar excursion, which are characteristics of hyperactivation (Harper et al, 2004; Bedu-Addo et al, 2008). This repetitive modulation of flagellar activity may underlie repeated ‘switching’ of sperm behaviour in human spermatozoa which is believed to be important for sperm progression in the female tract (Harper et al, 2004; Bedu-Addo et al, 2008; Ho et al, 2009; Publicover, 2017).

I have made the first recordings of $[Ca^{2+}]_i$ in free-swimming human sperm. My data showed that (i) progesterone-stimulated free-swimming cells generated $[Ca^{2+}]_i$ oscillations and (ii) there is a clear correlation between $[Ca^{2+}]_i$ and sperm motility, particularly velocity (fig. 7.1). Velocity increases during the rise and as $[Ca^{2+}]_i$ decays the velocity slows. I also showed that the effect of $[Ca^{2+}]_i$ oscillations on velocity may regulate substrate attachment/detachment in human spermatozoa (fig. 7.2). When $[Ca^{2+}]_i$ oscillations were investigated at higher frame rate, I was able to detect that oscillation may also drive turning, decreasing the straightness of cell path, which is a kinematic parameter directly related to hyperactivated motility (fig. 7.3). Other aspects of hyperactivated motility, particularly lateral head movement (ALH) could not be assessed because these require a much faster image acquisition rate (50-60 Hz; Mortimer, 2000). During its journey through the female tract, sperm cells may bind to the oviductal epithelium and detaching from it requires driving force promoted by ‘switching’ sperm behaviour to hyperactivated motility (Pacey et al, 1995; Demott and Suarez, 1992; Gwathmey et al, 2003; Suarez and Ho, 2003).

Previous studies have reported that Ca^{2+} influx enhances sperm velocity (Fakih et al, 1986) and that CatSper null mice exhibited decreased sperm swimming speed parameters, such as path velocity, progressive velocity and track speed (Ren et al, 2001). CatSper-null mice sperm are motile but fail to hyperactivate and consequently to fertilise oocytes (Ren et al, 2001; Carlson et al, 2003; Quill et al, 2003; Ho et al, 2009). Since $[\text{Ca}^{2+}]_i$ oscillations in immobilised cells are dependent on CatSper activity (chapter 5), I investigated whether the ‘switching’ of swimming behaviour associated with $[\text{Ca}^{2+}]_i$ oscillations is dependent of CatSper activity (fig. 7.10). Treatment with RU prevented both the generation of $[\text{Ca}^{2+}]_i$ oscillations and switching of behaviour in free-swimming cells. This is the first report confirming the physiological relevance of $[\text{Ca}^{2+}]_i$ oscillations generation in regulating sperm motility, controlled by membrane potential and CatSper activation.

In the female tract, the spermatozoon has to penetrate mucus barriers with different viscosities, which range from 2800–10000 cp (Karni et al, 1971; Jansen, 1978; Suarez et al, 1997; Tung et al, 2015). I showed that perfusion of immobilised cells with high viscosity (4000 cp) medium induced a transient $[\text{Ca}^{2+}]_i$ increase followed by $[\text{Ca}^{2+}]_i$ oscillations in human spermatozoa and that these responses are dependent of CatSper activity (fig. 7.6 – fig. 7.8). The $[\text{Ca}^{2+}]_i$ responses induced by high viscosity perfusion are likely to be due to increased shear on the cell membrane. The voltage-gated proton channel Hv1, which are localised in the principal piece of the sperm flagellum (Lishko et al, 2010), has recently been shown to be shear sensitive (Pathak et al, 2016). Increased shear stimulus may therefore cause channel activation and raise pH_i , indirectly activating CatSper channels, which are localised in similar sperm region (Ren et al, 2001; Kirichok et al, 2006). This may play an important role in progression of sperm through viscous mucus. Similar to free-swimming cells in standard saline, $[\text{Ca}^{2+}]_i$ oscillations in free-swimming cells in viscous mucus also appeared to

drive sperm velocity (fig. 7.9).

Studies have shown that progesterone increases sperm penetration through viscous physiological barriers, such as cervical and oviduct mucus, cumulus cells layer and zona pellucida of the oocyte (Rathi et al, 2001; Suarez, 2008; Darszon et al, 2011; Alasmari et al, 2013). Some authors have reported that progesterone stimulates hyperactivated motility in mouse (Pérez-Cerezales et al, 2015) and human spermatozoa (Uhler et al, 1992, Gakamsky et al, 2009) under low viscosity environments, though this is controversial (Achikanu et al, 2018). However, once in a viscous environment, progesterone-stimulated sperm cells are believed to exhibit a more linear and progressive motility. This behaviour has been reported in sperm from different species: mice (Suarez and Dai, 1992; Pérez-Cerezales et al, 2016), hamster (Suarez et al, 1991) and bull (Hyakutake et al, 2015) and human (Tesarik et al, 1990).

Using the Kremer penetration I confirmed previous observations that CatSper blockade inhibits the stimulation of penetration induced by progesterone (Alasmari et al, 2013), but in this chapter I also present the first report suggesting that CatSper is crucial in regulating the ‘passive’ (unstimulated) behaviour responsible for sperm penetration ability (figs. 7.12 – 7.14). These data has been recently published (Rennhack et al, 2018). Moreover, CASA analysis within the glass capillary tubes showed that inhibition of CatSper blocks sperm penetration ability by altering the proportion of progressive and motile sperm population (fig. 7.15). Furthermore hyperpolarisation (valinomycin treatment), which will also suppress CatSper activity, blocks the stimulation of penetration induced by progesterone by reducing sperm velocity (fig. 7.16), which is consistent with the swimming characteristics induced by $[Ca^{2+}]_i$ oscillations that I demonstrated in this chapter.

CHAPTER EIGHT: GENERAL DISCUSSION

8.1 Key findings:

- Approximately a quarter of the human sperm population exhibit $[Ca^{2+}]_i$ oscillations induced by physiological concentrations of the hormone progesterone, independently of level of sperm capacitation;
- $[Ca^{2+}]_i$ oscillations are dependent of Ca^{2+} influx, start at the sperm flagellum and propagate actively towards the sperm head, where the signal becomes larger;
- RU1968-F1 is an effective inhibitor of CatSper channels and could be used as a new pharmacological tool in the study of these Ca^{2+} channels;
- Membrane potential (V_m), Slo3 channels and CatSper channels contribute to generation of $[Ca^{2+}]_i$ oscillations;
- SKF-96365 modulates $[Ca^{2+}]_i$ oscillations generation through similar mechanism as progesterone;
- $[Ca^{2+}]_i$ oscillations also occur in free-swimming sperm cells and are associated with switching of sperm swimming behaviour in both low and high viscosity environments;
- $[Ca^{2+}]_i$ oscillations drive swimming velocity, turning and hyperactivated motility in human spermatozoa and may regulate attachment/detachment from substrate
- Consistent with the involvement of CatSper in generation of $[Ca^{2+}]_i$ oscillations, regulation of sperm swimming velocity and cell progression are dependent on CatSper activity;
- Ability to penetrate into viscous environment is dependent on CatSper activity.

8.2 Thesis discussion:

The aim of this thesis was to investigate Ca^{2+} signalling pathways induced by progesterone, particularly induction of $[\text{Ca}^{2+}]_i$ oscillations, and determine whether and how they play physiological roles in human spermatozoa. Progesterone is a steroid hormone synthesised in the female tract by the cumulus cells surrounding the oocyte which modulates Ca^{2+} influx into the spermatozoa and, consequently, sperm function (Roldan et al, 1994; Ren et al, 2001; Harper et al, 2004; Eisenbach and Giojalas, 2006; Kirichok et al, 2006). In our studies, I used 3 μM progesterone which is a physiologically relevant concentration as progesterone is found at micromolar concentrations in the female tract (Osman et al, 1989; Baldi et al, 1998; Jaiswal et al, 1999) and can reach concentrations as high as 10 micromolar when close to the oocyte (Sagare-Patil et al, 2012; Tamburrino et al, 2014).

In human spermatozoa population, progesterone typically induces a biphasic Ca^{2+} response (transient peak followed by a sustained phase) through the activation of CatSper channels (Blackmore et al, 1990; Meizel and Turner, 1991, Kirkman-Brown et al, 2000, Strunker et al., 2011; fig. 3.2). The use of single-cell imaging allowed detailed analysis of the heterogeneity Ca^{2+} responses induced by the hormone. The observation that a large subpopulation of progesterone-stimulated sperm cells generate Ca^{2+} oscillations (~25%, fig. 3.4) motivated us to further investigate the mechanism of their generation and to understand their role in a physiological context. Progesterone-induced $[\text{Ca}^{2+}]_i$ oscillations in human sperm cells were first reported in 2004 (Harper et al, 2004; Kirkman-Brown et al, 2004) as large peaks showing a slow kinetics, each cycle lasting approximately 2 to 5 minutes. Basal or induced $[\text{Ca}^{2+}]_i$ oscillations were also detected in other species, such as hamster and sea urchin (Suarez et al, 1993; Wood et al, 2003) however, the kinetics of these signals were very

different: duration up to 1 second and period between 0.5-5 seconds. These discrepancies in the $[Ca^{2+}]_i$ oscillations kinetics observed in different species could indicate that they are generated by distinct mechanisms and may evoke different sperm responses.

To assist elucidating the mechanism on how the $[Ca^{2+}]_i$ oscillations are generated, I performed a spatial-temporal analysis of the progesterone-induced $[Ca^{2+}]_i$ oscillations propagation which showed that the signal starts in the sperm flagellum and spreads actively through the neck and then head, the signal becoming enhanced as it spreads forward (figs. 3.7 and 3.8). This observation was important since it suggests the involvement of CatSper channel activation (in the tail) and, subsequently, Ca^{2+} mobilisation from intracellular stores by calcium-induced calcium release system (CICR) in the neck/head. The $[Ca^{2+}]_i$ oscillations observed in *Strongylocentrotus purpuratus* sperm showed similar complex distribution throughout the cell, with signal starting from the tail and propagating to the sperm head (Wood et al, 2003). However, in hamster sperm, the Ca^{2+} influx necessary for the $[Ca^{2+}]_i$ oscillations generation occurred both tail and head of the sperm (Suarez et al, 1993).

Typically $[Ca^{2+}]_i$ oscillations in somatic cells are generated and maintained by periodic mobilisation of intracellular $[Ca^{2+}]_i$ stores (reviewed in Dupont et al, 2011). In our work, I showed that not only Ca^{2+} influx is crucial to generation of $[Ca^{2+}]_i$ oscillations but I also reported for the first time that membrane potential (V_m) regulates progesterone-induced $[Ca^{2+}]_i$ oscillations in human spermatozoa (fig. 3.6 and 3.9 - 3.17). Mechanisms of membrane potential regulation have been described in sperm of different species including mouse, bovine, sea urchin and human (Espinosa and Darszon, 1995; Zeng et al, 1995; Arnoult et al, 1996; Beltran et al, 1996) and are believed to be responsible for the modulation of Ca^{2+} influx and consequent changes in the sperm function. Based on data presented in chapter 3 and 5, we suggested a tentative model for progesterone-induced $[Ca^{2+}]_i$ oscillations generation in human

spermatozoa (fig. 5.8): Ca^{2+} influx through progesterone-stimulated CatSper activates Slo3 channels triggering Vm hyperpolarisation and promotes CatSper closure; Ca^{2+} sequestration mechanisms re-establish Ca^{2+} concentration in the cytosol, which allows Slo3 to close and membrane potential to be restored; CatSper re-opens again allowing Ca^{2+} influx and the oscillation cycle restarts. Although I have not done pharmacological manipulations on the intracellular Ca^{2+} stores or pumps to confirm their participation on the $[\text{Ca}^{2+}]_i$ oscillations generation, Harper and colleagues (2004) showed that inhibition of ryanodine receptors (RyRs) with tetracaine, caffeine and ryanodine clearly altered the oscillations kinetics, but not the inhibition of IP_3 receptors (IP_3Rs). Recently, Mata-Martinez and colleagues (2018) suggested a similar model (including contribution of CatSper) for generation of small, spontaneous $[\text{Ca}^{2+}]_i$ oscillations in human sperm cells, but the role of membrane potential was not investigated. In their model, Ca^{2+} influx through CatSper activates RyRs and PLC, which generates IP_3 and then activates IP_3Rs . Ca^{2+} mobilisation from stores increases $[\text{Ca}^{2+}]_i$ and re-establishment of Ca^{2+} concentration are promoted by Ca^{2+} -ATPases, PMCA4 and SPCA1 in the sperm membranes. In marine organisms, CatSper and membrane potential are both believed to be essential in induced $[\text{Ca}^{2+}]_i$ oscillations generation. The proposed model for three species of sea urchins *Strongylocentrotus purpuratus*, *Arbacia punctulata* and *Lytechinus pictus* involves the binding of a chemoattractant peptide released by the egg (for example, speract and resact) to its receptor, which triggers Vm hyperpolarisation by activation of cyclic nucleotide-gated K^+ channels. Alteration in membrane potential leads to pH_i alkalisation and, consequently, activation of CatSper channels and increase of $[\text{Ca}^{2+}]_i$ (Darszon et al, 2011; Seifert et al, 2014; Espinal-Enrquez et al, 2017).

In a physiological context, Ca^{2+} influx is believed to be critical for sperm motility and acrosome reaction, especially in mammalian sperm cells (reviewed in Rahman et al, 2014). In

marine organisms, with external fertilisation, alterations of behaviour are mainly associated with sperm-egg chemotaxis. In the case of sea urchin spermatozoa, the binding of the chemoattractant peptide speract leads to Ca^{2+} oscillations which drive increased asymmetry of the flagellar beat causing a change in swimming direction (Kaupp et al, 2003; Wood et al, 2005; Friedrich and Julicher, 2007). During the Ca^{2+} rise, sperm cells show a turning behaviour with an increased curvature of the flagellum alternating with straighter swimming episodes when Ca^{2+} decreases between oscillations (Kaupp et al, 2003; Bohmer et al, 2005; Wood et al, 2005; Shiba et al, 2008). Similar Ca^{2+} -dependent swimming behaviour towards the chemoattractant was also observed in the starfish *Asterias amurensis* (Bohmer et al, 2005). On the other hand, in species with internal fertilisation, changes in motility are critical to the progress of the sperm in the female tract, whereas a role for chemotaxis is not yet established (Suarez et al, 1993). During its journey towards the oocyte the sperm cell faces several barriers which require adoption of vigorous motility, such as hyperactivation, to enable sperm progression. Hyperactivation has been associated with aiding sperm penetration into viscous and viscoelastic environment, which are presented in the cervix, in the oviductal lumen and the cumulus cells layer, though more recent data are equivocal (Suarez et al, 1991; Suarez and Dai, 1992; Darszon et al, 2011; Alasmari et al, 2013). Also hyperactivated motility may be required both for sperm penetration of zona pellucida that surrounds the oocyte (Stauss et al, 1995; Quill et al, 2003) and for detachment from oviductal epithelium (Suarez and Osman, 1987; DeMott and Suarez, 1992; Ho et al, 2009). Hyperactivation is an event dependent on Ca^{2+} influx and studies have shown that $[\text{Ca}^{2+}]_i$ in a hyperactivated cells ranges from 200-1000 nM against 30-50 nM in an activated spermatozoon (Suarez and Dai, 1995; Ho et al, 2002; Achikanu et al, 2018).

In order to investigate whether $[Ca^{2+}]_i$ oscillations occur in free-swimming sperm cells and are responsible for regulation of behaviour, I developed a technique to track and measure Ca^{2+} probe signals in free-swimming sperm, the first recordings of $[Ca^{2+}]_i$ signals in individual, free-swimming human sperm (chapter 7). In our work, I confirmed the occurrence of $[Ca^{2+}]_i$ oscillations in free-swimming, progesterone-stimulated cells. The observed changes in fluorescence were not an artefact of cell rotation (10-20 Hz) or re-orientation occurring during cell movement; the long duration (> 1 min) and high amplitudes, resembling those detected in immobilised cells and continuing even when cells attached and ‘crawled’ on the coverslip. Moreover, I showed that $[Ca^{2+}]_i$ oscillations drive different swimming behaviour as there is a clear correlation between $[Ca^{2+}]_i$ and sperm motility, particularly velocity (figs. 7.1 and 7.3). The data reported here confirm that $[Ca^{2+}]_i$ oscillations are the cause of the increase in velocity rather than the result of changes in flagellar beating occurring in immobilised cells. Data obtained at 31°C, using a 10 Hz frame rate, revealed that $[Ca^{2+}]_i$ oscillations may also drive turning: decreasing the straightness of cell path and increasing fractal dimension, a kinematic parameter directly related to hyperactivated motility (figs. 7.4 and 7.5). Although tracking the sperm cells at 10 Hz provided us enough details to observe correlations between the Ca^{2+} signal and some kinematic parameters associated with hyperactivation, other aspects of hyperactivated motility, particularly lateral head movement (ALH) could not be assessed because these require a much faster image acquisition rate (50-60 Hz; Mortimer, 2000), which was not possible to achieve with our technique due to effects of photo-damage on the samples. Furthermore, the observation that ‘switching’ of swimming behaviour associated with $[Ca^{2+}]_i$ oscillations is dependent of CatSper activity (fig. 7.10) corroborates the work in mouse sperm which showed that CatSper null sperm exhibited impaired motility as sperm swam in circles or in straight trajectories with lower curvilinear velocity (VCL), amplitude of

lateral head displacement (ALH) and beat cross frequency (BCS) (Marquez et al, 2007). $[Ca^{2+}]_i$ oscillations may therefore regulate substrate attachment/detachment in human spermatozoa (fig. 7.2). This observation is physiological relevant as sperm cells are known to swim close to the surfaces in the female tract (Ooi et al, 2014) and $[Ca^{2+}]_i$ oscillations could be an essential mechanism to help the sperm cell to swim freely in the oviduct. Correlations between $[Ca^{2+}]_i$ oscillations and sperm behaviour have been described before, however mainly addressing the flagellar beating cycle (Suarez et al, 1993; Harper et al, 2004; Corkidi et al, 2008).

Additionally, in this thesis I presented the first report suggesting that CatSper is crucial in regulating the ‘passive’ (unstimulated) behaviour responsible for sperm penetration ability into viscous environment (Rennhack et al, 2018; figures 7.12 – 7.14). The observation that inhibition of CatSper and ‘clamping’ of membrane potential with valinomycin blocks the stimulation of penetration induced by progesterone (figures 7.13 – 7.16) through the decrease of sperm velocity, and progressive motility is consistent with the data showing the swimming characteristics are regulated by $[Ca^{2+}]_i$ oscillations and suggests the physiological relevance of CatSper activation and $[Ca^{2+}]_i$ oscillations for the sperm penetration ability. In summary, I have demonstrated that $[Ca^{2+}]_i$ oscillations are strongly associated with switching of human sperm swimming behaviour: driving velocity, attachment/detachment from substrate, sperm turning and hyperactivated motility and that CatSper channels are critical in regulating the swimming behaviour responsible for sperm ability to penetrate into viscous environment.

Although I have not analysed the role of progesterone-induced $[Ca^{2+}]_i$ oscillations on acrosome reaction (AR), Harper and colleagues (2004) reported that the percentage of progesterone-stimulated cells undergoing AR is lower in oscillating than non-oscillating cells and Mata-Martinez and colleagues (2018) showed that spontaneous $[Ca^{2+}]_i$ oscillations

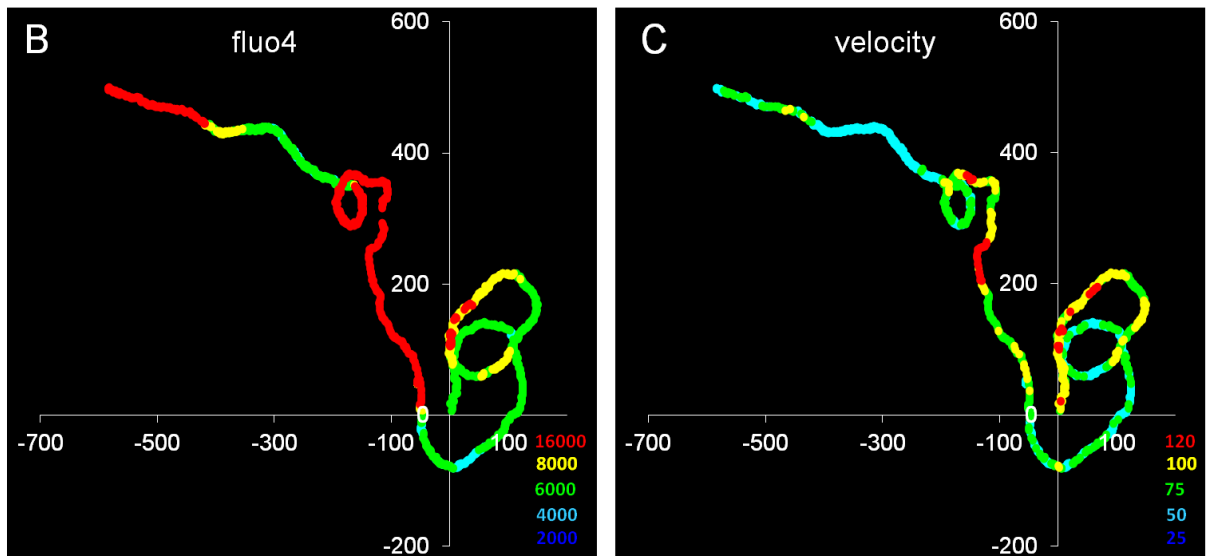
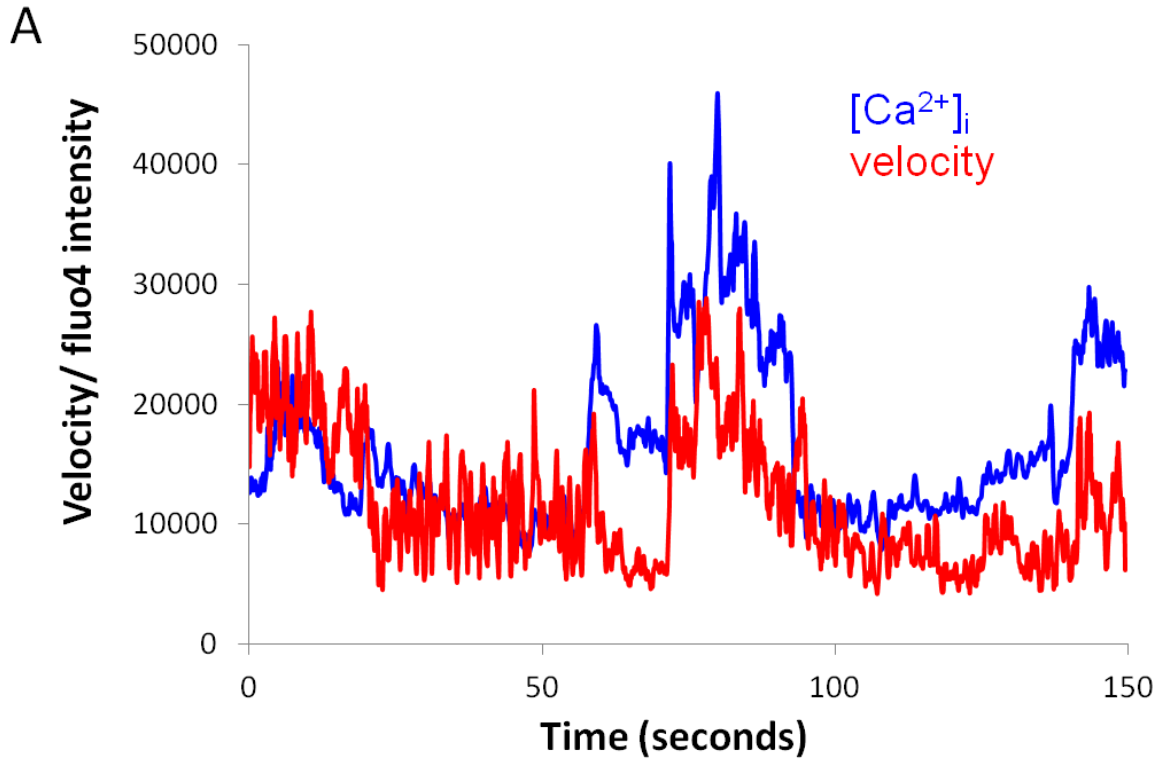
actually prevent acrosome reaction in human spermatozoa, suggesting another role for the $[Ca^{2+}]_i$ oscillations as a potential mechanism to prevent premature acrosome reaction. The sperm sub-population that exhibits a sustained phase instead of $[Ca^{2+}]_i$ oscillations, following progesterone stimulation, may lack the capacity to regulate $[Ca^{2+}]_i$.

The understanding of how $[Ca^{2+}]_i$ oscillations are generated and what physiological roles they might play in the sperm cell functions is crucial to identifying potential targets for pharmacological manipulation. For example, in chapter 3, I reported the contribution of membrane potential to $[Ca^{2+}]_i$ oscillations generation and many drugs which block V_m could be used as potential regulators of sperm motility, once we now know these processes are correlated. In chapter 4, I showed an improved drug, RU1968-F1, which can potentially be used as a new pharmacological tool to study CatSper channels and, moreover, could be used as a lead structure to develop non-hormonal contraceptives, since it mimics the lack of CatSper associated with male infertility and fertilisation prevention. The knowledge that generation of $[Ca^{2+}]_i$ oscillations is the mechanism that drives switching of sperm behaviour and hyperactivation could be used as a parameter for gamete selection in clinic. Finally, elucidating the $[Ca^{2+}]_i$ oscillation mechanisms in human spermatozoa may bring important information for evolutionary biology on the study of conserved signalling pathways between different species.

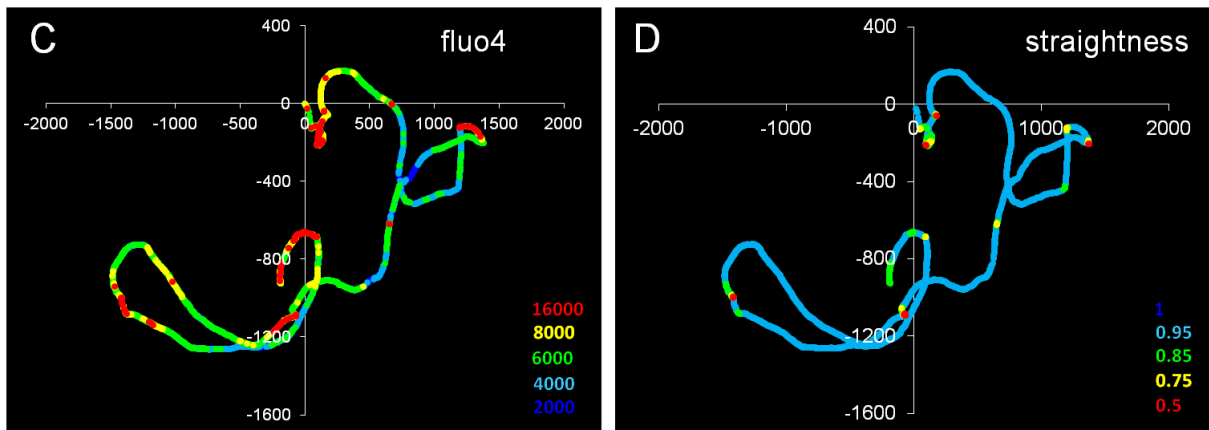
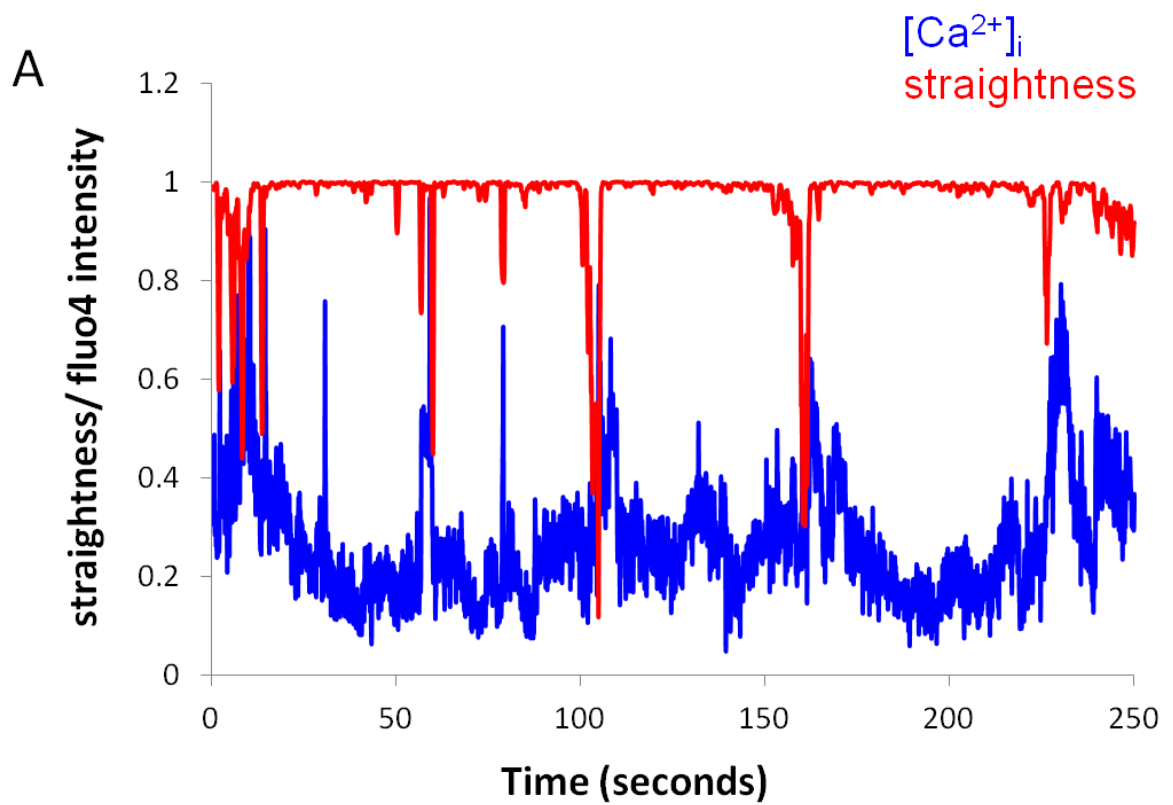
8.3 Future work:

- Investigate Ca^{2+} stores and pumps involved in the generation of $[\text{Ca}^{2+}]_i$ oscillations *downstream* to CatSper activation and whether these machinery could also contribute to complex behavioral changes in human sperm, as hyperactivation;
- Further study the SKF-96365 mechanism of action by which it modulates the generation of $[\text{Ca}^{2+}]_i$ oscillations;
- Perform assays in samples of patients with defects in Ca^{2+} signalling machinery to confirm our tentative model for $[\text{Ca}^{2+}]_i$ oscillations generation;
- Increase the number of cells analysed on the fluo4-labelled free-swimming cells assay in order to improve understanding of the correlation between $[\text{Ca}^{2+}]_i$ oscillations and swimming behaviour;
- Improve the fluo4-labelled free-swimming cells technique to be able to perform faster recordings (50-60 Hz) and analyse other aspects of hyperactivated motility, such as ALH;
- Investigate the $[\text{Ca}^{2+}]_i$ oscillation and sperm swimming behaviour in viscoelastic environments;
- Study the role of progesterone-induced $[\text{Ca}^{2+}]_i$ oscillations in acrosome reaction.

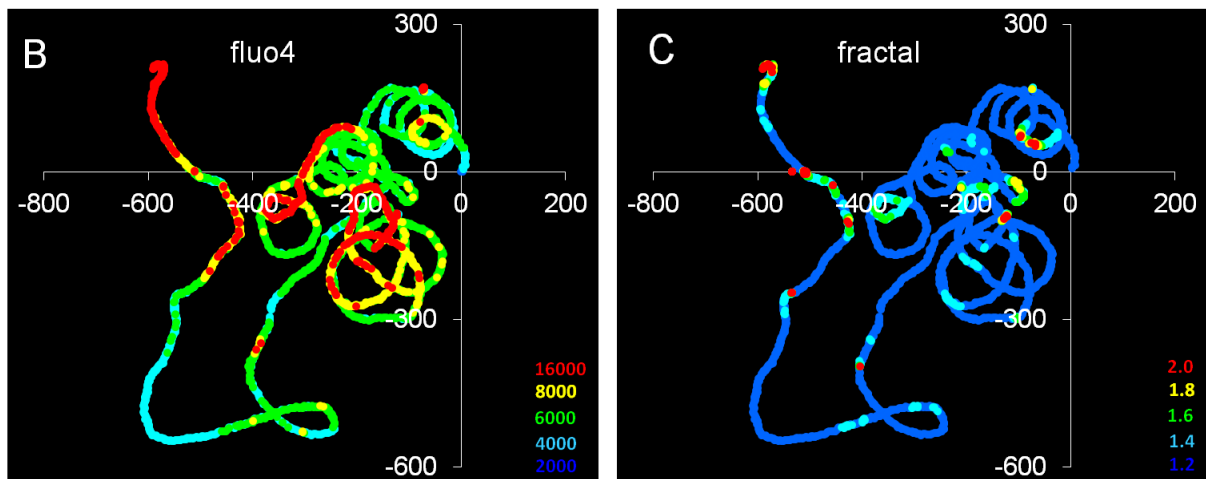
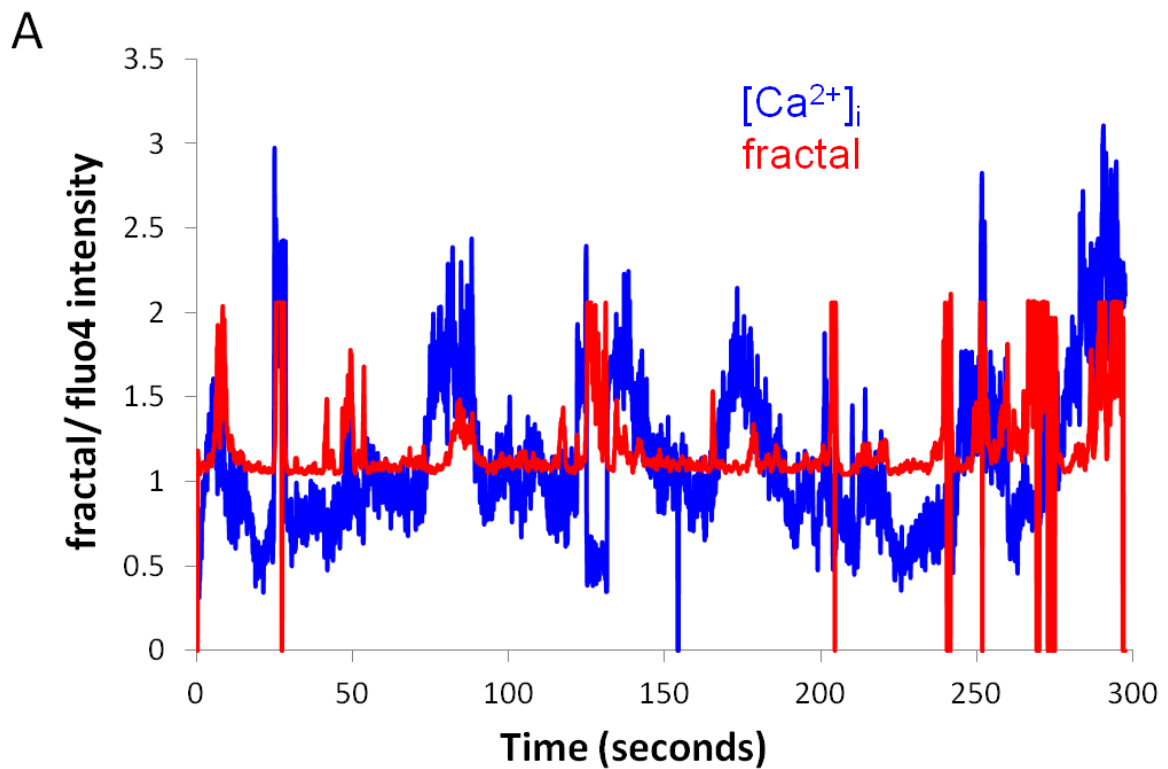
APPENDIX I



Appendix I.1 Correlation between $[Ca^{2+}]_i$ and velocity - example. (A) shows relationship between $[Ca^{2+}]_i$ (fluo4 fluorescence – blue) and average path velocity (VAP), in a progesterone-stimulated, free-swimming human sperm (velocity has been normalised to maximum value). Lower panel shows sperm track coordinates plotted with colour coding to indicate fluo4 fluorescence (B) and VAP (C). Analysis was performed in collaboration with Dr. Hector A. Guidobaldi, Universidad Nacional de Cordoba.



Appendix I.2 Correlation between [Ca²⁺]_i and straightness - example. (A) shows relationship between [Ca²⁺]_i (fluo4 fluorescence – blue) and straightness in a progesterone-stimulated, free-swimming human sperm. Lower panel shows sperm track coordinates plotted with colour coding to indicate fluo4 fluorescence (B) and straightness (C). Analysis was performed, in collaboration with Dr. Hector A. Guidobaldi, Universidad Nacional de Cordoba.



Appendix I.3 Correlation between $[Ca^{2+}]_i$ and fractal dimension - example. (A) shows relationship between $[Ca^{2+}]_i$ (fluo4 fluorescence – blue) and fractal dimension in a progesterone-stimulated, free-swimming human sperm. Lower panel shows sperm track coordinates plotted with colour coding to indicate fluo4 fluorescence (B) and fractal dimension (C). Analysis was performed, in collaboration with Dr. Hector A. Guidobaldi, Universidad Nacional de Cordoba.

APPENDIX II

PUBLICATIONS AND PRESENTATIONS OF RESEARCH

RENNHACK, A.; SCHIFFER, C.; BRENKER, C.; FRIDMAN, D.; **NITAO, E.T.**; CHENG, Y.M.; TAMBURRINO, L.; BALBACH, M.; STÖLTING, G.; BERGER, T.K.; KIERZEK, M.; ALVAREZ, L.; WACHTEN, D.; ZENG, X.H.; BALDI, E.; PUBLICOVER, S.J.; BENJAMIN KAUPP, U.; STRÜNKER, T. (2018) A novel cross-species inhibitor to study the function of CatSper Ca²⁺ channels in sperm. Br J Pharmacol. 175(15):3144-3161.

Open calcium conference, Milton Keynes (UK) – July, 2018 (oral + poster presentation)

Membrane potential contributes to generation of [Ca²⁺]_i oscillations and sperm behaviour in human spermatozoa. Elis Torrezan-Nitao, Sean Brown, Hector Guidobaldi and Stephen Publicover.

Fertility, Liverpool (UK) – January, 2018 (oral presentation)

Characterisation of [Ca²⁺]_i oscillations induced by progesterone and their role in human sperm swimming behaviour. Elis Torrezan-Nitao and Stephen Publicover.

Gordon Research conference - Fertilization and Activation of Development, Holderness (USA) - July, 2017 (poster presentation)

Different signalling mechanisms modulate sperm swimming behaviour in a low and high viscosity environment. Elis Torrezan-Nitao and Stephen Publicover.

Annual conference Society for Reproduction and Fertility, Winchester (UK) - July, 2016 (poster presentation)

Membrane potential contributes to generation of high amplitude [Ca²⁺]_i oscillations and sperm behaviour in human spermatozoa. Elis Torrezan-Nitao and Stephen Publicover.

Bioscience Graduate School Symposium, Birmingham (UK) - April, 2016 (poster presentation)

[Ca²⁺]_i oscillations patterns induced by progesterone in human spermatozoa are regulated by membrane potential and CatSper activation. Elis Torrezan-Nitao and Stephen Publicover.

Annual conference Society for Reproduction and Fertility, Oxford (UK) - July, 2015 (poster presentation)

Membrane potential is crucial for one of the [Ca²⁺]_i oscillations profiles induced by progesterone in human spermatozoa. Elis Torrezan-Nitao and Stephen Publicover.

REFERENCES

- ABRAMOWITZ, J.; BIRNBAUMER, L. (2009) Physiology and pathophysiology of canonical transient receptor potential channels. *The FASEB Journal*. 23:297–328.
- ACHIKANU, C.; PENDEKANTI, V.; TEAGUE, R.; PUBLICOVER, J. (2018) Effects of pH manipulation, CatSper stimulation and Ca²⁺-store mobilisation on [Ca²⁺]_i and behaviour of human sperm. *Human reproduction*.
- AITKEN, R.J. (1997) Molecular mechanisms regulating human sperm function. *Molecular Human Reproduction* 3:169-173.
- AITKEN, R.J.; BAKER, M.A.; SAWYER, D. (2003) Oxidative stress in the male germ line and its role in the aetiology of male infertility and genetic disease. *Reprod Biomed Online*. 7:65-70.
- AITKEN, R.J.; BAKER, M.A. (2006) Oxidative stress, sperm survival and fertility control. *Mol Cell Endocrinol* 250:66 – 69.
- AITKEN, R.J.; MCLAUGHLIN, E.A. (2007) Molecular mechanisms of sperm capacitation: progesterone-induced secondary calcium oscillations reflect the attainment of a capacitated state. *Soc Reprod Fertil Suppl*. 63:273-93.
- AITKEN, R.J.; HENKEL, R.R. (2011) Sperm cell biology: current perspectives and future prospects. *Asian J Androl*. 13(1):3-5.
- AITKEN, R.J.; NIXON, B. (2013) Sperm capacitation: a distant landscape glimpsed but unexplored. *Mol Hum Reprod*. 19:785–93.
- ALASMARI, W.; COSTELLO, S.; CORREIA, J.; OXENHAM, S.K.; MORRIS, J.; FERNANDES, L.; RAMALHO-SANTOS, J.; KIRKMAN-BROWN, J.; MICHELANGELI,

F.; PUBLICOVER, S.; BARRATT, C.L. (2013) Ca^{2+} signals generated by CatSper and Ca^{2+} stores regulate different behaviors in human sperm. *J Biol Chem.* 288(9):6248-6258.

ALVAREZ, L.; FRIEDRICH, B.M.; GOMPPER, G.; KAUPP, U.B. (2014) The computational sperm cell. *Trends Cell Biol.* 24(3):198-207.

AMANN, R.P.; HOWARDS, S.S. (1980) Daily spermatozoal production and epididymal spermatozoal reserves of the human male. *J Urol.* Aug;124(2):211-5.

ARMON, L.; EISENBACH, M. (2011) Behavioral mechanism during human sperm chemotaxis: involvement of hyperactivation. *PLoS ONE* 6(12): e28359.

ARNOULT, C.; CARDULLO, R.A.; LEMOS, J.R.; FLORMAN, H.M. (1996) Activation of mouse sperm T-type Ca^{2+} channels by adhesion to the egg zona pellucida. *Proc. Natl. Acad. Sci. USA* 93:13004–13009.

ARNOULT, C.; KAZAM, I.G.; VISCONTI, P.E.; KOPF, G.S.; VILLAZ, M.; FLORMAN, H.M. (1999) Control of the low voltage-activated calcium channel of mouse sperm by egg ZP3 and by membrane hyperpolarization during capacitation. *Proc. Natl. Acad. Sci. USA* 96:6757–6762.

AUSTIN, C. (1951) Observations on the penetration of the sperm in the mammalian egg. *Aust J Sci Res B.* 4:581-596.

AUSTIN, C. (1952) The capacitation of the mammalian sperm. *Nature.* 170:326-332.

BAKER, T.G.; FRANCHI, L.L. (1967) The fine structure of oogonia and oocytes in human ovaries. *J Cell Sci.* Jun;2(2):213-24.

BALDERAS, E.; ARTEAGA-TLECUITL, R.; RIVERA, M.; GOMORA, J.C.; DARSZON, A. (2012) Niflumic acid blocks native and recombinant t-type channels. *J Cell Physiol.* 227(6): 2542–2555.

- BALDI, E.; LUCONI, M.; BONACCORSI, L.; FORTI, G. (1998) Nongenomic effects of progesterone on spermatozoa: mechanisms of signal transduction and clinical implications. *Frontiers in Bioscience* 3:d1051–d1059.
- BALTZ, J.M.; WILLIAMS, P.O.; CONE, R.A. (1990) Dense fibers protect mammalian sperm against damage. *Biol Reprod.* 43:485–91.
- BARRATT, C.L.; MANSELL, S.; BEATON, C.; TARDIF, S.; OXENHAM, S.K. (2011). Diagnostic tools in male infertility-the question of sperm dysfunction. *Asian J Androl.* 13(1). p.53-58.
- BARROS, C.; VIGIL, P.; HERRERA, E.; ARGUELLO; WALKER, R. (1984) Selection of morphologically abnormal sperm by human cervical mucus. *Archs Androl. (Suppl.)* 12, 95-107.
- BAUSKIN, A.R.; FRANKEN, D.R.; EBERSPAECHER, U.; DONNER, P. (1999) Characterization of human zona pellucida glycoproteins. *Mol Hum Reprod* 5:534–540.
- BEDFORD, J.M. (1970) The saga of mammalian sperm from ejaculation to syngamy. In *Mammalian Reproduction*. Eds. H. Gibian and E. J. Plotz. Springer, Berlin.
- BEDU-ADDO, K.; COSTELLO, S.; HARPER, C.; MACHADO-OLIVEIRA, G.; LEFIEVRE, L.; FORD, C.; BARRATT, C.; PUBLICOVER, S. (2008) Mobilisation of stored calcium in the neck region of human sperm –a mechanism for regulation of flagellar activity. *International J Dev Biol* 52:615–626.
- BEERS, W.H.; STRICKLAND, S.; REICH, E. (1975) Ovarian plasminogen activator: Relationship to ovulation and hormonal regulation. *Cell* 6:387–394.
- BELTRÁN, C.; ZAPATA, O.; DARSZON, A. (1996) Membrane potential regulates sea urchin sperm adenylcyclase. *Biochemistry* 35(23):7591–7598.

- BERRIDGE, M.J. (1993). Inositol trisphosphate and calcium signalling. *Nature* 361. p.315–325.
- BERRIDGE, M.J. (1997) Elementary and global aspects of calcium signaling. *J Physiol.* 499:291–306.
- BERRIDGE, M.J. (2004) Calcium signal transduction and cellular control mechanisms. *Biochim Biophys Acta.* 1742(1-3):3-7.
- BEZPROZVANNY, I.; WATRAS, J.; EHRLICH, B.E. (1991) Bell-shaped calcium response curves of Ins(1,4,5)P₃- and calcium-gated channels from endoplasmic reticulum of cerebellum. *Nature.* 351:751–754.
- BIANCHI, E.; DOE, B.; GOULDING, D.; WRIGHT, G.J. (2014) Juno is the egg Izumo receptor and is essential for mammalian fertilization. *Nature.* 508(7497):483-7.
- BILLINGTON, R.A.; HARPER, C.; BELLOMO, E.A.; PUBLICOVER, S.; BARRATT, C.L.; GENAZZANI, A.A. (2006) Characterization of cyclic adenine dinucleotide phosphate ribose levels in human spermatozoa. *Fertility and Sterility* 86:891–898.
- BLACKMORE, P.F.; BEEBE, S.J.; DANFORTH, D.R.; ALEXANDER, N. (1990) Progesterone and 17 α -hydroxyprogesterone. Novel stimulators of calcium influx in human sperm. *Journal of Biological Chemistry* 265:1376–1380.
- BOERKE, A.; BROUWERS, J.F.; OLKKONEN, V.M.; VAN DE LEST, C.H.; SOSTARIC, E.; SCHOEVERS, E.J.; HELMS, J.B.; GADELLA, B.M. (2013) Involvement of bicarbonate-induced radical signaling in oxysterol formation and sterol depletion of capacitating mammalian sperm during in vitro fertilization. *Biol Reprod.* 88(1):21.
- BÖHMER, M.; VAN, Q.; WEYAND, I.; HAGEN, V.; BEYERMANN, M.; MATSUMOTO, M.; HOSHI, M.; HILDEBRAND, E.; KAUPP, U.B. (2005) Ca²⁺ spikes in the flagellum control chemotactic behavior of sperm. *EMBO J* 24(15):2741-52.

- BRAUN, R.E.; BEHRINGER, R.R.; PESCHON, J.J.; BRINSTER, R.L.; PALMITER, D. (1989) Genetically haploid spermatids are phenotypically diploid. *Nature* 337, 373–376.
- BRAUN, R.E. (2001) Packaging paternal chromosomes with protamine. *Nature Genetics* 28, 10–12.
- BREITBART, H. (2002) Intracellular calcium regulation in sperm capacitation and acrosomal reaction. *Molecular and Cellular Endocrinology* 187:139–144.
- BRENKER, C.; GOODWIN, N.; WEYAND, I.; KASHIKAR, N.D.; NARUSE, M.; KRÄHLING, M.; MÜLLER, A.; KAUPP, U.B.; STRÜNKER, T. (2012) The CatSper channel. A polymodal chemosensor in human sperm. *EMBO J.* 31. p.1654-1665.
- BRENKER, C.; ZHOU, Y.; MÜLLER, A.; ECHEVERRY, F.A.; TRÖTSCHER, C.; POETSCH, A.; XIA, X.M.; BÖNIGK, W.; LINGLE, C.J.; KAUPP, U.B.; STRÜNKER, T. (2014) The Ca^{2+} -activated K^+ current of human sperm is mediated by Slo3. *Elife*. 26(3):e01438.
- BROUWERS, J.F.; BOERKE, A.; SILVA, P.F.N.; GARCIA-GIL, N.; VAN GESTEL, R.A.; HELMS, J.B.; VAN DE LEST, C.H.A.; GADELLA, B.M. (2011) Mass spectrometric detection of cholesterol oxidation in bovine sperm. *Biology of Reproduction* 85:128–136.
- BROWN, R.L.; STRASSMAIER, T.; BRADY, J.D.; KARPEN, J.W. (2006) The pharmacology of cyclic nucleotide-gated channels: emerging from the darkness. *Curr Pharm Des* 12: 3597–3613.
- BRUGH, V.M.; LIPSHULTZ, L.I. (2004) Male factor infertility: evaluation and management. *Med Clin North Am.* 88(2):367–85.
- BUCCIONE, R.; SCHROEDER, A.C.; EPPIG, J.J. (1990) Interactions between somatic cells and germ cells throughout mammalian oogenesis. *Biol. Reprod.*, 43:543–547.

- BURGESS, D.L.; GEFRIDES, L.A.; FOREMAN, P.J.; NOEBELS, J.L. (2001) A cluster of three novel Ca²⁺ channel gamma subunit genes on chromosome 19q13.43: evolution and expression profile of the gamma subunit gene family. *Genomics* 71:339–350.
- BURGOS, M.H.; FAWCETT, D.W. (1956) An electron microscope study of spermatid differentiation in the toad, *Bufo arenarum* Hensel. *J Biophys Biochem Cytol.* May 25;2(3):223–240.
- BUSSO, D.; COHEN, D.J.; MALDERA, J.A.; DEMATTEIS, A.; CUASNICU, P.S. (2007) A novel function for CRISP1 in rodent fertilization: Involvement in sperm-zona pellucida interaction. *Biol.Reprod.* 77:848–854.
- BYSKOV, A.G.; HOYER, P.E. (1994) Embryology of mammalian gonads and ducts. E. Knobil, J.D. Neill (Eds.), *The Physiology of Reproduction* (2nd ed), Raven Press, New York, pp. 487–540.
- CAHALAN, M.D. (2009) STIMulating store-operated Ca²⁺ entry. *Nature Cell Biology* 11:669–677.
- CAI, X.; WANG, X.; PATEL, S.; CLAPHAM, D.E. (2005) Insights into the early evolution of animal calcium signaling machinery: a unicellular point of view. *Cell Calcium.* 57(3):166-73.
- CAMPBELL, N.A.; REECE, J.B.; MITCHELL, L.G. (1999) *Biology* (5th Edition) Benjamin-Cummings Pub Co.
- CANCEL, A.M.; LOBDELL, D.; MENDOLA, P.; PERREAULT, S.D. (2000) Objective evaluation of hyperactivated motility in rat spermatozoa using computer-assisted sperm analysis, *Human Reproduction* 15(6):1322–1328.
- CANEGUIM, B.H.; CERRI, P.S.; SPOLIDÓRIO, L.C.; MIRAGLIA, S.M.; SASSO-CERRI, E. (2009). Structural alterations in the seminiferous tubules of rats treated with immunosuppressor tacrolimus. *Reproductive Biology and Endocrinology : RB&E*, 7:19.

CANTI, C.; DAVIES, A.; DOLPHIN, A.C. (2003) Calcium channel $\alpha 2\delta$ subunits: structure, functions and target site for drugs. *Curr Neuropharmacol* 1:209–217.

CARLSON, A.E.; WESTENBROEK, R.E.; QUILL T.; REN, D.; CLAPHAM, D.E.; HILLE, B, GARBERS, D.L.; BABCOCK, D.F. (2003) CatSper1 required for evoked Ca^{2+} entry and control of flagellar function in sperm. *Proc Natl Acad Sci USA*. 100:14864-14868.

CARLSON, A.E.; QUILL, T.A.; WESTENBROEK, R.E.; SCHUH, S.M.; HILLE, B.; BABCOCK, D.F. (2005) Identical phenotypes of CatSper1 and CatSper2 null sperm. *J Biol Chem*. 280:32238–44.

CARLSON, A.E.; BURNETT, L.A.; DEL CAMINO, D.; QUILL, T.A.; HILLE, B.; CHONG, J.A.; et al. (2009). Pharmacological targeting of native CatSper channels reveals a required role in maintenance of sperm hyperactivation. *PloS One* 4: e6844.

CASTELLANO, L.E.; TREVIÑO, C.L.; RODRÍGUEZ, D.; SERRANO, C.J.; PACHECO, J.; TSUTSUMI, V.; FELIX, R.; DARSZON, A. (2003) Transient receptor potential (TRPC) channels in human sperm: expression, cellular localization and involvement in the regulation of flagellar motility. *FEBS Lett*. 541:69–74.

CATTERALL, W.A. (2000) Structure and regulation of voltage-gated Ca^{2+} channels. *Annu Rev Cell Dev Biol*. 16:521–555.

CHAKRABORTY, J.; NELSON, L. (1975) Fate of surplus sperm in the fallopian tube of the white mouse. *Biol Reprod*. 12(4):455-63.

CHAMBERLIN, M.E.; DEAN, J. (1990) Human homolog of the mouse sperm receptor. *Proc Natl Acad Sci USA*. 87(16):6014–6018.

CHAN, H.C.; WU, W.L.; SUN, Y.P.; LEUNG, P.S.; WONG, T.P.; CHUNG, Y.W.; et al. (1998) Expression of sperm Ca^{2+} -activated K^+ channels in *Xenopus* oocytes and their modulation by extracellular ATP. *FEBS Letters*. 438:177–182.

CHAN, H.C.; SHI, Q.X.; ZHOU, C.X.; WANG, X.F.; XU, W.M.; CHEN, W.Y.; CHEN, A.J.; NI, Y.; YUAN, Y.Y. (2006) Critical role of CFTR in uterine bicarbonate secretion and the fertilizing capacity of sperm. *Mol Cell Endocrinol* 250:106-113.

CHANG, M.C. (1951) Fertilizing capacity of spermatozoa deposited into the fallopian tubes. *Nature*. 168:697-698.

CHANG, H.; SUAREZ, S.S. (2011). Two distinct Ca^{2+} signaling pathways modulate sperm flagellar beating patterns in mice. *Biol. Reprod.* 85:296–305.

CHÁVEZ, J.C.; FERREIRA, J.J.; BUTLER, A.; DE LA VEGA BELTRÁN, J.L.; TREVIÑO, C.L.; DARSZON, A.; SALKOFF, L.; SANTI, C.M. (2014) Slo3 K^+ channels control calcium entry through CatSper channels in sperm. *J Biol Chem.* 289(46):32266-75.

CHÁVEZ, J.C.; DE LA VEGA-BELTRÁN, J.L.; JOSÉ, O.; TORRES, P.; NISHIGAKI, T.; TREVIÑO, C.L.; et al. (2018). Acrosomal alkalization triggers Ca^{2+} release and acrosome reaction in mammalian spermatozoa. *J Cell Physiol* (6):4735-4747.

CHEN, C.C.; LAMPING, K.G.; NUNO, D.W.; BARRESI, R.; PROUTY, S.J.; LAVOIE, J.L.; CRIBBS, L.L.; ENGLAND, S.K.; SIGMUND, C.D.; WEISS, R.M. et al. (2003) Abnormal coronary function in mice deficient in $\alpha_1\text{H}$ T-type Ca^{2+} channels. *Science*. 302:1416–8.

CHEN, W.Y.; XU, W.M.; CHEN, Z.H.; NI, Y.; YUAN, Y.Y.; ZHOU, S.C.; et al. (2009) Cl^- is required for HCO_3^- entry necessary for sperm capacitation in guinea pig: Involvement of a $\text{Cl}^-/\text{HCO}_3^-$ exchanger (SLC26A3) and CFTR. *Biology of Reproduction*. 80:115–123.

CHIU, P.C.; WONG, B.S.; LEE, C.L.; PANG, R.T.; LEE, K.F.; et al (2008) Native human zonapellucida glycoproteins: purification and binding properties. *Hum Reprod* 23:1385–93.

CHUNG, J.J.; NAVARRO, B.; KRAPIVINSKY, G.; KRAPIVINSKY, L.; CLAPHAM, D.E. (2011) A novel gene required for male fertility and functional CATSPER channel formation in spermatozoa. *Nature Communications* 2:153.

CHUNG, J.J.; MIKI, K.; KIM, D.; SHIM, S.H.; SHI, H.F.; HWANG, J.Y.; CAI, X.; ISERI, Y.; ZHUANG, X.; CLAPHAM, D.E. (2017) CatSper ζ regulates the structural continuity of sperm Ca^{2+} signaling domains and is required for normal fertility. *Elife*. 6:e23082.

CLERMONT, Y.; OKO, R.; HERMO, L. (1993) Cell and molecular biology of the testis. In: Desjardins C, Ewing L, editors. *Cell biology of mammalian spermatogenesis.*, New York: Oxford University Press. pp. 332–376.

COETZEE, W.A.; AMARILLO, Y.; CHIU, J.; CHOW, A.; LAU, D.; MCCORMACK, T.; MORENO, H.; NADAL, M.S.; OZAITA, A.; POUNTNEY, D.; SAGANICH, M.; VEGA-SAENZ DE MIERA, E.; RUDY, B. (1999) Molecular diversity of K^{+} channels. *Ann N Y Acad Sci*. 868:233-85.

COOPER, T.G. (2002) Recent advances in sperm maturation in the human epididymis. *Andrologie*. 12:38–51.

COOPER, T.G.; YEUNG, C.H. (2007) Involvement of potassium and chloride channels and other transporters in volume regulation by spermatozoa. *Current Pharmaceutical Design*. 13:3222–3230.

COOPER, T.G.; NOONAN E.; VON ECKARDSTEIN, S.; AUGER, J.; BAKER, H.W.; BEHRE, H.M.; HAUGEN, T.B.; KRUGER, T.; WANG, C.; MBIZVO, M.T.; VOGELSONG, K.M. (2010) World Health Organization reference values for human semen characteristics. *Hum Reproduction Update*. 16:231–45.

CORKIDI, G.; TABOADA, B.; WOOD, C.D.; GUERRERO, A.; DARSZON, A. (2008) Tracking sperm in three-dimensions. *Biochem. Biophys. Res. Commun*. 373:125-129.

CORREIA, J.; MICHELANGELI, F.; PUBLICOVER, S. (2015) Regulation and roles of Ca²⁺ stores in human sperm. *Reproduction*. 150(2):R65-76.

COSKER, F.; CHEVIRON, N.; YAMASAKI, M.; MENTEYNE, A.; LUND, F.E.; MOUTIN, M.J.; GALIONE, A. CANCELA, J.M. (2010) The ecto-enzyme CD38 is a mammalian NAADP synthase which couples receptor activation to Ca²⁺ mobilization from lysosomes. *Journal of Biological Chemistry* 285:38251–38259.

COSTELLO, S.; MICHELANGELI, F.; NASH, K.; LEFIEVRE, L.; MORRIS, J.; MACHADO-OLIVEIRA, G.; BARRATT, C.; KIRKMAN-BROWN, J.; PUBLICOVER, S. (2009) Ca²⁺-stores in sperm: their identities and functions. *Reproduction*. 138(3):425-437.

CROSS, N. (1998) Role of cholesterol in sperm capacitation. *Biol Reprod* 59:7-11.

CROSS, N.L. (2003) Decrease in order of human sperm lipids during capacitation. *Biol Reprod*. 69(2):529-34.

CUASNICU, P.S.; COHEN, D.J.; ELLERMAN, D.A.; BUSO, D.; DA ROS, V.G.; MORGENFELD, M. (2002) Changes in sperm proteins during epididymal maturation. In: Robaire B, Hinton BT, eds. *The Epididymis. From Molecules to Clinical Practice*. New York, NY: Kluwer Academic/ Plenum Publishers; 389–404.

DARSZON, A.; LABARCA, P.; NISHIGAKI, T.; ESPINOSA, F. (1999) Ion channels in sperm physiology. *Physiol Rev* 79:481 – 510.

DARSZON, A.; NISHIGAKI, T.; WOOD, C.; TREVINO, C.L.; FELIX, R.; BELTRAN, C. (2005) Calcium channels and Ca²⁺ fluctuations in sperm physiology. *International Review of Cytology* 243:79–172.

DARSZON, A.; ACEVEDO, J.J.; GALINDO, B.E.; HERNANDEZ-GONZALEZ, E.O.; NISHIGAKI, T.; TREVINO, C.L.; WOOD, C.; BELTRAN, C. (2006) Sperm channel diversity and functional multiplicity. *Reproduction* 131:977-988.

DARSZON, A.; LOPEZ-MARTINEZ, P.; ACEVEDO, J.J.; HERNANDEZ-CRUZ, A.; TREVINO, C.L. (2006) T-type Ca²⁺ channels in sperm function. *Cell Calcium* 40:241– 252.

DARSZON, A.; GUERRERO, A.; GALINDO, B.E.; NISHIGAKI, T.; WOOD, C.D. (2008) Sperm-activating peptides in the regulation of ion fluxes, signal transduction and motility. *Int J Dev Biol* 52: 595– 606.

DARSZON, A.; NISHIGAKI, T.; BELTRAN, C.; TREVINO, C.L. (2011) Calcium channels in the development, maturation, and function of spermatozoa. *Physiological Reviews* 91:1305–1355.

DARSZON, A.; SANCHEZ-CARDENAS, C.; ORTA, G.; SANCHEZ-TUSIE, A.A.; BELTRAN, C.; LOPEZ-GONZALEZ, I.; GRANADOS-GONZALEZ, G.; TREVINO, C.L. (2012) Are TRP channels involved in sperm development and function? *Cell and Tissue Research* 349:749–764.

DeCOURSEY, T.E. (2010) Voltage-gated proton channels find their dream job managing the respiratory burst in phagocytes. *Physiology (Bethesda)* 25:27-40.

DE JONGE, C. (2005) Biological basis for human capacitation. *Hum Reprod Update*. 11(3):205-14.

DE LAMIRANDE, E.; LECLERC, P.; GAGNON, C. (1997) Capacitation as a regulatory event that primes spermatozoa for the acrosome reaction and fertilization. *Mol Hum Reprod*. 3:175–94.

DE LA VEGA-BELTRAN, J.L.; SANCHEZ-CARDENAS, C.; KRAPP, D.; HERNANDEZGONZALEZ, E.O.; WERTHEIMER, E.; TREVINO, C.L.; DARSZON, A. (2012) Mouse sperm membrane potential hyperpolarization is necessary and sufficient to prepare sperm for the acrosome reaction. *J Biol Chem* 287: 44384 – 44393.

DEMARCO, I.A.; ESPINOSA, F.; EDWARDS, J.; SOSNIK, J.; DE LA VEGA-BELTRAN, J.L.; HOCKENSMITH, J.W.; KOPF, G.S.; DARSZON, A.; VISCONTI, P.E. (2003) Involvement of a $\text{Na}^+/\text{HCO}_3^-$ cotransporter in mouse sperm capacitation. *Journal of Biological Chemistry* 278:7001–7009.

DEMOTT, R.P.; SUAREZ, S.S. (1992) Hyperactivated sperm progress in the mouse oviduct. *Biol Reprod.* 46(5):779–785.

DE ROOIJ, D.G. (1973) Spermatogonial stem cell renewal in the mouse. I. Normal situation. *Cell Tissue Kinet.* 6(3):281-7.

DE ROOIJ, D.G.; RUSSELL, L.D. (2000) All you wanted to know about spermatogonia but were afraid to ask. *J Androl.* 21(6):776-98.

DIETERT, S.E. (1966) Fine structure of the formation and fate of the residual bodies of mouse spermatozoa with evidence for the participation of lysosomes. *J. Morphol.*, 120:317–346.

DOWNS, S.; LONGO, F.J. (1983) Prostaglandins and preovulatory follicular maturation in mice. *J. Exp. Zool.* 228:99–108.

DOYLE, D.A.; MORAIS CABRAL, J.; PFUETZNER, R.A.; KUO, A.; GULBIS, J.M.; COHEN, S.L.; CHAIT, B.T.; MACKINNON, R. (1998) The structure of the potassium channel: Molecular basis of K^+ conduction and selectivity. *Science* 280:69–77.

DRAGILEVA, E.; RUBINSTEIN, S.; BREITBART, H. (1999) Intracellular $\text{Ca}^{2+}\text{Mg}^{2+}$ -ATPase regulates calcium influx and acrosomal exocytosis in bull and ram spermatozoa. *Biological Reproduction* 61:1226–1234.

DUPONT, G.; COMBETTES, L.; BIRD, G.S.; PUTNEY, J.M. (2011) Calcium Oscillations. *Cold Spring Harb Perspect Biol.* 3(3):a004226.

DYM, M.; FAWCETT, D.W. (1971) Further observations on the numbers of spermatogonia, spermatocytes, and spermatids connected by intercellular bridges in the mammalian testis. *Biol Reprod* 4:195–215.

DYM, M. (1994) Spermatogonial stem cells of the testis. *Proceedings of the National Academy of Sciences of the United States of America*. 91(24):11287–11289.

EISENBACH, M. (1999) Sperm chemotaxis. *Reviews of Reproduction* 4:56–66.

EISENBACH, M.; GIOJALAS, L.C. (2006). Sperm guidance in mammals - an unpaved road to the egg. *Nature Rev. Mol. Cell. Biol.* 7:276-285.

ENG, L.A.; OLIPHANT, G. (1978) Rabbit sperm reversible decapacitation by membrane stabilization with a highly purified glycoprotein from seminal plasma. *Biol. Reprod.* 19, 1083-1094.

ERICKSON, G.F. (1986) An analysis of follicle development and ovum maturation. *Semin.Reprod. Endocrinol.* 4:233–254.

ERTEL, E.A.; CAMPBELL, K.P.; HARPOLD, M.M.; HOFMANN, F.; MORI, Y.; PEREZ-REYES, E.; SCHWARTZ, A.; SNUTCH, T.P.; TANABE, T.; BIRNBAUMER, L.; TSIEN, R.W.; CATTERALL, W.A. (2000) Nomenclature of voltage-gated calcium channels. *Neuron*. 25:533–535.

ESCOFFIER, J.; BOISSEAU, S.; SERRES, C.; CHEN, C.C.; KIM, D.; STAMBOULIAN, S.; SHIN, H.S.; CAMPBELL, K.P.; DE WAARD, M.; ARNOULT, C. (2007) Expression, localization and functions in acrosome reaction and sperm motility of Ca(V)3.1 and Ca(V)3.2 channels in sperm cells: an evaluation from Ca(V)3.1 and Ca(V)3.2 deficient mice. *J Cell Physiol* 212:753–763.

ESPINAL-ENRÍQUEZ, J.; PRIEGO-ESPINOSA, D.A.; DARZON, A.; BELTRÁN, C.; MARTÍNEZ-MEKLER, G. (2017) Network model predicts that CatSper is the main Ca^{2+} channel in the regulation of sea urchin sperm motility. *Scientific Reports Sci Rep* 7(1):4236.

ESPINOSA, F.; DARZON, A. (1995) Mouse sperm membrane potential: changes induced by Ca^{2+} . *FEBS Lett.* 372:119–125.

ESPINOSA, F.; DE LA VEGA-BELTRAN, J.L.; LOPEZ-GONZALEZ, I.; DELGADO, R.; LABARCA, P.; DARZON, A. (1998) Mouse sperm patch-clamp recordings reveal single Cl^- channels sensitive to niflumic acid, a blocker of the sperm acrosome reaction. *FEBS Letters.* 426:47–51.

FAKIH, H.; MACLUSKY, N.; DECHERNEY, A.; WALLIMANN, T.; HUSZAR, G. (1986) Enhancement of human sperm motility and velocity *in vitro*: Effects of calcium and creatine phosphate. *Fertil Steril* 46:938–944.

FAWCETT, D.W. (1975). The mammalian spermatozoon. *Dcv. Biol.* 44, 394-436.

FELIX, R.; SERRANO, C.J.; TREVINO, C.L.; MUNOZ-GARAY, C.; BRAVO, A.; NAVARRO, A.; PACHECO, J.; TSUTSUMI, V.; DARZON, A. (2002) Identification of distinct K^+ channels in mouse spermatogenic cells and sperm. *Zygote* 10:183–188.

FENG, M.; GRICE, D.M.; FADDY, H.M.; NGUYEN, N.; LEITCH, S.; WANG, Y.; MUEND, S.; KENNY, P.A.; SUKUMAR, S.; ROBERTS-THOMSON, S.J. et al. (2010) Store independent activation of Orai1 by SPCA2 in mammary tumors. *Cell* 143 84–98.

FICARRO, S.; CHERTIHIN, O.; WESTBROOK, V.A.; WHITE, F.; JAYES, F.; KALAB, P.; MARTO, J.A.; SHABANOWITZ, J.; HERR, J.C.; HUNT, D.F.; VISCONTI, P.E. (2003) Phosphoproteome analysis of capacitated human sperm. Evidence of tyrosine phosphorylation of a kinase-anchoring protein 3 and valosin-containing protein/p97 during capacitation. *J Biol Chem.*278:11579–11589.

FIGUEIRAS-FIERRO, D.; ACEVEDO, J.J.; MARTINEZ-LOPEZ, P.; ESCOFFIER, J.; SEPULVEDA, F.V.; BALDERAS, E.; ORTA, G.; VISCONTI, P.E.; DARSZON, A. (2013) Electrophysiological evidence for the presence of cystic fibrosis transmembrane conductance regulator (CFTR) in mouse sperm. *J Cell Physiol* 228:590–601.

FLESCH, F.M.; GADELLA, B.M. (2000) Dynamics of the mammalian sperm plasma membrane in the process of fertilization. *Biochim Biophys Acta*. 1469(3):197-235.

FLORMAN, H.M.; TOMBES, R.M.; FIRST, N.L.; BABCOCK, D.F. (1989) An adhesion-associated agonist from the zona pellucida activates G protein-promoted elevations of internal Ca^{2+} and pH that mediate mammalian sperm acrosomal exocytosis. *Dev Biol*. 135:133–146.

FLORMAN, H.M. (1994) Sequential focal and global elevations of sperm intracellular Ca^{2+} are initiated by the zona pellucida during acrosomal exocytosis. *Developmental Biology* 165:152–164.

FLORMAN, H.M.; ARNOULT, C.; KAZAM, I.G.; LI, C.; O'TOOLE, C.M. (1998) A perspective on the control of mammalian fertilization by egg-activated ion channels in sperm: a tale of two channels. *Biol Reprod* 59:12 – 16.

FRENETTE, G.; LESSARD, C.; SULLIVAN, R. (2002) Selected proteins of “prostasome-like particles” from epididymal cauda fluid are transferred to epididymal caput spermatozoa in bull. *Biol. Reprod.* 67:308–313.

FRIEDRICH, B.M.; JÜLICHER F. (2007) Chemotaxis of sperm cells. *Proc. Natl. Acad. Sci. USA*. 104:13256–13261.

FUKAMI, K.; YOSHIDA, M.; INOUE, T.; KUROKAWA, M.; FISSORE, R.A.; YOSHIDA, N.; MIKOSHIBA, K.; TAKENAWA, T. (2003) Phospholipase Cdelta4 is required for Ca^{2+} mobilization essential for acrosome reaction in sperm. *Journal of Cell Biology* 161:79–88.

FURST, J.; GSCHWENTNER, M.; RITTER, M.; BOTTA, G.; JAKAB, M.; MAYER, M.; et al. (2002) Molecular and functional aspects of anionic channels activated during regulatory volume decrease in mammalian cells. *Pflügers Archiv.* 444:1–25.

GADELLA, B.M.; HARRISON, R.A. (2000) The capacitating agent bicarbonate induces protein kinase A-dependent changes in phospholipid transbilayer behavior in the sperm plasma membrane. *Development.* 127(11):2407-20.

GADELLA, B.M.; VAN GESTEL, R.A. (2004) Bicarbonate and its role in mammalian sperm function. *Anim Reprod Sci.* 82-83:307-19.

GADELLA, B.M. (2008) The assembly of a zona pellucida binding protein complex in sperm. *Reprod Domest Anim* 43:12–9.

GAKAMSKY, A.; ARMON, L.; EISENBACH, M. (2009) Behavioral response of human spermatozoa to a concentration jump of chemoattractants or intracellular cyclic nucleotides. *Hum Reprod.* 24:1152–63.

GARCIA, M.A.; MEIZEL, S. (1999) Regulation of intracellular pH in capacitated human spermatozoa by a Na⁺/H⁺ exchanger. *Mol. Reprod. Develop.* 52:189-195.

GIANNINI, G.; CONN, A.; MAMMARELLA, S.; SCROBOGNA, M.; SORRENTINO, V. (1995) The ryanodine receptor/ calcium channel genes are widely and differentially expressed in murine brain and peripheral tissues. *J. Cell Biol.* 128:893-904.

GONDOS, B.; WESTERGAARD, L.; BYSKOV, A.G. (1986) Initiation of oogenesis in the human fetal ovary: ultrastructural and squash preparation study. *Am J Obstet Gynaecol.* 155:189–195.

GONZÁLEZ-MARTÍNEZ, M.T.; GALINDO, B.E.; DE LA TORRE, L.; ZAPATA, O.; RODRÍGUEZ, E.; FLORMAN, H.M.; DARSZON, A. (2001) A sustained increase in

intracellular Ca^{2+} is required for the acrosome reaction in sea urchin sperm. *Dev Biol.* 236(1):220-9.

GOUGEON, A. (1996) Regulation of ovarian follicular development in primates: facts and hypotheses. *Endocr Rev.* 17(2):121-55.

GRISWOLD, M.D. (1998) The central role of Sertoli cells in spermatogenesis. *Semin. Cell Dev. Biol.* 9:411–416.

GUNARATNE, H.J; VACQUIER, V.D. (2006) Evidence for a secretory pathway Ca^{2+} -ATPase in sea urchin spermatozoa. *FEBS Letters* 580(16):3900-3904.

GUPTA, S. K.; JETHANANDANI, P.; AFZALPURKAR, A.; KAUL, R.; SANTHANAM, R. (1997) Prospects of zona pellucida glycoproteins as immunogens for contraceptive vaccine *Human Reproduction Update* 3(4):311–324.

GUPTA, S.K.; BHANDARI, B. (2011) Acrosome reaction: relevance of zona pellucida glyco-proteins. *Asian J Androl* 13:97–105.

GURAYA, S.S. (1987) *Biology of Spermatogenesis and Spermatogonia in Mammals.* Springer-Verlag Berlin, pp 248-251.

GWATHMEY, T.M.; IGNOTZ, G.G.; SUAREZ, S.S. (2003) PDC-109 (BSP-A1/A2) promotes bull sperm binding to oviductal epithelium in vitro and may be involved in forming the oviductal sperm reservoir. *Biol Reprod.* 69:809–815.

HAFEZ, E.S.E.; BLACK, D.L. (1969) The mammalian uterotubal junction. In Hafez ESE and Blandau RJ (eds), *The Mammalian Oviduct: Comparative Biology and Methodology.* The University of Chicago Press, Chicago, IL, pp. 85–128.

HAMILL, O.P.; MARTY, A.; NEHER, E.; SAKMANN, B.; SIGWORTH, F.J. (1981) Improved patch clamp techniques for high resolution current recording from cells and cell-free membrane patches. *Pflugers Arch.* 391:85-100.

HANSON, F.W.; OVERSTREET, J.W. (1981) The interaction of human spermatozoa with cervical mucus *in vitro*. *Am. J. Obstet. Gynecol.* 140:173–178.

HARPER, C.V., BARRATT, C.L.; PUBLICOVER, S.J. (2004) Stimulation of human spermatozoa with progesterone gradients to simulate approach to the oocyte. Induction of $[Ca^{2+}]_i$ oscillations and cyclical transitions in flagellar beating. *J. Biol. Chem.* 279:46315–46325.

HARPER, C.; WOOTTON, L.; MICHELANGELI, F.; LEFIEVRE, L.; BARRATT, C.; PUBLICOVER, S. (2005) Secretory pathway Ca^{2+} -ATPase (SPCA1) Ca^{2+} pumps, not SERCAs, regulate complex $[Ca^{2+}]_i$ signals in human spermatozoa. *J Cell Sci* 118:1673–1685.

HARPER, C.V.; PUBLICOVER, S.J. (2005) Reassessing the role of progesterone in fertilization-compartmentalized calcium signalling in human spermatozoa? *Human Reproduction* 20:2675-2680.

HARRIS, J.D.; HIBLER, D.W.; FONTENOT, G.K.; et al (1994) Cloning and characterization of zona pellucida genes and cDNAs from a variety of mammalian species: the ZPA, ZPB and ZPC gene families. *DNA Sequence* 4:361–393.

HARRISON, R.A.; MILLER, N.G. (2000) cAMP-dependent protein kinase control of plasma membrane lipid architecture in boar sperm. *Molecular Reproduction and Development* 55:220-228.

HASHIMOTO, Y.; EGUCHI, Y. (1955) Histological observations on the gonads in the cattle and the horse foetus. 1. The cattle foetus. *Jap.J. zootech. Sci.* 26:259.

HERNÁNDEZ-GONZÁLEZ, E.O.; SOSNIK, J.; EDWARDS, J.; ACEVEDO, J.J.; MENDOZA-LUJAMBIO, I.; LÓPEZ GONZÁLEZ, I.; DEMARCO, I.; WERTHEIMER, E.; DARSZON, A.; VISCONTI, P.E. (2006) Sodium and epithelial sodium channels participate in the regulation of the capacitation-associated hyperpolarization in mouse sperm. *J Biol Chem.* 281:5623-3563.

HERNANDEZ-GONZALEZ, E.O.; TREVINO, C.L.; CASTELLANO, L.E.; DE LA VEGA-BELTRAN, J.L.; OCAMPO, A.Y.; WERTHEIMER, E. et al. (2007) Involvement of cystic fibrosis transmembrane conductance regulator in mouse sperm capacitation. *The Journal of Biological Chemistry* 282:24397–24406.

HIBINO, H.; INANOBE, A.; FURUTANI, K.; MURAKAMI, S.; FINDLAY, I.; KURACHI, Y. (2010) Inwardly rectifying potassium channels: their structure, function, and physiological roles. *Physiol Rev.* 90(1):291-366.

HILDEBRAND, M.S.; AVENARIUS, M.R.; FELLOUS, M.; ZHANG, Y.; MEYER, N.C.; AUER, J.; SERRES, C.; KAHRIZI, K.; NAJMABADI, H.; BECKMANN, J.S.; SMITH, R.J. (2010) Genetic male infertility and mutation of CATSPER ion channels. *Eur J Hum Genet.* 18(11):1178-84.

HINO, T.; MURO, Y.; TAMURA-NAKANO, M.; OKABE, M.; TATENO, H.; YANAGIMACHI, R. (2016) The behavior and acrosomal status of mouse spermatozoa in vitro, and within the oviduct during fertilization after natural mating. *Biol Reprod.* 95(3):50.

HIROHASHI, N.; VACQUIER, V.D. (2003) Store-operated calcium channels trigger exocytosis of the sea urchin sperm acrosomal vesicle. *Biochem Biophys Res Commun.* 304(2):285-92.

HIRSH, A. (2003). Male subfertility. *BMJ.* 327 (7416). p.669-672.

HO, H.C.; SUAREZ, S.S. (2001). An inositol 1,4,5-trisphosphate receptor-gated intracellular Ca^{2+} store is involved in regulating sperm hyperactivated motility. *Biol. Reprod.* 65:1606–1615.

HO, H.C., GRANISH, K.A.; SUAREZ, S.S. (2002). Hyperactivated motility of bull sperm is triggered at the axoneme by Ca^{2+} and not cAMP. *Dev. Biol.* 250:208–217.

HO, H.C.; SUAREZ, S.S. (2003) Characterization of the intracellular calcium store at the base of the sperm flagellum that regulates hyperactivated motility. *Biol. Reprod.* 68:1590–1596.

HO, K.; WOLFF, C.A; SUAREZ, S.S. (2009) CatSper-null mutant spermatozoa are unable to ascend beyond the oviductal reservoir. *Reprod Fertil Dev.* 21:345–350.

HODGKIN, A.L.; KEYNES, R.D. (1955) The potassium permeability of a giant nerve fibre. *J Physiol.* 128:61–88.

HOGG, R.C.; WANG, Q.; LARGE, W.A. (1994) Action of niflumic acid on evoked and spontaneous calcium-activated chloride and potassium currents in smooth muscle cells from rabbit portal vein. *British Journal of Pharmacology* 112(3): 977–984.

HOODBHOY, T.; JOSHI, S.; BOJA, E.S.; WILLIAMS, S.A.; STANLEY, P.; DEAN, J. (2005) Human sperm do not bind to rat zonae pellucidae despite the presence of four homologous glycoproteins. *J Biol Chem.* 280:12721–12731.

HOLT, W.V.; VAN LOOK, K.J.W. (2004) Concepts in sperm heterogeneity, sperm selection and sperm competition as biological foundations for laboratory tests of semen quality. *Reproduction* 127:527-535.

HUCKINS, C. (1971) The spermatogonial stem cell population in adult rats. I. Their morphology, Proliferation and maturation *Anatomical Record* 169:533-548.

- HUGGINS, M.L. (1942) Thermodynamic properties of solutions of long-chain compounds. *Annals of the New York Academy of Sciences* 43(1):1-32.
- HUNTER, R.H.; LÉGLISE, P.C. (1971) Polyspermic fertilization following tubal surgery in pigs, with particular reference to the rôle of the isthmus. *J Reprod Fertil.* 24(2):233–246.
- HUNTER, R.H. (1972) Local action of progesterone leading to polyspermic fertilization in pigs. *J Reprod Fertil.* 31(3):433–444.
- HUNTER, R.H. (1973) Polyspermic fertilization in pigs after tubal deposition of excessive numbers of spermatozoa. *J Exp Zool.* 183(1):57–63.
- HYAKUTAKE, T.; SUZUKI, H.; YAMAMOTO, S. (2015) Effect of non-Newtonian fluid properties on bovine sperm motility. *J Biomech.* 48(12):2941-7.
- IBORRA, A.; COMPANYÓ, M.; MARTÍNEZ, P.; MORROS, A. (2000) Cholesterol efflux promotes acrosome reaction in goat spermatozoa. *Biol Reprod.* 62(2):378-83.
- INO, M.; YOSHINAGA, T.; WAKAMORI, M.; MIYAMOTO, N.; TAKAHASHI, E.; SONODA, J.; KAGAYA, T.; OKI, T.; NAGASU, T.; NISHIZAWA, Y.; et al (2001) Functional disorders of the sympathetic nervous system in mice lacking the $\alpha 1B$ subunit (Cav 2.2) of N-type calcium channels. *Proc Natl Acad Sci USA.* 98:5323–8.
- INOUE, N.; IKAWA, M.; ISOTANI, A.; OKABE, M. (2005) The immunoglobulin superfamily protein Izumo is required for sperm to fuse with eggs. *Nature* 434: 234–238.
- IQBAL, M.; SHIVAJI, S.; VIJAYASARATHY, S.; BALARAM, P. (1980) Synthetic peptides as chemoattractants for bull spermatozoa structure activity correlations. *Biochem. Biophys. Res. Commun.* 96:235–242.
- IRVINE, D.S. (1998) Epidemiology and etiology of male infertility. *Hum Reprod* 13 (Suppl 1). p.33-44.

JAGANNATHAN, S.; PUNT, E.L.; GU, Y.; ARNOULT, C.; SAKKAS, D.; BARRATT, C.L.; PUBLICOVER, S.J. (2002) Identification and localization of T-type voltage-operated calcium channel subunits in human male germ cells. Expression of multiple isoforms. *Journal of Biological Chemistry* 277:8449–8456.

JAGANNATHAN, S.; PUBLICOVER, S.J.; BARRATT, C.L. (2002) Voltage-operated calcium channels in male germ cells. *Reproduction* 123:203–215.

JAIWAL, B.S., TUR-KASPA, I., DOR, J., MASHIACH, S. & EISENBACH, M. (1999). Human sperm chemotaxis: is progesterone a chemoattractant? *Biology of Reproduction*. 60:1314-1319.

JANSEN, R.P. (1978). Fallopian tube isthmus mucus and ovum transport. *Science*, 201(4353):349-351.

JANSEN, R.P. (1980) Cyclic changes in the human fallopian tube isthmus and their functional importance. *Am J Obstet Gynecol*. 136(3):292-308.

JENTSCH, T.J.; NEAGOE, I.; SCHEEL, O. (2005) CLC chloride channels and transporters. *Current Opinion in Neurobiology*. 15:319–325.

JIMENEZ-GONZALEZ, C.; MICHELANGELI, F.; HARPER, C.V.; BARRATT, C.L.; PUBLICOVER, S.J. (2006) Calcium signalling in human spermatozoa: a specialized ‘toolkit’ of channels, transporters and stores. *Human Reproduction Update*. 12:253–267.

JIN, J.; JIN, N.; ZHENG, H.; RO, S.; TAFOLLA, D.; SANDERS, K.M.; YAN, W. (2007) *Catsper3* and *Catsper4* are essential for sperm hyperactivated motility and male fertility in the mouse. *Biol Reprod*. 77:37–44.

JIN, M.; FUJIWARA, E.; KAKIUCHI, Y.; OKABE, M.; SATOUH, Y.; BABA, S.A.; CHIBA, K.; HIROHASHI, N. (2011) Most fertilizing mouse spermatozoa begin their

acrosome reaction before contact with the zona pellucida during *in vitro* fertilization. Proceedings of the National Academy of Sciences, 108(12):4892-4896.

JIN, S.K.; YANG, W.X. (2017) Factors and pathways involved in capacitation: how are they regulated? Oncotarget 8(2):3600-3627.

JONGE, C. (2005) Biological basis for human capacitation. Human Reproduction Update. 11:205–214.

JUNGNICKEL, M.K.; MARRERO, H.; BIRNBAUMER, L.; LEMOS, J.R.; FLORMAN, H.M. (2001) Trp2 regulates entry of Ca²⁺ into mouse sperm triggered by egg ZP3. Nature Cell Biology 3:499–502.

KARNI, Z.; POLISHUK, W. Z.; ADONI, A.; DIAMANT, Y. (1971) Newtonian viscosity of the human cervical mucus during the menstrual cycle. Int J Fertil, 16:185-8.

KATZ, D.F.; MORALES, P. et al (1990) Mechanisms of filtration of morphologically abnormal human sperm by cervical mucus. Fertility and Sterility 54(3):509-512.

KATZ, D.F.; SLADE, D.A.; NAKAJIMA, S.T. (1997) Analysis of preovulatory changes in cervical mucus hydration and sperm penetrability. Adv Contracep 13:143–151.

KAUPP, U.B. (1995) Family of cyclic nucleotide gated ion channels. Current Opinion in Neurobiology 5:434–442.

KAUPP, U.B.; SEIFERT, R. (2002) Cyclic nucleotide-gated ion channels. Physiol Rev 82: 769 – 824.

KAUPP, U.B.; SOLZIN, J.; HILDEBRAND, E.; BROWN, J.E.; HELBIG, A.; HAGEN, V.; BEYERMANN, M.; PAMPALONI, F.; WEYAND, I. (2003) The signal flow and motor response controlling chemotaxis of sea urchin sperm. Nat. Cell Biol. 5:109–117.

KAUPP, U.B., HILDEBRAND, E.; WEYAND, I. (2006). Sperm chemotaxis in marine invertebrates molecules and mechanisms. *J. Cell Physiol.* 208:487-494.

KAUPP, U.B.; KASHIKAR, N.D.; WEYAND, I. (2008) Mechanisms of sperm chemotaxis. *Annu Rev Physiol* 70:93–117.

KELLY, M.; BROWN, S.; COSTELLO, S.; RAMALINGAM, M.; DREW, E.; BARRATT, C.; PUBLICOVER, S.J.; MARTINS DA SILVA, S. (2018) Single-cell analysis of $[Ca^{2+}]_i$ signalling in sub-fertile men: characteristics and relation to fertilization outcome. *Human Reproduction.* 33(6):1023–1033.

KERVANCIOGLU, M.E., DJAHANBACKHCH, O.; AITKEN, R.J. (1994) Epithelial cell co-culture and the induction of sperm capacitation. *Fertil. Steril.* 61:1103–1108.

KIM, D.; SONG, I.; KEUM, S.; LEE, T.; JEONG, M.J.; KIM, S.S.; MCENERY, M.W.; SHIN, H.S. (2001) Lack of the burst firing of thalamocortical relay neurons and resistance to absence seizures in mice lacking $\alpha(1G)$ T-type Ca^{2+} channels. *Neuron.* 31:35–45.

KIM, M.S.; ZENG, W.; YUAN, J.P.; SHIN, D.M.; WORLEY, P.F.; MUALLEM, S. (2009) Native store-operated Ca^{2+} influx requires the channel function of orai1 and TRPC1. *Journal of Biological Chemistry.* 284:9733–9741.

KIM, D.M.; NIMIGEAN, C.M. (2016) Voltage-Gated Potassium Channels: A Structural Examination of Selectivity and Gating. *Cold Spring Harb Perspect Biol.* 8(5):a029231.

KIRICHOK, Y.; NAVARRO, B.; CLAPHAM, D.E. (2006). Whole-cell patch-clamp measurements of spermatozoa reveal an alkaline-activated Ca^{2+} channel. *Nature.* 439:737–740.

KIRICHOK, Y.; LISHKO, P.V. (2011) Rediscovering sperm ion channels with the patch-clamp technique. *Mol Hum Reprod.* 17(8):478-99.

KIRKMAN-BROWN, J.C.; BRAY, C.; STEWART, P.M.; BARRATT, C.L.; PUBLICOVER, S.J. (2000) Biphasic elevation of $[Ca^{2+}]_i$ in individual human spermatozoa exposed to progesterone. *Dev Biol.* 222(2):326-35.

KIRKMAN-BROWN, J.C.; BARRATT, C.L.; PUBLICOVER, S.J. (2004) Slow calcium oscillations in human spermatozoa *Biochemical Journal* 378:827-832.

KOCH, H.P.; KUROKAWA, T.; OKOCHI, Y.; SASAKI, M.; OKAMURA, Y.; LARSSON, H.P. (2008) Multimeric nature of voltage-gated proton channels. *Proc Natl Acad Sci USA* 105:9111– 9116.

KRASZNAI, Z.; KRASZNAI, Z.T.; MORISAWA, M.; BAZSÁNÉ, Z.K.; HERNÁDI, Z.; FAZEKAS, Z.; TRÓN, L.; GODA, K.; MÁRIÁN, T. (2006) Role of the Na^+/Ca^{2+} exchanger in calcium homeostasis and human sperm motility regulation. *Cell Motil Cytoskeleton.* 63(2):66-76.

KREMER, J. (1965) A simple sperm penetration test. *International journal of fertility,* 10:209-215.

KURODA, Y.; KANEKO, S.; YOSHIMURA, Y.; NOZAWA, S.; MIKOSHIBA, K. (1999) Are there inositol 1,4,5-triphosphate (IP3) receptors in human sperm? *Life Sciences* 65:135– 143.

LAWSON, C.; DORVAL, V.; GOUPIL, S.; LECLERC, P. (2007) Identification and localisation of SERCA 2 isoforms in mammalian sperm. *Molecular Human Reproduction.* 13:307–316.

LEE, S.Y.; LETTS, J.A.; MACKINNON, R. (2008) Dimeric subunit stoichiometry of the human voltage-dependent proton channel Hv1. *Proc Natl Acad Sci USA* 105:7692 – 7695.

LEFIEVRE, L.; CONNER, S.J.; SALPEKAR, A.; OLUFOWOBI, O., ASHTON, P.; PAVLOVIC, B.; et al (2004). Four zona pellucida glycoproteins are expressed in the human. *Human Reproduction* 19(7):1580–6.

LEFIEVRE, L.; NASH, K.; MANSELL, S.; COSTELLO, S.; PUNT, E.; CORREIA, J.; MORRIS, J.; KIRKMAN-BROWN, J.; WILSON, S.M.; BARRATT, C.L.; PUBLICOVER, S. (2012) 2-APB-potentiated channels amplify CatSper-induced Ca^{2+} signals in human sperm. *Biochemistry Journal* 448:189–200.

LEMAIRE, W.J.; YANG, N.S.T.; BEHRAM, H.H.; MARSH, J.M. (1973) Pre-ovulatory changes in concentration of prostaglandin in rabbit graafian follicles. *Prostaglandins*. 3:367–376.

LEONETTI, M.D.; YUAN, P.; HSIUNG, Y.; MACKINNON, R. (2012) Functional and structural analysis of the human SLO3 pH- and voltage-gated K^+ channel. *Proc Natl Acad Sci USA*. 109(47):19274-9.

LESSEY, B.A.; YEH, I.; CASTELBAUM, A.J.; FRITZ, M.A.; ILESANMI, A.O.; KORZENIOWSKI, P.; SUN, J.; CHWALISZ, K. (1996) Endometrial progesterone receptors and markers of uterine receptivity in the window of implantation. *Fertil Steril*. 65(3):477-83.

LIEVANO, A.; SANTI, C.M.; SERRANO, C.J.; TREVINO, C.L.; BELLVE, A.R.; HERNANDEZ-CRUZ, A.; DARSZON, A. (1996) T-type Ca^{2+} channels and $\alpha 1E$ expression in spermatogenic cells, and their possible relevance to the sperm acrosome reaction. *FEBS Lett* 388:150– 154.

LI, C.Y.; JIANG, L.Y.; CHEN, W.Y.; LI, K.; SHENG, H.Q.; NI, Y.; LU, J.X.; XU, W.X.; ZHANG, S.Y.; SHI, Q.X. (2010) CFTR is essential for sperm fertilizing capacity and is correlated with sperm quality in humans. *Human Reproduction*. 25:317–327.

LI, M.; YU, Y.; YANG, J. (2011) Structural Biology of TRP Channels. *Adv Exp Med Biol*. 704:1–23.

LIESTE, J.R.; KOOPMAN, W.J.H.; REYNEN, V.J.; SCHEENEN, W.J.J.M.; JENKS, B.G.; ROUBOS, E.W. (1998) Action currents generate stepwise intracellular Ca²⁺ patterns in a neuroendocrine cell. *J. Biol. Chem.* 273:25686–25694.

LINCK, R.W.; OLSON, G.E.; LANGEVIN, G.L. (1981) Arrangement of tubulin subunits and microtubule-associated proteins in the central-pair microtubule apparatus of squid (*Loligo pealei*) sperm flagella. *J Cell Biol.* 89:309–22.

LINCK, R.W.; CHEMES, H.; ALBERTINI, D.F. (2016) The axoneme: the propulsive engine of spermatozoa and cilia and associated ciliopathies leading to infertility. *J Assist Reprod Genet.* 33:141–56.

LIU, J.; KIM, M.L.; HEO, W.D.; JONES, J.T.; MYERS, J.W.; FERRELL, J.E.JR; MEYER, T. (2005) STIM is a Ca²⁺ sensor essential for Ca²⁺-store-depletion-triggered Ca²⁺ influx. *Current Biology.* 15(13):1235–1241.

LISHKO, P.V.; KIRICHOK, Y. (2010) The role of Hv1 and CatSper channels in sperm activation. *J Physiol.* 588:4667–4672.

LISHKO, P.V.; BOTCHKINA, I.L.; FEDORENKO, A.; KIRICHOK, Y. (2010) Acid extrusion from human spermatozoa is mediated by flagellar voltage-gated proton channel. *Cell* 140:327 – 337.

LISHKO, P.V.; BOTCHKINA, I.L.; KIRICHOK, Y. (2011) Progesterone activates the principal Ca²⁺ channel of human sperm. *Nature* 471(7338):387-391.

LISHKO, P.V.; KIRICHOK, Y.; REN, D.; NAVARRO, B.; CHUNG, J.J.; CLAPHAM, D.E. (2012) The control of male fertility by spermatozoan ion channels. *Annual Reviews Physiology* 74:453–475.

- LITVIN, T.N.; KAMENETSKY, M.; ZARIFYAN, A.; BUCK, J.; LEVIN, L.R. (2003) Kinetic properties of “soluble” adenylyl cyclase. Synergism between calcium and bicarbonate. *J Biol Chem.* 278:15922–15926.
- LIU, J.; XIA, J.; CHO, K.H.; CLAPHAM, D.E.; REN, D. (2007) CatSper beta, a novel transmembrane protein in the CatSper channel complex. *J Biol Chem.* 282:18945–52.
- LIU, Y.; WANG, D.K.; CHEN, LM. (2012) The physiology of bicarbonate transporters in mammalian reproduction. *Biol Reprod.* 86(4):99.
- LOBLEY, A.; PIERRON, V.; REYNOLDS, L.; ALLEN, L.; MICHALOVICH, D. (2003) Identification of human and mouse CatSper3 and CatSper4 genes: characterisation of a common interaction domain and evidence for expression in testis. *Reprod Biol Endocrinol.* 1:53.
- LOTTI F.; MAGGI, M. (2014) Ultrasound of the male genital tract in relation to male reproductive health. *Human Reproduction Update.* 21(1):56-83.
- MAAS, D.H.; STOREY, B.T.; MASTROIANNI, L. (1977) Hydrogen ion and carbon dioxide content of the oviductal fluid of the rhesus monkey (*Macaca mulatta*). *Fertil. Steril.* 28:981–985.
- MANSELL, S.A.; PUBLICOVER, S.J.; BARRATT, C.L.R.; WILSON, S.M. (2014) Patch clamp studies of human sperm under physiological ionic conditions reveal three functionally and pharmacologically distinct cation channels. *Mol Hum Reprod* 20:392-408.
- MARQUEZ, B.; SUAREZ, S.S. (2004) Different signaling pathways in bovine sperm regulate capacitation and hyperactivation. *Biol. Reprod.* 70:1626-1633.
- MARQUEZ, B.; SUAREZ, S.S. (2006) Bovine sperm hyperactivation is promoted by alkaline-stimulated Ca²⁺ influx, *Biol Reprod* 76(4):660-5.

MARQUEZ, B.; SUAREZ, S.S. (2007) Bovine sperm hyperactivation is promoted by alkaline-stimulated Ca^{2+} influx. *Biol Reprod.* 76(4):660-5.

MARQUEZ, B.; IGNOTZ, G.; SUAREZ, S.S. (2007) Contributions of extracellular and intracellular Ca^{2+} regulation of sperm motility: release of intracellular stores can hyperactivate CatSper1 and CatSper2 null sperm. *Dev Biol.* 303:214–221.

MARTINEAU, J.; NORDQVIST, K.; TILMANN, C.; LOVELL-BADGE, R.; CAPEL, B. (1997) Male-specific cell migration into the developing gonad. *Current Biology* 7:958 – 968.

MARTINEZ-LOPEZ, P.; SANTI, C.M.; TREVINO, C.L.; OCAMPO-GUTIERREZ, A.Y.; ACEVEDO, J.J.; ALISIO, A.; et al (2009) Mouse sperm K^+ currents stimulated by pH and cAMP possibly coded by Slo3 channels. *Biochemical and Biophysical Research Communications.* 381:204–209.

MASON, M.J.; MAYER, B.; HYMEL, L.J. (1993) Inhibition of Ca^{2+} transport pathways in thymic lymphocytes by econazole, miconazole, and SKF 96365. *Am J Physiol.* 264:C654–C662.

MATA-MARTÍNEZ, E.; DARSZON, A.; TREVIÑO, C.L. (2018) pH-dependent Ca^{2+} oscillations prevent untimely acrosome reaction in human sperm. *Biochem Biophys Res Commun* 497:146–152.

MAZZOLINI, M.; MARCHESI, A.; GIORGETTI, A.; TORRE, V. (2010) Gating in CNGA1 channels. *Pflügers Arch* 459: 547–555.

MEIZEL, S.; TURNER, K.O. (1996) Chloride efflux during the progesterone-initiated human sperm acrosome reaction is inhibited by lavendustin A, a tyrosine kinase inhibitor. *Journal of Andrology* 17:327–330.

MERRITT, J.E.; ARMSTRONG, W.P.; BENHAM, C.D.; HALLAM, T.J.; JACOB, R.; JAXA-CHAMIEC, A.; et al. (1990) SKF 96365, a novel inhibitor of receptor-mediated calcium entry. *Biochem J.* 271:515–522.

MICHELANGELI, F.; EAST, J.M. (2011) A diversity of SERCA Ca²⁺ pump inhibitors. *Biochemical Society Transactions* 39:789–797.

MIZUTANI, H.; YAMAMURA, H.; MURAMATSU, M.; KIYOTA, K.; NISHIMURA, K.; SUZUKI, Y.; OHYA, S.; IMAIZUMI, Y. (2014) Spontaneous and nicotine-induced Ca²⁺ oscillations mediated by Ca²⁺ influx in rat pinealocytes. *Am J Physiol Cell Physiol.* 306(11):C1008-16.

MORALES, P.; OVERSTREET, J.W.; KATZ, D.F. (1988) Changes in human sperm motion during capacitation *in vitro*. *J. Reprod. Fertil.* 83:119–128.

MORALES, C.R.; NI, X.; SMITH, C.E.; INAGAKI, N.; HERMO, L. (2012) ABCA17 mediates sterol efflux from mouse spermatozoa plasma membranes. *Histol Histopathol.* 27(3):317-28.

MORTIMER, D.; TEMPLETON, A.A. (1982) Sperm transport in the female reproductive tract in relation to semen analysis characteristics and the time of ovulation. *J Reprod Fertil* 64:401-408.

MORTIMER, D.; PANDYA, I.J.; SAWERS, R.S. (1986) Relationship between human sperm motility characteristics and sperm penetration into human cervical mucus *in vitro*. *J Reprod Fertil.* 78(1):93-102.

MORTIMER, S.T.; MORTIMER, D. (1990) Kinematics of human spermatozoa incubated under capacitating conditions. *J Androl.* 11:195–203.

MORTIMER, S.T.; SWAN, M.A. (1995) Variable kinematics of capacitating human spermatozoa. *Hum.Reprod.* 10:3178–3182.

MORTIMER, D.; MORTIMER, S.T. (1998) Value and reliability of CASA systems. In:Ombelet W, Bosmans E, Vandeput H, Vereecken A, Renier M, Hoomans E, eds. Modern ART in the 2000s. London: Parthenon Publishing Group Limited. 73–89.

MORTIMER, S.T. 2000. CASA - Practical aspects. *Journal of Andrology*, 21:515-524.

MOSELEY, F.L.; JHA, K.N.; BJORND AHL, L.; BREWIS, I.A.; PUBLICOVER, S.J.; BARRATT, C.L.; LEFIEVRE, L. (2005) Protein tyrosine phosphorylation, hyperactivation and progesterone-induced acrosome reaction are enhanced in IVF media: an effect that is not associated with an increase in protein kinase A activation. *Mol Hum Reprod* 11:523–529.

MUANPRASAT, C.; SONAWANE, N.D.; SALINAS, D.; TADDEI, A.; GALIETTA, L.J.; VERKMAN, A.S. (2004) Discovery of glycine hydrazide pore-occluding CFTR inhibitors: mechanism, structure-activity analysis, and in vivo efficacy. *J Gen Physiol*. 124:125–137.

MUÑOZ-GARAY, C.; DE LA VEGA-BELTRÁN, J.L.; DELGADO, R.; LABARCA, P.; FELIX, R.; DARSZON, A. (2001) Inwardly rectifying K⁺ channels in spermatogenic cells: functional expression and implication in sperm capacitation. *Dev. Biol.* 234:261–274

NAABY -HANSEN S.; WOLKOWICZ M.J.; KLOTZ K., BUSH L.A.; WESTBROOK V.A.; SHIBAHARA H.; SHETTY J.; COONROD S.A.; REDDI P.P.; SHANNON J.; KINTER M.; SHERMAN N.E.; FOX J.; FLICKINGER C.J.; HERR J.C. (2001) Co-localization of the inositol 1,4,5-trisphosphate receptor and calreticulin in the equatorial segment and in membrane bounded vesicles in the cytoplasmic droplet of human spermatozoa. *Mol. Hum. Reprod.* 7:923-933.

NAKANISHI, T.; ISOTANI, A.; YAMAGUCHI, R.; IKAWA, M.; BABA, T.; SUAREZ, S.S.; OKABE, M. (2004) Selective passage through the uterotubal junction of sperm from a mixed population produced by chimeras of calmegin-knockout and wild-type male mice. *Biol. Reprod.* 71:959-965.

NASH, K.; LEFIEVRE, L.; PERALTA-ARIAS, R.; MORRIS, J.; MORALES-GARCIA, A.; CONNOLLY, T.; COSTELLO, S.; KIRKMAN-BROWN, J.C.; PUBLICOVER, S.J. (2010) Techniques for imaging Ca²⁺ signaling in human sperm. *J Vis Exp* pii:1996.

NAVARRO, B.; KIRICHOK, Y.; CLAPHAM, D.E. (2007) KSper, a pH-sensitive K⁺ current that controls sperm membrane potential. *Proc Natl Acad Sci USA* 104:7688–7692.

NAVARRO, B.; KIRICHOK, Y.; CHUNG, J.J.; CLAPHAM, D.E. (2008) Ion channels that control fertility in mammalian spermatozoa. *International Journal of Developmental Biology* 52:607–613.

NAZ, R.K.; RAJESH, P.B. (2004) Role of tyrosine phosphorylation in sperm capacitation/acrosome reaction. *Reproductive Biology and Endocrinology* 2:75.

NEILD, D.M.; BROUWERS, J.F.H.M.; COLENBRANDER, B.; AGUERO, A.; GADELLA, B.M. (2005) Lipid peroxide formation in relation to membrane stability of fresh and frozen thawed stallion spermatozoa. *Mol. Reprod. Dev.* 72:230–238.

NEILL, J.M.; OLDS-CLARKE, P. (1987) A computer-assisted assay for mouse sperm hyperactivation demonstrates that bicarbonate but not bovine serum albumin is required. *Gamete Res.* 18:121–140.

NILIUS, B.; HESS, P.; LANSMAN, J.B.; TSIEN, R.W. (1985) A novel type of cardiac Ca²⁺ channel in ventricular cells. *Nature* 316:433-446.

NILIUS, B.; DROOGMANS, G. (2003) Amazing chloride channels: An overview. *Acta Physiologica Scandinavica.* 177:119–147.

NILIUS, B.; OWSIANIK, G.; VOETS, T.; PETERS, J.A. (2007) Transient receptor potential cation channels in disease. *Physiol Rev.* 87:165–217.

NOLAN, J.P.; HAMMERSTEDT, R.H. (1997) Regulation of membrane stability and the acrosome reaction in mammalian sperm. *FASEB J.* 11:670-682.

OAKBERG, E.F. (1971) Spermatogonial stem-cell renewal in the mouse. *Anat. Rec.* 169:515–531.

OGUNBAYO, O.A.; ZHU, Y.; ROSSI, D.; SORRENTINO, V.; MA, J.; ZHU, M.X.; EVANS, A.M. (2011) Cyclic adenosine diphosphate ribose activates ryanodine receptors, whereas NAADP activates two-pore domain channels. *Journal of Biological Chemistry* 286:9136–9140.

O'FLAHERTY, C.; BECONI, M.; BEORLEGUI, N. (1997) Effect of natural antioxidants, superoxide dismutase and hydrogen peroxide on capacitation of frozen-thawed bull spermatozoa. *Andrologia* 29(5):269-275.

OOI, E.H.; SMITH, D.J.; GADÉLHA, H.; GAFFNEY, E.A.; KIRKMAN-BROWN, J. (2014) The mechanics of hyperactivation in adhered human sperm. *R Soc open sci.* 1:140230.

ORTA, G.; FERREIRA, G.; JOSE, O.; TREVINO, C.L.; BELTRAN, C.; DARSZON, A. (2012) Human spermatozoa possess a calcium-dependent chloride channel that may participate in the acrosomal reaction. *The Journal of Physiology* 590:2659–2675.

OSMAN, R.A., ANDRIA, M.L., JONES, A.D.; MEIZEL, S. (1989) Steroid-induced exocytosis: the human sperm acrosome reaction. *Biochem. Biophys. Res. Commun.* 160:828–833.

OKABE, M. (2013) The cell biology of mammalian fertilization. *Development* 140:4471–4479.

OKO, R.; CLERMONT, Y. (1998) Spermiogenesis. In: Knobil E, Neill JD, editors. *Encyclopedia of Reproduction*. San Diego: Academic Press. pp. 602–609.

OKUNADE, G.W.; MILLER, M.L.; PYNE, G.J.; SUTLIFF, R.L.; O'CONNOR, K.T.; NEUMANN, J.C.; ANDRINGA, A.; MILLER, D.A.; PRASAD, V.; DOETSCHMAN, T. et al. (2004) Targeted ablation of plasma membrane Ca²⁺-ATPase (PMCA) 1 and 4 indicates a major housekeeping function for PMCA1 and a critical role in hyperactivated sperm motility and male fertility for PMCA4. *J Biol Chem* 279:33742– 33750.

O'TOOLE, C.M.B.; ARNOULT, C.; DARSZON, A.; STEINHARDT, R.A.; FLORMAN, H.M. (2000) Ca²⁺ entry through store-operated channels in mouse sperm is initiated by egg ZP3 and drives the acrosome reaction. *Molecular Biology of the Cell* 11:1571–1584.

PACEY, A.A.; HILL, C.J.; SCUDAMORE, I.W.; WARREN, M.A.; BARRATT, C.L.R.; COOKE, I.D. (1995) The interaction *in vitro* of human spermatozoa with epithelial cells from the human uterine (fallopian) tube. *Hum Reprod* 10:360–366.

PRAKRIYA, M.; FESKE, S.; GWACK, Y.; SRIKANTH, S.; RAO, A.; HOGAN, P.G. (2006) Orai1 is an essential pore subunit of the CRAC channel. *Nature*. 443(7108):230-233.

PARK, K.H.; KIM, B.J.; KANG, J.; NAM, T.S.; LIM, J.M.; KIM, H.T.; PARK, J.K.; KIM, Y.G.; CHAE, S.W.; KIM, U.H. (2011) Ca²⁺ signaling tools acquired from prostasomes are required for progesterone-induced sperm motility. *Sci. Signal.* 4:31.

PATHAK, M.M.; TRAN, T.; HONG, L.; JOÓŠ, B.; MORRIS, C.E.; TOMBOLA, F. (2016) The Hv1 proton channel responds to mechanical stimuli. *J Gen Physiol* 148:405–418.

PEREZ-CEREZALES, S.; BORYSHPOLETS, S.; EISENBACH, M. (2015) Behavioral mechanisms of mammalian sperm guidance. *Asian J Androl.* 2015;17:628–32.

PESCHON, J.J.; BEHRINGER, R.R.; BRINSTER, R.L.; PALMITER, R.D. (1987) Spermatid-specific expression of protamine-1 in transgenic mice. *Proc. Natl. Acad. Sci. USA.* 84:5316–5319.

- PETERS, H.; BYSKOV, A.G.; HIMELSTEIN-BRAW, R.; FABER, M. (1975) Follicular growth: the basic event in the mouse and human ovary. *J Reprod Fertil.* 45:559–566.
- PINKERTON, J.H; MCKAY, D.G; ADAMS, E.C; HERTIG, A.T. (1961) Development of the human ovary—a study using histochemical techniques. *Obstet Gynecol.* 18:152–181.
- PINTO, F.M.; RAVINA, C.G.; FERNÁNDEZ-SÁNCHEZ, M.; GALLARDO-CASTRO, M.; CEJUDO-ROMÁN, A.; CANDENAS, L. (2009) Molecular and functional characterization of voltage-gated sodium channels in human sperm. *Reprod Biol Endocrinol.* 7:71.
- PLATZER, J.; ENGEL, J.; SCHROTT-FISCHER, A.; STEPHAN, K.; BOVA, S.; CHEN, H.; ZHENG, H.; STRIESSNIG, J. (2000) Congenital deafness and sinoatrial node dysfunction in mice lacking class D Ltype Ca^{2+} channels. *Cell.* 102:89–97.
- POPLI, K.; STEWART, J. (2007) Infertility and its management in men with cystic fibrosis: review of literature and clinical practices in the UK. *Hum Fertil (Camb)* 10:217–221.
- PUBLICOVER, S.J.; BARRATT, C.L. (1999) Voltage-operated Ca^{2+} channels and the acrosome reaction: which channels are present and what do they do? *Hum Reprod* 14:873 – 879.
- PUBLICOVER, S.; HARPER, C.V.; BARRATT, C. (2007) $[\text{Ca}^{2+}]_i$ signalling in sperm - making the most of what you've got. *Nature Cell Biol.* 9:235–242.
- PUBLICOVER, S.J.; GIOJALAS, L.C.; TEVES, M.E.; DE OLIVEIRA, G.S.; GARCIA, A.A.; BARRATT, C.L.; HARPER, C.V. (2008) Ca^{2+} signalling in the control of motility and guidance in mammalian sperm. *Front Biosci.* 13:5623-37.
- PUBLICOVER S. Regulation of Sperm Behaviour. *The Sperm Cell* (2nd Ed), De Jonge and Barratt. 423 Cambridge University Press. 2017.
- PUTNEY, J.W. Jr (1986) A model for receptor-regulated calcium entry. *Cell Calcium* 71–12.

QI, H.; MORAN, M.M.; NAVARRO, B.; CHONG, J.A.; KRAPIVINSKY, G.; KRAPIVINSKY, L.; KIRICHOK, Y.; RAMSEY, I.S.; QUILL, T.A.; CLAPHAM, D.E. (2007) All four CatSper ion channel proteins are required for male fertility and sperm cell hyperactivated motility. *Proc Natl Acad Sci USA*. 104(4):1219-23.

QUILL, T.A.; REN, D.; CLAPHAM, D.E.; GARBERS, D.L. (2001). A voltage-gated ion channel expressed specifically in spermatozoa. *Proc. Natl. Acad. Sci. U.S.A.* 98:12527–531.

QUILL, T.A.; SUGDEN, S.A.; ROSSI, K.L.; DOOLITTLE, L.K.; HAMMER, R.E.; GARBERS, D.L. (2003). Hyperactivated sperm motility driven by CatSper2 is required for fertilization. *Proc. Natl. Acad. Sci. U.S.A.* 100:14869-14874.

QUILL, T.A.; WANG, D.; GARBERS, D.L. (2006) Insights into sperm cell motility signaling through sNHE and the CatSper. *Mol Cell Endocrinol* 250:84–92.

RAHMAN M.S.; KWON, W.S.; PANG M.G. (2014) Calcium influx and male fertility in the context of the sperm proteome: an update. *Biomed Res Int*. 2014:841615.

RAMSEY, I.S.; MORAN, M.M.; CHONG, J.A.; CLAPHAM, D.E. (2006) A voltage-gated proton-selective channel lacking the pore domain. *Nature* 440:1213– 1216.

RASWEILER, J.J. (1987) Prolonged receptivity to the male and the fate of spermatozoa in the female black mastiff bat, *Molossus ater*. *J Reprod Fertil* 79:643–654.

RATHI, R.; COLENBRANDER, B.; BEVERS, M.M.; GADELLA, B.M. (2001) Evaluation of *in vitro* capacitation of stallion spermatozoa. *Biol. Reprod.* 65:462-470.

REDDY, J.M.; AUDHYA, T.K.; GOODPASTURE, J.C.; ZANEVELD, L.J. (1982) Properties of a highly purified antifertility factor from human seminal plasma. *Biology of Reproduction* 27(5):1076-1083.

REDGROVE, K.A.; NIXON, B.; BAKER, M.A.; HETHERINGTON, L.; BAKER, G.; LIU, D.Y.; et al. (2012) The molecular chaperone HSPA2 plays a key role in regulating the expression of sperm surface receptors that mediate sperm-egg recognition. PLoS ONE 7:e50851.

REDGROVE, K.A.; ANDERSON, A.L.; MCLAUGHLIN, E.A.; O'BRYAN, M.K.; AITKEN, R.J.; NIXON, B. (2013) Investigation of the mechanisms by which the molecular chaperone HSPA2 regulates the expression of sperm surface receptors involved in human sperm-oocyte recognition. Mol Hum Reprod 19:120–35.

REIJO, R.; LEE, T.Y.; SALO, P.; ALAGAPPAN, R.; BROWN, L.G.; ROSENBERG, M.; ROZEN, S.; JAFFE, T.; STRAUS, D.; HOVATTA, O.; et al (1995) Diverse spermatogenic defects in humans caused by Y chromosome deletions encompassing a novel RNA-binding protein gene. Nature Genet. 10:383–393.

REN, D.; NAVARRO, B.; PEREZ, G.; JACKSON, A.C.; HSU, S.; SHI, Q., TILLY, J.L.; CLAPHAM, D.E. (2001). A sperm ion channel required for sperm motility and male fertility. Nature 413:603–609.

RENNHACK, A.; SCHIFFER, C.; BRENKER, C.; FRIDMAN, D.; NITAO, E.T.; CHENG, Y.M.; TAMBURRINO, L.; BALBACH, M.; STÖLTING, G.; BERGER, T.K.; KIERZEK, M.; ALVAREZ, L.; WACHTEN, D.; ZENG, X.H.; BALDI, E.; PUBLICOVER, S.J.; BENJAMIN KAUPP, U.; STRÜNKER, T. (2018) A novel cross-species inhibitor to study the function of CatSper Ca²⁺ channels in sperm. Br J Pharmacol. 175(15):3144-3161.

REUTER, H. (1983) Calcium channel modulation by neurotransmitters, enzymes and drugs. Nature 301:569-574.

RIVLIN, J.; MENDEL, J.; RUBINSTEIN, S.; ETKOVITZ, N.; BREITBART, H. (2004) Role of hydrogen peroxide in sperm capacitation and acrosome reaction. Biol Reprod, 70:518-522.

ROLDAN, E.R.; MURASE, T.; SHI, Q.X. (1994) Exocytosis in spermatozoa in response to progesterone and zona pellucida. *Science* 266:1578–1581.

ROSSATO, M.; DI VIRGILIO, F.; RIZZUTO, R.; GALEAZZI, C.; FORESTA, C. (2001) Intracellular calcium store depletion and acrosome reaction in human spermatozoa: role of calcium and plasma membrane potential. *Molecular Human Reproduction*. 7:119–128.

RU, Y.; ZHOU, Y.; ZHANG, Y. (2015) Transient receptor potential-canonical 3 modulates sperm motility and capacitation associated protein tyrosine phosphorylation via $[Ca^{2+}]_i$ mobilization. *Acta Biochim Biophys Sin.* 47(6):404–413.

RUSSELL, L.D.; ETTLIN, R.A.; SINHA-HIKIM, A.P. (1990) *Histological and Histopathological Evaluation of the Testis*. Vienna, IL: Cache River Press.

SAEGUSA, H.; KURIHARA, T.; ZONG, S.; MINOWA, O.; KAZUNO, A.; HAN, W.; MATSUDA, Y.; YAMANAKA, H.; OSANAI, M.; NODA, T.; TANABE, T. (2000) Altered pain responses in mice lacking alpha 1E subunit of the voltage-dependent Ca^{2+} channel. *Proc Natl Acad Sci USA*. 97:6132–7.

SAGARE-PATIL, V.; GALVANKAR, M. (2012) Differential concentration and time dependent effects of progesterone on kinase activity, hyperactivation and acrosome reaction in human spermatozoa. *Int J Androl* 35:633–644.

SAKAI, Y.; YAMASHINA, S. (1989) Mechanism for the removal of residual cytoplasm from spermatids during mouse spermiogenesis. *Anat Rec*. 223(1):43-8.

SAKATA, Y.; SAEGUSA, H.; ZONG, S.; OSANAI, M.; MURAKOSHI, T.; SHIMIZU, Y.; NODA, T.; ASO, T.; TANABE, T. (2002) CaV2.3 (a1E) Ca_v2p channel participates in the control of sperm function. *FEBS Letters* 516:229–233.

SALICIONI, A.M.; PLATT, M.D.; WERTHEIMER, E.V.; ARCELAY, E.; ALLAIRE, A.; SOSNIK, J.; VISCONTI, P.E. (2007) Signalling pathways involved in sperm capacitation. *Soc Reprod Fertil Suppl.* 65:245-59.

SANCHEZ-CARDENAS, C.; SERVIN-VENCES, M.R.; JOSE, O.; TREVINO, C.L.; HERNANDEZ-CRUZ, A.; DARSZON, A. (2014) Acrosome reaction and Ca^{2+} imaging in single human spermatozoa: new regulatory roles of $[Ca^{2+}]_i$. *Biol Reprod* 91:67.

SANTI, C.M.; MARTÍNEZ-LÓPEZ, P.; DE LA VEGA-BELTRÁN, J.L.; BUTLER, A.; ALISIO, A.; DARSZON, A.; SALKOFF, L. (2010) The SLO3 sperm-specific potassium channel plays a vital role in male fertility. *FEBS Lett.* 584(5):1041-6.

SASAKI, M.; TAKAGI, M.; OKAMURA, Y. (2006) A voltage sensor-domain protein is a voltage-gated proton channel. *Science* 312:589– 592.

SATI, L.; CAYLI, S.; DELPIANO, E.; SAKKAS, D.; HUSZAR, G. (2014) The pattern of tyrosine phosphorylation in human sperm in response to binding to zona pellucida or hyaluronic acid. *Reproductive Sciences* 21:573-581.

SATOUH, Y.; INOUE, N.; IKAWA, M.; OKABE, M. (2012) Visualization of the moment of mouse sperm-egg fusion and dynamic localization of IZUMO1. *J. Cell Sci.* 125:4985–4990.

SCHAEFER, M.; HABENICHT, U.F.; BRÄUTIGAM, M.; GUDERMANN, T. (2000) Steroidal sigma receptor ligands affect signaling pathways in human spermatozoa. *Biol Reprod* 63: 57-63.

SCHWARZ, G.; DROOGMANS, G.; NILIUS, B. (1994) Multiple effects of SKF 96365 on ionic currents and intracellular calcium in human endothelial cells. *Cell Calcium.* 15:45–54.

SCHUH, K.; CARTWRIGHT, E.J.; JANKEVICS, E.; BUNDSCHU, K.; LIEBERMANN, J.; WILLIAMS, J.C.; ARMESILLA, A.L.; EMERSON, M.; OCEANDY, D.; KNOBELOCH,

K.P. et al. (2004) Plasma membrane Ca^{2+} ATPase 4 is required for sperm motility and male fertility. *J Biol Chem* 279:28220–28226.

SEIFERT, R.; FLICK, M.; BONIGK, W.; ALVAREZ, L.; TROTSCHER, C.; POETSCH, A.; ... STRUNKER, T. (2014) The CatSper channel controls chemosensation in sea urchin sperm. *The EMBO Journal* 34(3):379–392.

SELVA, D.M.; HIRSCH-REINSHAGEN, V.; BURGESS, B.; ZHOU, S.; CHAN, J.; MCISAAC, S.; HAYDEN, M.R.; HAMMOND, G.L.; VOGL, A.W.; WELLINGTON, C.L. (2004) The ATP-binding cassette transporter 1 mediates lipid efflux from Sertoli cells and influences male fertility. *J. Lipid Res.* 45:1040–1050.

SEO, M.D.; VELAMAKANNI, S.; ISHIYAMA, N.; STATHOPOULOS, P.B.; ROSSI, A.M.; KHAN, S.A.; DALE, P.; LI, C.; AMES, J.B.; IKURA, M. et al. (2012) Structural and functional conservation of key domains in InsP3 and ryanodine receptors. *Nature* 483:108–112.

SHALGI, R.; SMITH, T.; YANAGIMACHI, R. (1992) A quantitative comparison of the passage of capacitated and uncapacitated hamster spermatozoa through the uterotubal junction. *Biol. Reprod.* 46: 419-424.

SHARPE, R.M. (2012). Sperm counts and fertility in men: a rocky road ahead. *EMBO Rep* 13 (5):398-403.

SHIBA, K.; BABA, S.A.; INOUE, T.; YOSHIDA, M. (2008) Ca^{2+} bursts occur around a local minimal concentration of attractant and trigger sperm chemotactic response. *Proc. Natl. Acad. Sci. USA* 105:19312–19317.

SIGNORELLI, J.; DIAZ, E.; MORALES, P. (2012) Kinases, phosphatases and proteases during sperm capacitation. *Cell and Tissue Research* 349:765-782.

SINGH, A.P.; RAJENDER, S. (2015) CatSper channel, sperm function and male fertility. *Reprod Biomed Online*. 30(1):28-38.

SLAMA, R., HANSEN, O.K., DUCOT, B., BOHET, A., SORENSEN, D., GIORGIS ALLEMAND, L., EIJKEMANS, M.J., ROSETTA, L., THALABARD, J.C., KEIDING N. & BOUYER, J. (2012). Estimation of the frequency of involuntary infertility on a nation-wide basis. *Hum Reprod*. 27:1489-1498.

SMITH, C.E.; HERMO, L.; FAZEL, A.; LALLI, M.F.; BERGERON, J.J. (1990) Ultrastructural distribution of NADPase within the Golgi apparatus and lysosomes of mammalian cells. *Prog Histochem Cytochem* 21:1–120.

SOBRERO, A.J.; MACLEOD, J. (1962) The immediate postcoital test. *Fertil. Steril*. 13, 184–189.

STAUSS, C.R.; VOTTA, T.J.; SUAREZ, S.S. (1995). Sperm motility hyperactivation facilitates penetration of the hamster zona pellucida. *Biol. Reprod*. 52:1280-1285.

STRANGE, K.; YAN, X.; LORIN-NEBEL, C.; XING, J. (2007) Physiological roles of STIM1 and Orai1 homologs and CRAC channels in the genetic model organism *Caenorhabditis elegans*. *Cell Calcium*. 42:193–203.

STRÜNKER, T.; WEYAND, I.; BÖNIGK, W.; VAN, Q.; LOOGEN, A.; BROWN, J.E.; KASHIKAR, N.; HAGEN, V.; KRAUSE, E.; KAUPP, U.B. (2006) A K⁺-selective cGMP-gated ion channel controls chemosensation of sperm. *Nat. Cell Biol*. 8:1149–1154.

STRÜNKER, T.; GOODWIN, N.; BRENKER, C.; KASHIKAR, N.D.; WEYAND, I.; SEIFERT, R.; KAUPP, U.B. (2011) The CatSper channel mediates progesterone-induced Ca²⁺ influx in human sperm. *Nature* 471:382–386.

SUAREZ, S.S., KATZ, D.F. & OVERSTREET, J.W. (1983). Movement characteristics and acrosomal status of rabbit spermatozoa recovered at the site and time of fertilization. *Biol. Reprod.* 29:1277-1287.

SUÁREZ, S.S.; OSMAN, R.A. (1987) Initiation of hyperactivated flagellar bending in mouse sperm within the female reproductive tract. *Biol Reprod* 36(5):1191-1198.

SUAREZ, S.S.; KATZ, D.F.; OWEN, D.H.; ANDREW, J.B.; POWELL, R.L. (1991) Evidence for the function of hyperactivated motility in sperm. *Biol Reprod.* 44:375-381.

SUAREZ, S.S.; DAI, X.B.; DEMOTT, R.P.; REDFERN, K., MIRANDO, M.A. (1992) Movement characteristics of boar sperm obtained from the oviduct or hyperactivated *in vitro*. *J Androl.* 13:75-80.

SUAREZ, S.S.; VAROSI, S.M.; DAI, X. (1993) Intracellular calcium increases with hyperactivation in intact, moving hamster sperm and oscillates with the flagellar beat cycle. *Proc Natl Acad Sci USA.* 90:4660–4664.

SUAREZ, S.S.; DAI, X. (1995) Intracellular calcium reaches different levels of elevation in hyperactivated and acrosome-reacted hamster sperm. *Mol Reprod Dev* 42:325-333.

SUAREZ, S.S.; BROCKMAN, K.; LEFEBVRE, R. (1997) Distribution of mucus and sperm in bovine oviducts after artificial insemination *Biology of Reproduction* 56:447–453.

SUAREZ, S.S.; HO, H.C. (2003). Hyperactivated motility in sperm. *Reprod. Domest. Anim.* 38:1191–24.

SUAREZ, S.S.; PACEY, A.A. (2006) Sperm transport in the female reproductive tract. *Hum Reprod update* 12:23–37.

SUAREZ, S.S. (2008). Control of hyperactivation in sperm. *Hum Reprod Update.* 14 (6):647-657.

SUSI, F.R.; LEBLOND, C.P.; CLERMONT, Y. (1971) Changes in the Golgi apparatus during spermiogenesis in the rat. *Am J Anat* 130:251–267.

SUTOVSKY, P.; MANANDHAR, G. (2006) Mammalian spermatogenesis and sperm structure: anatomical and compartmental analysis. In *The Sperm Cell: Production, Maturation, Fertilization, Regeneration*, pp. 1–30.

TAMBURRINO, L.; MARCHIANI, S.; MINETTI, F.; FORTI, G.; MURATORI, M.; BALDI, E. (2014). The CatSper calcium channel in human sperm: relation with motility and involvement in progesterone-induced acrosome reaction. *Hum Reprod* 29:418-428.

TANG, X.M.; LALLI, M.F.; CLERMONT, Y. (1982) A cytochemical study of the Golgi apparatus of the spermatid during spermiogenesis in the rat. *Am J Anat* 163:283–294.

TANG, Q.Y.; ZHANG, Z.; XIA, J.; REN, D.; LOGOTHETIS, D.E. (2010) Phosphatidylinositol 4,5-bisphosphate activates Slo3 currents and its hydrolysis underlies the epidermal growth factor-induced current inhibition. *J Biol Chem* 285:19259 – 19266.

TATENO, H.; KRAPF, D.; HINO, T.; SÁNCHEZ-CÁRDENAS, C.; DARSON, A.; YANAGIMACHI, R.; VISCONTI, P.E. (2013) Ca²⁺ ionophore A23187 can make mouse spermatozoa capable of fertilizing in vitro without activation of cAMP-dependent phosphorylation pathways. *Proceedings of the National Academy of Sciences* 110:18543-18548.

TEGELENBOSCH, R.A.; DE ROOIJ, D.G.A. (1993) Quantitative study of spermatogonial multiplication and stem cell renewal in the C3H/101 F1 hybrid mouse. *Mutat Res.* 290(2):193-200.

TESARÍK, J.; MENDOZA OLTRAS, C.; TESTART, J. (1990) Effect of the human cumulus oophorus on movement characteristics of human capacitated spermatozoa. *J Reprod Fertil.* 88(2):665-75.

TEVES, M.E.; GUIDOBALDI, H.A.; UÑATES, D.R.; SANCHEZ, R.; MISKA, W.; PUBLICOVER, S. J.; GIOJALAS, L.C. (2009) Molecular Mechanism for Human Sperm Chemotaxis Mediated by Progesterone. PLoS ONE, 4(12):e8211.

TILMANN, K.; CAPEL, B. (1999) Mesonephric cell migration induces testis cord formation and Sertoli cell differentiation in the mammalian gonad. Development. 126:2883–2890.

TOMBOLA, F.; ULBRICH, M.H.; ISACOFF, E.Y. (2008) The voltage-gated proton channel Hv1 has two pores, each controlled by one voltage sensor. Neuron 58:546 – 556.

TRAVIS, A.J.; KOPF, G.S. (2002) The spermatozoon as a machine: compartmentalized pathways bridge cellular structure and function. In: De Jonge CJ, Barratt CL, editors. Assisted Reproductive Technology: Accomplishments and New Horizons. Cambridge University Press; Cambridge. pp. 26–39.

TREVINO, C.L.; SANTI, C.M.; BELTRAN, C.; HERNANDEZ-CRUZ, A.; DARZON, A.; LOMELI, H. (1998) Localisation of inositol trisphosphate and ryanodine receptors during mouse spermatogenesis: possible functional implications. Zygote. 6:159–172.

TREVINO, C.L.; SERRANO, C.J.; BELTRAN, C.; FELIX, R.; DARSZON, A. (2001) Identification of mouse trp homologs and lipid rafts from spermatogenic cells and sperm. FEBS Letters. 509:119-125.

TREVINO, C.L.; FELIX, R.; CASTELLANO, L.E.; GUTIERREZ, C.; RODRIQUEZ, D.; PACHECO, J.; LOPEZ-GONZALEZ, I.; GOMORA, J.C.; TSUTSUMI, V.; HERNANDEZ-CRUZ, A.; FIORDELISIO, T.; SCALING, A.L.; DARSZON, A. (2004) Expression and differential cell distribution of low-threshold Ca^{2+} channels in mammalian male germ cells and sperm. FEBS Letters. 563:87-92.

TREVIÑO, C.L.; DE LA VEGA-BELTRÁN, J.L.; NISHIGAKI, T.; FELIX, R.; DARSZON, A. (2006) Maitotoxin potently promotes Ca^{2+} influx in mouse spermatogenic cells and sperm, and induces the acrosome reaction. J Cell Physiol. 206(2):449-56.

TUNG, C.K.; HU, L.; FIORE, A.G.; ARDON, F.; HICKMAN, D.G.; GILBERT, R.O.; SUAREZ, S.S.; WUA, M. (2015) Microgrooves and fluid flows provide preferential passageways for sperm over pathogen *Tritrichomonas foetus*. Proc Natl Acad Sci USA. 112(17):5431–5436.

UHLER, M.; LEUNG, A.; CHAN, S.; WANG, C. (1992) Direct effects of progesterone and antiprogestosterone on human sperm hyperactivated motility and acrosome reaction. Fertil Steril. 58:1191–1198.

URNER, F.; SAKKAS, D. (2003) Protein phosphorylation in mammalian spermatozoa. Reproduction 125:17-26.

VANNIER, B.; ZHU, X.; BROWN, D.; BIRNBAUMER, L. (1998) The membrane topology of human transient receptor potential 3 as inferred from glycosylation-scanning mutagenesis and epitope immunocytochemistry. J. Biol. Chem. 273:8675 – 8679.

VILLANUEVA-DIAZ, C.; ARIAS-MARTINEZ, J.; BERMEJO-MARTINEZ, L.; VADILLO-ORETEGA, F. (1995) Progesterone induces human sperm chemotaxis. Fertil. Steril. 64:1183–1188.

VISCONTI, P.E.; NING, X.; FORNES, M.W.; ALVAREZ, J.G.; STEIN, P.; CONNORS, S.A.; KOPF, G.S. (1999) Cholesterol efflux-mediated signal transduction in mammalian sperm: cholesterol release signals an increase in protein tyrosine phosphorylation during mouse sperm capacitation. Dev Biol 214:429–443.

VISCONTI, P.E.; WESTBROOK, V.A.; CHERTIHIN, O.; DEMARCO, I.; SLEIGHT, S.; DIEKMAN, A.B. (2002) Novel signaling pathways involved in sperm acquisition of fertilizing capacity. Journal of Reproductive Immunology 53:133–150.

VISCONTI, P.E. (2009) Understanding the molecular basis of sperm capacitation through kinase design. PNAS 106 (3) 667-668.

VISHWAKARMA, P. (1962) The pH and bicarbonate-ion content of the oviduct and uterine fluids. *Fertil. Steril.* 13:481–485.

XIA, X.M.; ZHANG, X.; LINGLE, C.J. (2004) Ligand-dependent activation of Slo family channels is defined by interchangeable cytosolic domains. *J Neurosci* 24:5585 – 5591.

XIA, J.; REIGADA, D.; MITCHELL, C.H.; REN, D. (2007) CatSper channel-mediated Ca^{2+} entry into mouse sperm triggers a tail-to-head propagation. *Biol Reprod* 77:551–559.

XIA, J.; REN, D. (2009) Egg coat proteins activate calcium entry into mouse sperm via CATSPER channels. *Biology of Reproduction.* 80:1092–1098.

XIA, J.; REN, D. (2009) The BSA-induced Ca^{2+} influx during sperm capacitation is CATSPER channel-dependent. *Reprod Biol Endocrinol.* 7:119.

XU, W.M.; SHI, Q.X.; CHEN, W.Y.; ZHOU, C.X.; NI, Y.; ROWLANDS, D.K.; LIU, G.Y.; ZHU, H.; MA, Z.G.; WANG, X.F.; CHEN, Z.H.; ZHOU, S.C.; DONG, H.S.; ZHANG, X.H.; CHUNG, Y.W.; YUAN, Y.Y.; YANG, W.X.; CHAN, H.C. (2007) Cystic fibrosis transmembrane conductance regulator is vital to sperm fertilizing capacity and male fertility. *Proc Natl Acad Sci USA* 104:9816–9821.

WALKER, D.; DE WAARD, M. (1998) Subunit interaction sites in voltage dependent Ca^{2+} channels. *Trends Neurosci* 21:148 –154.

WANG, D.; KING, S.M.; QUILL, T.A.; DOOLITTLE, L.K.; GARBERS, D.L. (2003) A new sperm-specific Na^+/H^+ exchanger required for sperm motility and fertility. *Nat Cell Biol* 5:1117–22.

WANG, D.; HU, J.; BOBULESCU, I.A.; QUILL, T.A.; MCLEROY, P.; et al. (2007) A sperm-specific Na^+/H^+ exchanger (sNHE) is critical for expression and *in vivo* bicarbonate regulation of the soluble adenylyl cyclase (sAC). *Proc Natl Acad Sci USA* 104:9325–30.

WANG, Y.; DENG, X.; HEWAVITHARANA, T.; SOBOLOFF, J.; GILL, D.L. (2008) Stim, ORAI and TRPC channels in the control of calcium entry signals in smooth muscle. *Clinical and Experimental Pharmacology and Physiology*. 35:1127–1133.

WANG, H.; LIU, J.; CHO K.H.; REN, D. (2009) A novel, single, transmembrane protein CATSPERG is associated with CATSPER1 channel protein. *Biol Reprod*. 81:539–544.

WASSARMAN, P. M. (1988). Zona pellucida glycoproteins. *Annu. Rev. Biochem.* 57:415-442.

WASSARMAN, P.M. (1999) Mammalian fertilization: molecular aspects of gamete adhesion, exocytosis, and fusion. *Cell* 96:175-183.

WARTENBERG H. (1978) Human testicular development and the role of the mesonephros in the origin of a dual Sertoli cell system. *Andrologia*. 10(1):1-21.

WENNEMUTH, G., WESTENBROEK, R.E., XU, T., HILLE, B.; BABCOCK, D.F. (2000) Cav2.2 and Cav2.3 (N- and R-type) Ca²⁺ channels in depolarization-evoked entry of Ca²⁺ into mouse sperm. *J. Biol. Chem.* 275:21210–21217.

WENNEMUTH, G.; CARLSON, A.E.; HARPER, A.J.; BABCOCK, D.F. (2003) Bicarbonate actions on flagellar and calcium channel responses: initial events in sperm activation. *Development*. 130:1317–1326.

WERTHEIMER, E.V.; SALICIONI, A.M.; LIU, W.; TREVINO, C.L.; CHAVEZ, J.; HERNANDEZ-GONZALEZ, E.O.; et al (2008) Chloride is essential for capacitation and for the capacitation-associated increase in tyrosine phosphorylation. *The Journal of Biological Chemistry*. 283:35539–35550.

WESTENBROEK, R.E.; BABCOCK, D.F. (1999) Discrete regional distributions suggest diverse functional roles of calcium channel alpha1 subunits in sperm. *Dev Biol* 207:457– 469.

WEYAND, I.; GODDE, M.; FRINGS, S.; WEINER, J.; MÜLLER, F.; ALTENHOFEN, W.; HATT, H.; KAUPP, U.B. (1994) Cloning and functional expression of a cyclic nucleotide-gated channel from mammalian sperm. *Nature*. 368:859–863.

WIESNER, B.; WEINER, J.; MIDDENDORFF, R.; HAGEN, V.; KAUPP, U.B.; WEYAND, I. (1998) Cyclic nucleotide-gated channels on the flagellum control Ca^{2+} entry into sperm. *Journal of Cell Biology* 142:473–484.

WILLIAMS, H.L.; MANSELL, S.; ALASMARI, W.; BROWN, S.G.; WILSON, S.M.; SUTTON, K.A.; MILLER, M.R.; LISHKO, P.V.; BARRATT, C.L.; PUBLICOVER, S.J. et al (2015) Specific loss of CatSper function is sufficient to compromise fertilizing capacity of human spermatozoa. *Hum Reprod* 30:2737–2746.

WITSCHI, E. (1948) Migration of the germ cells of human embryos from the yolk sac to the primitive gonadal folds. *Contrib Embryol* 32:67–80.

WOOD, C.D.; DARSZON, A.; WHITAKER, M. (2003) Speract induces calcium oscillations in the sperm tail. *J. Cell Biol.* 161:89–101.

WOOD, C.D.; NISHIGAKI, T.; FURUTA, T.; BABA, S.A.; DARSZON, A. (2005) Real-time analysis of the role of Ca^{2+} in flagellar movement and motility in single sea urchin sperm. *J Cell Biol* 169:725–731.

WOOTTON, L.L.; ARGENT, C.C.; WHEATLEY, M.; MICHELANGELI, F. (2004) The expression, activity and localisation of the secretory pathway Ca^{2+} -ATPase (SPCA1) in different mammalian tissues. *Biochim Biophys Acta*. 1664(2):189-97.

WU, W.L.; SO, S.C.; SUN, Y.P.; ZHOU, T.S.; YU, Y.; CHUNG, Y.W.; WANG, X.F.; BAO, Y.D.; YAN, Y.C.; CHAN, H.C. (1998) Functional expression of a Ca^{2+} -activated K^+ channel in *Xenopus* oocytes injected with RNAs from the rat testis. *Biochimica et Biophysica Acta* 1373:360–365.

YANAGIMACHI, R. (1969) *In vitro* capacitation of hamster spermatozoa by follicular fluid. *J Reprod Fertil.* 18:275–286.

YANAGIMACHI, R. (1988) Mammalian fertilization. In Knobil, E. and Neill, J.D. (eds), *The Physiology of Reproduction*. Raven Press, New York, USA, 135–185.

YANAGIMACHI, R. (1994). Mammalian fertilization. In: Knobil, E., Neill, J. (Eds.), *The Physiology of Reproduction*. Raven Press, New York, p.189–317.

YEUNG, C.H.; BARFIELD, J.P.; COOPER, T.G. (2005) Chloride channels in physiological volume regulation of human spermatozoa. *Biology of Reproduction* 73:1057–1063.

YOSHIMOTO, H.; TAKEO, T.; IRIE, T.; NAKAGATA, N. (2017) Fertility of cold-stored mouse sperm is recovered by promoting acrosome reaction and hyperactivation after cholesterol efflux by methyl-beta-cyclodextrin. *Biology of Reproduction*. 96(2): 446-455.

ZHAO, M.; DEAN, J. (2002) The zona pellucida in folliculogenesis, fertilization and early development. *Rev Endocr Metab Disord.* 3(1):19–26.

ZAMIR, N.; RIVEN-KREITMAN, R.; MANOR, M.; MAKLER, A.; BLUMBERG, S.; RALT, D.; EISENBACH, M. (1993) Atrial natriuretic peptide attracts human spermatozoa in vitro. *Biochem. Biophys. Res. Commun.* 197:116–122.

ZEGERS-HOCHSCHILD, F.; ADAMSON, G.D.; DE MOUZON, J.; ISHIHARA, O.; MANSOUR, R.; NYGREN, K.; SULLIVAN, E.; VANDERPOEL, S. (2009) The International Committee for Monitoring Assisted Reproductive Technology (ICMART) and the World Health Organization (WHO) Revised Glossary on ART Terminology, Fertility and Sterility. 92(5):1520-1524.

ZENG, Y.; CLARK, E.N.; FLORMAN, H.M. (1995) Sperm membrane potential: hyperpolarization during capacitation regulates zona pellucida-dependent acrosomal secretion. *Developmental Biology* 171(2):554-563.

ZENG, X.H.; YANG, C.; KIM, S.T.; LINGLE, C.J.; XIA, X.M. (2011) Deletion of the Slo3 gene abolishes alkalization activated K^+ current in mouse spermatozoa. *Proceedings of the National Academy of Sciences of the United States of America*. 108:5879–5884.

ZHU, G.; XIE, C.; YANG, Z.; WANG, Y.; CHEN, D.; WANG, X. (2018) Expression of TRPC5 is decreased in the sperm of patients with varicocele-associated asthenozoospermia. *Biomed Rep*. 8(6):529–534.